Leveraging Thermal Remote Sensing and Unmanned Aerial Vehicle High-Throughput Phenotyping for Assessing and Monitoring the Water Status of Neglected and Underutilised Taro Crops in Smallholder Farming Systems

by

Helen Snethemba Ndlovu

216016417

Submitted in fulfilment of the academic requirements of

Doctor of Philosophy

in Environmental Science

School of Agricultural, Earth and Environmental Sciences

College of Agriculture, Engineering and Science

University of KwaZulu-Natal

Pietermaritzburg

South Africa

2025

Source: Helen Snethemba Ndlovu

"One of the most impactful ways to increase food security around the world is the empowerment of smallholder farmers, who produce about one-third of the world's food supply"

– World Economic Forum

ABSTRACT

As threats posed by climate change and variability continue to intensify, smallholder farming systems are challenged by the urgent need to sustain crop production and ensure food security. Taro (*Colocasia esculenta* (L)), a Neglected and Underutilised Crop Species (NUS), has emerged as a promising future-smart crop due to its resilience to drought and heat stresses, holding great potential for diversifying existing cropping systems and enhancing smallholder farming resilience. Despite its reported adaptive capabilities, taro remains vulnerable to prolonged water stress. Such conditions can disrupt internal water balance, leading to reduced equivalent water thickness, increased foliar temperature and decreased stomatal conductance, which can ultimately compromise taro's tuber quality and productivity. Therefore, accurate and robust monitoring of taro crop water status indicators is essential for the rapid detection of water deficits, facilitating proactive and targeted interventions aimed at mitigating stress impacts and maintaining optimal productivity. Cutting-edge remote sensing technologies, particularly Unmanned Aerial Vehicles (UAVs) equipped with high-resolution thermal cameras integrated with multispectral sensors, have revolutionised precision agriculture. Such technologies have emerged as invaluable tools that enable near-real-time crop monitoring at ultra-high spatial and temporal resolutions, suitable for continuous field-scale assessments of water status. Hence, this study sought to evaluate the utility of UAV thermal remote sensing in assessing and monitoring the crop water status of neglected and underutilised taro crop within smallholder farming systems. Taro is classified as a NUS owing to its limited inclusion in mainstream agricultural research and policy, particularly in Africa and many other regions worldwide, despite its potential to support food security in climate-vulnerable regions. Specifically, this study first adopted a systematic approach to review the progress, challenges, and opportunities in utilising UAV thermal remote sensing to assess and monitor the water status within crop farming systems. The findings revealed that studies utilising UAV thermal remote sensing to assess crop water status are disproportionately concentrated in the global north, with a limited focus on neglected and underutilised crops (> 4 %) and smallholder rainfed systems in the global south (2.3 %). Furthermore, results highlighted that while UAV-derived thermal datasets have gained significant traction, integrating thermal imagery with multispectral data is crucial for leveraging their complementary strengths, enhancing accuracy, and providing a more comprehensive assessment of crop water status. The findings further highlighted the importance of advanced image segmentation techniques in mitigating soil background interference, which

can distort crop thermal signatures and compromise the precision of crop water status assessments. As a result, the second objective of the study was to assess the utility of index-based image segmentation techniques and UAV thermal remotely sensed data in enhancing the estimation of smallholder taro equivalent water thickness (EWT_{canopy}) as a proxy of crop water status. To achieve this objective, a comparative analysis was conducted to assess the predictive performance of models with and without the thermal band, while also evaluating the effectiveness of Excess Green (ExG), Excess Red (ExR), and Excess Green minus Excess Red (ExGR) image segmentation techniques in improving taro EWT_{canopy} estimations. The findings revealed that incorporating the thermal band and applying image segmentation, particularly using the ExGR technique, significantly enhanced the prediction accuracy of taro EWT_{canopy}, leading to a substantial increase in the R^2 value from 0.32 to 0.92, while the rRMSE was significantly reduced from 60.51% to 15.31%. Having established the importance of integrating thermal data with the ExGR image segmentation technique, the third objective aimed to evaluate the utility of UAV remotely sensed data for high-throughput crop phenotyping of taro equivalent water thickness, fuel moisture content, stomatal conductance, foliar temperature and chlorophyll content as proxies for water status within smallholder farms. The findings revealed that a multi-modal approach, integrating thermal and multispectral data outperforms single-modal methods, yielding R^2 values greater than 0.91 and rRMSEs less than 14.15%. Notably, the thermal waveband and derived thermal indices emerged as the most influential variables for estimating stomatal conductance and leaf temperature, with R^2 values of 0.96 and 0.95, respectively. In contrast, for equivalent water thickness and fuel moisture content, other spectral variables ranked higher in importance. However, incorporating thermal spectral variables substantially improved the prediction accuracy for these traits, increasing R^2 from 0.73 to 0.95 (rRMSE reduced from 33.82 % to 14.15 %) for equivalent water thickness, and from 0.77 to 0.94 (rRMSE reduced from 6.55 % to 3.32 %) for fuel moisture content. Subsequently, the fourth objective sought to conduct a multi-temporal analysis of NUS taro crop water status using multi-modal UAV remotely sensed data and deep learning techniques to estimate stomatal conductance and foliar temperature as key physiological indicators across different growth stages of smallholder taro crops. The findings highlighted distinct trends in stomatal conductance and leaf temperature, with the emergence stage exhibiting the highest leaf temperatures and lowest stomatal conductance, while the vegetative stage showed the lowest leaf temperatures and a peak in stomatal conductance. Notably, the vegetative growth stage exhibited the highest prediction accuracies for stomatal conductance (R^2 of 0.96, RMSE of

29.34 mmol m^{-2} s^{-1} and rRMSE of 12.86 %) and leaf temperature (R^2 of 0.95, RMSE of 0.33 °C and rRMSE of 1.11 %). This pattern may be attributed to the limited canopy cover during the emergence stage, where exposed soil temperatures to interfere with crop thermal signatures, in contrast to the vegetative stage where increased foliage reduces soil influence and supports optimal physiological activity. Finally, the fifth objective evaluated the utility of a data-driven approach using UAV thermal and multispectral remotely sensed data, along with topographic variables, to estimate the stomatal conductance and leaf temperature of smallholder taro crops across different growth stages (emergence, vegetative, and maturity) as proxies for crop water status. While integrating multi-source datasets provides a comprehensive evaluation of crop water conditions, it is recommended that advanced feature selection and model optimisation are employed to address challenges of redundancy, multicollinearity and overfitting because of combing large feature subsets. To this end, the findings highlighted the utility of integrating diverse yet relevant datasets, including thermal, multispectral, and topographic data, into a unified data-driven framework for estimating crop water status. Additionally, this study applied critical water stress thresholds (50 mmol m^{-2} s^{-1} for stomatal conductance and 35 °C for leaf temperature) to the optimised models, enabling the spatially explicit identification of water-stressed areas within the taro field. Results revealed significant stress during the emergence stage, with 14.18 % of crops showing low stomatal conductance and 37.14 % exceeding the leaf temperature threshold. In contrast, minimal stress was observed in the vegetative growth stage (1.85 %), while the maturity stage showed a slight increase in stress, with 9.36% of the area exceeding the leaf temperature threshold. The findings of this study highlight the critical importance of early-stage monitoring and targeted interventions, especially during the emergence stage, to manage potential negative impacts caused by water stress on taro. Overall, the findings of this study demonstrated the transformative potential of integrating UAV thermal remote sensing with advanced deep learning techniques in providing rapid and robust spatially explicit information on smallholder taro crop water status for ensuring crop productivity and developing early warning systems of water stress. The findings make a significant contribution to the anecdotal knowledge of neglected and underutilised crops, such as taro. Additionally, they play a crucial role in promoting climate-smart agriculture and enhancing climate resilience within smallholder farming systems. Lastly, the implications of this study are aligned with global and regional developmental goals, including Sustainable Development Goals (2 and 13) and the African Union's Agenda 2063 Goals (5), contributing to sustainable agricultural practices that enhance food security and climate resilience. Ultimately, this study is a pathway

towards transformative, data-driven frameworks and actionable solutions that could empower decision-makers to support smallholder farmers in proactively adapting to climate variability, enhancing long-term crop viability and fostering resilience and sustainability in the face of intensifying climate stress.

Keywords: Unmanned aerial vehicles, thermal remote sensing, taro, neglected and underutilised crops, climate resilience, crop water status monitoring, high-throughput phenotyping, smallholder farmers.

PREFACE

The research contained in this dissertation was completed by the candidate while based in the School of Agricultural, Earth and Environmental Sciences of the College of Agriculture, Engineering and Science, University of KwaZulu-Natal, Pietermaritzburg, South Africa, from April 2022 to December 2024, under the supervision of Prof. John Odindi, Prof. Onisimo Mutanga and Dr. Mbulisi Sibanda. The research was financially supported by the National Research Foundation and the Water Research Commission of South Africa.

The contents of this work have not been submitted in any form to another university and, except where the work of others is acknowledged in the text, the results reported are due to investigations by the candidate.

Helen Snethemba Ndlovu Signed_[redacted]_ Date: 25/01/2025

As the candidate's supervisor, I certify the statement and have approved this thesis for submission.

Professor John Odindi Signed_[redacted]_ Date: 25/01/2025

Professor Onisimo Mutanga Signed_[redacted] Date: 28/01/2025

Dr Mbulisi Sibanda Signed_[redacted]_ Date: 29/01/2025

DECLARATION ONE: PLAGIARISM

I Helen Snethemba Ndlovu declare that:

1. The research reported in this dissertation is my original work unless otherwise indicated.

2. This dissertation has not been submitted for the attainment of a degree or examination purposes at another university.

3. This dissertation does not contain any data, graphics, and other information from other persons unless duly acknowledged.

4. This dissertation does not contain other persons' writings unless duly acknowledged as such. In cases where written sources have been cited:

    a. Their words have been paraphrased and general information attributed to them has been referenced.
    b. Where exact words have been used, they were placed inside quotation marks and referenced.

5. This dissertation does not contain text, graphics, and or tables directly copied and pasted from the internet unless otherwise sources were duly acknowledged within the content of this dissertation.

Signed  Date: 25/01/2025

DECLARATION TWO: PUBLICATIONS AND MANUSCRIPTS

1. **Ndlovu, H. S**., Odindi, J., Sibanda, M., & Mutanga, O. (2024). A systematic review on the application of UAV-based thermal remote sensing for assessing and monitoring crop water status in crop farming systems. *International Journal of Remote Sensing*, 45(15), 4923-4960.

2. **Ndlovu, H. S**., Odindi, J., Sibanda, M., & Mutanga, O. (2024). Enhancing Taro Equivalent Water Thickness Estimation through Index-Based Image Segmentation using Unmanned Aerial Vehicle Multispectral Thermal Imagery. *Proceedings of the 3rd African Conference on Precision Agriculture*, 229-235. African Plant Nutrition Institute, Benguérir, Morocco.

3. **Ndlovu, H. S**., Odindi, J., Sibanda, M., & Mutanga, O. (2024). Enhancing Taro Equivalent Water Thickness Estimation through Index-Based Image Segmentation using Unmanned Aerial Vehicle Multispectral Thermal Imagery. *Remote Sensing Applications: Society and Environment*, Under Review, Manuscript ID: RSASE-D-24-01546

4. **Ndlovu, H. S**., Odindi, J., Sibanda, M., & Mutanga, O. (2024). Assessing Neglected and Underutilised Taro Crop Water Status using Physiological Indicators and UAV Multi-Modal Thermal-Multispectral Data. *Precision Agriculture*, Under Review, Manuscript ID: PRAG-D-24-01162

5. **Ndlovu, H. S**., Odindi, J., Sibanda, M., & Mutanga, O. (2025). Multi-Temporal Analysis of Taro Crop Water Stress Using High-Resolution Thermal and Multispectral Proximal Sensing for Improved Resilience of Smallholder Farming Systems. *Computers and Electronics in Agriculture*, Under Preparation.

6. **Ndlovu, H. S**., Odindi, J., Sibanda, M., & Mutanga, O. (2025). Optimising Neglected and Underutilised Taro Crop Water Status Estimations using UAV-Acquired Thermal and Multispectral Remotely Sensed Data. *Smart Agricultural Technology*, Under Preparation.

DEDICATION

This work is dedicated to my younger self, the little girl who dared to dream, and to the love of my life who makes every dream possible.

"The pain of discipline is better than the pain of regret"

ACKNOWLEDGEMENTS

Firstly, to the Universe, I offer my deepest gratitude for guiding me on this journey. May my heart remain open to the infinite wisdom, love and light that surrounds me and may I remain a vessel for the divine, allowing its presence to guide me towards my highest potential.

I would like to thank the University of KwaZulu-Natal, particularly the School of Agricultural, Earth, and Environmental Sciences, for granting me the opportunity to pursue my doctoral degree and for providing the academic foundation essential for completing this research.

I would like to express my sincere appreciation to my supervisors, Prof. John Odindi, Prof. Onisimo Mutanga and Dr. Mbulisi Sibanda, for their invaluable guidance, constructive feedback and professional expertise that have contributed significantly to the success of this research. Your mentorship, support and encouragement have been instrumental in shaping my academic and professional growth over the past seven years as an honours, masters and doctoral student. May your teachings, wisdom and inspiration continue to guide me through my future research endeavours. I would also like to acknowledge and thank Dr. Trylee Matongera for his words of encouragement and moral support throughout my academic journey.

I extend my heartfelt appreciation to my dear colleagues in the Department of Geography who have been an incredible source of motivation, support and encouragement throughout my research. Specifically, I would like to thank Anela Mkwenkwana, Celuxolo Dlamini, Bheka Mlambo, Siphiwokuhle Buthelezi, Tembela Vimbi, Kuhlekonke Mathenjwa, Siphamandla Maseko, Dr. Collins Matiza, Dr Mthembeni Mngadi, Dr. Odebiri Omosalewa, Sfundo Mthiyane, Ntuthuko Mncwabe, Dr. Dadirai Matarira, Dr. Adeola Arougundade and Anita Masenyama for their assistance with fieldwork and overall support. I would like to particularly thank Celuxolo Dlamini for his invaluable contributions with programming concepts, proofreading and strengthening the outputs of this research. I extend my sincere appreciation to the community of Swayimane and the smallholder farmers, particularly Mr. Mkhize and Mr. Nene, for their invaluable support and generosity in granting access to their fields. I also thank the Department of Geography Staff, Ms. Andile Mshengu, Mr. Brice Gijsbertsen, Mr. Donavin

Devos, Ms. Celeste Clark and Ms. Alison Young for their assistance with technical and administrative matters**.**

To my Mom and Dad, Ncamisile and Ronnie Ndlovu, thank you for enduring my love and passion for academia. Your unwavering support and unconditional love have carried me through this journey and held me steady through life's storms and challenges. I am eternally grateful for the countless sacrifices you have made to nurture my dreams and guide me toward a purposeful and meaningful life. *Ngiyabonga kakhulu!*

To Lindokuhle Luthuli – I could not have done this without you. Your encouragement to think in abundance has been a reminder that our reality is shaped by our thoughts and intentions. Your love and support have been a constant source of strength enabling me to push through and follow my dreams. Thank you - I am forever grateful for your presence in my life!

This work is based on the research funded by the Water Research Commission of South Africa through the project [WRC C2022/2023 – 00930] titled "Unmanned Aerial Vehicle (UAV) High-Throughput Phenotyping (HTP) of Neglected and Underutilised Crop species (NUS) for improved water use and productivity in smallholder farms". I would like to also acknowledge the National Research Foundation (NRF) through the Research Chair in Land Use Planning and Management Grant Number 84157, NRF Postgraduate Scholarships Grant Number 144765 and the Sustainable and Healthy Food Systems – Southern Africa project [227749/Z/23/Z] for their financial support.

TABLE OF CONTENTS

LIST OF TABLES

LIST OF FIGURES

ABBREVIATIONS

A	Above
Adam	Adaptive Moment Estimation
ANOVA	Analysis of Variance
ASTER	Advanced Spaceborne Thermal Emission and Reflection Radiometer
AWS	Automatic Weather Station
AWiFS	Advanced Wide Field Sensor
B	Below
CRP	Calibrated Reflectance Panel
CV	Coefficient of Variation
CVCT	Coefficients Variance of Canopy Temperature
CSTD	Standard Deviation of Canopy Temperature Index
CWSI	Crop Water Stress Index
DACT	Degrees Above Critical Temperature
DANS	Degrees Above Non-Stressed Canopy
DEM	Digital Elevation Models
DLS 2	Downwelling Light Sensor 2
DNN	Deep Neural Networks
DOI	Digital Object Identifier
DOY	Day of Year
DW	Dry Weight
ECOSTRESS	Ecosystem Spaceborne Thermal Radiometer Experiment on Space Station
ET	Crop Evapotranspiration
EMT+	Enhanced Thematic Mapper Plus
EVI	Enhanced Vegetation Index
ExG	Excess Green
ExGR	Excess Green minus Excess Red
ExR	Excess Red
FW	Fresh Weight
GPS	Global Positioning System
HRMET	High-Resolution Mapping of Evapotranspiration

HTP	High-Throughput Phenotyping
I3	Second Formulation of the Stomatal Conductance Index
IG	Index of Relative Stomatal Conductance
IPCC	Intergovernmental Panel on Climate Change
KML	Keyhole Markup Language
LAI	Leaf Area Index
LASSO	Least Absolute Shrinkage and Selection Operator
LiDAR	Light Detection and Ranging
LR	Linear Regression
M300	DJI Matrice 300
MCARI	Modified Chlorophyll Absorption in Reflectance Index
MODIS	Moderate Resolution Imaging Spectroradiometer
MODTRAN	Moderate Resolution Atmospheric Transmission
MSR	Modified Spectral Ratio
N	Number Samples
NGRDI	Normalised Green-Red Difference Index
NDRE	Normalised Difference Red-Edge Index
NDVI	Normalised Difference Vegetation Index
NDWI	Normalised Difference Water Index
NRCT	Normalised Relative Canopy Temperature
NRMSE	Normalised Root Mean Square Error
NUS	Neglected and Underutilised Crop Species
OSAVI	Optimised Soil-Adjusted Vegetation Index
PLR	Partial Least Squares Regression
PRI	Photochemical Reflectance Index
PRISMA	Preferred Reporting Items for Systematic Reviews and Meta-Analyses
R^2	Coefficient of Determination
RDVI	Renormalised Difference Vegetation Index
ReLU	Rectified Linear Unit
RGB	Red-Green-Blue
RGRI	Red–Green Ratio Index
RMSE	Root Mean Square Error
SACAA	South African Civil Aviation Authority

SAVI	Soil-Adjusted Vegetation Index
SCTI	Standardised Canopy Temperature Index
SEM	Standard Error of Mean
SHAP	SHapley Additive exPlanations
SIPI	Structure Insensitive Pigment Index
SPI	Stream Power Index
SPAD	Soil Plant Analysis Development
SMMI	Surface Moisture Mapping Index
Std.	Standard Deviation
Ta	Air Temperature
Tc	Canopy Temperature
TCI	Temperature Condition Index
TCARI	Transformed Chlorophyll Absorption in Reflectance Index
TCARI/OSAVI	Transformed Chlorophyll Absorption in Reflectance Index / Optimised Soil-Adjusted Vegetation Index
TIRS	Thermal Infrared Sensors
TM	Thematic Mapper
TR	Terrain Ruggedness Index
TVDI	Temperature Vegetation Drought Index
TSEB	Two-Source Energy Balance
TWI	Topographic Wetness Index
UAV	Unmanned Aerial Vehicle
URL	Uniform Resource Locator
USA	United States of America
UTM	Universal Transverse Mercator
VI	Vegetation Indices
VIIRS	Visible Infrared Imaging Radiometer Suite
VTOL	Vertical Take-off and Landing
WDI	Water Deficit Index

CHAPTER ONE: GENERAL INTRODUCTION

1.1 Introduction

Global demand for food production is escalating rapidly due to the growing human population (Panday *et al.* 2020; Mugiyo *et al.* 2021a). Previous estimates have indicated that agricultural food production would need to increase by 50 – 70% by 2050 to sustain the projected global population of ~ 10 billion (Nhamo *et al.* 2020; Ghosh *et al.* 2024; Williamson *et al.* 2024). This is a critical concern as the population has already reached 8.2 billion as of 2024 (United Nations 2024). Meanwhile, the challenge of meeting rising food demand is exacerbated by the impacts of climate change, which particularly pose a significant threat to traditional agricultural systems (Nhamo *et al.* 2019b; Kephe *et al.* 2021a). Shifting rainfall patterns, rising temperatures and the increased frequency of extreme weather events, for instance, have adversely affected crop productivity and overall yields (Gomez-Zavaglia *et al.* 2020; Kumari *et al.* 2022). A recent Climate Change Synthesis Report by the Intergovernmental Panel on Climate Change (IPCC) has confirmed that developing regions, including Sub-Saharan Africa, are extremely vulnerable to the impacts of climate change and variability (Lee *et al.* 2023). These regions already face precedent challenges of hunger and food insecurity, which are further exacerbated by climate-related risks (Chakona and Mushangai 2021; Lee *et al.* 2023). This challenge is further pronounced in smallholder farming systems, that despite producing 80% of food in this region, remain disproportionally susceptible to the impacts of climate change due to their reliance on rainfall and lack of resources for climate adaptation and resilience (Antonaci *et al.* 2014; Hlophe-Ginindza and Mpandeli 2020; Silici *et al.* 2022). Hence, food and nutrition security continue to be ongoing challenges, as cropping systems struggle to adapt to the worsening climatic conditions (Chivenge *et al.* 2015; Aryal *et al.* 2020). Moreover, while existing agricultural systems consisting of a few mainstream crops have supported food demands in the past, their ability to sustain productivity in the 21st century is uncertain (Mabhaudhi *et al.* 2017a). This reality necessitates a transformative and climate-smart paradigm shift in agriculture, that prioritises diversification of cropping systems to incorporate crop species that build resilience and strengthen the adaptive capacity of smallholder agricultural landscapes against climate change (Mabhaudhi *et al.* 2017a; Nhamo *et al.* 2019b).

A promising approach to addressing these challenges is through the strategic promotion and integration of Neglected and Underutilised Crop Species (NUS) into agricultural systems.

NUS, as the term suggests, are crops that have been historically overlooked in mainstream agriculture, exhibit low utilisation rates, receive limited research attention and are predominately confined to smallholder farming systems (Chivenge *et al.* 2015; Ndlovu *et al.* 2024c). These crops are typically well-adapted to harsh agro-ecological conditions, including marginal lands and unpredictable climates, making them an ideal option for crop resilience amidst climate variability and change (Mabhaudhi *et al.* 2017a; Mugiyo *et al.* 2021a). Taro (*Colocasia esculenta* (L)), referred to as *Amadumbe* in South Africa, for instance, has been identified as a future-smart-crop due to its drought and heat tolerance and its adaptability to adverse environmental conditions (Mabhaudhi and Modi 2015; Oyeyinka and Amonsou 2020). Cultivated for its edible corms, leaves and petioles, taro's nutritional profile is rich in carbohydrates, protein, vitamins, and natural sterols, hence a promising option for addressing micronutrient deficiencies while ensuring food security (Chivenge *et al.* 2015; Haerussana *et al.* 2022). While taro has demonstrated significant potential for advancing climate-resilient and nutrition-sensitive agriculture, empirical research on its water requirement status and stress responses remains largely limited and anecdotal (Mabhaudhi *et al.* 2017a). Furthermore, a significant knowledge gap exists regarding the spatial and temporal dynamics of taro's water status and its stress responses throughout the growing season, hence, hindering its promotion and integration into existing agricultural systems. Moreover, as moisture content directly influences tuber quality, texture and palatability (Ferdaus *et al.* 2023), accurately monitoring its water status throughout the growth stages becomes imperative. Therefore, generating spatially and temporally explicit evidence-based information on taro's water status is critical for maintaining optimal moisture levels, enhancing productivity and informing climate-adaptive management practices.

Assessing variation of crop physiological processes in response to water stress is crucial for understanding the dynamics of crop water status and accurately quantifying water stress (Gerhards *et al.* 2019; Parkash and Singh 2020; Ahmad *et al.* 2021). Studies indicate that under moisture deficit conditions, crops exhibit several physiological changes that can serve as reliable indicators of their water status (Parkash and Singh 2020; Sobejano-Paz *et al.* 2020; Wang *et al.* 2022a). Stomatal conductance, a key indicator of gas exchange through leaf pores, for example, typically declines during water stress as crop close their stomata to minimise water loss through transpiration, leading to increased foliar temperature due to reduced evaporative cooling (Gerhards *et al.* 2019; Krishna *et al.* 2021). Similarly, equivalent water thickness and fuel moisture content, indicators of internal water reserves within plant tissues,

generally diminish as crops experience dehydration due to water deficits (Ndlovu *et al.* 2021a; Traore *et al.* 2021). Additionally, chlorophyll content, vital for capturing light energy during photosynthesis, declines under water stress due to structural damage to chloroplasts and the oxidative stress induced by moisture shortages (Shafiq *et al.* 2019; Parkash and Singh 2020). Therefore, quantifying and continuously monitoring these crop water physiological indicators is imperative for understanding taro's water status and developing targeted interventions that mitigate the impacts of water deficit, particularly during critical growth phases such as emergence, vegetative expansion and corm development (Mabhaudhi and Modi 2016; Abd El-Aal *et al.* 2019). Although taro is often classified as drought-tolerant, this tolerance is relative and not absolute. Its physiological performance and yield can be significantly constrained under persistent or severe water stress, especially when stress occurs at sensitive developmental stages (Hassanpanah and Khorshidi Benam 2004; Ramírez *et al.* 2016; Kunz *et al.* 2024a). Furthermore, taro's adaptive mechanisms, such as partial stomatal regulation or increased root uptake, may delay the onset of visible stress symptoms but do not eliminate underlying physiological strain, making the early detection of subtle water stress essential for timely intervention (Gouveia *et al.* 2020). Such efforts are particularly important for smallholder farming systems, where irrigation infrastructure and decision-support tools are limited (Nhamo *et al.* 2019b), resulting in timely detection of crop water stress through physiological indicators like stomatal conductance, leaf temperature, and chlorophyll content, being critical to avoid irreversible yield losses. Consequently, there is an urgent need for rapid, innovative, and effective techniques to monitor the spatial and temporal variability of these indicators to enable timely and data-driven management strategies that optimise water use efficiency, enhance crop productivity, and support resilience in agriculture.

While traditional techniques of retrieving crop water status physiological indicators are accurate, these methods are inherently time-intensive, laborious, expensive and often require exhaustive chemical analysis and direct visual observations conducted by trained experts (Maimaitiyiming *et al.* 2020a; Yin *et al.* 2023). Furthermore, these measurements are prone to human error, lack of efficiency and are not well-suited for the continuous monitoring across the spatial and temporal scales required to adequately capture field water status variability throughout the growing season (Mobasheri and Fatemi 2013a; Panday *et al.* 2020; Traore *et al.* 2021). Meanwhile, advances in earth observation technologies, particularly the advent of thermal remote sensing, have provided a robust and transformative tool for assessing and monitoring crop water status (Khanal *et al.* 2017; Messina and Modica 2020). Thermal remote

sensing, operating within the 8 – 14 μm of the thermal infrared region of the electromagnetic spectrum, is grounded on the principle that crops emit thermal radiation which is influenced by heat dissipation processes linked to transpiration, evaporation and overall crop water uptake (Khanal *et al.* 2017; Gerhards *et al.* 2019; Krishna *et al.* 2021). As crops transpire under adequate water conditions for instance, water evaporates from their leaves, creating a cooling effect that directly impacts leaf surface temperature, which can be accurately detected using thermal sensors (Maes and Steppe 2012; Hou *et al.* 2018). Therefore, by capturing crop thermal signatures associated with physiological processes, thermal remote sensing provides a robust framework for non-invasive quantification of crop water status and enables the early detection of crop water stress (Gerhards *et al.* 2019).

The adoption of thermal remote sensing technologies has significantly grown over the past decades (Gerhards *et al.* 2019; Awais *et al.* 2022a). This growth has been particularly driven by the deployment of satellite-based thermal sensors that include the Moderate Resolution Imaging Spectroradiometer (MODIS), Advanced Spaceborne Thermal Emission and Reflection Radiometer (ASTER), Ecosystem Spaceborne Thermal Radiometer Experiment on Space Station (ECOSTRESS), and the Landsat series (Malbéteau *et al.* 2018b; Gerhards *et al.* 2019; Xue *et al.* 2020a). These sensors have enabled detailed monitoring of surface temperature and thermal dynamics at various spatial and temporal scales, providing critical insights on vegetation water characteristics (Khanal *et al.* 2017; Awais *et al.* 2022a). Nonetheless, while thermal remote sensing offers valuable capabilities, the integration of thermal with multispectral data has been noted to provide a comprehensive understanding of crop water dynamics and overall health, enabling the capture of subtle variations in crop water status that may otherwise remain undetected by thermal sensors alone (Messina and Modica 2020; Gao *et al.* 2024). Multispectral sensors such as Sentinel-2 Multispectral Instrument, Landsat Thematic Mapper (TM)/Enhanced TM Plus (ETM+), WorldView-2/3, and PlanetScope, which capture reflectance in the visible, near-infrared and shortwave regions of the spectrum, provide complementary data that are sensitive to changes in crop water status (Ihuoma and Madramootoo 2019; Ahmad *et al.* 2021). Despite these advancements, it remains a significant challenge for existing satellite-based thermal and multispectral sensors to balance high spatial resolution with high revisit frequency, thereby limiting their capacity to offer continuous monitoring of crop water status at a field scale (Khanal *et al.* 2017; Mo *et al.* 2018; Kapari *et al.* 2024). Given these constraints, there is an urgent need for novel, spatially explicit, and time-

efficient alternatives capable of accurately assessing the variations in crop water status across the growing season of smallholder taro crops.

Recent advances in proximal remote sensing technologies, especially Unmanned Aerial Vehicles (UAVs) equipped with high-resolution sensors, have emerged as revolutionary tools for crop monitoring, offering a distinct advantage over traditional satellite-based remote sensing (Hussain *et al.* 2020; Nhamo *et al.* 2020). Unlike satellite remotely sensed data, UAVs can provide very-high spatial resolution datasets, often in centimetres, enabling detailed and precise monitoring of crop water conditions at the field level (Hoffmann *et al.* 2016b; Chivasa *et al.* 2020). Additionally, UAVs facilitate on-demand acquisition of thermal and multispectral imagery, providing an opportunity for near-real-time mapping of crop water status and variability across the growing season (Malbéteau *et al.* 2018b). Therefore, UAVs mounted with ultra-high resolution thermal cameras and multispectral sensors spanning the visible, near-infrared and red-edge regions of the electromagnetic spectrum, enable the development of optimal thermal, vegetation and topographic indices for estimating the crop water status of smallholder taro cropping systems (Gago *et al.* 2017a; Tang *et al.* 2020a; Elsherbiny *et al.* 2021). Despite these advantages, the application of UAV-proximal sensing for assessing and monitoring the water status of neglected and underutilised taro crops, particularly within marginalised and smallholder farming systems in the Global South, remains significantly underexplored. Moreover, a critical gap in the literature lies in the integration of UAV-based thermal remote sensing with advanced deep-learning techniques to model complex and non-linear NUS crop attributes, offering immense potential for enhancing crop water assessments and promoting data-driven decision-making in precision agriculture.

In addressing this gap, there is an urgent need for research that evaluates the utility of cutting-edge UAV technologies integrated with state-of-the-art spatial modelling techniques for monitoring and assessing taro crop water status. Developing advanced data-informed crop moisture models from multi-modal datasets holds great potential in advancing the precision and scalability of UAV-based crop monitoring, particularly for building early warning systems and contributing to broader climate-resilient agricultural frameworks. However, the effectiveness and adoption of these technologies in smallholder farming systems may be constrained by factors such as the high cost of UAV equipment, lack of technical expertise, limited data-processing infrastructure, and inadequate policy support. Recognising these limitations, this study does not merely aim to promote UAV use as a standalone solution but

rather as a science-to-proof-of-concept initiative, laying the groundwork for future integration into low-cost, farmer-support systems. By extracting simplified thermal and multispectral indicators of crop water stress, the findings can inform the development of context-appropriate advisory tools or mobile-based applications that local extension officers or cooperatives can use to support smallholders. By leveraging the advantages of UAVs equipped with high-resolution thermal and multispectral sensors, this study aims to contribute to the growing body of anecdotal knowledge on neglected and underutilised crops, such as taro, highlighting their role in promoting climate-smart agriculture and enhancing climate resilience within smallholder farming systems. In doing so, the research bridges the gap between advanced technologies and local farming realities by producing evidence that can support policy dialogue, guide investment in accessible innovations, and strengthen early detection of crop water stress, ultimately benefiting smallholder farmers in the long term. The findings will seek to contribute to climate action and policy by fostering resilient agricultural practices and promoting food and nutrition security in marginal and smallholder farming communities, addressing a pressing need for innovative and inclusive solutions in the era of precision agriculture.

1.2 Aims and objectives

The aim of this study was to evaluate the utility of UAV thermal remote sensing in assessing and monitoring the crop water status of neglected and underutilised taro crops within smallholder farming systems. The specific objectives were:

i. To review and offer an in-depth systematic assessment of the progress, challenges, and opportunities presented in the literature on the adoption of UAV thermal remote sensing in assessing and monitoring crop water status.

ii. To assess the utility of UAV thermal remotely sensed data and index-based segmentation techniques in enhancing the estimation of smallholder taro equivalent water thickness as a proxy of crop water status.

iii. To evaluate the utility of UAV remotely sensed data for high-throughput crop phenotyping of taro equivalent water thickness, fuel moisture content, stomatal

conductance, foliar temperature and chlorophyll content as proxies for water status within smallholder farms.

iv. To conduct a multi-temporal analysis of neglected and underutilised taro crop water status using multimodal UAV remotely sensed data to estimate stomatal conductance and foliar temperature as key physiological indicators across different growth stages of smallholder taro crops.

v. To optimise the estimation of taro stomatal conductance and leaf temperature through a data-driven approach that integrates UAV-derived thermal and multispectral data with topographic variables, enabling the quantification of crop water stress based on predefined stress thresholds.

1.3 Research questions

i. What are the current advancements, challenges, and opportunities in utilising UAV-based thermal remote sensing for assessing and monitoring crop water status?

ii. What knowledge gaps and future research directions exist in the application of UAV thermal remote sensing for crop water status assessment?

iii. To what extent can UAV-derived thermal remote sensing data be used exclusively to estimate physiological indicators of taro crop water status?

iv. Can index-based image segmentation techniques enhance the estimation of taro crop water status physiological indicators?

v. At which growth stages of the taro growing season can UAV remotely sensed data most accurately assess the variability in crop water status?

vi. Which combination of remotely derived UAV and non-UAV data configurations, including thermal data, multispectral bands, vegetation indices and topographic

variables, best describes the variability of taro crop water status indicators across the growing season?

vii. Can advanced optimisation techniques and deep learning models effectively predict taro crop water status indicators? How accurately can these models identify water-stressed areas using predefined stress thresholds?

1.4 Description of the study area

This study was conducted in Swayimane (29°31′ 24'' S; 30°41′ 37'' E), a rural village located within the uMshwathi Municipality, approximately 58 km northeast of Pietermaritzburg, KwaZulu-Natal, South Africa (Figure 1.1). Swayimane is located within the moist midlands mistbelt bioresource group and is characterised by a sub-humid climate, with average annual temperatures ranging from 11.8 ℃ to 24 ℃ and a mean annual temperature of 17 ℃ (Kapari *et al.* 2025). The region experiences distinct seasonal patterns of hot, wet summers and cool, dry winters with an annual rainfall ranging from 600 mm to 1100 mm that predominantly occur during summer (Cele and Mudhara 2024). Swayimane, characterised by arable clay loam soils, provides highly fertile land for agriculture, making the area well-suited for cropping and farming activities. Consequently, the local community heavily relies on the land for subsistence, with crops such as sweet potatoes, beans, maize, sugarcane, and taro being widely cultivated (Zaca *et al.* 2023). Swayimane's farming system is predominantly smallholdings, with local farmers practicing traditional farming techniques, including manual crop sowing, hand weeding, and the use of livestock manure as fertiliser. Crops grown in Swayimane are also distributed to local markets for domestic sale, therefore contributing to regional food security and sustaining local livelihoods. Despite the fertile land, Swayimane has been identified by the uMngeni Resilience Project as a high-risk area to the impacts of climate change, with projections suggesting an increase in temperatures and erratic changes in precipitation, that pose a threat to agricultural productivity and local food security (SANBI 2018; Mthethwa *et al.* 2022). These challenges have consequently positioned the area as a focal point for numerous research initiatives, including projects supported by the Water Research Commission and the Sustainable and Healthy Food Systems - Southern Africa project. These research efforts highlight the urgent need for climate-resilient strategies that build resilience of smallholder farming systems and support sustainable agricultural practices in the face of climate change.

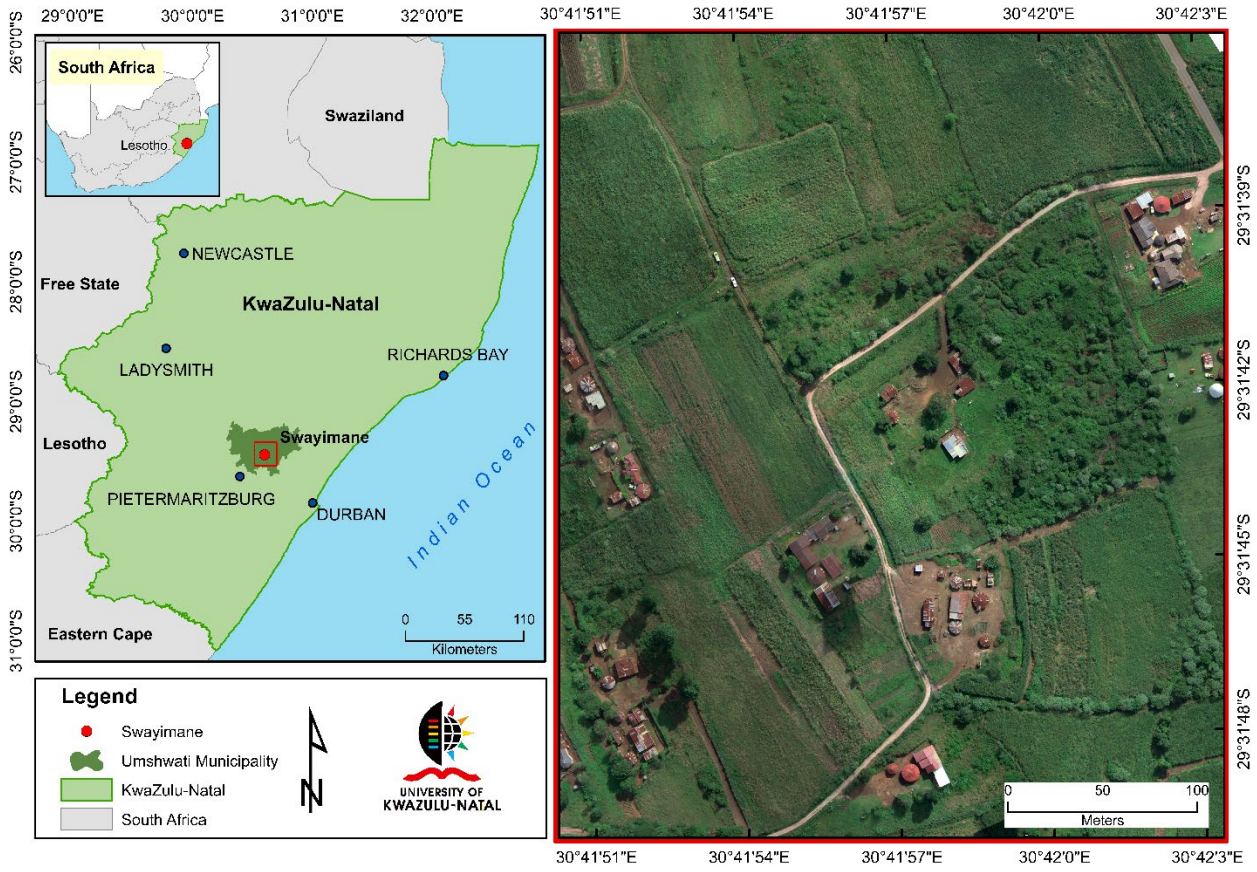

Figure 1.1 Location of the study area, Swayimane, KwaZulu-Natal, South Africa.

1.5 Structure of the dissertation

This dissertation comprises seven chapters, that include a general introduction and synthesis chapter. The structure aligns with the format requirements for a thesis by publication, with chapters two to six consisting of standalone manuscripts, each contributing to the objectives of this study. The manuscripts are structured in the traditional peer-reviewed article format, with their publication, submission, or preparation status indicated. Each manuscript starts with an introduction and concludes with a transition to the next chapter, resulting in potential commonalities and repetition of theoretical concepts. This overlap is inevitable given the concurrent development of key concepts and doctrines that underpin the current scientific understanding. Consequently, each chapter should be regarded as an independent and self-contained article, but this should not detract from the cohesive context of the thesis. A detailed outline of each chapter is presented below:

Chapter One: This introductory chapter provides an overview of the research and highlights the significance of the study. It contextualises the challenges faced by smallholder farmers in

managing crop water status, particularly in the context of climate change, and introduces the potential of UAV thermal remote sensing as a transformative tool for monitoring neglected and underutilised taro crop water variability. The chapter also outlines the study's aims, objectives, study site and the structure of the dissertation.

Chapter Two: This chapter presents a systematic literature review and in-depth assessment of the progress, challenges, and opportunities regarding the use of UAV thermal remotely sensed data in assessing and monitoring crop water status. It explores the advancements in thermal infrared sensor technologies, the diversity of crop types and farming systems studied, and the biophysical and biochemical proxies used to assess crop water status. The chapter also acknowledges the role of multispectral proximal data, optimal predictor variables and advanced modelling techniques for quantifying crop water status. Finally, this chapter synthesises trends in the literature and identifies research gaps for advancing the application of UAV thermal remote sensing in precision agriculture.

Chapter Three: This chapter focuses on evaluating the utility of UAV-acquired thermal remotely sensed data and index-based image segmentation techniques in enhancing the estimation of equivalent water thickness as a proxy of taro water status. It offers a comparative analysis of the performance of prediction models incorporating UAV thermal bands against those relying solely on multispectral data. Additionally, the chapter outlines a framework for isolating crop canopy pixels and eliminating soil background using index-based image segmentation techniques, thereby, enhancing the accuracy of smallholder taro equivalent water thickness estimations.

Chapter Four: This chapter evaluates the utility of UAV-based high-throughput crop phenotyping and the deep neural network algorithm in accurately estimating taro water status within smallholder farming systems. The study presents a snapshot of crop water status physiological indicators, including equivalent water thickness, fuel moisture content, stomatal conductance, foliar temperature and chlorophyll content during the critical vegetative growth stage, aiming to identify the most optimal indicators for quantifying crop water status using UAV remotely sensed data. Furthermore, this study highlights the combined strengths of multi-modal data by integrating thermal and multispectral imagery, enabling a comprehensive assessment of taro crop water status in smallholder farming systems.

Chapter Five: This chapter focuses on estimating stomatal conductance and foliar temperature as optimal proxies of crop water status. It leverages the integration of UAV-acquired thermal and multispectral data combined with the deep neural network algorithm to accurately predict stomatal conductance and foliar temperature across the emergence, vegetative and maturity growth stages of taro. Through a comparative analysis, the chapter identifies the most reliable growth stage for UAV-based estimations, offering valuable insights into the optimal timing for predicting these key indicators of water status using remotely sensed thermal and multispectral data.

Chapter Six: This chapter focuses on optimising the estimations of taro stomatal conductance and foliar temperature as proxies for crop water status across the emergence, vegetative and maturity growth stages of smallholder taro crops. The study evaluates the predictive performance of selected feature subsets, comprising thermal data, multispectral bands, vegetation indices and topographic variables in estimating crop water status proxies. Through the application of advanced deep learning model optimisation techniques, the study identifies optimal feature combinations for accurately predicting taro stomatal conductance and foliar temperature at each growth stage. Finally, by applying crop water stress thresholds for stomatal conductance and foliar temperature, the study establishes a framework for quantifying the area affected by water stress in smallholder taro crops. This chapter bridges the gap between UAV-based remotely sensed data and practical crop water management by refining predictive models and providing actionable insights for monitoring water stress across taro farming systems.

Chapter Seven: This chapter synthesises the findings and conclusions derived from the research objectives, offering a comprehensive summary of the key insights gained from using UAV thermal remote sensing for assessing and monitoring the crop water status of neglected and underutilised smallholder taro crops. The chapter further outlines the major implication and contribution of this research to advancing NUS precision agriculture, especially in smallholder taro farming systems, and provides actionable recommendations for future investigations.

CHAPTER TWO

A Systematic Review of the Application of UAV-Based Thermal Remote Sensing for Assessing and Monitoring Crop Water Status in Crop Farming Systems

This chapter is based on:

Ndlovu, H. S., Odindi, J., Sibanda, M., & Mutanga, O. (2024). A systematic review on the application of UAV-based thermal remote sensing for assessing and monitoring crop water status in crop farming systems. *International Journal of Remote Sensing*, 45(15), 4923-4960

Abstract

The accurate assessment and monitoring of crop water status is a critical component of precision agriculture. Over the past decade, Unmanned Aerial Vehicles (UAVs) integrated with high-resolution thermal technologies, have pioneered a new era in remote sensing, enabling the acquisition of near-real-time data essential for the efficient management of water resources within crop farming systems. With the application of UAV-based thermal sensors, a diverse array of key biophysical and biochemical indicators that serve as critical proxies for crop water status have been evaluated. Therefore, this study adopted a systematic approach to review the progress, challenges, and opportunities in utilising UAV thermal remote sensing to assess and map the water status within crop farming systems. Specifically, this study sought to explore the current state of the literature and identify existing research gaps by analysing bibliometric data and recent trends in literature. The findings showed that even though UAV thermal remote sensing hold great potential, there currently exists significant research gaps in their application for assessing and monitoring crop water status, particularly in the global south. Furthermore, the results of this study concluded that most reviewed literature focused on assessing canopy temperature, potentially resulting in the application of UAV thermal sensors in characterizing other crop water-related indicators remaining relatively underexplored in scientific research. Overall, the findings of the review highlight UAV thermal remote sensing as an innovative tool capable of providing high-resolution, robust, and near-real-time datasets for crop water status assessments, hence, revolutionising agricultural farming practices. By facilitating timely monitoring of crop water requirements, UAV thermal sensors present an opportunity to transform agricultural management strategies, optimise crop water use and ultimately enhance crop yields. This study serves as a stepping stone toward integrating UAV thermal technologies into agricultural practices and achieving robust and spatially explicit information on crop water status for the improved management of farming landscapes.

Keywords: Thermal remote sensing, drone technology, crop farming systems, water status.

2.1 Introduction

The rapidly rising global population and subsequent rise in demand for agricultural products have resulted in increased pressure on the agricultural sector to enhance crop production (Calicioglu *et al.* 2019). To achieve global food security, crop production must increase by approximately 102 % to meet the projected food demands by 2050 (Mall *et al.* 2017; Pawlak and Kołodziejczak 2020; Mugiyo *et al.* 2021b). Despite the various measures implemented to improve crop production, the changing environment has resulted in several abiotic stresses that negatively affect crop growth and yield (Kumari *et al.* 2022). Recent studies, for instance, have confirmed that climate change and variability will substantially modify weather conditions, affecting future agriculture and food systems (Calicioglu *et al.* 2019; Nhemachena *et al.* 2020; Shahzad *et al.* 2021). Specifically, the rising temperatures and declining rainfall, coupled with the increasing frequency and intensity of droughts have overwhelming impacts on crop productivity (Nhamo *et al.* 2019b; Nhemachena *et al.* 2020). Existing literature has confirmed that the effects of climate change are expected to be particularly damaging to crop production in southern Africa as this region is mainly characterised by semi-arid conditions with scarce and intermittent water resources (Rapholo and Diko Makia 2020; Sibanda *et al.* 2021a). To ensure maximum crop productivity and yield, implementing innovative and sustainable approaches to assess and monitor crop water status for early drought detection and warning systems is crucial, particularly in farming systems vulnerable to water stress.

Crop water stress is a critical abiotic factor influencing crop growth and yield (Ihuoma and Madramootoo 2017). Crop water stress is characterised by a shortage of water supply that induces physiological and biochemical changes that affect the rate of photosynthesis and the growth processes (Gerhards *et al.* 2019). Under limiting moisture conditions, crops induce stomatal closure, reducing transpiration and evaporative cooling, which increases leaf temperature (Matese *et al.* 2018a). The co-relationship between transpiration and temperature has allowed for monitoring crop water status using temperature measurements (Krishna *et al.* 2021). A variety of biochemical and biophysical crop water-related parameters, including crop temperature, stomatal conductance, soil moisture content, canopy water content and evapotranspiration, have been identified as potential indicators of crop water status (Berni *et al.* 2009a; Das *et al.* 2021b; Ndlovu *et al.* 2021b; Aboutalebi *et al.* 2022; Brewer *et al.* 2022c; Cheng *et al.* 2022). For example, canopy temperature is a widely used indicator of crop water levels, which increases when crops experience limited water availability as a result of the

reduction in evaporative cooling that occurs when leaf stomata close under stressful conditions (Perich *et al.* 2020; Han *et al.* 2021; Fukai and Mitchell 2022). Furthermore, due to the regulation of leaf stomata, stomatal conductance is another important indicator of crop water status (Pirasteh-Anosheh *et al.* 2016). When crops experience a state of water deficit, stomatal conductance reduces as stomata closure is initiated to minimise water loss through transpiration (Brewer *et al.* 2022c). While ground-based approaches and in-situ measurements of crop biophysical and biochemical characteristics are reliable, the approaches are time-consuming, laborious and costly, thus rendering them impractical for continuous and cost-effective crop monitoring (Zhang *et al.* 2019; Panday *et al.* 2020).

The evolution of earth observation technologies has proven invaluable for optimizing agricultural practices and maximizing crop production (Maes and Steppe 2012; Sishodia *et al.* 2020). As a result, crop water status monitoring has continued to benefit from the use of Earth observation data, with remote sensing approaches serving as a valuable tool for overcoming the limitations of ground-based measurements (Malbéteau *et al.* 2018a; Alexandris *et al.* 2021). Recent studies have proven that optical remote sensing techniques can be effectively utilised for the monitoring of crop water stress (El-Hendawy *et al.* 2019; Krishna *et al.* 2019; Ahmad *et al.* 2021; Yousaf *et al.* 2021). For example, El-Hendawy *et al.* (2019) confirmed that various regions along the electromagnetic spectrum act as indirect indicators of water stress, enabling the quantification of crop water status based on leaf biochemical attributes. The visible (blue, green, red (RGB)), near-infrared (NIR) and short-wave-infrared (SWIR) wavelengths have particularly exhibited potential in monitoring crop water due to their water absorption characteristics related to leaf pigmentation (Wijewardana *et al.* 2019). Nonetheless, a critical limitation of optical sensors is their inability to directly assess crop water deficit and sufficiently characterise the biochemical and biophysical characteristics of crop water status (Ishimwe *et al.* 2014; Li *et al.* 2022a).

Thermal infrared remote sensing systems have become a promising tool for crop water assessment and monitoring, providing a direct correlation with crop water biophysical and biochemical elements (Khanal *et al.* 2017; Messina and Modica 2020; Krishna *et al.* 2021). The application of thermal remote sensing lies in the fact that the thermal properties of crop leaves are influenced by the rate of transpiration, which in a state of water deficit, decreases and subsequently increases leaf and canopy temperature (Liu *et al.* 2020; Messina and Modica 2020). Monitoring the thermal signals of crops using remote sensing approaches allows

agricultural practitioners and researchers to promptly identify areas of water stress and adopt relevant corrective measures to maintain optimal crop health (Gerhards *et al.* 2019). Therefore, the application of thermal remote sensing for assessing and monitoring crop water status is invaluable in modern agriculture and has proven to be an effective tool for crop management (Krishna *et al.* 2021).

Thermal imaging applications in crop water status monitoring have gained popularity over the decades due to improvements in sensor technology and cost reduction (Ishimwe *et al.* 2014; Messina and Modica 2020). Various satellite-based thermal sensors have been used to assess and monitor crop water status, including Landsat Thematic Mapper (TM), moderate-resolution imaging Spectroradiometer (MODIS), Ecosystem Spaceborne Thermal Radiometer Experiment on Space Station (ECOSTRESS) and Visible Infrared Imaging Radiometer Suite (VIIRS) (Malbéteau *et al.* 2018a; Gerhards *et al.* 2019; Masina *et al.* 2020; Xue *et al.* 2020b). However, these datasets are constrained by their coarse spatial and low temporal resolutions, limiting their use for rapid crop water stress detection and monitoring at farm-scale (Berni *et al.* 2009a; Malbéteau *et al.* 2018a; Alexandris *et al.* 2021).

Recently, sensors mounted on unmanned aerial vehicle (UAV) platforms have become invaluable for precision agriculture research, offering ultra-high spatial and temporal resolutions (Hoffmann *et al.* 2016a). In contrast to satellites, UAVs offer near-real-time, high resolution datasets on demand and over a range of atmospheric conditions (Malbéteau *et al.* 2018a; Zhu *et al.* 2021b). UAVs, integrated with very-high resolution Thermal Infrared Sensors (TIRS) offer a robust solution for retrieving temperature measurements of crop canopy for the accurate quantification of crop water status at a field scale (Berni *et al.* 2009a). Research findings have shown that phenological metrics, developed from high resolution drone imagery obtained from thermal sensors, offer near-real-time spectral information to detect changes in biophysical and biochemical crop properties such as foliar temperature, stomatal conductance and canopy water content (Brewer *et al.* 2022c). Despite such synergies, UAV thermal remote sensing has remained underexploited for high-throughput phenotyping and crop water monitoring (Han *et al.* 2020).

Whereas previous studies have reviewed literature on crop water status (Ishimwe *et al.* 2014; Gago *et al.* 2015; Gerhards *et al.* 2019; Virnodkar *et al.* 2020; Ahmad *et al.* 2021; Zhou *et al.* 2021; Awais *et al.* 2022a), it is important to acknowledge that these works have laid essential groundwork in understanding crop water relations and UAV applications. Most of

these studies, however, have not specifically focused on the systematic adoption and bibliometric evaluation of UAV thermal remote sensing to assess crop biophysical and biochemical indicators related to water status. Some studies, including Gago *et al.* (2015) and Awais *et al.* (2022a), have meaningfully explored both the challenges and potential benefits of UAV thermal imaging in detecting water stress and monitoring crop water status. Nevertheless, these investigations primarily addressed the detection of water stress and crop health monitoring without conducting a bibliometric synthesis or comprehensive review of UAV thermal sensing studies in this context. In this regard, this review aims to fill this knowledge gap by conducting a comprehensive and systematic evaluation of the progress, challenges, and opportunities presented in the literature on the application of UAV thermal remote sensing in assessing and monitoring crop water status. The review seeks to further explore literature on the advancements in TIRS, the crop types and farm settings, and the trend in biophysical and biochemical proxies of crop water status. By understanding these aspects, this review will provide valuable insights into the contribution of UAV thermal imaging to precision agriculture and identify gaps in literature that require further enquiry to enhance the body of knowledge on UAV thermal approaches for crop water assessment.

2.2 Materials and Methods

This study followed the Preferred Reporting Items for Systematic Reviews and Meta-Analyses (PRISMA) in systematically identifying peer-reviewed articles that published original research on the assessment and monitoring of crop water status using thermal proximal sensing approaches. To achieve this objective, the review was organised into two sections. The first section aimed to assess the up-to-date progress of the application of thermal remote sensing in mapping and monitoring the crop water status of agricultural crops. This section will report on the physiological and biochemical parameters, sensor characteristics, sensor platforms and approaches developed and implemented within this research space. The second section highlights the challenges and opportunities for applying thermal remote sensing in assessing and monitoring crop water status within agricultural cropping systems. The detailed literature search and analysis were conducted in three phases which are *i*) literature search and screening, *ii*) data extraction, and *iii*) data analysis.

2.2.1 Literature search and screening

A preliminary search of relevant articles was conducted to identify literature that could assist in formulating key search terms. The title and objective of these articles were particularly considered in compiling a comprehensive list of keywords, terms, and phrases for the search strings. The preliminary literature search was conducted in Google Scholar due to its broader coverage compared to existing search platforms. Specifically, 15 highly cited and relevant articles were selected and thoroughly reviewed to extract pertinent keywords and search terms. The following keywords and their variants were identified: "Thermal remote sensing" OR "Infrared thermography" OR "Thermal Imaging" AND "Remote sensing" OR "Spectroscopy" OR "Spectrometry" OR "Earth observation" OR "Satellite" OR "Geographic information systems" OR "GIS" OR "Unmanned aerial vehicles" OR "UAV" AND "Crop" OR "Agriculture" AND "Water stress" OR "Water status" OR "Water deficit" OR "Water content" OR "Moisture stress" OR "Moisture status" OR "Moisture deficit" OR "Moisture content" OR "Stomatal conductance" OR "Temperature" OR "Canopy temperature" OR "Leaf temperature". The query strings employed across the various databases are outlined in Table 2.1. The searches were confined to titles, abstracts, and keywords.

Table 2.1 Key terms used in the literature search.

Search Platform	Search Criterion	Articles Retrieved
SCOPUS	(TITLE-ABS-KEY (thermal AND remote AND sensing) OR TITLE-ABS-KEY (infrared AND thermography) OR TITLE-ABS-KEY (thermal AND imaging) AND TITLE-ABS-KEY (remote AND sensing) OR TITLE-ABS-KEY (spectroscopy) OR TITLE-ABS-KEY (spectrometry) OR TITLE-ABS-KEY (earth AND observation) OR TITLE-ABS-KEY (satellite) OR TITLE-ABS-KEY (geographic AND information AND systems) OR TITLE-ABS-KEY (unmanned AND aerial AND vehicles) OR TITLE-ABS-KEY (GIS) AND TITLE-ABS-KEY (UAV) AND TITLE-ABS-KEY (crop) OR TITLE-ABS-KEY (agriculture) AND TITLE-ABS-KEY (water AND stress) OR TITLE-ABS-KEY (water AND deficit) OR TITLE-ABS-KEY (water AND content) OR TITLE-ABS-KEY (moisture AND stress) OR TITLE-ABS-KEY (moisture AND status) OR TITLE-ABS-KEY (water AND status) OR TITLE-ABS-KEY (	165

	moisture AND deficit) OR TITLE-ABS-KEY (moisture AND content) OR TITLE-ABS-KEY (temperature) OR TITLE-ABS-KEY (canopy AND temperature) OR TITLE-ABS-KEY (leaf AND temperature))	
Web of Science	((((((((((((((((((((((((TI=(Thermal remote sensing)) OR TI=(Thermal Imaging)) OR TI=(Infrared thermography)) AND TI=(Remote sensing)) OR TI=(Spectroscopy)) OR TI=(Spectrometry)) OR TI=(Earth observation)) OR TI=(Satellite*)) OR TI=(Geographic information systems)) OR TI=(Unmanned aerial vehicles)) OR TI=(GIS)) OR TI=(UAV)) AND TI=(Crop*)) OR TI=(Agricultur*)) AND TI=(Water stress)) OR TI=(Water status)) OR TI=(Water deficit)) OR TI=(Water content)) OR TI=(Moisture stress)) OR TI=(Moisture status)) OR TI=(Moisture deficit)) OR TI=(Moisture content)) OR TI=(Stomatal conductance)) OR TI=(Temperature)) OR TI=(Canopy temperature)) OR TI=(Leaf temperature) and 4.169 Remote Sensing (Citation Topics Meso)	443
Science Direct	((“Thermal”) AND (“remote sensing” OR “GIS” OR “UAV”) AND (“Crop”) AND (“Water stress” OR “Water status” OR “Water deficit” OR “Water content”))	87

The identified keywords were input into SCOPUS, Science Direct, and the Web of Science databases to construct the applicable literature database. Where full-text access to certain articles was restricted on these platforms, Google Scholar was used to locate and retrieve those articles. The literature search was accomplished without applying any constraints on the timespan. The number of studies identified, included, or excluded were documented in alignment with the PRISMA procedure (Figure 2.1) as described by Page *et al.* (2021). Articles deemed eligible for inclusion in the meta-analysis had to satisfy the following criteria: a) the study focuses exclusively on the application of thermal remote sensing in monitoring crop water status, b) the study uses UAV proximal remote sensing techniques in crop water

monitoring and assessment, c) the full text of the publication is available, d) the published article is in an accredited journal and e) the article is written in English.

Initially, the literature search as well as title screening in SCOPUS, Science Direct, and the Web of Science retrieved 167, 85 and 440 articles, respectively. No date restrictions were applied during the search, allowing for the comprehensive retrieval of literature at all available years up to the time of data collection in July 2023. All retrieved literature and its respective bibliographic information were exported to EndNote for further screening. Firstly, duplicate articles and literature not written in English were excluded. Subsequently, the descriptive information (title, abstract and journal) of the remaining articles were examined to verify that the studies employed UAV-derived thermal remote sensing techniques for crop water monitoring. Following this, a more detailed full-text screening was conducted to refine the selection. At this stage, an exclusion criterion was applied to exclude a) review articles, b) articles that employed UAV platforms but did not utilize thermal imagery, c) studies that used satellite-based or ground-based sensors only, without UAV integration, d) studies that focused on non-agricultural applications (e.g., forestry, urban heat mapping); and e) studies that were based on non-crop vegetation types (e.g., grasslands, natural vegetation, or mixed-use systems not specific to crop farming). Lastly, only accessible full-length articles that exclusively investigated UAV-acquired thermal imagery for crop-based water status monitoring were included for detailed analysis. Following the screening process, 85 articles were retained. The detailed information for each article was then captured in a Microsoft Excel spreadsheet and used for further assessment.

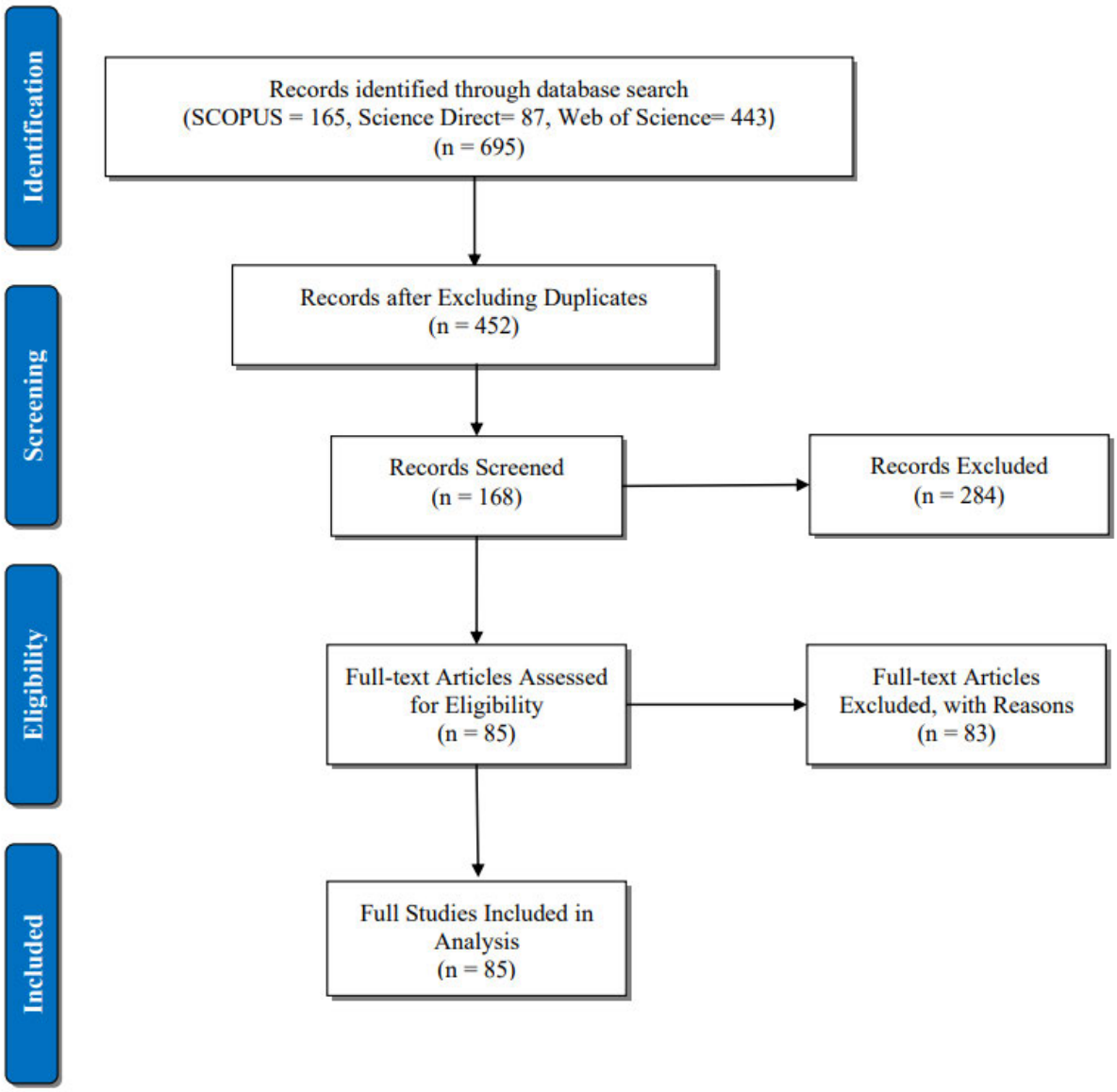

Figure 2.1 Topical concepts in mapping and monitoring crop water status derived from data extracted from titles, abstracts, and keywords.

2.2.2 *Data extraction*

In this phase, qualitative data were extracted. The data extracted included bibliographic information, including author name, publication year, article title, country, continent, journal name, keywords, abstract Digital Object Identifier (DOI), and Uniform Resource Locator (URL). Additionally, information on the crop type, spatial extent of the study, sensor attributes, biophysical or biochemical parameters, prediction algorithms and vegetation indices investigated were extracted from the articles. The categorical variables were subsequently transformed into numerical variables in preparation for the data analysis.

2.2.3 Data analysis

The extracted information was subjected to quantitative and qualitative analytical approaches. In relation to quantitative assessments, basic statistical frequencies and trend analysis were performed using Microsoft Excel. Subsequently, bibliometric analysis, a widely utilised meta-analytical tool for quantitatively assessing the co-occurrence and frequency of terms in the retrieved literature, was conducted. (Moral-Muñoz *et al.* 2020). Specifically, VOSviewer, a freely available bibliometric software (Van Eck and Waltman 2010; Orduña-Malea and Costas 2021), was employed to assess the occurrence and co-occurrence of terms and their linkages from literature that monitored crop water status through thermal remote sensing approaches. The titles, abstracts, and keywords of the retrieved articles were utilised as input data in VOSviewer to assess the occurrence and linkages of key terms within the research space. To ensure that the analysis of retrieved literature was not biased, the PRISMA checklist and procedure were adhered to for guidance (Page *et al.* 2021).

To address the research objectives, this review is subsequently presented in two sections. The initial section investigated the advancements made in the application of UAV-based thermal remote sensing for mapping and monitoring agricultural crop water status. This section of the review highlights literature search characteristics, biophysical and biochemical proxies of crop water status, trends in the distribution of studies and thermal remote sensing technologies applied within crop water monitoring research. The second section summarise and review the challenges, gaps, and opportunities in the context of knowledge creation in assessing and monitoring the water status of agricultural crops using thermal remotely sensed data.

2.3 Results

2.3.1 The literature characteristics

In analysing the characteristics of retrieved literature, a network map categorised the identified key terms from literature into three clusters as illustrated in Figure 2.2. The key terms in the red cluster were ‘precision agriculture’, ‘crop water stress’, ‘evapotranspiration’, ‘estimation’, ‘thermal image’, and ‘land surface temperature’. This cluster articulates the ability of thermal imagery in monitoring crop water status proxies such as evapotranspiration and temperature. The inclusion of the term’s ‘accuracy’, ‘rmse’, ‘performance’, ‘spatial resolution’, ‘machine’

and ‘model’ in this cluster suggest the accuracy and performance of machine learning techniques in estimating crop water biophysical and biochemical parameters at high spatial resolutions associated with UAV-derived thermal remote sensing. The second cluster (green) included key terms such as ‘Normalised Difference Vegetation Index (NDVI)’, ‘plant’, ‘vegetation index’, and ‘research’. This relates to the influence of vegetation indices within research, especially the use of the NDVI in estimating and monitoring crop water status. Lastly, the blue cluster contained key terms such as ‘Crop Water Stress Index (CWSI)’, ‘stomatal conductance’, ‘indicator’, and ‘determination’, which relate to the usage of the CWSI and stomatal conductance as a proxy for determining the water status and stress in cropping systems. The inclusion of the terms ‘plant’, ‘water status’, ‘thermal imagery’, and ‘camera’ in this cluster suggest the utility of UAV-derived thermal imagery as a high-resolution proximal sensing system for mapping water status of cropping systems (Figure 2.2).

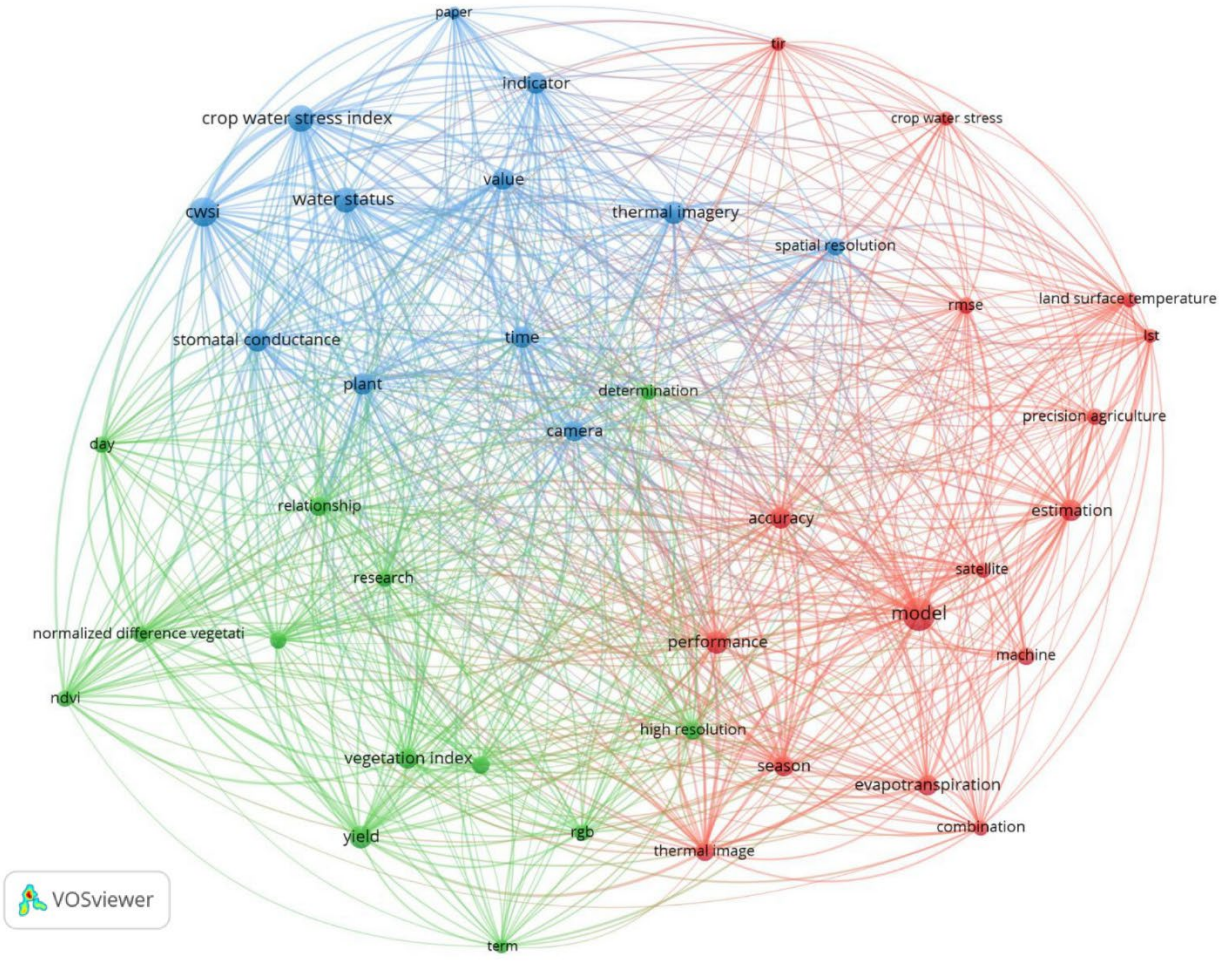

Figure 2.2 Topical concepts in mapping and monitoring crop water status derived from data extracted from titles, abstracts, and keywords.

2.3.2 The progress in the use of thermal remote sensing approaches in assessing and monitoring crop water status

2.3.2.1 Publication trends and geographic distribution

As aforementioned, over the recent decade, there has been a major focus on the utility of UAV-derived thermal remote sensing data for assessing and monitoring crop water status. This is evident in the growing number of studies that have employed thermal proximal sensing techniques for monitoring water status within cropping systems (Figure 2.3). The earliest publication within this field was reported in 2007. Between 2007 and 2017, a fluctuation in publications is observed, followed by a steady increase in studies between 2018 and 2022 (Figure 2.3).

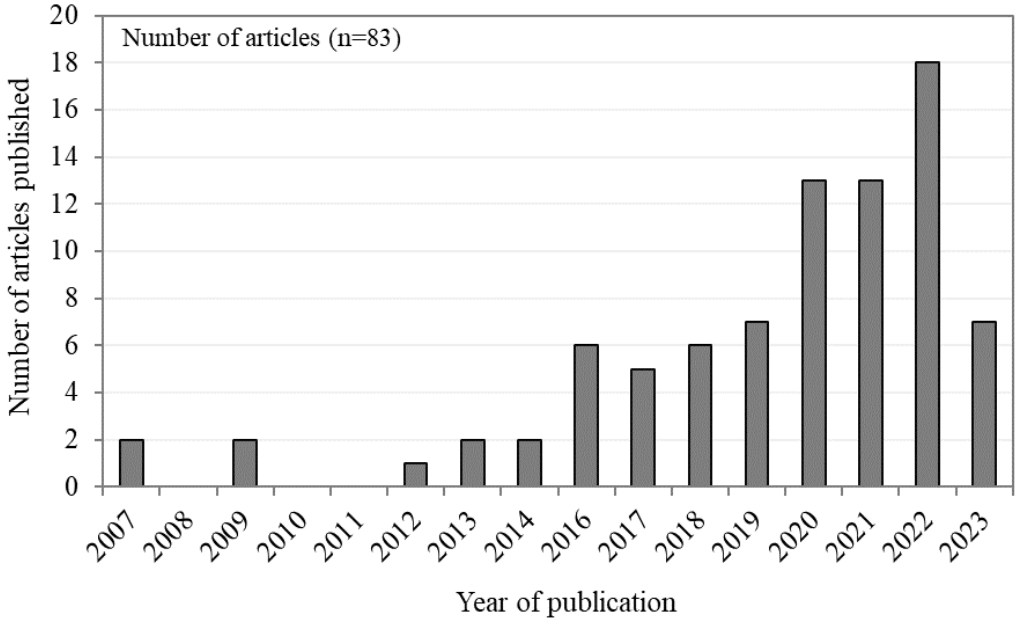

Figure 2.3 Frequency of studies published on UAV-derived thermal remote sensing applications in crop water monitoring.

Figure 2.4 illustrates the geographic distribution of studies considered in the meta-analysis. Publications of studies focusing on thermal proximal sensing approaches in assessing crop water status are distributed unevenly across 20 countries and mainly concentrated in the global north. The top three countries with the highest proportions of publications are the United States of America (USA), China and Spain, with a total of 24%, 16% and 15% articles, respectively. In reviewing the frequency of studies published, it was observed that publications on UAV-derived thermal remote sensing applications in crop water monitoring were conducted

across all continents, except Antarctica (Figure 2.4). The geographic distribution of published articles showed considerable gaps, especially in South America and several regions in Africa. Surprisingly, only 7 out of 85 studies on crop water status monitoring using thermal remote sensing approaches were conducted in the global south, with only 3.5% of studies published in Africa. Subsequently, there is a critical need to consider and prioritise research efforts to assess crop water parameters and machine learning techniques in monitoring water stress within cropping systems, especially in developing countries with pre-existing challenges of food insecurity.

Figure 2.4 Global distribution of studies (2007-2023) that used UAV-derived thermal remote sensing to assess and monitor crop water status.

2.3.2.2 Crop types and farming systems

Results of this study showed that 24 different crop types were mentioned in the retrieved literature (Table 2.2). Maize (24.7%), grapes (23.5%), wheat (11.8%) and soybean (10.6 %) were identified as the most widely researched crops within studies that focus on drone-based thermal applications for crop water monitoring. Only two crop types, sorghum and the African eggplant, are categorised as neglected and underutilised crop species, with a frequency of just three studies (Sagan *et al.* 2019b; Mwinuka *et al.* 2021b; Li *et al.* 2022b). Furthermore, results showed that 85.8% of reviewed studies were conducted within commercial farms, while only 2.3% of research focused on smallholder farming systems. Similarly, majority of the reviewed studies were conducted on irrigated croplands (54.1%), while only 9.41% of studies focused

on rainfed cropping systems. These findings highlight a concentration of studies on UAV-thermal mapping and monitoring of crop water status in irrigated commercial systems that primarily cultivate maize, grapes (vineyards) and wheat crops.

Table 2.2 Summary of crops identified in the reviewed literature.

Crop Type	Crop Name (Frequency)
Cereal Crops	Maize (21), Wheat (10), Barley (3), Sorghum (2)
Beverage and Spice Crops	Tea (3)
Oilseed Crops	Soybean (9), Olive (5)
Fibre Crops	Cotton (4)
Leguminous Crops	Dry bean (1)
Root/tuber Crops	Potato (3), African eggplant (1)
Sugar Crops	Sugar Beet (4)
Fruits and nuts - Subcategory: Grapes	Grapes (19)
Fruits and nuts - Subcategory: Berries	Pomegranate (2), Kiwi (1)
Fruits and nuts - Subcategory: Nuts	Almond (1), Pecan (1)
Fruits and nuts - Subcategory: Pome and stone fruits	Apple (1), Apricot (1), Peach (1)
Fruits and nuts - Subcategory: Citrus fruits	Nectarine (3), Orange (2), Lemon (1), Mandarin (1)

2.3.2.3 Biophysical and biochemical proxies of crop water status

Results of this study showed that 19 crop water indicator variables were mentioned in the retrieved literature (Figure 2.5). The widely studied crop water indicators were canopy temperature (Chen *et al.* 2019; Chakraborty *et al.* 2020; Han *et al.* 2021), CWSI (Poblete *et al.* 2018; Lee and Park 2019; Pádua *et al.* 2022), stomatal conductance (Sullivan *et al.* 2007; Berni *et al.* 2009a; Marques *et al.* 2020; Sobejano-Paz *et al.* 2020; Brewer *et al.* 2022c), soil moisture content (Sobejano-Paz *et al.* 2020; Zhang *et al.* 2023b), evapotranspiration (Hoffmann *et al.* 2016c; Shao *et al.* 2023), stem water potential (Matese *et al.* 2018b; Caruso *et al.* 2022) and leaf temperature (Han *et al.* 2021), with a frequency of more than 10 studies (Figure 2.5).

Various studies, for instance Xue *et al.* (2020b) and Awais *et al.* (2022b) explored the utility of canopy and leaf temperature in characterising crop water status of tea, maize, winter wheat, barley and grape fields, respectively. Furthermore, the findings illustrated that 32 studies explored the capabilities of the CWSI for assessing crop water (Park *et al.* 2017;

Alexandris *et al.* 2021; Ekinzog *et al.* 2022). In addition, 27 studies, including Brewer *et al.* (2022c) and Maimaitiyiming *et al.* (2020b), investigated the use of stomatal conductance as an indicator of crop water status. Results also showed that studies explored the utility of soil moisture content (n = 24) (Acorsi and Gimenez 2021; Li *et al.* 2022e) and evapotranspiration (n = 15) in crop water status monitoring (Chávez *et al.* 2018; Aboutalebi *et al.* 2022).

Results further illustrated that nine studies focused on chlorophyll content and four studies on leaf chlorophyll fluorescence as proxies of crop water status (Li *et al.* 2022a; Wang *et al.* 2022b). A study by Berni *et al.* (2009b) estimated chlorophyll content of commercially cultivated peach, maize and olive orchards using drone-based thermal and multispectral imagery, while Wang *et al.* (2022b) explored the potential of chlorophyll fluorescence in the detection of water stress within a sugar beet field. Studies also explored the utility of stem water potential (n = 13) (Matese *et al.* 2018b; Caruso *et al.* 2022) and leaf water potential (n = 6) (Berni *et al.* 2009a; Alimonti *et al.* 2020; Marques *et al.* 2020) in crop water status monitoring. Meanwhile, other studies explored leaf gas exchange, transpiration and photosynthesis and soil temperature in conjunction with other crop water indicators (Sobejano-Paz *et al.* 2020; Hou *et al.* 2021). Lastly, 14 studies investigated other crop water indicators, including equivalent water thickness, canopy water content, gravimetric water content, relative water content and dry matter content (Ndlovu *et al.* 2021b; Zhu *et al.* 2021b; Das *et al.* 2022). Li *et al.* (2022a) explored the combination of thermal, multispectral and LiDAR datasets to predict chlorophyll content and canopy water content of Tea (*Camellia sinensis (L.) O. Kuntze*), while Marques *et al.* (2020) investigated relative water content together with stomatal conductance, canopy temperature and leaf water potential of olive orchards.

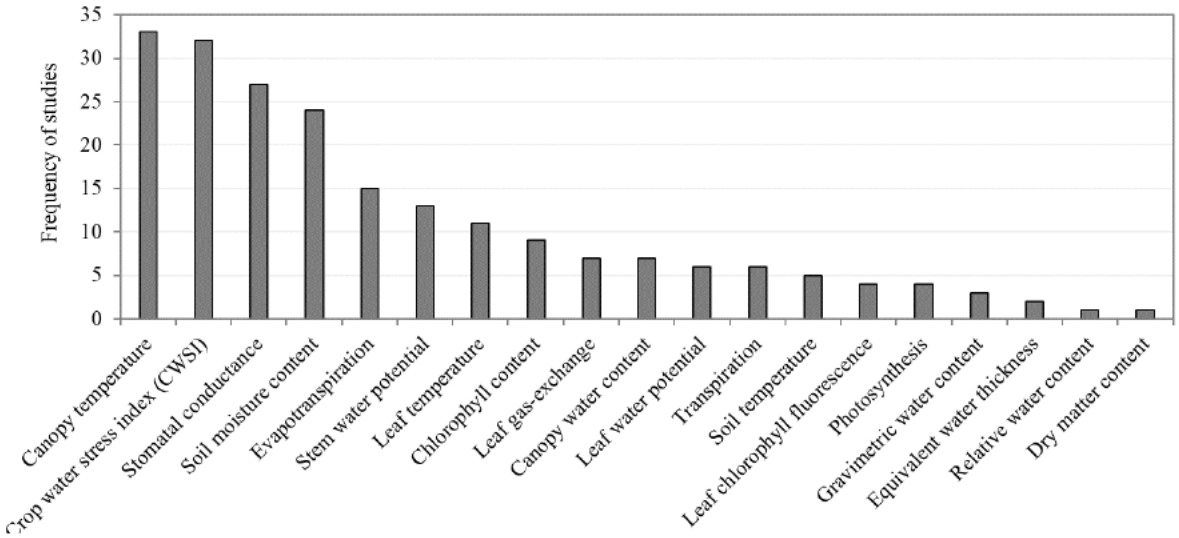

Figure 2.5 Frequency of crop water indicator variables identified in the reviewed literature.

2.3.2.4 UAV-based thermal remote sensing platforms

Results showed that the majority of studies (approximately 73%) on crop water status monitoring using drone-based thermal imagery were conducted using multi-copter systems, while only 15.7% used fixed-wing platforms. Similarly, the findings illustrated that 79.6% of studies acquired multispectral imagery through multi-copter platforms. The dominance of multi-copter platforms in crop water assessments in comparison to fixed-wing platforms is attributable to the fact that fixed-wing systems are relatively more expensive, do not have hovering capabilities and have a higher flight altitude that reduces image resolution (Gago *et al.* 2015). Additionally, fixed-wing platforms lack the capacity for Vertical Take-off and Landing (VTOL) and are limited by the inability to hover over areas of interest (Sibanda *et al.* 2021a). Surprisingly, even though quadcopters were the most dominant platform, it is evident that innovative hexacopters and octocopters have been extensively employed for assessing crop water status using both thermal and multispectral datasets (Santesteban *et al.* 2017b; Perich *et al.* 2020; Shao *et al.* 2023).

Figure 2.6 illustrates the frequency of each drone platform used in mapping crop water status using thermal and multispectral images. The DJI Matrice 600 Pro, Mikrokopter ARF Okto XL 6S12, DJI Spreading Wings S1000+ Professional and the DJI Matrice 600 are the most frequently used drone platforms in crop water assessment studies (Figure 2.6). It is also worth noting that DJI-manufactured UAV platforms are popular in studies using both thermal and multispectral imaging. The findings of this study showed that more than 50% of thermal and multispectral imagery (i.e., 50.5% and 62.9% respectively) have been acquired using UAV platforms manufactured by the Chinese company, Shenzhen DJI Sciences and Technologies Ltd. DJI-manufactured drone systems are equipped with advanced technology that enhances their capabilities for thermal and multispectral imaging, including their compatibility with a variety of sensors and specialised software for data analysis. Furthermore, the majority of DJI drone platforms possess VTOL capabilities and have established a benchmark for user-friendly interface and effortless controls, ensuring that even users with limited drone knowledge can easily operate and access advanced features.

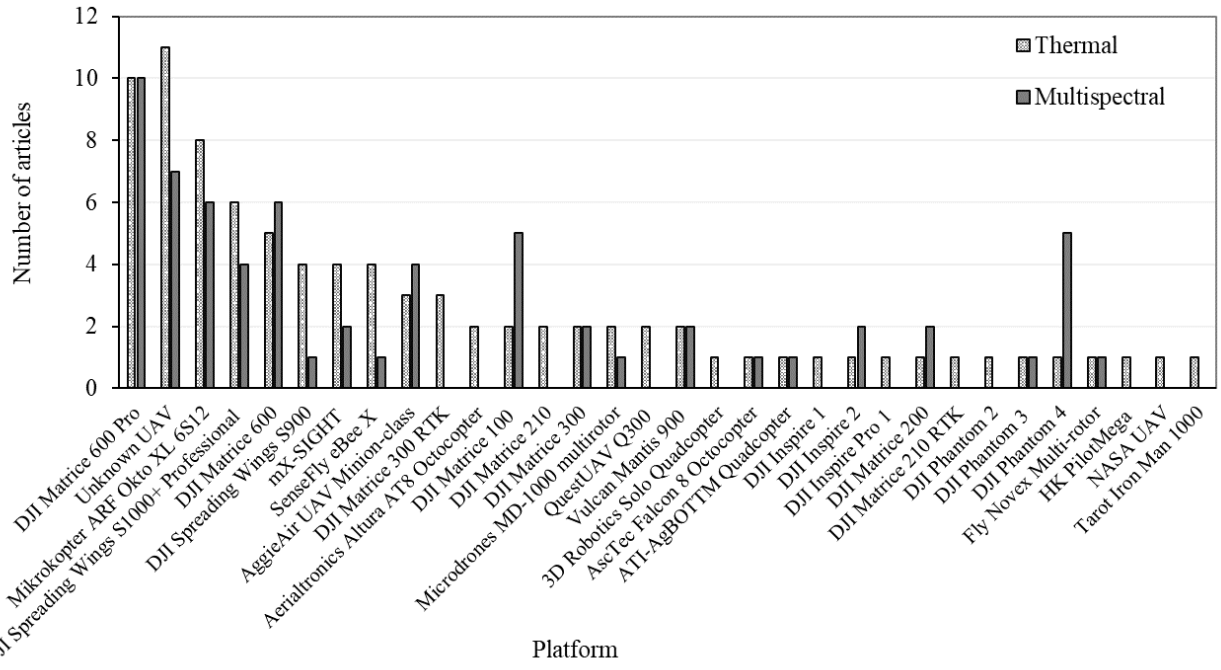

Figure 2.6 UAV platform types and platforms used in thermal and multispectral applications of crop water status monitoring.

2.3.2.5 Thermal sensor technologies and spectral settings

There has been a considerable increase in the use of thermal sensors for the remote quantification of crop water status, with 24 drone-based sensors noted in the literature reviewed (Table 2.3). The results of this review revealed that the FLIR Tau 2 thermal sensor (red cluster) was the most frequently employed (22.7%), followed by the FLIR Vue Pro R 640 (13.6%), DJI Zenmuse-XT2 (6.8%) and FLIR A65 (6.8%). The results of this study further illustrated that the application of drone-based thermal sensors in crop water assessments started trending in the early 2000s (Figure 2.7). Thermal-Eye X-50 and FLIR ThermaCam P40 were the first thermal sensors introduced in 2007 for crop water monitoring using UAV technology. In 2016, a greater variety of sensors such as FLIR A65, Micasense Altum, SenseFly ThermoMAP, ICI 8640 P-Series and DJI Zenmuse-XT were recorded (Figure 2.7). The findings also illustrated that FLIR Tau 2 began trending in literature in 2014 and FLIR Vue Pro R 640 in 2019 (Figure 2.7). Generally, there is also a high popularity of FLIR-manufactured thermal sensors (55.7%) within the reviewed studies that focused on crop water status monitoring.

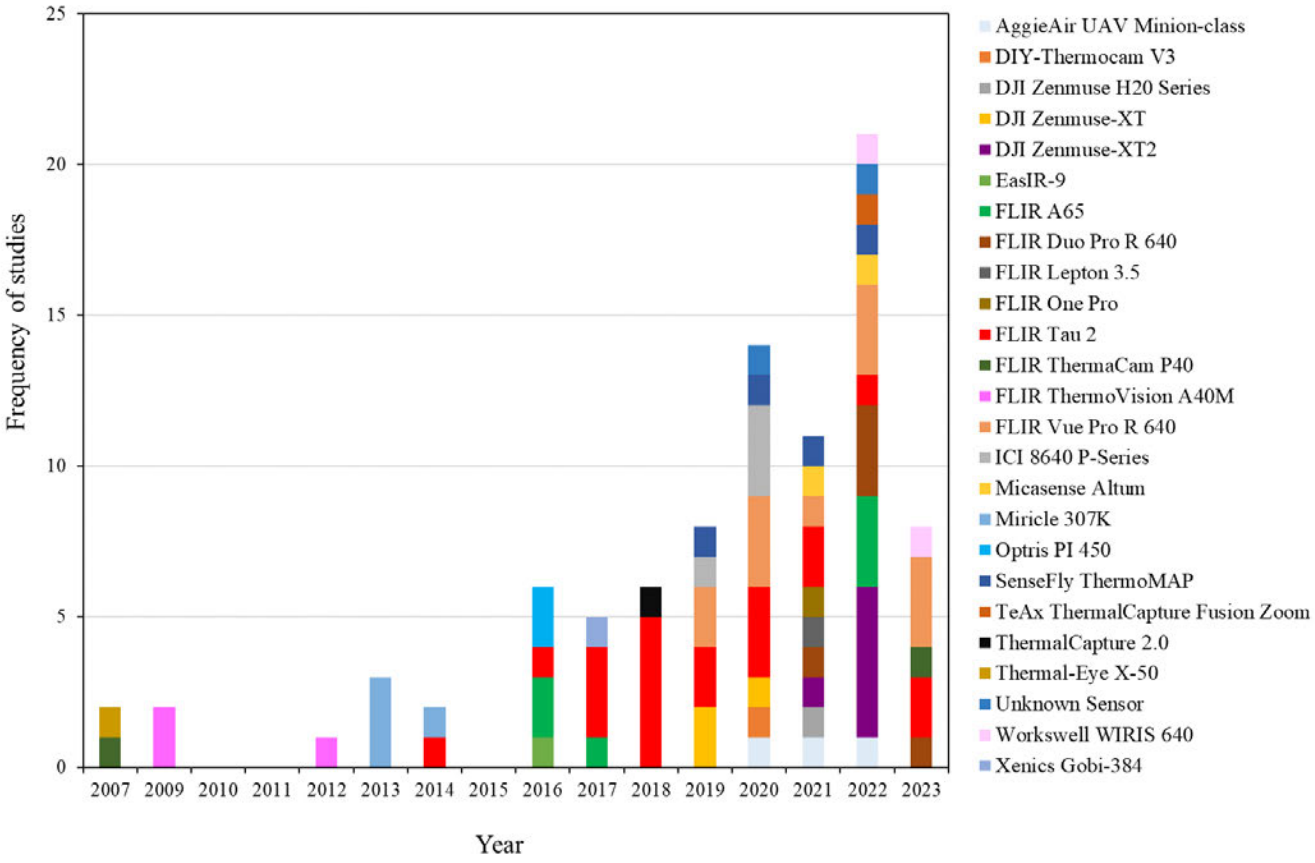

Figure 2.7 Progression of drone-based thermal sensors used in assessing and monitoring crop water status between 2007 and 2023.

Table 2.3 Summary of thermal sensors and platforms used in assessing and monitoring crop water status between 2007 and 2023.

Sensor Name	Frequency (n)	Onboarded UAV	Pixel Resolution	Spectral Range (µm)	Reference
FLIR Tau 2	20	ATI-AgBOTTM; DJI Spreading Wings S900; DJI Matrice 100; DJI Matrice 600; DJI Phantom 2; Mikrokopter ARF Okto XL 6S12; Microdrones MD-1000 multirotor; AscTec Falcon 8; DJI Inspire Pro 1	640 × 512	7.5 -13.5	(Espinoza *et al.* 2017; Martínez *et al.* 2017; Chávez *et al.* 2018; Matese and Di Gennaro 2018; Poblete *et al.* 2018; Chakraborty *et al.* 2020; Sobejano-Paz *et al.* 2020)
FLIR Vue Pro R 640	12	Fly Novex Multi-rotor; DJI Matrice 600 Pro; DJI Phantom 3; 3D Robotics Solo Quadcopter; DJI Inspire 2; DJI Spreading Wings S1000+ Professional; DJI Matrice 600; DJI Spreading Wings S900	640 × 512	7.5 -13.5	(Alimonti *et al.* 2020; Perich *et al.* 2020; Han *et al.* 2021; Lacerda *et al.* 2022; Zhang *et al.* 2022)
DJI Zenmuse-XT2	6	DJI Matrice 200; DJI Matrice 210; DJI Matrice 300 RTK; DJI Matrice 210 RTK	640 × 512	7.5-13.5	(Alexandris *et al.* 2021; Araújo-Paredes *et al.* 2022; Awais *et al.* 2022b; Li *et al.* 2022e)
FLIR A65	6	Vulcan Mantis 900; DJI Matrice 600 Pro; DJI Spreading Wings S900; DJI Spreading Wings S1000+ Professional	640 × 512	7.5-13.5	(Katsigiannis *et al.* 2016; Park *et al.* 2017; Park *et al.* 2021a; Lu *et al.* 2022a)
FLIR Duo Pro R 640	5	DJI Matrice 600; DJI Spreading Wings S1000+ Professional; DJI Matrice 600 Pro	640 × 512	7.5-13.5	(Hou *et al.* 2021; Maguire *et al.* 2021; Caruso *et al.* 2022; Cheng *et al.* 2023)

Sensor Name	Frequency (n)	Onboarded UAV	Pixel Resolution	Spectral Range (µm)	Reference
ICI 8640 P-Series	4	DJI Matrice 600 Pro; DJI Spreading Wings S1000+ Professional; DJI Matrice 300; mX-SIGHT	640 × 512	7.5 -13.5	(Sagan *et al.* 2019b; Maimaitiyiming *et al.* 2020b; Zhou *et al.* 2020)
Miricle 307K	4	mX-SIGHT	640 × 480	8.0 –12.0	(Calderón *et al.* 2013; Gonzalez-Dugo *et al.* 2013; Gonzalez-Dugo *et al.* 2014)
SenseFly ThermoMAP	4	SenseFly eBee X	640 × 512	7.5 -13.5	(Sagan *et al.* 2019b; Zhu *et al.* 2021b; Pádua *et al.* 2022)
AggieAir UAV Minion-class	3	AggieAir UAV Minion-class	not specified	8.0 –14.0	(Nieto *et al.* 2019; Aboutalebi *et al.* 2022)
DJI Zenmuse-XT	3	DJI Matrice 600; DJI Inspire 1; DJI Matrice 210	640 × 512	7.5 -13.5	(Bian *et al.* 2019; Chen *et al.* 2019; Masina *et al.* 2020)
FLIR ThermoVision A40M	3	Unknown UAV	320 × 240	7.5 -13.5	(Berni *et al.* 2009a; Berni *et al.* 2009b; Baluja *et al.* 2012b)
Micasense Altum	2	DJI Matrice 300	160 × 120	8.0 –14.0	(Ndlovu *et al.* 2021b; Brewer *et al.* 2022c)
Optris PI 450	2	QuestUAV Q300	382 × 288	7.5 -13.5	(Hoffmann *et al.* 2016a; Hoffmann *et al.* 2016c)
Workswell WIRIS 640	2	Aerialtronics Altura AT8 Octocopter	640 × 512	7.5 -13.5	(Wang *et al.* 2022b; Wang *et al.* 2023)

Sensor Name	Frequency (n)	Onboarded UAV	Pixel Resolution	Spectral Range (µm)	Reference
Unknown Sensor	2	Unknown UAV; unspecified DJI-manufactured UAV	not specified	not specified	(Bhatti *et al.* 2020; Mokari *et al.* 2022)
DIY-Thermocam V3	1	Tarot Iron Man 1000	160 ×120	7.5 -13.5	(Crusiol *et al.* 2020a)
DJI Zenmuse H20 Series	1	DJI Matrice 300 RTK	640 × 512	8.0 –14.0	(Awais *et al.* 2021)
EasIR-9	1	HK PilotMega	384 × 288	8.0 –14.0	(Sepúlveda-Reyes *et al.* 2016)
FLIR Lepton 3.5	1	DJI Phantom 4	160 × 120	8.0 –14.0	(Acorsi and Gimenez 2021)
FLIR One Pro	1	Unknown UAV	240 × 320	8.0 –14.0	(Mwinuka *et al.* 2021b)
FLIR ThermaCam P40	1	Unknown UAV	320 x 240	7.5 -13.5	(Tilling *et al.* 2007)
TeAx ThermalCapture Fusion Zoom	1	Unknown UAV	640 × 512	7.5 -13.5	(Ekinzog *et al.* 2022)
ThermalCapture 2.0	1	DJI Matrice 100	640 × 512	7.5 -13.5	(Malbéteau *et al.* 2018a)
Thermal-Eye X-50	1	NASA UAV	160 × 120	7.5 -14.0	(Sullivan *et al.* 2007)
Xenics Gobi-384	1	Mikrokopter ARF Okto XL 6S12	384 × 288	8.0 –14.0	(Gago *et al.* 2017b)

While the use of proximal thermal imagery in crop water monitoring has considerably increased, it is worth noting that 60% (n = 51) of published literature has explored the combination of thermal imagery and multispectral channels for estimating crop water status parameters. This signifies the growing interest in leveraging both thermal and multispectral sensing capabilities for collecting comprehensive data on biophysical and biochemical proxies of crop water status using drone technology. The integration of the two characteristics allows for better understanding of not only crop temperature but also other properties, including crop health and productivity. Table 2.4 shows a summary of multispectral sensors and platforms used in crop water status monitoring. From the results, it can be observed that the most widely used sensors were MicaSense RedEdge-MX (35.3 %), Tetracam Agricultural Digital Camera ADC-Lite (19.6 %) and the Tetracam Micro-Multiple Camera Array (MCA-6) (13.7 %). The popularity of the MicaSense RedEdge-MX sensor is due to its optimally high spatial resolution and a wider spectral range, capturing spectral reflectance across the RGB, NIR and red-edge sections of the electromagnetic spectrum, which is essential for understanding crop health attributes at field scale. The findings also included studies that utilised RGB sensors such as the Cannon S95, DJI Zenmuse Z3 and Sony A6000. However, RGB sensors, when applied on their own, cannot provide sufficient information required for monitoring the status of water within cropping systems. As a result, RGB sensors were often used in conjunction with other multispectral sensors to increase the spectral variability (Santesteban *et al.* 2017b; Lee and Park 2019; Perich *et al.* 2020; Aboutalebi *et al.* 2022; Li *et al.* 2022b; Peng *et al.* 2023; Zhang *et al.* 2023a).

Furthermore, studies (n = 25) reviewed combined drone-based thermal imagery with UAV-derived hyperspectral data, satellite imagery and Light Detection and Ranging (LiDAR) datasets derived from UAV platforms. Approximately 10% and 4% of publications integrated hyperspectral and LiDAR datasets such as Nano-Hyperspec, Rikola hyperspectral, DJI Zenmuse P1 and DJI Zenmuse L1, demonstrating a growing interest in these sensors for crop water assessments using drone technology. Studies (n = 4) also conducted a comparative assessment of UAV-derived thermal data and satellite thermal imagery including Landsat 8, Visible Infrared Imaging Radiometer Suite (VIIRS) and Ecosystem Spaceborne Thermal Radiometer Experiment on Space Station (ECOSTRESS). This indicates a comparatively lower level of emphasis and research focus on using thermal imaging derived from satellite platforms in crop water assessments. Additionally, from the publications included in this study,

less than 10% have used satellite multispectral data, such as Landsat 7 and 8, Sentinel-2 Multispectral Instrument and Planet Scope, alongside UAV-derived thermal images for modelling crop water biophysical and biochemical parameters. While satellite-based thermal imagery offer the advantage of capturing thermal data on a larger scale and spectral resolution, allowing for regional scale assessments, their spatial resolutions are limited for high-accuracy near-real-time monitoring of crop water stress (Chivasa *et al.* 2020).

Lastly, the findings of the current study indicate that most of the retrieved studies utilised the RGB, red-edge, NIR and thermal sections of the electromagnetic spectrum. However, there is scarcity in literature evaluating other sections of the electromagnetic spectrum and their applicability in assessing crop water status. While the shortwave infrared wavelength is valuable in crop water assessments, many drone-based sensors lack this sensor, hence reducing its popularity.

.

Table 2.4 Summary of multispectral sensors and platforms used in assessing and monitoring crop water status between 2007 and 2023.

Sensor Name	Frequency (n)	Bands	Spectral Coverage	Pixel Resolution	Onboarded UAV	Reference
MicaSense RedEdge-MX	18	5	Blue, green, red, near infrared, and red-edge	1280 x 960	ATI-AgBOTTM Quadcopter; DJI Matrice 600 Pro; DJI Matrice 100; DJI Matrice 600; DJI Spreading Wings S1000+ Professional; DJI Inspire 2; DJI Phantom 4	(Chakraborty *et al.* 2020; Hou *et al.* 2021; Maguire *et al.* 2021; Das *et al.* 2022; Ekinzog *et al.* 2022; Zhang *et al.* 2023b)
Tetracam Agricultural Digital Camera ADC-Lite	10	3	Red, green and near infrared	2048 x 1536	Vulcan Mantis 900	(Katsigiannis *et al.* 2016; Tattaris *et al.* 2016; Santesteban *et al.* 2017b; Alimonti *et al.* 2020)
Tetracam Micro-Multiple Camera Array (MCA-6)	7	6	Visible to near-infrared spectral range at 530, 550, 570, 670, 700 and 800 nm	1280 × 1024	DJI Matrice 100	(Berni *et al.* 2009b; Calderón *et al.* 2013; Chávez *et al.* 2018; Gracia-Romero *et al.* 2019b; Tang *et al.* 2020b; Peng *et al.* 2023)
DJI Zenmuse X3	2	3	RGB	4000 × 3000	DJI Matrice 600; DJI Matrice 100	(Zhu *et al.* 2021b; Shao *et al.* 2023)
MicaSense Altum camera	2	6	Blue, green, red, red-edge, and near-infrared and a radiometric longwave infrared thermal sensor	2064 × 1544	DJI Matrice 300	(Ndlovu *et al.* 2021b; Brewer *et al.* 2022c)

Sensor Name	Frequency (n)	Bands	Spectral Coverage	Pixel Resolution	Onboarded UAV	Reference
DJI Zenmuse X3	2	3	RGB	4000 × 3000	DJI Matrice 600; DJI Matrice 100	(Zhu *et al.* 2021b; Shao *et al.* 2023)
MicaSense Altum camera	2	6	Blue, green, red, red-edge, and near-infrared and a radiometric longwave infrared thermal sensor	2064 × 1544	DJI Matrice 300	(Ndlovu *et al.* 2021b; Brewer *et al.* 2022c)
DJI Phantom 4 Pro	2	3	RGB	1280 × 960	DJI Phantom 4	(Zhang *et al.* 2022; Zhang *et al.* 2023a)
DJI Zenmuse X5R	2	3	RGB	5280 x 3956	DJI Matrice 600 Pro; DJI Inspire 2	(Lee and Park 2019; Li *et al.* 2022b)
AggieAir UAV Minion-class	1	4	Blue, green, red, and near infrared	Not specified	AggieAir UAV Minion-class	(Nieto *et al.* 2019)
Foxtech MS600 Series	1	6	Blue, green, red, dual red-edge, near infrared	1280 × 960	DJ Matrice 200	(Li *et al.* 2022a)
Sentera AGX710	1	5	Blue, green, red, red-edge, and near-infrared	1248 x 950	DJI Matrice 200	(Alexandris *et al.* 2021)
SixCam multispectral camera	1	6	Center wavelengths at 530, 550, 570, 670, 700 and 800 nm	2592 × 1944	mX-SIGHT	(Zarco-Tejada *et al.* 2013)
Airinov MultiSPEC 4C	1	4	Green, red, red-edge and near-infrared	1280 x 960	SenseFly eBee X	(Mwinuka *et al.* 2021b)
Sequoia camera	1	4	Green, red, red-edge and near infrared	1280 × 960	Microdrones MD-1000 multirotor	(Mwinuka *et al.* 2021b)

Sensor Name	Frequency (n)	Bands	Spectral Coverage	Pixel Resolution	Onboarded UAV	Reference
DuncanTech 3-band Imager	1	3	Narrow wavelength bands across the red-edge including Red, far red and NIR	1392 x 1040	Unknown UAV	(Tilling *et al.* 2007)
AccuRange 4000	1	1	Near-Infrared	1024 X 2048	Unknown UAV	(Hoffmann *et al.* 2016a)
Lumenera Lt65R Monochrome	1	1	Near-Infrared	4240 × 2832	AggieAir UAV Minion-class	(Aboutalebi *et al.* 2022)
Canon Powershot ELPH 340 HS	1	3	Red, green, and near infrared	4608 x 3456	Mikrokopter ARF Okto XL 6S12	(Sankaran *et al.* 2019)
NiteCanon ELPH110	1	3	Red, green and near infrared	4608 × 3456	Mikrokopter ARF Okto XL 6S12	(Espinoza *et al.* 2017)
MaxMax R-G-NIR Camera	1	3	Red, green and near infrared	4608 × 3456	DJI Matrice 600 Pro	(Zhou *et al.* 2020)
Canon Eos M	1	3	RGB	5184 x 3456	Mikrokopter ARF Okto XL 6S13	(Santesteban *et al.* 2017b)
Canon IXUS 12 7 HS	1	3	RGB	Not specified	DJI Phantom 4	(Pádua *et al.* 2022)
DJI Phantom 3 Professional	1	3	RGB	4000 × 3000	DJI Matrice 100	(Malbéteau *et al.* 2018a)
DJI Phantom 4 Advanced	1	3	RGB	4096 x 2160	DJI Phantom 4 Advanced	(Chen *et al.* 2019)
DJI Zenmuse Z3	1	3	RGB	640 × 512	DJI Matrice 600 Pro	(Perich *et al.* 2020)
GoPro Hero 5 Black	1	3	RGB	4000 × 3000	DJ Matrice 600 Pro	(Zhou *et al.* 2020)
Lumenera Lt65R Color	1	3	RGB	4240 × 2832	AggieAir UAV Minion-class	(Aboutalebi *et al.* 2022)

Sensor Name	Frequency (n)	Bands	Spectral Coverage	Pixel Resolution	Onboarded UAV	Reference
Panasonic DMC-LX5 Lumix camera	1	3	RGB	3648 x 2736	Unknown UAV	(Hoffmann *et al.* 2016c)
Sony A6000	1	3	RGB	6000 × 4000	DJI Spreading Wings S1000+ Professional	(Wang *et al.* 2023)
Cannon S95	1	3	RGB	3648 x 2736	AggieAir UAV Minion-class	(Aboutalebi *et al.* 2022)

2.3.2.6 The role of remotely sensed vegetation indices, algorithms, and models in assessing and monitoring crop water status

Remotely sensed vegetation indices play a crucial role in monitoring crop water status using thermal imagery. A wide range of thermal indices have been identified in the literature, each providing valuable insights into the water stress levels and health of crops (Table 2.5). The most widely applied index is the CWSI, which compares the crop canopy temperature to reference wet and dry temperatures to determine water stress levels (Idso *et al.* 1981). Several studies, including Berni *et al.* (2009a); Calderón *et al.* (2013); Gago *et al.* (2017b) and Alexandris *et al.* (2021) have investigated the use of drone-based thermal imagery together with the CWSI for assessing water status over a variety of crops, including maize, grape vineyards, olive orchards and potato fields.

The findings of this study also reported the use of indices such as Index of Relative Stomatal Conductance (IG) and the Normalised Relative Canopy Temperature (NRCT) (Baluja *et al.* 2012b; Gago *et al.* 2017b; Crusiol *et al.* 2020a; Li *et al.* 2022b). The IG was formulated based on the close relationship between water status and stomatal conductance and its influence on transpiration (Baluja *et al.* 2012b; Espinoza *et al.* 2017; Maimaitiyiming *et al.* 2020b; Awais *et al.* 2021). Notably, the terms CWSI, stomatal conductance and canopy temperature were also detected during the bibliometric analysis illustrated in Figure 2.2. These indices, along with others mentioned in Table 2.5, play a crucial role in remotely monitoring crop water status using thermal proximal images, allowing for effective irrigation management and improved crop productivity.

The findings of this study further illustrated the importance of multispectral indices, which served as support variables for most of the reviewed studies (Table 2.5). Despite the abundance of vegetation indices found in the literature, Table 2.5 displays multispectral indices that have been utilised in more than three studies. The exclusion of most indices is due to their limited application in crop water assessments, as they were employed in fewer than three studies. In the studies reviewed, the red and NIR regions of the electromagnetic spectrum were extensively employed for deriving vegetation indices. Specifically, the Normalised Difference Vegetation Index (NDVI) was utilised in more than 45% of the studies, followed by the Soil-Adjusted Vegetation Index (SAVI) in 14%, and Normalised Difference Red-Edge Index (NDRE) and Transformed Chlorophyll Absorption in Reflectance Index (TCARI) in 10% of

the studies. Notably, approximately 19% of studied vegetation indices were derived from the red-edge region of the electromagnetic spectrum (Tilling *et al.* 2007; Mwinuka *et al.* 2021b; Ndlovu *et al.* 2021b). Whereas most studies predominantly utilised vegetation indices, a limited number (n = 2) explored the potential of topographic indices, including the Topographic Wetness Index (TWI) and Surface Moisture Mapping Index (SMMI), derived from (DEM) in assessing crop water status. This suggests a growing interest in harnessing the capabilities of both vegetation and topographic indices for comprehensive analysis and understanding of crop water dynamics and overall health.

As suggested in various studies, the combination of thermal indices, spectral variables with robust and efficient algorithms are valuable for producing accurate models on crop water status (Sibanda *et al.* 2021a). The findings of this research showed that 19 algorithms and nine modelling techniques were utilised in characterising crop water and stress levels. Specifically, Support Vector Machine (SVM), Random Forest (RF), Linear Regression (LR) and Partial Least Squares Regression (PLSR) were the most extensively used algorithms in characterising water status and crop biophysical and biochemical parameters (Figure 2.8). Additionally, the Pearson correlation test was identified as the most frequently used parametric exploratory test within crop water monitoring studies. Furthermore, the results of this study also demonstrated several Crop Evapotranspiration (ET) models with the Two-Source Energy Balance (TSEB) model, Moderate Resolution Atmospheric Transmission (MODTRAN) radiative transfer model and the Three-Temperature (3T) model as the most popular techniques for modelling crop ET. Nonetheless, it is essential to note that there is limited usage of other crop evapotranspiration models, highlighting the need for further exploration and evaluation of alternative models to enhance our understanding of crop ET processes. Therefore, it is necessary for more efforts to explore the potential of robust machine learning algorithms, such as decision tree ensemble, artificial neural network and deep neural network, and ET models, including the High-Resolution Mapping of Evapotranspiration (HRMET) model in assessing and monitoring crop water status using drone-based thermal data.

Table 2.5 Summary of thermal and multispectral vegetation indices in crop water status assessment studies.

Index Name	Equation	Reference
Thermal Indices		
Standard Deviation of Canopy Temperature Index	$CSTD = \sqrt{\frac{\sum_{i=1}^{n}(Tci - \overline{Tc})^2}{n}}$	(Han *et al.* 2016)
Coefficients Variance of Canopy Temperature	$\mathbf{CTCV} = \frac{\mathbf{CSTD}}{\mathbf{Tc}}$	(Awais *et al.* 2021)
Degrees Above Critical Temperature	$\mathbf{DACT} = \max[0,\ T_c\ (h) - T_{critical}]$	(DeJonge *et al.* 2015)
Degrees Above Non-Stressed Canopy	$\mathbf{DANS} = T_c\ (h) - T_c\ NS\ (h)$	(Taghvaeian *et al.* 2014)
ΔT canopy-air	$\Delta T_{canopy-air} = T_{canopy} - T_{air}$	(Costa *et al.* 2013)
Index of Relative Stomatal Conductance	$\mathbf{IG} = \frac{T_{dry} - T_{canopy}}{T_{canopy} - T_{wet}}$	(Jones 1999)
Second Formulation of the Stomatal Conductance Index	$\mathbf{I3} = \frac{T_{canopy} - T_{wet}}{T_{dry} - T_{canopy}}$	(Baluja *et al.* 2012b)
Normalised Relative Canopy Temperature	$\mathbf{NRCT} = \frac{T_{canopy} - T_{min}}{T_{max} - T_{min}}$	(Elsayed *et al.* 2015)
Standardised Canopy Temperature Index	$\mathbf{SCTI} = \frac{T_{canopy} - \mathbf{mean}\ T_{canopy}}{\mathbf{Standard\ deviation}}$	(Das *et al.* 2021a)

Index Name	Equation	Reference
Temperature Condition Index	$\mathbf{TCI} = \frac{\mathbf{T_{canopy\ max}} - \mathbf{T_{canopy}}}{\mathbf{T_{canopy\ max}} - \mathbf{T_{canopy\ min}}} \mathbf{x\ 100}$	(Kogan 1995)
Temperature Vegetation Drought Index	$\mathbf{TVDI} = \frac{\mathbf{T_s} - \mathbf{T_{s\ min}}}{\mathbf{a} + \mathbf{b_{NDVI}} - \mathbf{T_{smin}}}$	(Sandholt *et al.* 2002)
Water Deficit Index	$\mathbf{WDI} = \mathbf{1} - \frac{\boldsymbol{\lambda}\mathbf{E_{act}}}{\boldsymbol{\lambda}\mathbf{E_{pot}}} = \frac{(\mathbf{T_s} - \mathbf{T_a})_{\mathbf{min-}} (\mathbf{T_s} - \mathbf{T_a})_{\mathbf{mes}}}{(\mathbf{T_s} - \mathbf{T_a})_{\mathbf{min-}} (\mathbf{T_s} - \mathbf{T_a})_{\mathbf{max}}}$	(Moran *et al.* 1994)
Crop Water Stress Index	$\mathbf{CWSI} = \frac{\mathbf{T_{canopy}} - \mathbf{T_{wet}}}{\mathbf{T_{dry}} - \mathbf{T_{wet}}}$	(Idso *et al.* 1981)
Multispectral Indices		
Normalised Difference Vegetation index	$\mathbf{NDVI} = \frac{\mathbf{R_{Nir}} - \mathbf{R_{red}}}{\mathbf{R_{Nir}} + \mathbf{R_{red}}}$	(Rouse *et al.* 1974)
Soil-Adjusted Vegetation Index	$\mathbf{SAVI} = \frac{\mathbf{R_{Nir}} - \mathbf{R_{red}}}{\mathbf{R_{Nir}} + \mathbf{R_{red}} + \mathbf{L}} \times (\mathbf{1} + \mathbf{L})$	(Huete 1988)
Normalised Difference Red-Edge Index	$\mathbf{NDRE} = \frac{\mathbf{R_{Nir}} - \mathbf{R_{Redegde}}}{\mathbf{R_{Nir}} + \mathbf{R_{Rededge}}}$	(Gitelson and Merzlyak 1994)
Transformed Chlorophyll Absorption in Reflectance Index	$\mathbf{TCARI} = \mathbf{3} \times (\mathbf{R_{Rededge}} - \mathbf{R_{Red}}) - \mathbf{0.2} \times (\mathbf{R_{Rededge}} - \mathbf{R_{Green}}) \times \frac{\mathbf{R_{Redegde}}}{\mathbf{R_{Red}}}$	(Haboudane *et al.* 2002)

Index Name	Equation	Reference
Optimised Soil-Adjusted Vegetation Index	$\mathbf{OSAVI} = \frac{(\mathbf{1}+\mathbf{L})\ \mathbf{x}\ (\mathbf{R_{Nir}} - \mathbf{R_{red}})}{\mathbf{R_{Nir}} + \mathbf{R_{red}} + \mathbf{L}}$	(Haboudane *et al.* 2002)
Photochemical Reflectance Index	$\mathbf{PRI} = \frac{\mathbf{R_{530}} - \mathbf{R_{570}}}{\mathbf{R_{530}} + \mathbf{R_{570}}}$	(Gamon *et al.* 1992)
Modified Chlorophyll Absorption in Reflectance Index	$\mathbf{MCARI} = (\mathbf{R_{700}} - \mathbf{R_{670}}) - \mathbf{0.2\ x}\ (\mathbf{R_{700}} - \mathbf{R_{550}}) \times \frac{\mathbf{R_{700}}}{\mathbf{R_{670}}}$	(Daughtry *et al.* 2000)
Renormalised Difference Vegetation Index	$\mathbf{RDVI} = \frac{\mathbf{R_{Nir}} - \mathbf{R_{red}}}{\sqrt{\mathbf{R_{Nir}} + \mathbf{R_{red}}}}$	(Roujean and Breon 1995)
Transformed Chlorophyll Absorption in Reflectance Index / Optimised Soil-Adjusted Vegetation Index	$\mathbf{TCARI\vert\ OSAVI} = \frac{\mathbf{TCARI}}{\mathbf{OSAVI}}$	(Haboudane *et al.* 2002)
Enhanced Vegetation Index	$\mathbf{EVI} = \mathbf{2.5} \times \frac{\mathbf{R_{Nir}} - \mathbf{R_{red}}}{\mathbf{R_{Nir}} + \mathbf{6} \times \mathbf{R_{red}} - \mathbf{7.5} \times \mathbf{R_{Blue}} + \mathbf{1}}$	(Huete *et al.* 2002)
Normalised Green-Red Difference Index	$\mathbf{NGRDI} = \frac{\mathbf{R_{Green}} - \mathbf{R_{red}}}{\mathbf{R_{Green}} + \mathbf{R_{red}}}$	(Hunt Jr *et al.* 2013)
Red–Green Ratio Index	$\mathbf{RGRI} = \frac{\mathbf{R_{Red}}}{\mathbf{R_{Green}}}$	(Sims and Gamon 2002)
Modified Spectral Ratio	$\mathbf{MSR} = \frac{\mathbf{R_{Nir}} - \mathbf{R_{red}} - \mathbf{1}}{\sqrt{\mathbf{R_{Nir}} + \mathbf{R_{red}} + \mathbf{1}}}$	(Chen 1996)

Index Name	Equation	Reference
Normalised Difference Water Index	$\mathbf{NDWI} = \frac{\mathbf{R_{Green}} - \mathbf{R_{Nir}}}{\mathbf{R_{Green}} + \mathbf{R_{Nir}}}$	(Gao 1996; McFeeters 1996)
Red-edge Chlorophyll Index	$\frac{\mathbf{R_{Nir}}}{\mathbf{R_{rededge}}} - \mathbf{1}$	(Gitelson *et al.* 2003; Gitelson *et al.* 2006)

Thermal Indices: Where T_c = canopy temperature; $T_{critical}$ = canopy temperature threshold; $T_c\ (h)$ = canopy temperature at given time; $T_c\ NS\ (h)$ = non-stressed canopy temperature at given time; T_{canopy} = canopy temperature, T_{dry} = lower boundary canopy temperature; T_{wet} = upper boundary canopy temperature; T_s = surface temperature onserved at the given pixel; T_{smin} = minimum surface temperature; a and b = parameters defining the dry edge modelled as a linear fit to data (Tsmax = a + bNDVI); T_{max} = maximum temperature; T_{min} = minimum temperature; $\lambda Eact$ = actual latent heat flux density; $\lambda Epot$ = the potential latent heat flux density; T_a = air temperature and the subscripts "*min*", "*max*" and "*mes*" refer to minimum, maximum and measured.

Multispectral Indices: Where R is the reflectance and L is a constant value that varies from –1 to 1 depending on the green vegetation density

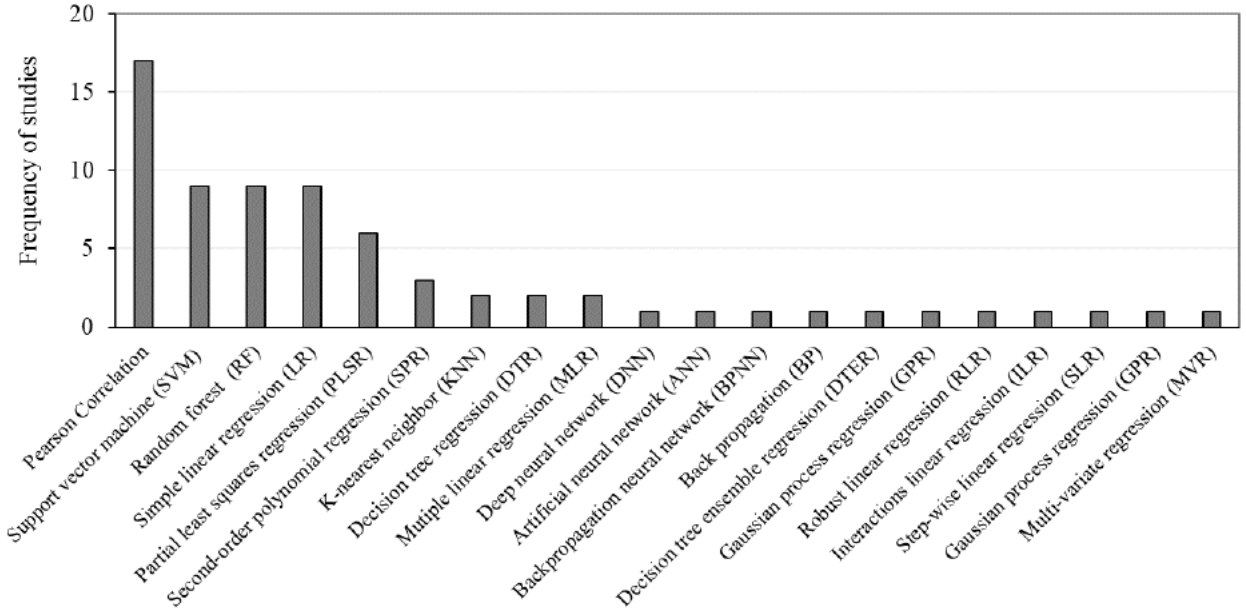

Figure 2.8 Algorithms used for assessing and monitoring crop water biophysical and biochemical parameters

2.4 Discussion

2.4.1 Progress in the use of UAV thermal remote sensing approaches in assessing and monitoring crop water status

2.4.1.1 Publication trends and geographic distribution

The results of this study showed that most crop water monitoring studies that used UAV-based thermal remote sensing approaches were conducted in USA, China and Spain. The USA and China are at the forefront of technological advancements, have well-established research institutions, government research support, financial investment and private sector initiatives to support research (Clarke 2014; Hodgkinson and Johnston 2018; Sibanda *et al.* 2021a). For instance, the acclaimed DJI drone series was designed and launched in China, while the widely used FLIR thermal cameras range are a product of the USA (Chakraborty *et al.* 2020; Park *et al.* 2021b). Furthermore, the USA and China have two of the largest agricultural sectors, making substantial contributions to food security. Consequently, there is greater emphasis on research and adoption of advanced technologies for crop water management and precision agriculture in these regions (Chen *et al.* 2018). In contrast, the results indicated substantial gaps in the

geographic distribution of articles published in the global south, especially in Africa and South America. There is a lack of adequate research, funding and public awareness and knowledge on UAV applications, particularly within the smallholder agricultural sector (Ayamga *et al.* 2021; Quiroga-Garza *et al.* 2022). Addressing these challenges and promoting investments in research and infrastructure can help bridge research gaps, leading to more comprehensive studies and publications in these regions. Furthermore, it is essential to note that most of these studies were conducted in research fields and experimental plots rather than in smallholder agricultural croplands. Therefore, there is a need for increased research efforts aimed at assessing the applicability of technologies and methodologies in the context of small, fragmented, and heterogeneous croplands typically found in developing regions, such as Southern Africa.

It was observed that the number of publications on UAV thermal mapping of crop water status is significantly increasing. The increase in publications reflects the confluence of technological advancements, increasing global concerns about food security, and introduction of drone technologies to local markets (Dinar *et al.* 2019; Zhao *et al.* 2023). The rapid evolution of drone technology has made UAV systems more accessible and cost-effective for various applications, including precision agriculture (Delavarpour *et al.* 2021). Their high efficiency in capturing near-real-time imagery at high spatial, spectral and temporal resolutions makes them a valuable tool for obtaining critical information on crop water levels in a time-efficient manner. Furthermore, the refinement of thermal imaging sensors has enabled detailed mapping, allowing the detection of subtle differences in canopy and foliar temperature at a field scale. This precision provides an accurate indication of water stress levels (Awais *et al.* 2022a). Lastly, with the intensifying threats of climate change, leading to unpredictable rainfall patterns and prolonged droughts, there is an increased need for strategies to maintain agricultural productivity and increase the resilience of cropping systems.

2.4.1.2 Crop types and farming systems

The results of this study showed that maize, grapes, wheat and soybean are the most widely researched crops in drone-based thermal studies for crop water status monitoring. These crops play a crucial role in the global food supply chain and are cultivated extensively across various regions, hence significant research efforts have been exerted towards them. For example, maize and wheat are staple food crops for a vast proportion of the world's population,

while grapes not only hold direct consumption value but also serve as the primary source for wine production (Hefferon 2015; Espinoza *et al.* 2017). Meanwhile, neglected and underutilised crop species, such as taro and sweet potato, remain under-researched despite their potential to address food and nutrition insecurity, highlighting a critical gap in scientific literature. Therefore, expanding research efforts on these crops is crucial for maximizing their contribution to sustainable agricultural practices and global food security.

The results also showed an overall bias in research settings and farming systems. The predominance of studies conducted within commercial farms (85.8%), compared to 2.3% on smallholder farms, sheds light on the ignored challenges and dynamics associated to smaller-scale farmers. The extensive focus on commercial agriculture may be driven by the economic gains associated with commercial farming, which often receives more funding and resources to facilitate research. Moreover, the emphasis on irrigated croplands over rainfed systems highlights potential neglect of areas that rely primarily on seasonal rainfall, which, given the increasing unpredictability of global weather patterns, represents a critical area of concern. Such focus on major commercial crops within irrigated farms reduces the applicability of UAV-thermal remote sensing, particularly in regions where smallholder farming plays a crucial role in local food security and where irrigation infrastructure is less developed.

2.4.1.3 Biophysical and biochemical proxies of crop water status identified in the literature.

The results of this study have demonstrated that various biophysical and biochemical proxies, such as canopy temperature, stomatal conductance and soil moisture content, have been widely applied in mapping and monitoring agricultural crop water status and stress. The rationale for measuring canopy temperature as an indicator of crop response to water stress is based on a study by Tanner (1963), which confirmed that leaf temperature is inversely correlated with the rate of transpiration in plant leaves. The underlying principle is that when crops are in a state of water deficit, leaf transpiration rates decrease due to the active regulation of stomata, reducing the evaporative cooling effect and resulting in an increase in leaf temperature (Gracia-Romero *et al.* 2019b). Additionally, the initial response of crops to water stress is stomatal closure, which prevents the loss of water through transpiration, making stomatal conductance a vital proxy of crop water status (Sobejano-Paz *et al.* 2020). As illustrated in a recent study by Brewer *et al.* (2022c), canopy temperature and stomatal conductance serve as adequate indicators for quantifying water stress in maize crops throughout

the entire growing period. Additionally, Sibanda *et al.* (2023) demonstrated the use of leaf temperature for the accurate assessment of moisture stress induced by natural hazards such as hailstorms. Therefore, the use of thermal remote sensing approaches and temperature measurements has become an established technique for detecting water stress and monitoring crop water levels.

Additionally, indicators such as the equivalent water thickness and canopy water content provide insights into the amount of water present in each crop, offering a direct measure of water status (Berni *et al.* 2009b; Zhu *et al.* 2021b). Such insights corroborate findings by Ndlovu *et al.* (2021b), where equivalent water thickness and fuel moisture content were identified as effective indicators of water stress in maize cropping systems. While these indicators are valuable and require less sophisticated equipment, Ihuoma and Madramootoo (2017) argue that their destructive nature makes them time-consuming and unfeasible, especially over larger landscapes. As technology evolves and the demands of precision agriculture grow, a balanced integration of both non-destructive and traditional indicators will be essential for comprehensive and efficient crop water status monitoring. This synthesis reinforces the importance of continued research and innovation in this field, ensuring that agricultural practices remain sustainable, efficient, and informed by the best available tools and practices.

2.4.1.4 UAV thermal remote sensing platforms, sensor technologies and spectral settings

The results of this study observed a high popularity of DJI-manufactured UAV systems within thermal remote sensing applications. The preference for DJI-manufactured drones may be linked to their cutting-edge technological characteristics, such as VTOL, in their products. These drones are highly reliable and stable in flight and offer an adaptable platform compatible with a wide array of sensors, ranging from multispectral to thermal and even hyperspectral and LIDAR sensors. This flexibility makes them particularly attractive for agricultural practitioners and researchers looking to integrate high-level drone systems with thermal sensors for agricultural crop monitoring. Similarly, this study noted a high utilisation of FLIR-manufactured thermal sensors. The reputation and preference towards FLIR are attributed to its longstanding history of producing high-quality thermal imaging systems. Moreover, the strategic collaboration established in 2015 between FLIR thermal cameras and DJI-produced

drones has made the integration of the two products common in cropping systems research (Thomas 2018).

While the use of proximal thermal imagery in crop water monitoring has considerably increased, it is worth noting that many studies have also explored the combination of thermal imagery and multispectral channels for estimating crop water status. This integrated approach underscores the broader recognition in the scientific community of the complementary information that both imaging methods can offer. Thermal imagery, for instance, primarily reflects the canopy temperature, which is related to plant processes, including leaf transpiration and stomatal conductance, thereby providing direct insights into crop water status (Zarco-Tejada *et al.* 2013; Han *et al.* 2021; Krishna *et al.* 2021). Whereas, multispectral imagery captures reflectance across various wavelengths, including the red-edge and NIR spectral channels, which are sensitive to crop health, productivity, and other physiological parameters, but are indirectly linked to crop water status (Ndlovu *et al.* 2021b; Brewer *et al.* 2022c). In the context of this study, the prominent use of multispectral sensors such as MicaSense RedEdge-MX (35.3%), Tetracam Agricultural Digital Camera ADC-Lite (19.6%) and the Tetracam Micro-Multiple Camera Array (13.7%) in literature is due to their broad spectral configuration. These sensors not only capture reflectance within the visible region but also extends to the NIR and red-edge portions of the electromagnetic spectrum. This capability provides a holistic understanding of crop health and water conditions (Chakraborty *et al.* 2020). For instance, the red-edge portion is known for its sensitivity to chlorophyll content, associated with water absorption and reflectance characteristics linked to plant water status (Peng *et al.* 2020). This is due to the wilting and yellowing of crop leaves under water deficit conditions, therefore, making this spectral region an effective predictor variable for both crop water stress and health (Berni *et al.* 2009b; Brewer *et al.* 2022a). Therefore, integrating both thermal and multispectral data may provide a comprehensive understanding of crop water status and overall growth conditions. This convergence of technologies in precision agriculture reflects the evolving nature of the field, where multi-modal data sources are leveraged for improved crop water management outcomes.

2.4.1.5 The role of remotely sensed vegetation indices, algorithms, and models in assessing and monitoring crop water status

Literature has illustrated several thermal indices that have been developed for assessing crop water status (Baluja *et al.* 2012b; Espinoza *et al.* 2017; Gago *et al.* 2017b; Alexandris *et al.* 2021). The majority of these indices primarily rely on canopy temperature as the main input variable, obtained as daily measurements taken at a presumed peak stress time or by assessing the time spent above a temperature threshold (Ihuoma and Madramootoo 2017). The Crop Water Stress Index (CWSI) is a prominent example of such indices, leveraging infrared canopy temperature measurements to offer insights into crop water status. In particular, the CWSI offers a non-invasive method to detect and quantify crop water stress, providing a numerical value that ranges from 0 (no stress) to 1 (severe stress) (Alexandris *et al.* 2021). However, a major limitation of using the CWSI in crop water status mapping is the associated computation difficulties, particularly pertaining to the reliable measurement of canopy and air temperature boundaries in the field (Veysi *et al.* 2017).

As a result, recent studies have explored alternative indices that demand fewer data inputs in comparison to the CWSI when assessing crop water conditions. For example, Alimonti *et al.* (2020) investigated the potential of the Degrees Above Critical Temperature (DACT) and Degrees Above Non-Stressed Canopy (DANS) in predicting water stress of maize crops, while Awais *et al.* (2021) evaluated the utility of UAV thermal imagery and the Index of Relative Stomatal Conductance (IG) for characterising water content in commercial tea fields. Furthermore, through a comparative study of thermal remote sensing indices, Kullberg *et al.* (2017) concluded that thermal indices with fewer data requirements, such as DACT and DANS, are more responsive to evapotranspiration and crop water stress, in comparison to more data-intensive methods such as the CWSI.

Although literature has highlighted the significance of thermal indices derived from UAV infrared imagery, there exist physiological and operational concerns that advocate for the exploration of alternative spectral indices, constructed on the RGB, NIR and red-edge regions for monitoring crop water status (Ihuoma and Madramootoo 2019). The shift towards utilising indicators beyond thermal indices for tracking crop water stress arises from the fact that while leaf temperature provides a direct measure of crop transpiration, it fails to inherently consider other physiological variations, including the changes in photosynthetic pigment or reductions

in photosynthesis not tied to stomatal activities during periods of water stress (Zarco-Tejada *et al.* 2013; Ihuoma and Madramootoo 2017). For instance, the NDVI, a widely recognised metric in precision agriculture, is instrumental in detecting plant vigour by examining the contrast between the visible and NIR reflectance by unhealthy or water-stressed crops, making it a valuable tool for assessing stress, even before visible symptoms appear (Espinoza *et al.* 2017; Gracia-Romero *et al.* 2019b).

However, Ihuoma and Madramootoo (2017) argue that the reliability of empirically derived NDVI products is compromised by their susceptibility to soil reflectance, spectral saturation and variations in sun-view geometry. To enhance the accuracy of NDVI, several indices, including the Renormalised Difference Vegetation Index (RDVI), Optimised Soil-Adjusted Vegetation Index (OSAVI), and Transformed Chlorophyll Absorption in Reflectance Index (TCARI), have been introduced to stabilise the variability of photosynthetic activity and minimise the effects of soil brightness on spectral vegetation indices, particularly those based in the red and NIR channels (Calderón *et al.* 2013; Gracia-Romero *et al.* 2019b). Moreover, the Photochemical Reflectance Index (PRI) offers valuable information about the efficiency of light utilization and can indicate immediate changes in xanthophyll pigments during stressful conditions, thus PRI emerges as a possible early warning indicator for water stress (Zarco-Tejada *et al.* 2013; Wang *et al.* 2022b; Tang *et al.* 2023). While thermal and spectral indices provide vital insights into crop water status and stress levels, their true potential is realised when integrated with advanced analytical methods.

Recent advancements in remote sensing algorithms present an opportunity to harness the intricate relationships embedded within thermal and spectral indices to predict and monitor crop water stress with increased precision. The findings of this study illustrated that machine learning algorithms are frequently used to monitor crop water status using UAV-derived thermal imagery. The efficacy of machine learning algorithms is attributed to their non-parametric nature, which allows them to operate without relying on any assumptions about data distribution (Basukala *et al.* 2017). Such flexibility means that these algorithms can accurately handle diverse and often non-linear datasets, making them particularly suited for decoding complex remote sensing data where various environmental factors interplay (Virnodkar *et al.* 2020). Whereas the use of machine learning algorithms such as Random Forest (RF) and Support Vector Machine (SVM) is highly popular, limited research reported on the use of deep learning approaches for UAV-thermal crop water applications. This novel area of machine

learning approaches has demonstrated outstanding robustness with computation models constructed with multiple processing layers to learn intricate data representations through the utilization of multiple levels of abstraction (Liakos *et al.* 2018). The under-representation of deep learning techniques signals an untapped potential and underscores the need for a more exhaustive investigation into the capabilities of deep learning in the context of UAV-derived thermal remote sensing for crop water status monitoring.

2.4.2 Challenges in the application of UAV thermal remote sensing in assessing and monitoring crop water status.

The application of UAV-based thermal remote sensing in crop water assessment and monitoring has demonstrated great potential in precision agriculture. However, there are several challenges that hinder its seamless adoption and widespread implementation in agricultural systems. One of the primary challenges is their high cost, especially UAVs equipped with high-resolution thermal cameras, making them less accessible for smallholder farmers or researchers with limited budgets (Yinka-Banjo and Ajayi 2019; Nhamo *et al.* 2020). This cost factor is particularly pronounced in the global south where economic constraints limit investments in advanced technologies. Secondly, UAV operations necessitate specialised knowledge and training. While piloting a UAV aircraft might seem straightforward, ensuring safe and effective flights that capture consistent and high-quality data requires expertise. For instance, in South Africa, the utilisation of drones is subject to stringent regulations imposed by the South African Civil Aviation Authority (SACAA), mandating potential operators to undergo rigorous training and certification processes (Mokoena *et al.* 2022). However, the cost and time associated with this training is a barrier for many farmers and remains beyond the reach of many researchers (Sibanda *et al.* 2022). Additionally, statutory regulations that govern UAV operations still impose restrictions on where and how UAVs should be operated, thus often limiting research efforts within agricultural (Cracknell 2017).

The calibration of thermal images is another challenge that cannot be understated. Ensuring the precision and accuracy of thermal data requires meticulous calibration processes, which, if improperly executed, can lead to significant deviations in water stress estimations (Han *et al.* 2020; Han *et al.* 2021). Similarly, atmospheric interference, varying weather conditions, and changes in solar radiation can also impact the quality and consistency of thermal data captured by UAVs, therefore demanding a rigorous calibration and validation processes (Bellvert *et al.*

2014). Additionally, soil background interference can lead to inconsistencies in thermal imagery during image analysis, affecting the accuracy of crop water status assessments. To address this, the implementation of advanced image segmentation techniques becomes imperative, with the need for methods that aim to isolate regions of interest to specifically focus on the vegetation cover, through image processing techniques such as the Canny Edge Detection and Otsu algorithm (Bian *et al.* 2019; Chakraborty *et al.* 2020; Awais *et al.* 2022a).

2.4.3 Research gaps and opportunities

The study identified the following gaps in the context of monitoring crop water status using UAV thermal remote sensing:

- There exist significant gaps, with a limited number of studies that have aimed to evaluate the utility of UAV thermal remote sensing techniques in assessing and monitoring crop water status, especially neglected and underutilised crop species, particularly in the global south.
- There is a scarcity of research attention directed towards mapping water status in rainfed and smallholder farming systems.
- The evaluation of crop water status using UAV-derived thermal datasets has garnered increased attention and interest from the scientific community over the recent years.
- While the assessment of canopy temperature has proven invaluable in crop water status assessments, there is a lack of studies that explore other biophysical and biochemical indicators of crop moisture such as, stomatal conductance, equivalent water thickness, canopy water content, leaf temperature and relative water content.
- There is limited research on how crop water status changes diurnally and throughout the various growth stages. Therefore, there is need for research that conducts time-series analyses using UAV datasets to understand the diurnal and phenological variations in crop water status.
- Minimal efforts have been made to explore the potential synergies between drone-derived data and satellite-borne datasets. Research efforts should be expanded to integrate UAV thermal data with satellite data, especially with the emerging availability of high-resolution datasets like PlanetScope.

- There is a notable scarcity of studies that probe the efficacy of robust machine algorithms, including deep learning techniques, in conjunction with thermal and spectral indices in mapping and monitoring crop water status.

By addressing these gaps, researchers can refine the methodologies, enhance the precision of assessments, and extend the applicability of UAV thermal remote sensing for monitoring crop water status on a larger extent.

2.5 Conclusion

The primary objective of this study was to systematically review and analyse the existing literature to comprehensively assess the progress, research gaps, and opportunities related to the application of UAV thermal remote sensing in assessing and monitoring crop water status. The study identified several research gaps and opportunities that collectively illustrated the need for additional research. For instance, the findings demonstrated a lack of research on UAV thermal applications, particularly on neglected and underutilised crops and in smallholder rainfed farming systems. Additionally, there is a need to explore and understand the diurnal and phenological variations of biophysical indicators and to assess the potential synergies between drone-derived data and satellite-borne datasets for crop water status assessments. Furthermore, leveraging robust machine algorithms including deep learning techniques for mapping crop water status remains underexplored. By addressing these gaps and increasing research efforts, UAV thermal remote sensing technologies hold great promise for providing spatially explicit very-high-resolution datasets for the near-real-time monitoring of agricultural crop water status. Therefore, this study serves as a fundamental step toward enhancing crop water status assessments and contributing to sustainable agriculture frameworks.

2.6 Summary

Literature has explicitly highlighted the transformative potential of UAV-based thermal remote sensing technologies in assessing and monitoring crop water status. While significant progress has been made, existing research has predominantly focused on mainstream crops and commercial farming systems, with limited attention given to neglected and underutilised crops, such as taro, in smallholder farming contexts. Additionally, the findings of the systematic review highlighted the need for enhanced methodologies integrating UAV-acquired thermal and

multispectral data to improve the accuracy and reliability of crop water status assessments. To ensure robustness, advanced image segmentation techniques are critical for minimising background noise, particularly soil interference, which can distort and reduce the accuracy of water status estimations. In this regard, Chapter Three explores the utility of image segmentation techniques and thermal imagery in enhancing the estimation of equivalent water thickness of smallholder neglected and underutilised taro crops.

CHAPTER THREE

Enhancing the Estimation of Equivalent Water Thickness in Neglected and Underutilised Taro Crops using UAV acquired Multispectral Thermal Image data and Index-Based Image Segmentation

This chapter is based on:

Ndlovu, H. S., Odindi, J., Sibanda, M., & Mutanga, O. (2024). Enhancing Taro Equivalent Water Thickness Estimation through Index-Based Image Segmentation using Unmanned Aerial Vehicle Multispectral Thermal Imagery. *Remote Sensing Applications: Society and Environment*, Under Review, Manuscript ID: RSASE-D-24-01546

Abstract

Due to the impact of climate variability and change, smallholder farmers are increasingly confronted by the challenge of sustaining crop production. Taro, recognised as a future smart neglected and underutilised crop as a result of its resilience to abiotic stresses, has emerged as valuable for diversifying crop farming systems and sustaining local livelihoods. Nonetheless, a significant research gap exists in spatially explicit information on the water status of taro, contributing to the paradox of its ability to adapt to diverse agro-ecological conditions. Precision agriculture, including the use of Unmanned Aerial Vehicles (UAVs) fitted with high-resolution multispectral and thermal imagery, has proven effective in farm-scale monitoring and provides near-real-time information on crop water status. Hence, this study sought to evaluate the applicability of multispectral and thermal infrared UAV imagery in understanding taro's water status. Leveraging deep learning techniques to evaluate the use of thermal remote sensing and three index-based segmentation techniques in predicting the canopy Equivalent Water Thickness (EWT) of taro crops, this study sought to determine EWT as a proxy to its water status in smallholder farmlands. The study findings illustrated a significant difference in the prediction accuracies of taro EWT with and without the thermal band ($P < 0.05$). Additionally, results (R^2 = 0.92, RMSE = 8.04 g/m^2, and rRMSE = 15.31% including the thermal band and 0.91, 8.73 g/m^2, and 16.64% excluding the thermal band) reveal the value of the Excessive Green minus Excessive Red (ExGR) technique in accurately predicting EWT_{canopy}. Furthermore, the near-infrared, red-edge, and thermal sections of the electromagnetic spectrum, together with their derived indices, were critical in estimating taro EWT. This study serves as a foundation for developing an effective and efficient monitoring framework that provides a spatially explicit overview of neglected and underutilised crops such as taro. The study offers valuable insights into neglected and underutilised crop water use within smallholder farming systems, critical for optimizing crop productivity and mitigating the effects of climatic variability and change.

Keywords: Thermal remote sensing, equivalent water thickness, crop water status, taro, unmanned aerial vehicles, index-based segmentation, smallholder farming.

3.1 Introduction

The world is confronted by the pressing need to sustain food supply and ensure food security due to climate change and the rising global human population (Mugiyo *et al.* 2021c; Din *et al.* 2022b). In southern Africa, climate variability, among other factors, has led to water scarcity, restricting crop production, and significantly reducing the available arable land (Mugiyo *et al.* 2021c; Zulu 2022; Kapari *et al.* 2023). This has particularly affected smallholder farmers in the sub-Saharan regions of Africa, who contribute up to 80% of food production and are therefore vital actors in addressing local food security (Hlophe-Ginindza and Mpandeli 2020). Despite their crucial role, smallholder farms commonly encounter sporadic water stress and drought, leading to substantial losses in crop yields (Gomez Paloma *et al.,* 2020). Addressing this challenge necessitates a shift toward crop diversification and incorporating crop species that demonstrate resilience to abiotic stresses (Chivenge *et al.* 2015; Hilary van Wyk and Oscar Amonsou 2021; Mugiyo *et al.* 2021a).

Recently, driven by water scarcity, there has been increasing interest in the potential use of Neglected and Underutilised Crop Species (NUS) in addressing food and nutrition challenges (Chivenge *et al.* 2015; Mabhaudhi *et al.* 2017b; Mugiyo *et al.* 2021c). NUS, characterised by historical domestication with limited scientific research and predominantly confined to smallholder farming systems, have emerged as key drought-tolerant crops for diversifying communal agricultural settings (Chivenge *et al.* 2015; Mabhaudhi *et al.* 2017b). Taro (*Colocasia esculenta* (L)) is one of the oldest and most widely cultivated NUS crops in the world's tropical and subtropical regions (Mabhaudhi *et al.* 2011; Mawoyo *et al.* 2017; Van Wyk 2021). In South Africa, taro, locally known as *amadumbe,* is known to be heat tolerant and primarily cultivated for subsistence, especially within small and marginalised communities (Mabhaudhi *et al.* 2014; Joshi *et al.* 2020; Oyeyinka and Amonsou 2020; Van Wyk 2021). Taro is identified as a future smart food under the NUS category because of its edible tubers, which are rich in carbohydrates, protein, and vitamins (Li and Siddique 2018; Kapoor *et al.* 2022). Despite taro and indeed other NUS's value, literature showed that they have largely been ignored.

Whereas advocation for taro as a valuable drought and heat-tolerant crop in diversifying the smallholder farming systems has gained traction, evidence is predominantly anecdotal (Joshi *et al.* 2020). Notedly, there is a significant research gap in understanding the crop's water status,

hence knowledge on its ability to adapt to diverse agroecological environments remains limited (Mabhaudhi *et al.* 2017a). Consequently, this presents challenges for decision-makers aiming to streamline taro into the existing agricultural systems (Mugiyo *et al.* 2021a). Therefore, it is imperative that further research on the canopy water status of taro be conducted as a proxy of water use to optimise its productivity and ultimately facilitate its integration into sustainable agricultural practices.

Equivalent Water Thickness (EWT), the relation between the amount of water per unit area and the leaf area of a crop, is a critical metric in assessing and understanding a crop's canopy water status (Traore *et al.* 2021) (Yi *et al.* 2014). The indicator quantifies the amount of water present in the plant canopy, hence provide a valuable measure of a crop's hydration level (Traore *et al.* 2021). Furthermore, EWT is critical in understanding bio-geochemical processes such as photosynthesis, primary productivity and overall crop health (Zhang and Zhou 2019b). Traditionally, EWT is measured using in-situ measurements that are laborious, time-consuming and often require trained experts in field sampling (Chivasa *et al.* 2020; Traore *et al.* 2021). However, over the past few decades, the application of satellite-borne earth observation technologies has provided a valuable alternative to quantifying agronomic properties and understanding the changes in crop water status (Pasqualotto *et al.* 2018). For example, Yilmaz *et al.* (2008) utilised a time series of Landsat 5 Thematic Mapper (TM), Advanced Spaceborne Thermal Emission and Reflection Radiometer (ASTER) and Advanced Wide Field Sensor (AWiFS) imagery to estimate the water status of maize and soybean at optimal accuracies (R^2 = 0.87 and R^2 = 0.47, respectively). Then, Neinavaz *et al.* (2017) successfully estimated canopy EWT using hyperspectral thermal infrared data to an R^2 of 0.81 and RMSE of 0.003 g cm^{-2}. The success of these studies could be explained by the presence of the thermal band, which facilitates the accurate estimation of canopy water content (Khanal *et al.* 2017).

Thermal infrared remote sensing has emerged as a valuable tool for crop water assessment and monitoring, offering a direct correlation with crop water biophysical and biochemical elements (Khanal *et al.* 2017; Messina and Modica 2020). Specifically, the emitted radiance in the thermal infrared region exhibits sensitivity to variations in canopy temperature, influenced by changes in crop water status (Gerhards *et al.* 2019). In states of water deficit, the rate of leaf transpiration decreases, leading to a linear decrease in leaf and canopy temperature, inducing a cooling effect (Maes and Steppe 2012; Hou *et al.* 2018). Therefore, thermal imagery can be utilised to indicate areas of water stress, valuable for the implementation of appropriate

management strategies to improve crop water status and overall productivity. The adoption of thermal remote sensing for estimating crop water status has gained popularity over the decades (Krishna *et al.* 2021). Various satellite-based thermal sensors that include Moderate Resolution Imaging Spectroradiometer (MODIS), Advanced Spaceborne Thermal Emission and Reflection Radiometer (ASTER), and the Landsat series (Malbéteau *et al.* 2018a; Gerhards *et al.* 2019; Masina *et al.* 2020; Xue *et al.* 2020b) have been used to assess and monitor crop water status. However, these datasets are constrained by their relatively coarse spatial resolutions, limiting their suitability for monitoring taro water status in smallholder farms (Malbéteau *et al.* 2018a).

The recent advancements in image acquisition, such as the use of lightweight thermal and multispectral sensors onboarded Unmanned Aerial Vehicles (UAVs), enable the provision of spatially explicit, near-real-time crop water status information (Hussain *et al.* 2020). UAV proximal sensors with a sub-centimetre resolution deliver rapid, cost-effective and accurate measurements suitable for monitoring the water stress and health attributes of crops at a plot level (Chivasa *et al.* 2020). Specifically, UAVs, integrated with very-high resolution Thermal Infrared Sensors (TIRS) provide an optimal approach of retrieving crop attributes for the accurate quantification of crop water status at a field scale (Berni *et al.* 2009a).

In addition to ultra-high spatial resolutions of UAV multispectral thermal imagery, image enhancement techniques and robust algorithms have been demonstrated to improve model accuracies. For instance, index-based image segmentation has been demonstrated to be effective in robustly segmenting plants in colour images, enabling the extraction of vegetation cover and removing soil background for enhanced crops spectral signatures (Hamuda *et al.* 2016). Meanwhile, color indices can improve the visual contrast of vegetation against the soil elements and mitigate the effects of varying light conditions, resulting in enhanced accuracy for plant segmentation compared to original Red-Green-Blue (RGB) imagery (Lu *et al.* 2022b). The Excess Green (ExG) and Excess Red (ExR) indices were proposed by Woebbecke *et al.* (1995) and Meyer *et al.* (1999), respectively, to enhance plant segmentation accuracy by emphasizing plant greenness by accounting for the relative proportions of red and physiological green. Additionally, Meyer and Neto (2008) leveraged the strength of both ExG and ExR to develop the Excess Green minus Excess Red (ExGR) index to improve crop water assessment and monitoring using thermal remote sensing systems. While colour index-based segmentations have been proven to be effective in improving estimation accuracies, they remain relatively underexplored, prompting the need for further inquiry to fully leverage their potential in

enhancing crop water assessment and monitoring through UAV multispectral thermal remote sensing systems.

In addition to traditional techniques, the use of machine learning methods, particularly deep learning, has recently shown great potential for assessing crop water status (Zhou *et al.* 2021). Deep learning techniques, such as Deep Neural Networks (DNN) have shown robustness and high accuracy in identifying and quantifying water deficits in various crops (e.g., sugarcane and maize) using thermal remote sensing (de Melo *et al.* 2022; Rajwade *et al.* 2023). In contrast to traditional machine learning algorithms, the DNN can comprehend complex nonlinear relationships between various environmental attributes by using feature representations that are only learned from data (Yuan *et al.* 2020; Omosalewa *et al.* 2022). Despite these advantages, the integration of the DNN algorithm with UAV thermal remote sensing for crop water estimations, especially in smallholder farming systems, has been infrequent (Abrahams *et al.* 2023). Consequently, there is dire need for further research to explore and incorporate the potential of DNN algorithms in precision agriculture for more accurate and efficient crop water status assessments.

In this regard, leveraging the capabilities of deep learning, this study aimed to evaluate the effectiveness of thermal remote sensing and index-based segmentation techniques in improving canopy EWT estimation of smallholder taro crops using UAV multispectral thermal imagery. Specifically, the study sought to: (1) assess the potential of the UAV thermal band in estimating EWT of smallholder taro, (2) compare the performance of crop canopy images extracted using the ExG, ExR, and ExGR color indices in improving EWT estimations of taro crop, and (3) evaluate the potential of UAV multispectral and thermal imagery in EWT estimations of taro crop in smallholder farmlands.

3.2 Materials and Methods

3.2.1 Study area description and the experimental field

This research was carried out in the rural community of Swayimana (29°31′ 24’’ S; 30°41′ 37’’ E), situated within the uMshwathi Municipality, northeast of Pietermaritzburg city, KwaZulu-Natal, South Africa (Figure 3.1). With an average annual temperature of 17 °C and an average temperature range of 11.8 °C to 24 °C, Swayimana is part of the moist midlands mistbelt

bioresource group (Cele and Mudhara 2024; Kapari *et al.* 2025). The region experiences hot, humid summers and arid winters, with an average precipitation of 600 –1200 mm per annum (Gokool *et al.* 2024). The study area is suitable for growing crops, including maize, sugarcane, sweet potatoes, and taro, as it has arable clay loam soils and considered among South Africa's top 2% of high-potential land (Ndlovu *et al.* 2021c; Zaca *et al.* 2023). The communal nature of farming practices in Swayimane emphasises traditional techniques such as applying intensive manual labour techniques and using cow dung for fertiliser. The region is primarily known for its smallholder subsistence farming and domestic sale of produce, underscoring its value in contributing to both food security and sustaining local livelihoods.

The taro experimental plot was cultivated during the early rainy season, aligning with its optimal growing conditions. The selected plot covered 2864.56 m^2 and was rainfed. The taro crop was sown in mid-October 2022 and was approximately 171 days old at the time of the experiment. Specifically, the crop was intermediate between the late vegetative and early maturity growth stages. The selection of this growth stage is crucial for capturing the developmental dynamics of the crop during a period of heightened canopy growth, providing valuable insights for the research objectives.

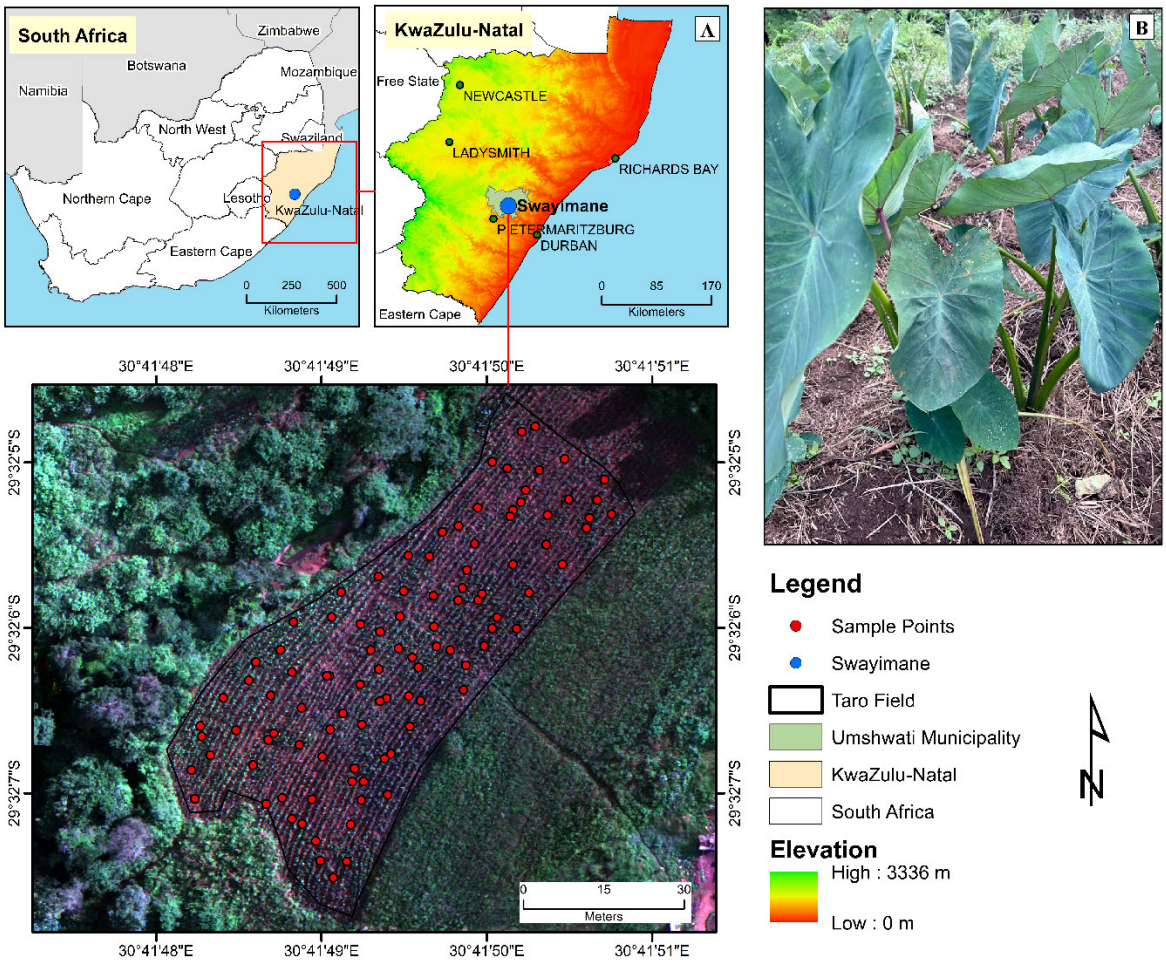

Figure 3.1 . a) Location of the experimental field in Swayimane and b) taro crop.

3.2.2 Field Sampling and in-situ measurements

Using Google Earth Pro, a polygon defining the taro field was developed and imported into ArcGIS Pro to facilitate the generation of 100 stratified random sampling points. The field was divided into three topographic strata, stratum A (upper slope), stratum B (mid-slope) and stratum C (lower slope), to capture the variability linked to elevation and water distribution across the slope. Stratified random sampling was then conducted by allocating sampling points within each of the three strata, ensuring comprehensive spatial representation of the taro crop. The Trimble handheld Global Positioning System (GPS), with a positional accuracy of approximately 1 meter, was then updated with these sampling points, enabling the precise location of each point within the taro field. In-situ measurements were obtained at each sampling point to compute respective EWT values.

A portable LiCOR-2200C Plant Canopy Analyser was used to obtain the Leaf Area Index (LAI) of the crops. The ABBBB sequence and a 38° zenith angle with a 270° view cap were used to measure the LAI, with A denoting a reference reading "above" the canopy and B denoting a reading "below" the canopy. Subsequently, the fresh weight (FW) of every crop sampled was determined by measuring its above-ground biomass using a calibrated scale that had a measurement error of 0.5 g. The sampled biomass was then placed in a labelled brown paper bag that was dried in an oven at 60 °C for about 72 hours or until a constant dry weight (DW) was reached. Thereafter, using the following equation, the LAI, FW, and DW were used to compute taro EWT_{canopy} indicators (Zhang and Zhou 2019a; Ahmad *et al.* 2021):

$$EWTcanopy = \frac{\mathrm{FW-DW}}{\mathrm{LAI}} \qquad \text{Units: g/m}^2 \qquad (3.1)$$

Lastly, in-situ measurements were conducted from 10:00 am to 2:00 pm local time on a sunny day as it aligns with the ideal period for crop photosynthesis, ensuring that the collected data accurately reflects the maximum reflectance and photosynthetic activity of the taro crops.

3.2.3 UAV platform and multispectral-thermal camera

Multispectral-thermal imagery was collected using the DJI Matrice 300 (M300) platform, which was equipped with a MicaSense Altum camera and a Downwelling Light Sensor 2 (DLS 2). The M300 platform is equipped with four rotary wings and incorporates Vertical Take-off and Landing (VTOL) technology, hence highly suitable for imaging smallholder farms, especially those near settlements. The MicaSense Altum camera is a multispectral and thermal imaging sensor that combines a radiometric longwave infrared thermal channel (11 μm) with five high-resolution narrow bands to measure reflectance in blue (475 nm), green (560 nm), red (668 nm), red-edge (717 nm), and NIR (840 nm) regions. This advanced camera provides synchronised capture of multispectral and thermal images, utilising a global shutter that facilitates a 1-second capture rate, ensuring clear and precisely aligned imagery (Hutton *et al.* 2020b). The multispectral channels have a sensor resolution of 2064 × 1544 pixels (equivalent to 3.2 megapixels per multispectral band), while the thermal band has a sensor resolution of 160 × 120 pixels, at a 120 m platform altitude. Lastly, the calibrated reflectance panel and equipped DLS 2 allows the Altum sensor to measure ambient light and sun angle, improving the quality of the captured radiation intensity.

3.2.4 Image acquisition and pre-processing

For the development of the UAV flight plan, a shapefile delineating the experimental field was created and transferred to the M300 handheld smart controller. To account for incident light conditions, the Altum sensor was calibrated both before and after flight using a Calibrated Reflectance Panel (CRP). This entailed utilizing established reflectance values throughout the spectral range to perform radiometric calibrations on the sensor by capturing an unshaded image of the CRP to account for the lighting and atmospheric conditions that prevailed during the flight. The automated flying mission was conducted at an altitude of 100 m, yielding a ground sampling distance of 10.08 cm per pixel produced a 10.08 cm per pixel. Additionally, the flight plan incorporated 80% forward and side overlap to ensure adequate image coverage and stitching quality. Given the extent of the study area and UAV battery capabilities, a single flight mission was sufficient to cover the entire taro field. The flight was conducted under clear sky conditions between 10:00 am and 2:00 pm local time when the solar zenith angle is minimal, and solar radiation reaches its peak. The UAV flight and in-situ measurements of taro water status were carried out concurrently.

A total of 1626 raw images of the experimental field were obtained and pre-processed in Pix4D photogrammetry software. The software allows for the stitching of the imagery to create a composite otho-mosaic of the taro field while accounting to atmospheric conditions during image acquisition. The CRP images, together with the raw images, are automatically recognised by the software and used to perform radiometric corrections by calibrating the image reflectance to align to the atmospheric conditions during the time of image acquisition. Pre-surveyed ground control points were employed to enhance the geometric accuracy of the collected images using ArcGIS Pro. A total of four ground control points were collected using a Trimble Handheld GPS device with an estimated positional accuracy of approximately one meter. The acquired points were placed on fixed, clearly identifiable locations surrounding the taro field to ensure adequate spatial coverage and effective georeferencing. Lastly, EWT_{canopy} in-situ measurements and the locationa of each sampled taro point were overlaid with UAV multispectral-thermal image. The multispectral and thermal reflectance data of taro was extracted from the UAV imagery and used to derive Vegetation Indices (VIs) for the development of the EWT_{canopy} prediction model. A list of VIs used in this study is summarised in Table 3.1. Based on their optimal performance in literature and relationship with crop water

status, these VIs were selected in this study (Baluja *et al.* 2012b) (Baluja *et al.* 2012a; Zhang and Zhou 2019a; Ozelkan 2020).

Table 3.1 UAV-derived vegetation indices utilised in this study.

Vegetation Index	Abbreviation and Equation	Reference
Normalised difference vegetation index	$NDVI = \frac{R_{Nir} - R_{red}}{R_{Nir} + R_{red}}$	(Rouse *et al.* 1974)
Soil-Adjusted Vegetation Index	$SAVI = \frac{R_{Nir} - R_{red}}{R_{Nir} + R_{red} + L} \times (1 + L)$	(Huete 1988)
Normalised Difference Red-Edge Index	$NDRE = \frac{R_{Nir} - R_{Redegde}}{R_{Nir} + R_{Rededge}}$	(Gitelson and Merzlyak 1994)
Transformed Chlorophyll Absorption in Reflectance Index	$TCARI = 3 \times (R_{Rededge} - R_{Red}) - 0.2 \times (R_{Rededge} - R_{Green}) \times \frac{R_{Redegde}}{R_{Red}}$	(Haboudane *et al.* 2002)
Modified Chlorophyll Absorption in Reflectance Index	$MCARI = (R_{Rededge} - R_{Red}) - 0.2 \times (R_{Rededge} - R_{Green}) \times \frac{R_{Rededge}}{R_{Red}}$	(Daughtry *et al.* 2000)
Normalised Green-Red Difference Index	$NGRDI = \frac{R_{Green} - R_{red}}{R_{Green} + R_{red}}$	(Hunt Jr *et al.* 2013)
Normalised difference water index	$NDWI = \frac{R_{Green} - R_{Nir}}{R_{Green} + R_{Nir}}$	(Gao 1996; McFeeters 1996)
Red-edge Chlorophyll Index	$CIrededge = \frac{R_{Nir}}{R_{rededge}} - 1$	(Gitelson *et al.* 2003; Gitelson *et al.* 2006)

3.2.5 Index-based image segmentation of taro crops' spectral signatures

Image segmentation to remove soil background is crucial for accurately assessing crop water status, especially in set-ups like smallholder taro fields, where the soil background effect is pronounced due to low planting density and high interrow spacing. The expansive growth of

taro tubers necessitates substantial space beneath the soil surface to access sufficient moisture and nutrients and to reduce competition, for optimal growth and development (Tumuhimbise 2015). To delineate the crop canopy and eliminate soil background from the multispectral thermal image, an index-based segmentation technique was employed. Specifically, The Excess Green (ExG), Excess Red (ExR), and Excess Green minus Excess Red (ExGR) color indices were computed using the green, red, and blue bands of the UAV multispectral thermal imagery (Woebbecke *et al.* 1995; Meyer *et al.* 1999; Meyer and Neto 2008; Hamuda *et al.* 2016). The ExG, ExR and ExGR were calculated using the following equations:

$$ExG = 2 \times R_{Green} - R_{Red} - R_{Blue} \quad (2)$$

$$ExR = 1.4 \times R_{Red} - R_{Green} \quad (3)$$

$$ExGR = ExG - ExR \quad (4)$$

Finally, the threshold method was used to generate a binary image from the gray-level histograms obtained during the index-based segmentation process (Shu *et al.* 2021). The ExG and ExR binary images of the taro crop canopy cover were generated using an automatic Otsu threshold, determined by the maximum interclass variance as defined by the Otsu method (Otsu 1979). The Otsu threshold was executed in Mathworks MatLab using the image toolbox graythresh function to develop a binary ExG image. Unlike the ExG index, the ExGR index does not require the calculation of a specific threshold, as all plant pixel values are positive, while the background pixels are negative (Meyer and Neto 2008; Riehle *et al.* 2020). Consequently, a fixed zero threshold was implemented to automatically generate a binary image with a consistent threshold of zero (Hamuda *et al.* 2016). Thereafter, the image pixels were reclassified to create a new layer where vegetation and soil pixels were assigned the values 1 and 0, respectively. The vegetation mask was subsequently converted into a shapefile that was used to extract the crop canopy cover from the UAV image and remove the soil background, as depicted in Figure 3.2.

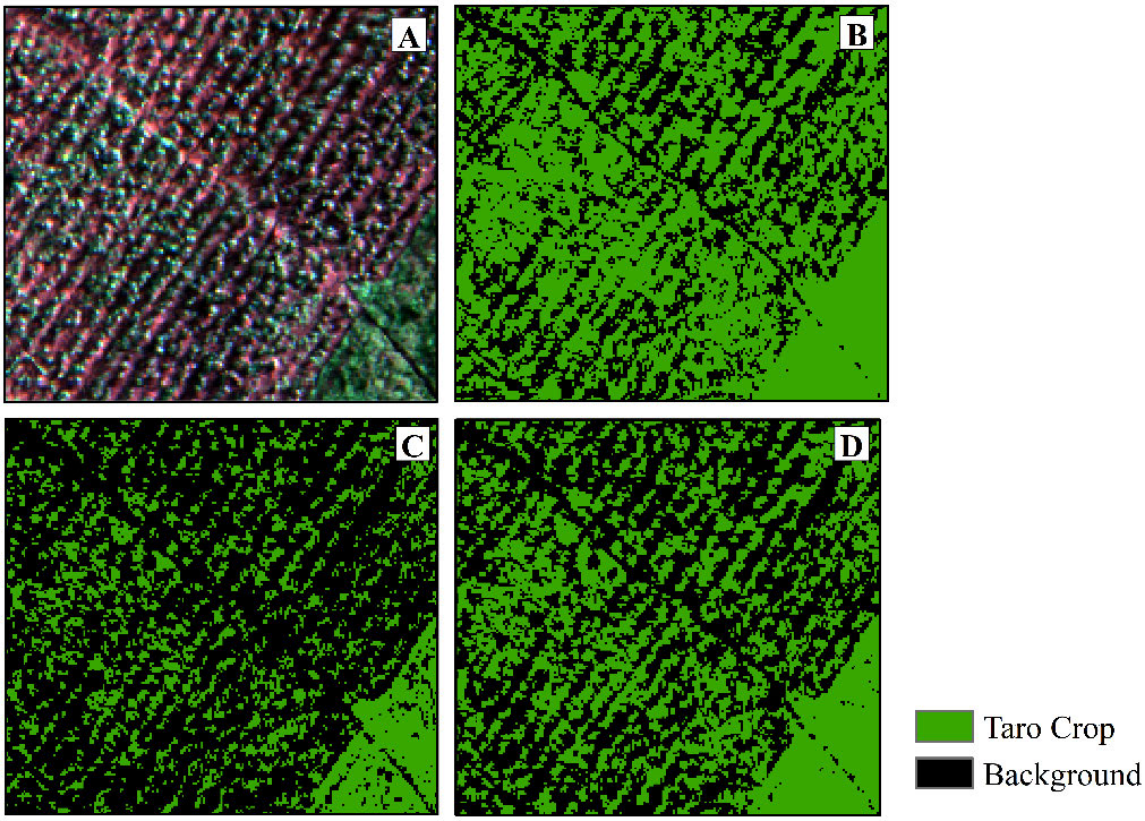

Figure 3.2 Taro crop canopy extraction: a) unsegmented UAV image, b) ExG, c) ExR and d) ExGR canopy extraction.

3.2.6 Model development and statistical analysis

This study employed a deep machine learning approach to estimate EWT_{canopy} using UAV derived multispectral optical and thermal datasets. Specifically, we utilised a Deep Neural Network (DNN), an artificial neural network characterised by multiple interconnected hidden layers (Traore *et al.* 2021). These hidden layers work in tandem to progressively learn higher-level features, facilitating the transformation of input data into meaningful output information (Chew *et al.* 2020; Bouguettaya *et al.* 2022). Unlike traditional machine learning techniques, which depend heavily on prior knowledge of parameters, DNNs utilise feature representations learned directly from the input dataset (Omosalewa *et al.* 2021). This unique approach allows the model to understand and capture complex non-linear relationships among variables, enhancing its ability to uncover intricate patterns and dependencies within the data (Omosalewa *et al.* 2021; Traore *et al.* 2021). Therefore, the combination of very-high resolution UAV multispectral-thermal imagery and sophisticated DNN architecture facilitated the precise and accurate estimation of EWT_{canopy} over smallholder taro farmland.

A three-layer neural network model, including an input layer, a hidden layer, and an output layer, was used in the study (Figure 3.3). A Rectified Linear Unit (ReLU) was applied to stimulate the EWT_{canopy} prediction model with the maximum epochs set to 200 interactions, indicating that the weights in the hidden layers were iteratively adjusted 200 times to reduce error and enhance EWT_{canopy} prediction accuracy. Following the use of the SoftMax activation function to convert the neural network's raw outputs into a vector of probabilities, the output model's performance was optimised using the Adaptive Moment Estimation (Adam) optimiser. Furthermore, the dropout regularisation technique was applied to avoid overfitting and improve the generalization of the model (Deepan and Sudha 2020). The hyperparameters of the DNN model were tuned to a learning rate of 0.001, batch size of 32 and an input and hidden layer dropout of 0.4 and 0.2, respectively. Lastly, the models were developed and adjusted using Python 3.8 within Anaconda Jupyter Notebooks.

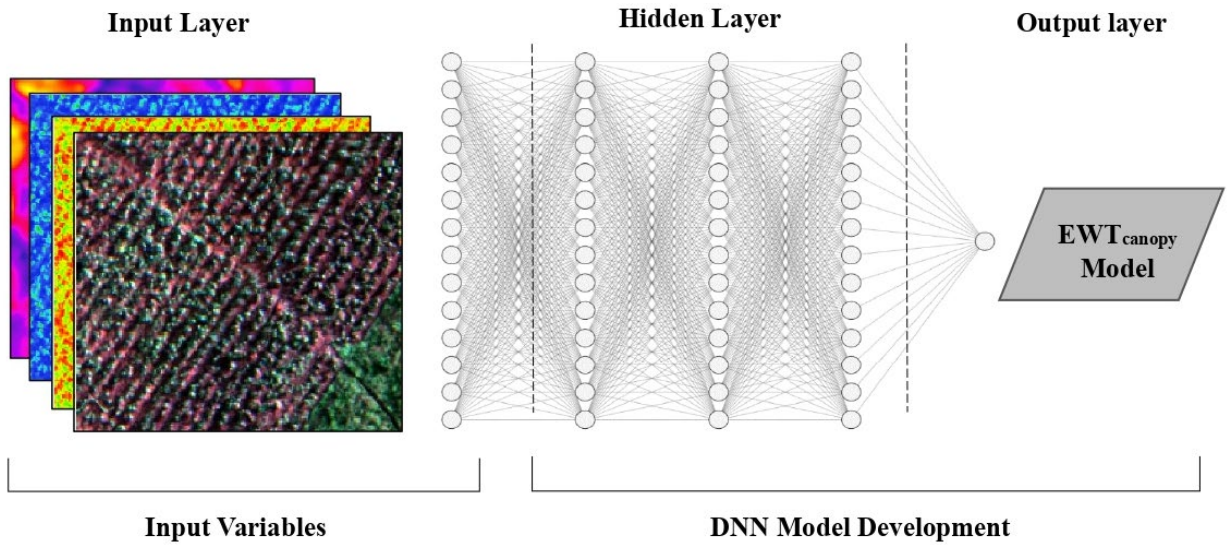

Figure 3.3 Graphical representation of the input, hidden, and output layer composition of the DNN structure.

3.2.7 Accuracy Assessment

To evaluate the performance EWT_{canopy} estimation model, the acquired dataset (n = 100) was divided into 70 % training data (n = 70) and 30 % testing data (n = 30). The training data was employed for the DNN model development, and the testing data used to assess the accuracy of the predictive model. The evaluation metrics included the Coefficient of Determination (R^2), the Root Mean Square Error (RMSE), and the Relative Root Mean Square Error (rRMSE). The

R^2 measures the variance between the in-situ measured and estimated taro EWT_{canopy}, while the RMSE assesses the magnitude of error between the field measurements and the modelled EWT_{canopy} field. Lastly, the rRMSE was used to compare the DNN model accuracies across the different image analysis techniques. The statistical indices are presented as follows:

$$R^2 = \frac{\left[\sum_{i=1}^{n}(y_i - \bar{y_i})\left(\hat{y_i} - \overline{\hat{y_i}}\right)\right]^2}{\left[\sum_{i=1}^{n}(y_i - \bar{y_i})^2 \sum_{i=1}^{n}\left(\hat{y_i} - \overline{\hat{y_i}}\right)^2\right]} \quad (5)$$

$$RMSE = \sqrt{\frac{1}{n}\sum_{i=1}^{n}(\hat{y_i} - y_i)^2} \quad (6)$$

$$rRMSE = \frac{RMSE}{\bar{y_i}} \times 100 \quad (7)$$

where $\hat{y_i}$ and y_i are the predicted and actual values; $\bar{y_i}$ and $\overline{\hat{y_i}}$ are the mean of the observed and predicted values, respectively; and *n* is the total number of data points. The higher the value of R^2, and the lower the values of RMSE and rRMSE, the greater the precision and accuracy of the EWT_{canopy} estimation model. The accuracy metrices were subjected to a statistical analysis using a Two-Way Analysis of Variance (ANOVA), in IBM SPSS software version 29.0.2, to assess the significant differences between the means of the prediction accuracies.

Lastly, the SHapley Additive exPlanations (SHAP) approach was used to assess the impact and contribution of predictor variables within the developed models. SHAP ranks the importance of model variables by calculating the average marginal contribution value of each predictor variable (Nahiduzzaman *et al.* 2023b). By leveraging the SHAP approach, a comprehensive understanding of the relative importance of each predictor variable is gained, enhancing the interpretability of the developed EWT_{canopy} estimation models. An overall workflow of this study is presented in Figure 3.4.

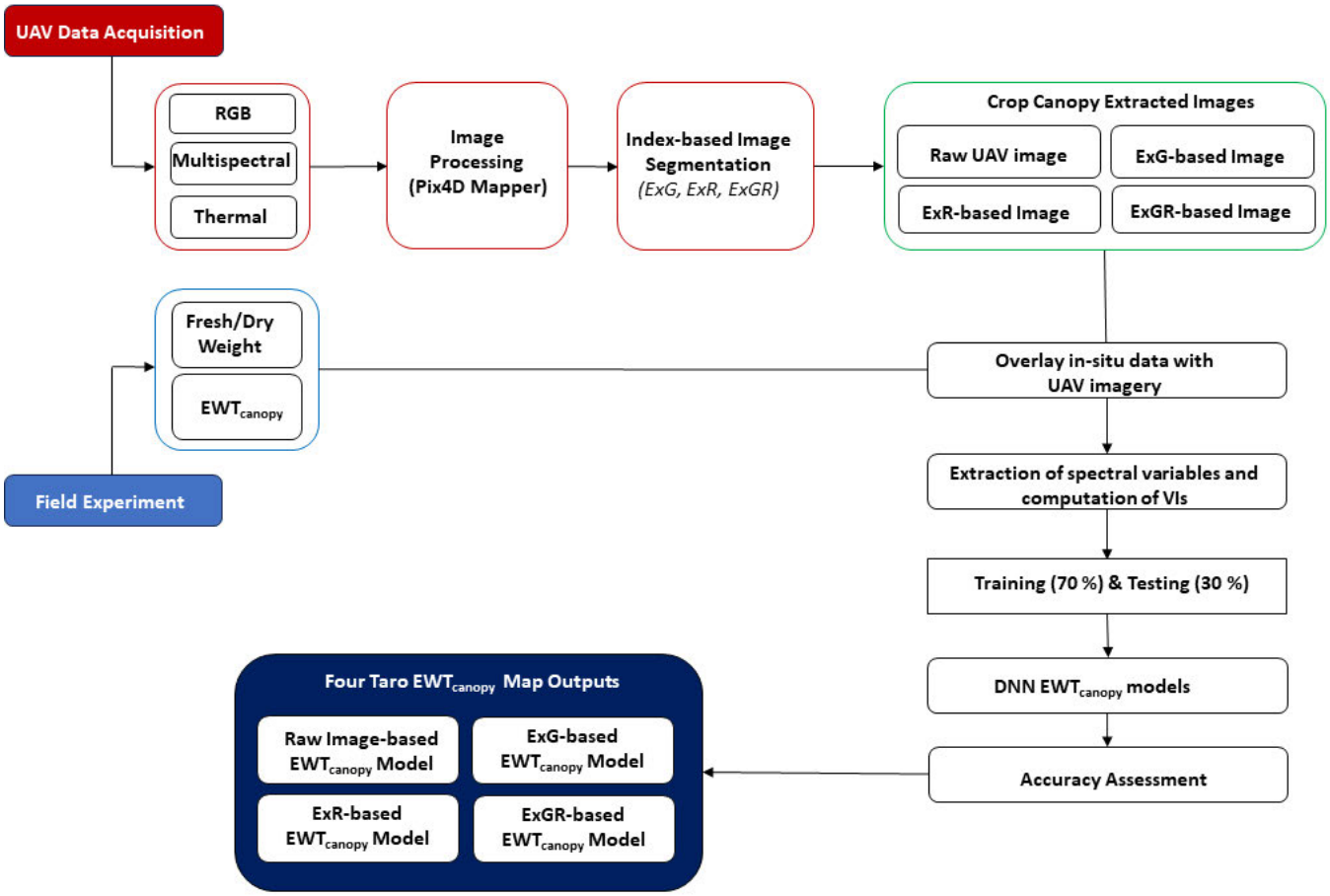

Figure 3.4 Workflow diagram for this study.

3.3 Results

3.3.1 Descriptive Statistics of In-situ EWT_{canopy} of taro crops

Table 3.2 presents the descriptive statistics of in-situ measurements of EWT_{canopy} across the taro field. A total of 100 samples (N) were collected during the peak vegetative growth stage. The mean and median of EWT_{canopy} were 60.90 g/m^2 and 47.70 g/m^2, respectively, with a Standard Error of Mean (SEM) of 4.45 g/m^2. A high spatial variability with a range of 8.72 g/m^2 – 220.77 g/m^2 was observed, underscoring the variability of crop water content across the sampled taro field. The Standard Deviation (Std.) was 44.49 g/m^2, and the Coefficient of Variation (CV) was 72.70 %.

Table 3. 2 Descriptive statistics of in-situ measured EWTcanopy of taro crops.

EWTcanopy (g/m^2)	n	Mean	Median	Minimum	Maximum	SEM	Std	CV%
Entire Dataset	100	60.70	47.70	8.72	220.77	4.45	44.49	72.70
Training Data	70	62.85	47.72	8.79	220.77	5.61	46.94	74.14
Testing Data	30	56.33	41.54	8.72	173.30	7.04	38.54	67.26

The standard error of the mean is denoted by SEM, the standard deviation by Std., and the coefficient of variation by CV.

3.3.2 Predicting EWT_{canopy} of taro crops using Deep Neural Network Algorithm and Image Segmentation Techniques

Figure 3.5 illustrates the model accuracies achieved in predicting taro EWT_{canopy} across the various index-based image segmentation techniques, including ExG, ExR, and ExGR crop canopy extraction applied to the unsegmented UAV imagery. Figure 3.5 a – d represents the prediction accuracies from the analysis conducted without the thermal band, while Figure 3.5 e - h illustrates the estimation accuracies based on models including the thermal band.

Generally, the exclusion of the thermal band resulted in relatively low model accuracies for all index-based segmentation methods. For instance, when estimating EWT_{canopy} based on the unsegmented UAV image, excluding the thermal band yielded a poor R^2 of 0.35, RMSE of 34.96 g/m^2 and rRMSE of 60.51 % (Figure 3.5a), with blue, green, red, TCARI, NIR, red-edge, NGRDI, CIrededge, NDVI and MCARI emerging as important predictor variables (Figure 3.6a). Meanwhile, the EWT_{canopy} estimation derived from the unsegmented UAV image, including the thermal band, resulted in moderately higher prediction accuracy of R^2 of 0.61, RMSE of 25.35 g/m^2, and rRMSE of 43.87% (Figure 3.5e). The most influential predictor variables were CIrededge, NDRE, blue, NGRDI, green, TCARI, thermal, NDWI, red-edge and NDVI, in descending order of importance (Figure 3.6e).

Overall, an increase in prediction accuracy was observed when index-based image segmentation techniques and thermal data were applied to the unsegmented UAV imagery. The ExR-based EWT_{canopy} model including the thermal band yielded an R^2 of 0.79, RMSE of 14.53 g/m^2 and rRMSE of 27.76 % (Figure 5g), while the ExG-based model including thermal achieved an R^2 of 0.90, RMSE of 10.69 g/m^2 and rRMSE of 18.82 % (Figure 5f). The most

important predictor variables were CIrededge, thermal, SAVI, red, and NIR, NGRDI, TCARI, blue, red-edge and NDWI for the ExR-based EWT_{canopy} model (Figure 3.5g), whereas the ExG-based model had CIrededge, TCARI, red, green, NGRDI, NDWI, thermal, red-edge, SAVI and blue band as the most influential predictor variables (Figure 3.55f). The ExGR-based EWT_{canopy} model, including thermal, exhibited the highest prediction accuracy, achieving an optimal R^2 of 0.92, RMSE of 8.04 g/m^2 and rRMSE of 15.31 %, based on TACRI, CIrededge, MCARI, NGRDI, NDWI, blue, red-edge, red, thermal and NDVI variables, in descending order of importance (Figure 3.5h & 3.6h).

Overall, the fitting degree between EWT_{canopy} ExGR-based model (R^2 = 0.92) was significantly higher than that of the unsegmented UAV image (R^2 of 0.61). By applying the ExGR technique and including the thermal band, the prediction accuracy of target taro EWT_{canopy} was significantly improved. These outcomes underscore the efficacy of the DNN model, particularly when integrated with thermal data and advanced image segmentation approaches in enhancing the precision of EWT_{canopy} estimations for taro crops.

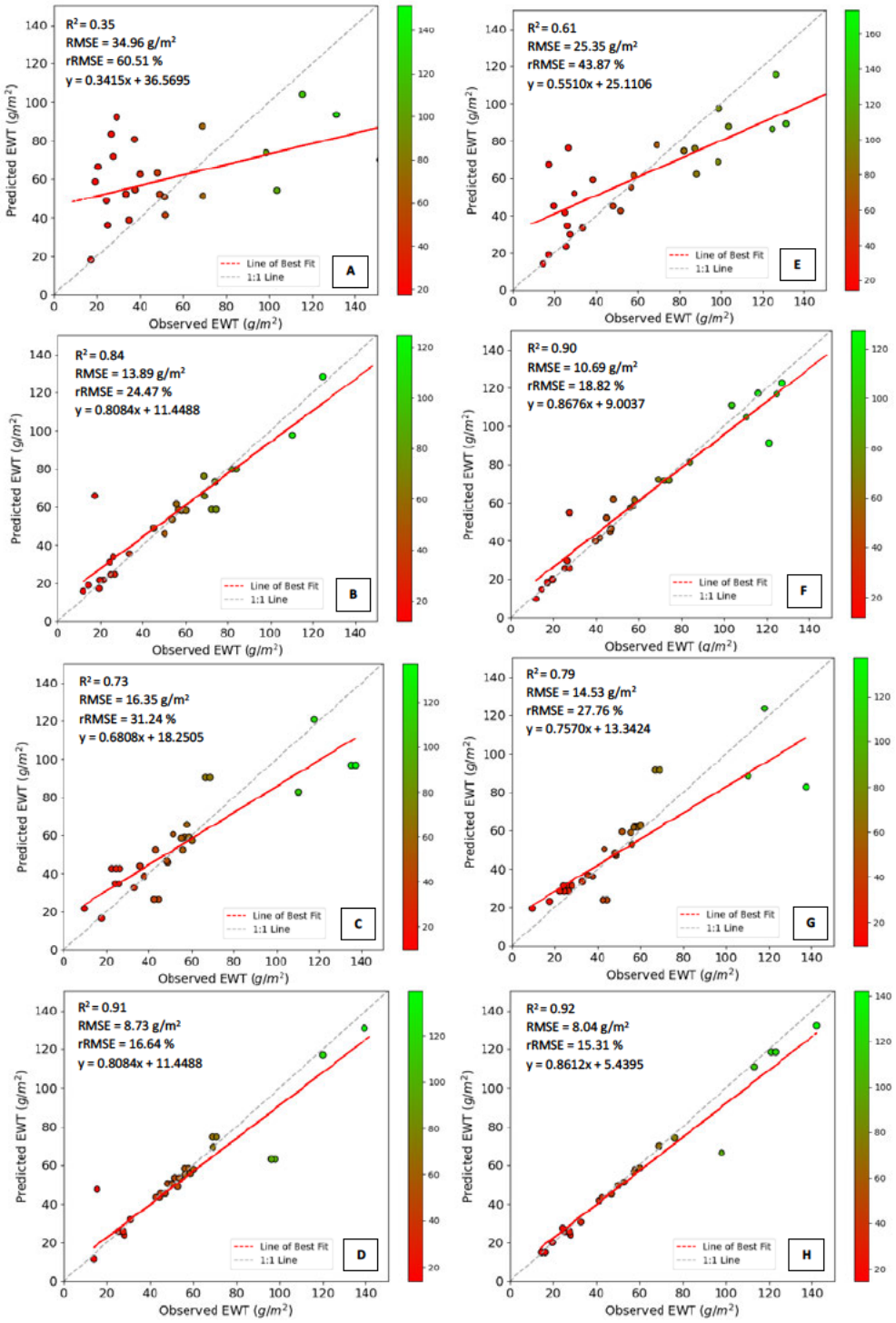

Figure 3.5 Relationship between the predicted and observed EWTcanopy based on the a) unsegmented UAV image excluding thermal, b) unsegmented UAV image including thermal, c) ExG excluding thermal, d) ExG including thermal e) ExR excluding thermal, f) ExR including thermal, g) ExGR excluding thermal and h) ExGR including thermal.

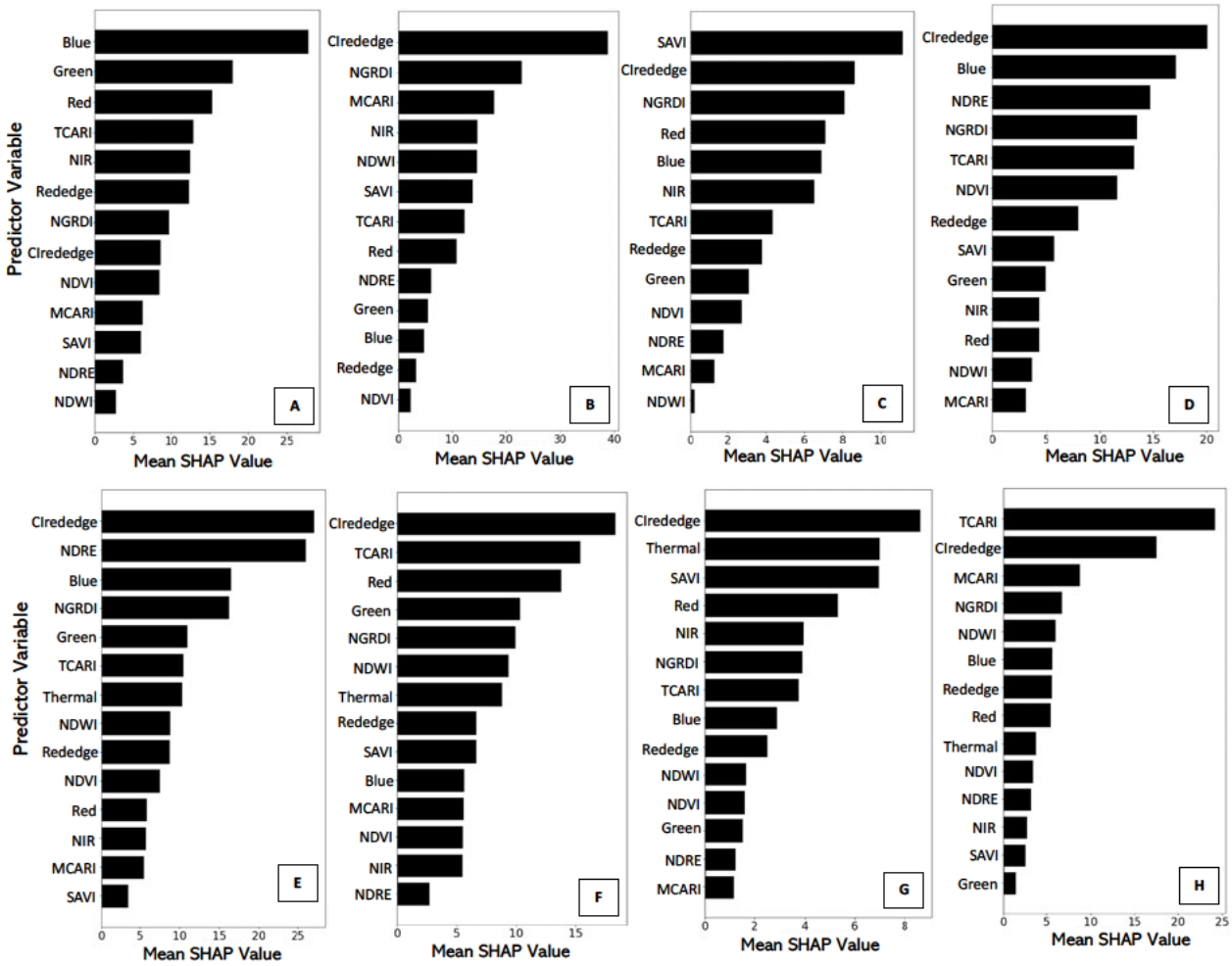

Figure 3.6 SHAP generated variable importance of predictor variables in estimating EWTcanopy based on the a) unsegmented UAV image excluding thermal, a) unsegmented UAV image including thermal, c) ExG excluding thermal, d) ExG including thermal e) ExR excluding thermal, f) ExR including thermal, g) ExGR excluding thermal and h) ExGR including thermal.

3.3.3 Assessment of the influence of the thermal band in conjunction with the Deep Neural Network Algorithm

Generally, excluding the thermal band resulted in comparatively lower model accuracies across the index-based segmentation methods. This pattern is consistent across the R^2, RMSE and rRMSE metrics for all segmentation techniques, with generally higher estimation accuracies achieved when the thermal band is considered in the taro EWT_{canopy} analysis. To investigate the impact of including the thermal band on prediction accuracies, an ANOVA test was conducted to assess differences in accuracy among segmentation techniques and the presence or absence

of the thermal channel. The two-way ANOVA revealed a significant interaction between prediction accuracies and segmentation techniques based on the inclusion and exclusion of the thermal band, implying that the trends of variation of parameters change with the inclusion of the thermal band and different segmentation techniques. This suggests that variations in prediction accuracies exhibit different trends depending on whether the thermal band is incorporated, and distinct segmentation techniques are employed. Statistical significance was observed in the accuracies of predicting EWT_{canopy} across all segmentation techniques ($P < 0.05$) (Figure 3.7 (A-C)). Additionally, significant differences in prediction accuracies ($P < 0.001$) were noted between the inclusion and exclusion of the thermal band across segmentation methods (Figure 3.7 (D-F)). The Segmentation factor, Thermal Band factor, and their interaction significantly contributed to the differences in R^2, RMSE and rRMSE (Figure 3.7). However, no significant difference in prediction accuracies was observed for the inclusion and exclusion of thermal characteristics for the ExGR-based technique. The ExGR data was the most optimal model, exhibiting an R^2 of 0.92, RMSE of 8.04 g/m^2 and rRMSE of 15.31 % with the thermal band (Figure 3.5 H), and achieving an R^2 of 0.91, RMSE of 8.73 g/m^2 and rRMSE of 16.64 %, even with the exclusion of the thermal band (Figure 3.5 D). Following the optimal performance of models that were based on the index-based image segmentation methods in conjunction with the thermal band, these models were adopted in mapping the spatial distribution of EWT_{canopy} in the study area.

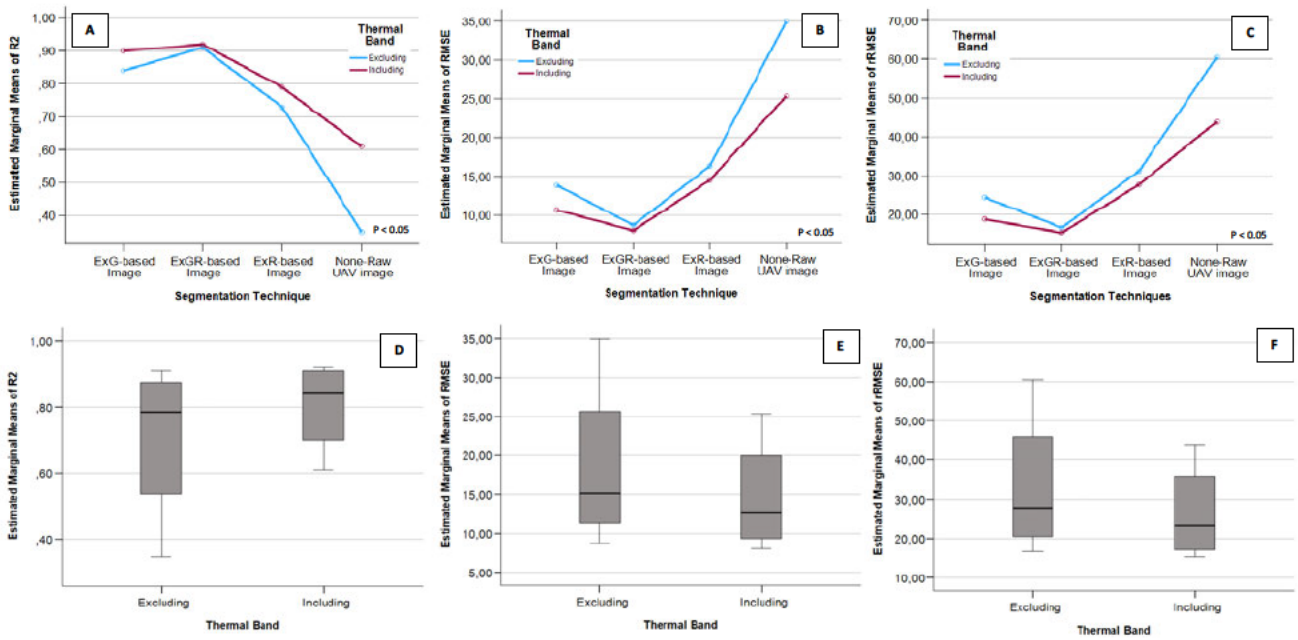

Figure 3.7 Comparative analysis of mean performance metrics, including a) R^2, b) RMSE and c) rRMSE across segmentation techniques between the inclusion and exclusion of the thermal band and overall mean d) R^2, e) RMSE and f) rRMSE obtained between including and excluding the thermal band.

3.3.4 Spatial Distribution of EWT_{canopy} of smallholder taro crops

Figure 3.8 presents the spatial distribution of estimated EWT_{canopy} using UAV-acquired multispectral thermal data as well as using the different image segmentation techniques, including ExG, ExR, and ExGR crop canopy extraction applied to the unsegmented UAV imagery. While the unsegmented UAV image achieved moderate prediction accuracy, this approach could not accurately assign EWT_{canopy} because of the overfitting problem (Figure 3.8a). On the contrary, the ExGR-based EWT_{canopy} model produced results close to the observed EWT_{canopy} within the taro field and achieved the highest accuracy in visual comparison (Figure 3.8d). Similarly, the ExG-based EWT_{canopy} model demonstrated comparable results in capturing the spatial distribution of EWT_{canopy} of taro crops (Figure 3.8d). A general trend was observed in the southwestern area (high elevation) of the field exhibiting higher EWT_{canopy} estimates in relation to the eastern parts (Figure 3.8).

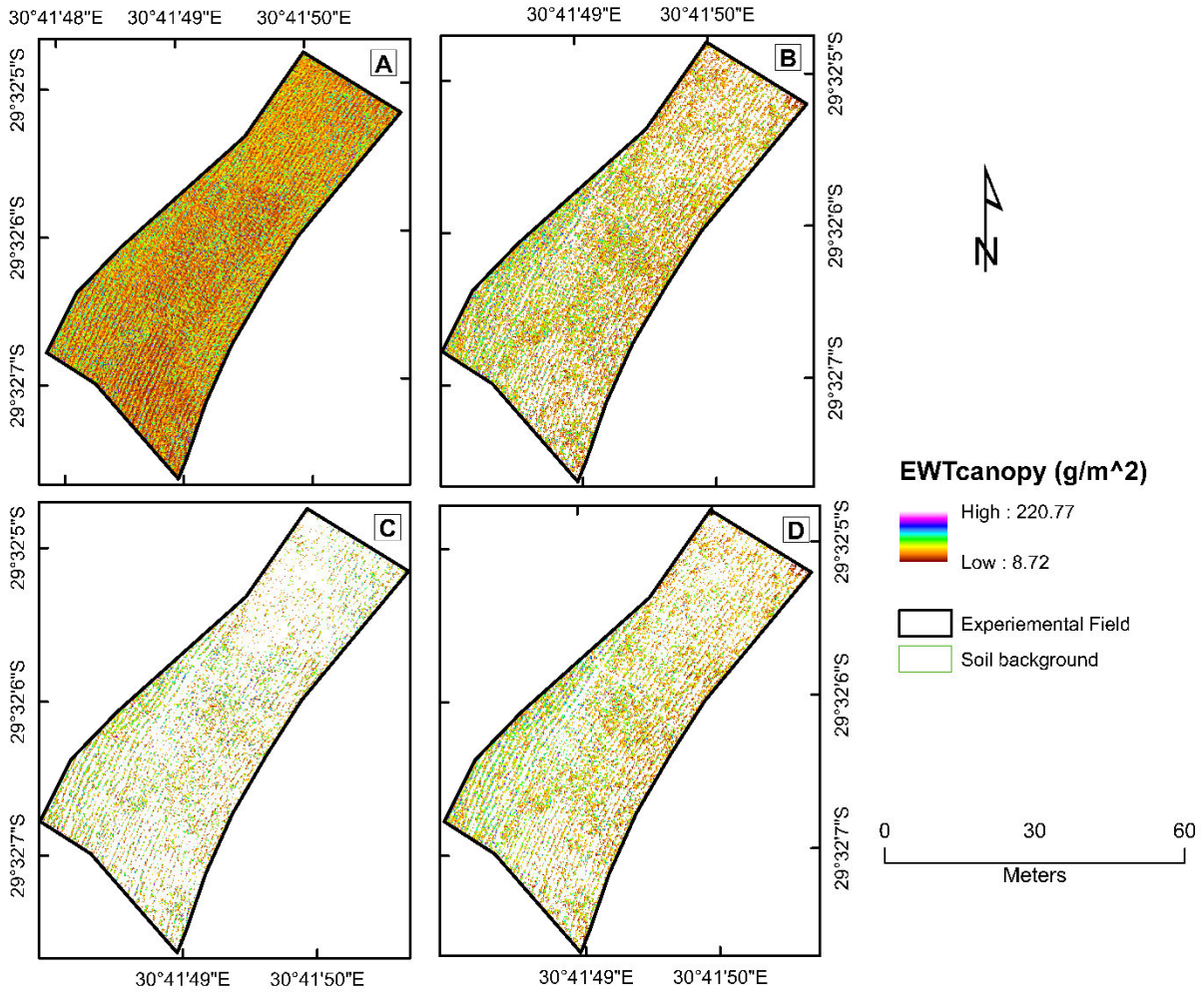

Figure 3.8 Spatial distribution of EWT_{canopy} within the taro field based on the a) unsegmented UAV image, b) ExG, c) ExR and d) ExGR canopy extraction techniques.

3.4 Discussion

This study aimed to assess the application of thermal remote sensing and index-based segmentation techniques in enhancing the estimation of EWT_{canopy} in a smallholder taro farm. Specifically, the study investigated the capability of the UAV thermal band in estimating the EWT_{canopy} of taro crop. Additionally, this study assessed the influence of soil background removal using ExG, ExR and ExGR segmentation indices in enhancing the prediction accuracy of taro EWT_{canopy}. Furthermore, the research sought to explore the capabilities of UAV-acquired multispectral and thermal data predicting EWT_{canopy} of taro crops.

3.4.1 Prediction of EWT_{canopy} using UAV multispectral thermal imagery

The findings of this study showed a wide variety of EWT_{canopy} measured within the taro field, ranging from 8.72 g/m^2 to 220.77 g/m^2 with the highest values recorded at the lower elevations of the field. This spatial variability can generally be attributed to water drainage and accumulation, particularly the gravity-driven flow that tends to accumulate at lower elevations. This fosters a wetter environment that enhances soil moisture availability for crops in the area, leading to higher EWT_{canopy} values. A study by Basile *et al.* (2020) also confirmed the contribution of topographic characteristics, such as slope on crop water status, with down-slope soils exhibiting higher water retention capacity that increases water available to the crop. Therefore, future studies should consider quantifying the relative contribution of topography on the spatial variability of crop moisture content within small-scale farming systems.

The results of this study also showed that taro EWT_{canopy} could be optimally estimated using the ExGR segmentation method, including thermal (R^2 = 0.92, RMSE = 8.04 g/m^2 and rRMSE = 15.31 %), with the most influential variable being TACRI, CIrededge, MCARI, NGRDI, NDWI, blue, red-edge, red, thermal and NDVI (Figure 3.6). These findings demonstrated the sensitivity of EWT_{canopy} to the NIR and red-edge sections of the electromagnetic spectrum. Literature has confirmed that the NIR section is effective in characterizing crop water status, attributed to its high water absorption capacity that enables the detection of variations in crop water content through changes in canopy reflectance under different water statuses (Pasqualotto *et al.* 2018; El-Hendawy *et al.* 2019; Brewer *et al.* 2022b). The importance of red-edge-based indices such as TCARI, CIrededge and MCARI is attributed to the unique properties of the red-edge region, which is particularly sensitive to subtle changes in vegetation structure and leaf pigmentation due to water stress, hence invaluable for assessing crop water status (Ballester *et al.* 2019; Colovic *et al.* 2022). The results of this study further reported indices such as CIrededge and TCARI among the influential variables in estimating EWT_{canopy} of taro crops (Figure 3.6). These findings are consistent with Zhang and Zhou (2019a) and Colovic *et al.* (2022) that demonstrated the CIrededge to be sensitive to variations in crop water conditions and highly influenced by changes in irrigation treatments. Similarly, Baluja *et al.* (2012a) identified TCARI as a valuable predictor variable of vineyard water status, yielding an optimal correlation of R^2 of 0.80.

3.4.2 Performance of the thermal band in predicting EWT_{canopy} of taro crops

The performance of the thermal band in predicting EWT_{canopy} of taro crops revealed a consistent trend across the various index-based segmentation techniques. It was observed that the exclusion of the thermal band in EWT_{canopy} analysis resulted in lower estimation accuracies ($P < 0.05$), emphasising the importance of the thermal band in characterising taro crop water status (Figure 3.7). Surprisingly, our study found no significant difference in prediction accuracies when thermal data was considered in comparison to its exclusion in the ExGR-based model. This unexpected finding suggests that the ExGR technique has a superior ability to isolate the taro canopy and reduce background interference, enabling multispectral data alone to capture sufficient spectral information related to EWT_{canopy} variations. Consequently, the added value of thermal data in this context appears diminished compared to other segmentation methods.

Additionally, it was observed that the thermal band was among the topmost predictor variable across all EWT_{canopy} models. Literature confirms the invaluable role of thermal infrared remote sensing in assessing and monitoring crop water status, establishing a direct correlation with crop water biophysical and biochemical elements (Khanal *et al.* 2017; Messina and Modica 2020; Krishna *et al.* 2021). The use of thermal remote sensing is based on the premise that the thermal characteristics of crop leaves are affected by leaf transpiration, which decreases in a state of water deficit, resultantly reducing leaf and canopy temperatures (Maes and Steppe 2012; Gerhards *et al.* 2019). The findings of this study align with a recent study by Guan and Grote (2023), which achieved an R^2 of 0.74 when incorporating the thermal channel, compared to an R^2 of 0.63 with the thermal band excluded, highlighting the integration of multispectral and thermal data and its combined value in understanding crop water status. These findings are further corroborated by García-Tejero *et al.* (2018), who concluded that the thermal band is feasible for monitoring almond water stress for irrigation scheduling, and Cheng et al. (2023), who highlighted the applicability of thermal imaging in assessing the crop water conditions of summer maize crop.

In concert, these results indicate that while thermal imagery generally enhances $EWTc_{anopy}$ prediction, its contribution depends on the segmentation method employed. The robustness of the ExGR segmentation in effective background exclusion reduces reliance on thermal data, suggesting that the importance of thermal bands should be carefully interpreted relative to the segmentation approach used. Further studies are recommended to evaluate this

interaction across different crops, environmental conditions, and segmentation workflows to better understand when thermal data provides substantial incremental value.

3.4.3 Performance of index-based segmentation techniques for the estimation of taro EWT_{canopy}

This study showed that the inclusion of soil background reduces the accuracy of EWT_{canopy} predictions within taro crop (R^2 of 0.61, RMSE of 25.35 g/m^2, and rRMSE of 43.87%). It was noted that the prediction accuracy of taro EWT_{canopy} improved significantly after the removal of soil background through the ExGR-based image segmentation technique, yielding an optimal R^2 of 0.92, RMSE of 8.04 g/m^2 and rRMSE of 15.31. These results align with the broader consensus in the literature. Xu *et al.* (2021) and Li *et al.* (2022d) for instance emphasised the challenge posed by soil background in influencing crop canopy spectra, particularly in UAV-derived imagery. Notably, while the ExG and ExR techniques demonstrated acceptable accuracy in quantifying taro EWT_{canopy} (R^2 of 0.90, and R^2 of 0.76, respectively), the ExGR method outperformed both these techniques. This notable enhancement can be attributed to the inherent capabilities of the ExGR technique in effectively mitigating soil background interference (Zhai *et al.* 2023). The comprehensive nature of the ExGR method combines the advantages of both the ExG and ExR by simultaneously leveraging ExG for extracting the crop canopy and ExR for eliminating background noise (Meyer *et al.* 2004; Hamuda *et al.* 2016; Riehle *et al.* 2020; Upendar *et al.* 2021).

Overall, the removal of soil background has proven imperative for enhancing the accuracy of taro EWT_{canopy} predictions. These results are further supported by Shu *et al.* (2021) who observed a significant increase in prediction accuracy from R^2 of 0.45 and RMSE of 7.13 before to an R^2 of 0.74 and RMSE of 3.68 after performing soil background removal in estimating the SPAD chlorophyll content of a maize crop. These parallel findings underscore the significance of addressing soil background interference for accurate and reliable estimations in crop water-related assessments.

Lastly, it is important to note that while the ExGR segmentation method demonstrated superior performance in this study by effectively isolating the taro canopy and minimizing soil background interference, its effectiveness may vary under different conditions. Factors such as crop type, variations in soil colour and texture, as well as changing lighting and environmental

conditions, can influence the accuracy of ExGR-based segmentation (Hamuda *et al.* 2016; Hernández-Hernández *et al.* 2016; Sabzi *et al.* 2018). Therefore, further research should aim to assess the ExGR method across diverse crops, backgrounds, and illumination scenarios to establish its broader applicability and generalizability across other cropping systems.

3.4.4 Implications of the study, limitations and recommendations for future research

The results of this study underscore the significant potential accurately assessing and monitoring the EWT_{canopy} of taro in smallholder rainfed croplands using UAV-derived multispectral-thermal and the ExGR image segmentation. The value of UAV thermal band in this study highlights its significance in enhancing the precision of EWT estimations for taro crops. The application of UAV-based multispectral and thermal data offers exceptional accuracy in predicting taro water status, providing valuable insights into smallholder taro farming practices. These findings emphasise the significance of precision agricultural technologies, particularly UAVs, in enhancing smallholder agricultural management. The near-real-time capabilities of UAV-derived data enable rapid and effective decision-making, contributing to improved crop health and productivity, particularly of NUS crops such as taro. Despite the promising outcomes, it is worth noting the limitations. The high spatial resolution provided by the UAV onboard sensor contrasts with limitations in spectral resolution, constraining the available multispectral bands and derived vegetation index options. Additionally, while the study employed high-precision GPS system, with up to centimeter accuracy, careful consideration is essential during the sampling procedure to maintain precision and accuracy of sample locations. Furthermore, to advance the understanding of crop water status, future studies should explore indicators beyond EWT, including stomatal conductance and more detailed assessments of canopy temperature, incorporating thermal-related indices. Further research should also consider integrating structural features, such as crop cover, plant height, chlorophyll content, and topographic variables including aspect, slope and elevation, to enhance the precision of crop water predictions. Additionally, exploring alternative image segmentation techniques can contribute to refining the accuracy and applicability of the models.

3.5 Conclusion

This study assessed the applicability of thermal remote sensing and index-based segmentation techniques in predicting EWT_{canopy} in smallholder taro farmlands. The results showed that UAV thermal data integrated with multispectral data and the ExGR segmentation technique is optimal for estimating EWT_{canopy} of taro crops. Based on the findings of this study, it can be concluded that:

- The exclusion of the thermal band in EWT_{canopy} estimations reduces the prediction accuracies of taro water status.
- The ExGR segmentation technique proved most effective in extracting crop canopy spectra and removing soil background, thereby enhancing the prediction accuracies of taro EWT_{canopy}.
- The NIR, red-edge, and thermal sections of the electromagnetic spectrum were identified as most influential in estimating EWT_{canopy} of taro crops.

These results highlight the potential of near-real-time spatial information provided by UAV proximal remote sensing techniques for evaluating the crop water status of smallholder NUS taro crops. The results of this study will aid the development of an accurate and reliable monitoring framework for taro water status that is spatially explicit, filling the knowledge gap essential for integrating taro into sustainable agricultural practices. The findings serve as a steppingstone to improved agricultural management practices and resource optimization in small-scale cultivation of NUS crops, aligning with the ongoing efforts to bridge the gap between research and practical implementation. Therefore, the insights gained from this study are imperative for decision-makers aiming to streamline NUS crops, particularly taro, into existing agricultural systems, thereby enhancing food security and promoting resilient farming practices in diverse agroecological environments.

3.6 Summary

Chapter Three demonstrated the effectiveness of UAV thermal data, integrated with image segmentation techniques, in significantly enhancing the estimation of equivalent water thickness in smallholder taro crops. The findings highlighted the efficacy of the Excess Green minus Excess Red segmentation method in improving the prediction accuracy of taro equivalent water thickness estimations, serving as a foundational metric setting for refining crop water status assessments. Chapter Four builds on these findings by evaluating the utility of remotely sensed thermal and multispectral data for high-throughput crop phenotyping of additional crop

water physiological indicators, including stomatal conductance, leaf temperature, fuel moisture content and chlorophyll content.

CHAPTER FOUR

Assessing Neglected and Underutilised Taro Crop Water Status using Physiological Indicators and UAV Multi-Modal Thermal-Multispectral Data

This chapter is based on:

Ndlovu, H. S., Odindi, J., Sibanda, M., & Mutanga, O. (2024). Assessing Neglected and Underutilised Taro Crop Water Status using Physiological Indicators and UAV Multi-Modal Thermal-Multispectral Data. *Precision Agriculture*, Under Review, Manuscript ID: PRAG-D-24-01162

Abstract

Taro (*Colocasia esculenta* (L)), a neglected and underutilised crop species, holds great potential as a future smart crop that can thrive under climate variability and change, hence sustaining food security. While taro exhibits tolerance to drought conditions, variations in physiological attributes such as leaf temperature that rises under water stress and the associated stomatal closure initiated to conserve water, compromise crop productivity and overall yield. Therefore, monitoring taro crop physiological indicators of water status allows the implementation of timely interventions and targeted adaption strategies to mitigate the effects of water deficit on taro crop productivity. Unmanned Aerial Vehicles (UAV), integrated with high-resolution thermal sensors, provide valuable platform for generating near-real-time spatially explicit information suitable for assessing taro crop water status physiological indicators at farm scale. Hence, this study sought to evaluate the utility of UAV multi-modal thermal remote sensing and deep neural network techniques to estimate the equivalent water thickness, fuel moisture content, stomatal conductance, canopy temperature, and chlorophyll content of smallholder taro crops. Findings showed that the multi-modal variable method achieved higher estimation accuracies in comparison to a single-modal technique, with R^2 values greater than 0.91 and rRSME values less than 14.15% of equivalent water thickness, fuel moisture content, stomatal conductance, canopy temperature, and chlorophyll content. Additionally, the results illustrated that the thermal wavebands and derived thermal indices were the most influential variables in estimating stomatal conductance and leaf temperature, yielding R^2 of 0.96 and 0.95, respectively. Although not among the top predictors, the thermal spectral variables proved valuable in estimating equivalent water thickness and fuel moisture content, resulting in increased prediction accuracies from R^2 = 0.73, rRMSE =33.82 % to R^2 = 0.95 and rRMSE = 14.15 % for equivalent water thickness, and R^2 = 0.77 and rRMSE = 6.55 % to R^2 = 0.94 and rRMSE = 3.32 % for fuel moisture content. These research findings underscore the applicability of UAV-acquired thermal remote sensing in providing rapid and robust spatially explicit information on smallholder taro crop water status for ensuring crop productivity and developing early warning systems of water stress. These findings serve as a stepping stone towards advancing agricultural monitoring frameworks and integrating neglected and underutilised crop species such as taro into traditional farming landscapes.

Keywords: Thermal remote sensing, unmanned aerial vehicles, deep neural network, neglected and underutilised crop species

4.1 Introduction

Neglected and Underutilised Crop Species (NUS) have emerged as vital assets in sustainable agricultural practices, offering opportunities to diversify cropping systems and enhance resilience, in light of the escalating climate change impacts and the need to ensure food security (Chivenge *et al.* 2015; Popoola *et al.* 2019; Mugiyo *et al.* 2021a). In developing regions such as southern Africa, where pre-existing challenges of hunger and nutrition insecurity persist, the cultivation of NUS, commonly confined to smallholder farms, plays a critical role in sustaining local food security (Chivenge *et al.* 2015; Kapari *et al.* 2023). Despite contributing approximately 80% of food production, smallholder farmers are disproportionately susceptible to the effects of climate change and frequently experience periods of water stress and drought, leading to substantial crop yield losses (Gomez y Paloma *et al.* 2020; Hlophe-Ginindza and Mpandeli 2020). Taro (*Colocasia esculenta* (L)), renowned for its drought and heat tolerance, holds great potential as a future smart crop capable of thriving in diverse agroecological environments (Mabhaudhi and Modi 2015; Oyeyinka and Amonsou 2020; Talucder *et al.* 2024). Locally (South Africa) referred to as *amadumbe*, taro has garnered significant attention as a priority crop due to its resilience to drought and heat stress and edible tubers of high nutritional value (Mabhaudhi *et al.* 2017a; Munialo *et al.* 2024). Despite its promising attributes, there is a dearth in literature on its crop water status variations, hindering a comprehensive understanding of its adaptive capabilities. Therefore, research on taro water status becomes imperative for optimizing its productivity and as a step towards integrating into the mainstream agricultural systems.

Understanding the variations of taro crops' physiological indicators in response to water deficit is essential for designing and implementing effective crop water stress management strategies (Huang *et al.* 2020; Parkash and Singh 2020). During periods of water deficit, plants undergo a variety of physiological changes aimed at conserving water and mitigating stress (Shafiq *et al.* 2019; Wang *et al.* 2022a). For example, stomatal conductance, the measure of gas exchange through leaf stomata, typically decreases under water stress conditions as plants close their stomata to reduce water loss through transpiration (Gerhards *et al.* 2019; Wang *et al.* 2022a). This decrease limits carbon dioxide uptake for photosynthesis, leading to reduced plant

productivity and growth (Ahmad *et al.* 2021). Also, chlorophyll content, essential for absorbing light energy during photosynthesis, declines due to the detrimental effects of water stress on the chloroplast membrane and photo-oxidation (Shafiq *et al.* 2019; Parkash and Singh 2020). Meanwhile, leaf temperature, influenced by evaporative cooling processes, often increases under water stress as plants close their stomata to conserve water, resulting in reduced transpiration cooling (Gerhards *et al.* 2019; Parkash and Singh 2020). Then, equivalent water thickness and fuel moisture content, reflecting the moisture levels within plant tissues, typically decrease during water stress as plants experience dehydration (Ahmad *et al.* 2021; Ndlovu *et al.* 2024b). Therefore, by monitoring the variations in these physiological indicators, we can effectively quantify crop water status and implement timely interventions to mitigate the impacts of water deficit on taro crop productivity. Although traditional methods of retrieving crop water status physiological indicators are accurate, these techniques are labour-intensive, time-consuming, and generally rely on exhaustive chemical analysis (Yin *et al.* 2023). Moreover, these measurements are prone to inaccuracies and do not sufficiently indicate the spatial variability of crop water status across the entire field (Mobasheri and Fatemi 2013b; Traore *et al.* 2021).

Thermal remote sensing has proven to be a robust tool for assessing crop water status and related physiological indicators due to its inherent ability to detect subtle variations in surface temperature, which are indicative of crop water status (Khanal *et al.* 2017; Awais *et al.* 2022a). By capturing thermal emissions from the Earth's surface, thermal sensors provide valuable insights into crop water status and related heat dissipation processes influenced by transpiration, evaporation, and plant water uptake dynamics (Gerhards *et al.* 2019; Zhai *et al.* 2023). Satellite-based thermal sensors, such as Landsat Thermal Infrared Sensor (TIRS), Advanced Spaceborne Thermal Emission and Reflection Radiometer (ASTER) and the Ecosystem Spaceborne Thermal Radiometer Experiment on Space Station (ECOSTRESS) have been instrumental in regional-scale crop water status assessments (Gerhards *et al.* 2019; Awais *et al.* 2022a). Despite their utility, satellite-based thermal sensors are restricted by their coarse spatial resolution, which limits the characterization of crop water status at a field scale (Khanal *et al.* 2017). Consequently, alternative approaches are necessary to capture finer-scale variations in crop water status and facilitate precision agricultural practices.

In recent years, advancements in earth observation technologies, specifically the use of Unmanned Aerial Vehicles (UAVs) equipped with multi-modal thermal multispectral sensors,

have revolutionised the characterization of crop water status and associated physiological indicators, particularly at local scales (Hussain *et al.* 2020). UAVs, equipped with very-high-spatial resolution sensors of up to sub-centimetre precision, enable the precise assessment of crop water status at a field scale (Chivasa *et al.* 2020). In comparison to satellites, UAVs offer flexibility in flight planning, and the ability to capture data on-demand, making them ideal for monitoring crop physiological dynamics such as taro crop water stress in fragmented heterogeneous smallholder agricultural systems (Zhu *et al.* 2021b). This is demonstrated by studies such as Marques *et al.* (2020) that utilised UAV-acquired thermal data to characterise the stomatal conductance and relative water content of a commercial olive orchard and studies by Han *et al.* (2021) that achieved an optimal R^2 value of 0.96 in estimating the canopy temperature of apple trees using UAV thermal imagery.

The integration of UAVs with machine learning methods, particularly deep learning approaches such as Deep Neural Networks (DNNs), has further enhanced the analysis of remotely sensed agricultural data (de Melo *et al.* 2022). The DNN algorithm is robust in characterizing complex relationships allowing for more accurate prediction of crop attributes, including water status (Omosalewa *et al.* 2022; Rajwade *et al.* 2023). Despite these advantages, the integration of DNN algorithms with UAV thermal remote sensing for field-scale crop monitoring, particularly on crop water variability remains elusive. Such integration could offer scalable insights into spatial crop water variability that are critical for improving water use efficiency and guiding precision interventions. As a result, there is need for further research to fully exploit and incorporate the capabilities of DNN algorithms into precision agricultural applications. Therefore, this study aimed to leverage the capabilities of UAV multi-modal thermal multispectral remote sensing and deep neural network techniques to assess the crop water status of neglected and underutilised smallholder taro crop. Specifically, the objectives of this study were to: (1) evaluate the performance of selected thermal and multispectral variables, along with their derived indices, in estimating the status of crop water physiological indicators (i.e. equivalent water thickness, fuel moisture content, stomatal conductance, canopy temperature, and chlorophyll content), and (2) optimise prediction models by utilizing optimal multi-modal variables derived from UAV-acquired thermal multispectral data.

4.2 Materials and Methods

4.2.1 Study area description and the experimental field

This study was conducted in a smallholder taro crop field located in Swayimane (- 29.534951; 30.697113), a rural community situated within the uMshwathi Municipality, Pietermaritzburg, South Africa (Figure 4.1). The area is predominantly characterised by smallholder agriculture, where maize, sugarcane, sweet potatoes, and taro are the primary crops cultivated in smallholdings (Sibanda *et al.* 2023). Within these farming systems, smallholder farmers practice traditional farming methods characterised by manual sowing of crop seeds, hand-weeding and use of cow manure. The yield from the croplands provides sustenance for the local community and is also marketed domestically, thereby contributing to local food security and livelihoods. Swayimane's crop production benefits from the area's climatic conditions of warm, humid summers and cool, arid winters. The area experiences an average temperature ranging from 11.8 ℃ to 24 ℃ annually, with precipitation averaging between 600 and 1200 mm per year (Gokool *et al.* 2024; Kapari *et al.* 2025). Majority of the rainfall across the study area is concentrated during the summer months, providing essential moisture for agricultural activities. The research focused on a smallholder taro field measuring 30 × 96 meters (2850 m^2), which was planted during the rainy season in October 2022. This taro cropland primarily relies on rainfall for irrigation and was approximately 171 days old at the time of the study. For this study, the transitional phase between the vegetative and late vegetative stages of the crop's development was considered. This phenological stage was chosen because it enabled the capture of changes occurring during a period of peak canopy growth, as it is the most critical growth stage when the crop is most susceptible to moisture stress that influences its productivity.

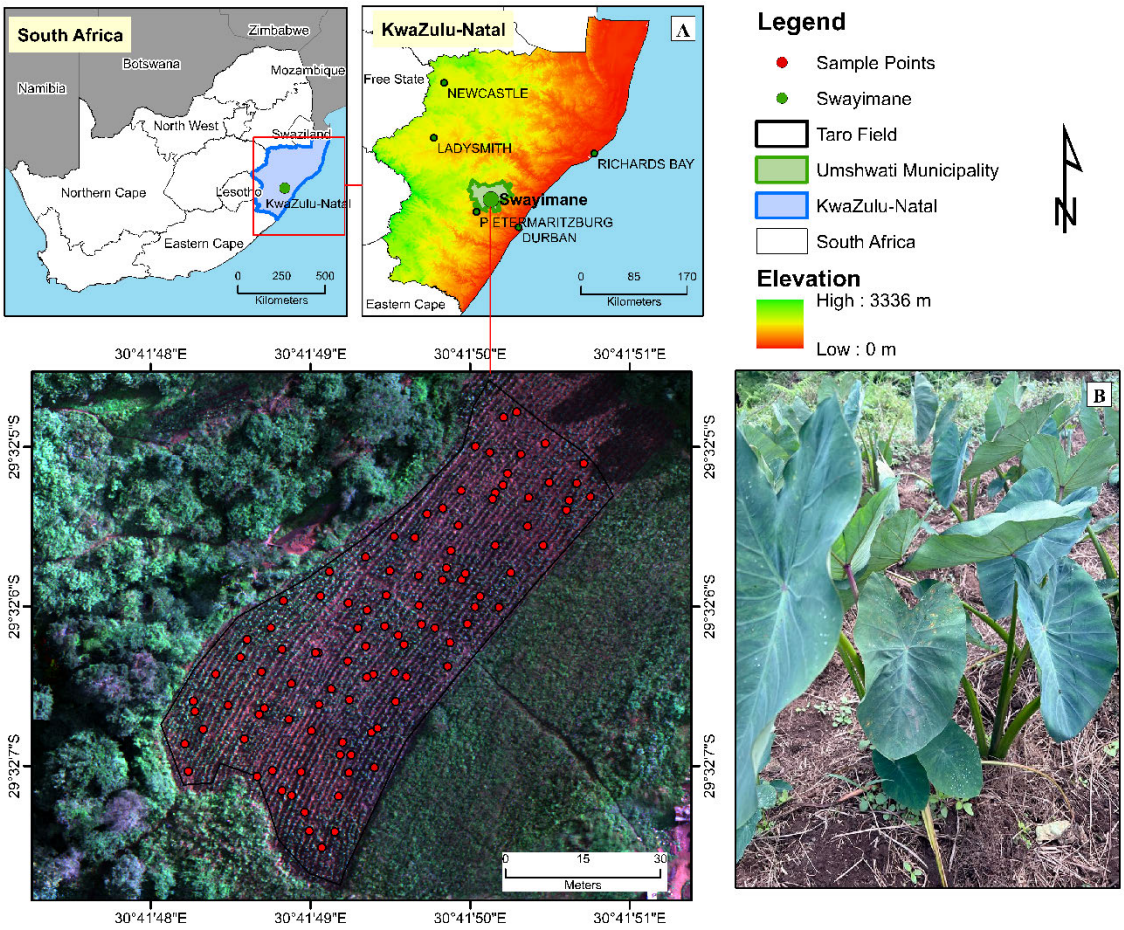

Figure 4.1 (a) Location of the smallholder taro field in Swayimane communal area in uMshwathi Municipality, Pietermaritzburg, South Africa and (b) the taro crop.

4.2.2 Field sampling and in-situ measurements

To establish sampling points within the taro field, a polygon delineating the field boundary was constructed using Google Earth Pro. After importing this polygon into ArcGIS Pro, the field was divided into three elevation-based strata: upper slope (stratum A), mid-slope (stratum B), and lower slope (stratum C). This topographic stratification was applied to capture variations in water availability and physiological responses linked to slope position. A total of 100 stratified random sampling points were then generated across the three strata to ensure comprehensive spatial representation and accuracy in reflecting the heterogeneity of taro crop conditions within the field. Subsequently, these sampling points were transferred to a Trimble handheld Global Positioning System (GPS) device (Trimble Inc., Sunnyvale, California, USA) with sub-centimetre accuracy, allowing for the precise location determination of each sampling point within the taro field. At each sampling point, in-situ measurements were taken to calculate

the respective values of equivalent water thickness, fuel moisture content, stomatal conductance, canopy temperature, and chlorophyll content. The sampling procedure of each physiological indicator is further explained below.

4.2.2.1 Equivalent water thickness and fuel moisture content

A handheld LiCOR-2200C Plant Canopy Analyser (LI-COR Biosciences, Lincoln, Nebraska, USA) was used to measure the Leaf Area Index (LAI) of taro crop. LAI measurements were taken at a 45° zenith angle with a 180° view cap, and a total of five readings were collected above (A) and below (B) the canopy, following the ABBBB sequence. Subsequently, the above-ground biomass of each sampled crop was recorded, with the fresh weight (FW) measured on an analytical balance with a measurement error of 0.5 g. The collected biomass was then transferred to a brown paper bag labelled with its identification, then placed to dry in an oven at 60 °C for approximately 72 hours until a consistent dry weight (DW) was reached. LAI, FW, and DW served as input variables for computing taro Equivalent Water Thickness (EWT) and Fuel Moisture Content (FMC) using the following equations (Danson and Bowyer 2004; Zhang and Zhou 2019a; Ahmad *et al.* 2021):

$$Equivalent\ Water\ Thickness = \frac{FW-DW}{LAI} \qquad \text{Units: g/m}^2 \qquad (4.1)$$

$$Fuel\ Moisture\ Content = \frac{FW-DW}{DW}\ x\ 100 \qquad \text{Units: \%} \qquad (4.2)$$

4.2.2.2 Stomatal conductance

An SC-1 leaf porometer (Decagon Devices Inc., Pullman, Washington, USA) was used to measure stomatal conductance. This device was selected based on its capability to record leaf conductance rates in relation to external environmental factors (Byambadorj *et al.* 2023). Prior to conducting measurements in the field, calibration of the SC-1 leaf porometer was conducted to ensure thermal equilibrium between the leaf clip and the environment. During the calibration process, filter paper saturated with distilled water from the sensor kit was placed over the aperture in the calibration plate. Subsequently, the sensor head was fixed to the calibration plate and an initial measurement period of 30 seconds was established. The sensor was equilibrated after each measurement and the head of the sensor was then reattached for subsequent calibrations (Brewer *et al.* 2022b). The calibration process was iterated up to ten times to ensure stable measurements, thus standardizing the instrument's readings. Subsequently, stomatal conductance measurements were conducted at each sampling point by positioning the SC-1 leaf

porometer at the centre of the leaf blade, perpendicular to the midrib of a sunlit taro leaf (Brewer *et al.* 2022b).

Leaf blades receiving full exposure to sunlight were selected to ensure accurate stomatal conductance measurements and avoid potential shading effects that could alter the crop's photosynthetic characteristics (Brewer *et al.* 2022b). The SC-1 leaf porometer simultaneously measured air temperature and humidity and automatically recorded leaf stomatal conductance (in mmol m^{-2} s^{-1}) for 30 seconds. Stomatal conductance measurements close to 0 mmol m^{-2} s^{-1} suggest the closure of stomata to minimise water loss, indicating extreme water deficit, while values close to 500 mmol m^{-2} s^{-1} suggest open leaf stomata, indicating minimal crop water stress and optimal physiological activity (Byambadorj *et al.* 2023).

4.2.2.3 Foliar temperature

The taro foliar temperature was assessed using a digital laser infrared GM320 handheld thermometer (Shenzhen Jumaoyuan Science and Technology Co., Ltd, Nanshan District, Shenzhen, China). The GM320 has a 1.5 °C error margin and is characterised by a wide measurement range spanning from -50 °C to 380 °C and a spectral response of 8-14 μm. At each sampling point, five foliar temperature measurements were taken and averaged to ensure accuracy. These measurements were acquired at specific locations on the taro leaf: (1) the centre of each leaf blade, near the primary leaf vein, (2) roughly one-third along from the tip of the leaf, (3) about two-thirds of the way down from the leaf tip, and (4) at the midpoint between the leaf vein and the leaf margin on both sides. This comprehensive approach facilitated a thorough assessment of leaf temperature distribution and variability across the taro foliage, providing valuable insights into its thermal characteristics.

4.2.2.4 Chlorophyll content

Using a Soil Plant Analysis Development (SPAD) 502 chlorophyll meter (Minolta Corporation Ltd., Osaka, Tokyo, Japan), the amount of chlorophyll in taro leaves was determined. The SPAD meter facilitates rapid measurements of chlorophyll content non-destructively by emitting light through crop leaves and quantifying the light transmitted in the red (650 nm) and near-infrared (940 nm) regions (Delegido *et al.* 2011). The device instantaneously generates a unitless value, which correlates with the chlorophyll content present in the sampled leaf (Uddling *et al.* 2007; Bayat *et al.* 2016). Five chlorophyll measurements

were obtained per sunlit leaf sampled at the top of the taro canopy at specific locations: (a) the middle point of every leaf blade, adjacent to the primary leaf vein, (b) about one-third down from the leaf tip, (c) about two-thirds from the leaf tip, and (d) at the middle point between the leaf vein and leaf margin on either side. These measurements were then averaged for each leaf and noted accordingly. To ensure accuracy when taking readings of chlorophyll, the SPAD meter was protected from direct sunlight. Finally, using the equation provided by Markwell *et al.* (1995) that demonstrated an R^2 of 0.94, SPAD measurements were converted to a value for chlorophyll content:

$$Chlorophyll\ Content = 10^{M^{0.265}} \qquad \text{units: } \mu\text{mol m}^{-2} \qquad (3)$$

Where chlorophyll content, measured in μmol m-2, is represented by the SPAD value (M), indicating the total chlorophyll per unit leaf area (Ling *et al.* 2011; Bayat *et al.* 2016).

All field measurements were performed from 10:00 am to 2:00 pm local time, on a sunny day, coinciding with the ideal timeframe for crop photosynthesis. This timing was selected to ensure that the gathered data precisely captures the peak reflectance and photosynthetic function of the taro plants.

4.2.3 Image acquisition and pre-processing

The DJI Matrice 300 (M300) (DJI-Innovations Inc., Shenzhen, China) multirotor platform and MicaSense Altum multispectral-thermal camera (MicaSense, Seattle, WA, USA) were flown over the taro field. The MicaSense Altum camera combines five narrow high-resolution bands to assess reflectance across various spectral ranges, including blue (475 nm), green (560 nm), red (668 nm), red-edge (717 nm), and near-infrared (NIR) (840 nm), and features a radiometric longwave infrared thermal channel (11 μm). To achieve optimal field coverage, a flight path was generated by transferring a shapefile of the experimental field directly to the smart controller of the DJI Matrice 300. Prior to and post each flight, the MicaSense Altum camera was calibrated using a Calibrated Reflectance Panel (CRP) based on known reflectance values across the spectrum to perform radiometric calibration on the sensor. Subsequently, an image of the CRP under consistent lighting conditions was captured and utilised to compensate for the atmospheric and environmental conditions encountered during the flight. The autonomous aerial survey was carried out at an altitude of 100 m, maintaining an 80% forward and sideward

image overlap, achieving 10.08 cm per pixel spatial resolution imagery. The drone flight was conducted during periods of peak solar radiation, typically from 10:00 am to 2:00 pm local time. This flight mission was executed concurrently with field measurements to ensure accurate synchronization and comprehensive data collection.

The automated flight mission produced a total of 1626 raw images, which were then imported into Pix4D photogrammetry software (Pix4D, Lausanne, Switzerland) for pre-processing. Within Pix4D, the software automatically identifies the CRP images, leveraging them to execute radiometric corrections and generate an ortho-mosaic of the smallholder taro field. Subsequently, ground reference points surveyed prior to fieldwork were utilised to refine the geometric accuracy of the acquired images within ArcGIS Pro software. The in-situ field measurements were superimposed on top of the obtained multispectral-thermal imagery, and both were georeferenced to the Universal Transverse Mercator zone 36S projection. Crop reflectance characteristics from both the multispectral and thermal wavelengths were extracted to compute thermal and spectral indices as outlined in Table 4.1. These specific indices were chosen due to their documented strong correlation with the plant water conditions, making them reliable indicators for assessing and monitoring crop water status (Baluja *et al.* 2012a; Gago *et al.* 2017a; Zhang and Zhou 2019a; Ozelkan 2020). In calculating the thermal indices, Normalised Relative Canopy Temperature (NRCT) and Second Formulation of the Stomatal Conductance Index (I3), T_{canopy} was determined by the canopy temperature of each sampled taro crop. Meanwhile, T_{wet} was determined using the lower boundary temperature, assuming that these crops were experiencing maximum transpiration (open stomata) and T_{dry} was determined using the higher boundary temperature, assuming that these crops were experiencing minimum transpiration conditions (closed stomata) (Baluja *et al.* 2012a; Crusiol *et al.* 2020b).

Table 4.1 UAV-derived spectral indices used in this study.

Vegetation Index	Abbreviation and Equation	Reference
Thermal Indices		
Normalised Relative Canopy Temperature	$NRCT = \frac{T_{canopy} - T_{wet}}{T_{dry} - T_{wet}}$	(Elsayed *et al.* 2015)
Second Formulation of the Stomatal Conductance Index	$I3 = \frac{T_{canopy} - T_{wet}}{T_{dry} - T_{canopy}}$	(Baluja *et al.* 2012b)
Spectral Indices		
Normalised difference vegetation index	$NDVI = \frac{R_{Nir} - R_{red}}{R_{Nir} + R_{red}}$	(Rouse *et al.* 1974)
Soil-Adjusted Vegetation Index	$SAVI = \frac{R_{Nir} - R_{red}}{R_{Nir} + R_{red} + L} \times (1 + L)$	(Huete 1988)
Normalised Difference Red-Edge Index	$NDRE = \frac{R_{Nir} - R_{Redegde}}{R_{Nir} + R_{Rededge}}$	(Gitelson and Merzlyak 1994)
Transformed Chlorophyll Absorption in Reflectance Index	$TCARI = 3 \times (R_{Rededge} - R_{Red}) - 0.2 \times (R_{Rededge} - R_{Green}) \times \frac{R_{Redegde}}{R_{Red}}$	(Haboudane *et al.* 2002)
Modified Chlorophyll Absorption in Reflectance Index	$MCARI = (R_{Rededge} - R_{Red}) - 0.2 \times (R_{Rededge} - R_{Green}) \times \frac{R_{Rededge}}{R_{Red}}$	(Daughtry *et al.* 2000)
Structural Insensitive Pigment Index	$SIPI = \frac{R_{Nir} - R_{Blue}}{R_{Nir} + R_{Red}}$	(Penuelas *et al.* 1995)
Normalised Green-Red Difference Index	$NGRDI = \frac{R_{Green} - R_{red}}{R_{Green} + R_{red}}$	(Hunt Jr *et al.* 2013)
Normalised difference water index	$NDWI = \frac{R_{Green} - R_{Nir}}{R_{Green} + R_{Nir}}$	(Gao 1996; McFeeters 1996)

Red-edge Chlorophyll Index	$CIrededge = \frac{R_{Nir}}{R_{rededge}} - 1$	(Gitelson *et al.* 2003; Gitelson *et al.* 2006)

4.2.4 Crop canopy index-based segmentations

Crop canopy index-based segmentation was executed on the UAV multispectral-thermal image using the Excess Green minus Excess Red (ExGR) index technique (Hamuda *et al.* 2016). This method was chosen to effectively delineate the crop canopy while eliminating soil background from the multispectral thermal image, ensuring the accuracy of crop water predictions across the taro field. Unlike other segmentation techniques, such as the Excess Green index, the ExGR index does not rely on a specific threshold for calculation as positive pixel values are classified as crop canopy, while negative values represent background (Riehle *et al.* 2020). Following calculation (Equation 4.4), a fixed zero threshold was used to automatically generate a binary image from the gray-level histogram in Mathworks MatLab (Hamuda *et al.* 2016; Shu *et al.* 2021). Subsequently, the resulting image was reclassified into vegetation pixels (assigned value 1) and soil pixels (assigned value 0). The crop canopy mask was then converted into a shapefile and overlaid onto the original UAV image in ArcGIS Pro, effectively removing soil background (Figure 4.2).

$$ExGR = (2 \times R_{Green} - R_{Red} - R_{Blue}) - (1.4 \times R_{Red} - R_{Green}) \quad (4.4)$$

where R represents the reflectance values obtained from the respective spectral band.

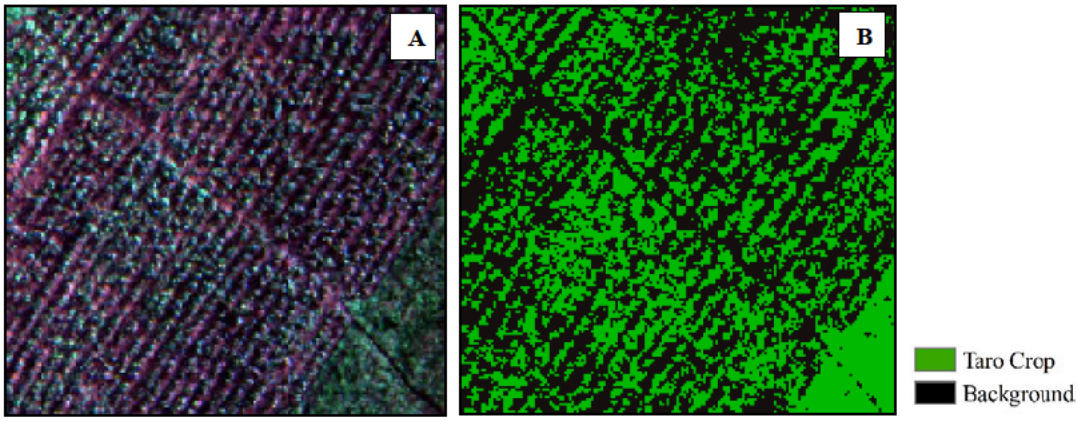

Figure 4.2 Taro crop canopy extraction using the ExGR index-based segmentation technique.

4.2.5 Model development and statistical analysis

This study utilised a deep machine learning approach to develop models for estimating taro crop water status physiological indicators, that include equivalent water thickness, fuel moisture content, stomatal conductance, temperature, and chlorophyll content. Specifically, we leveraged the abilities of the Deep Neural Network (DNN), which is an artificial neural network distinguishable by its multiple interconnected hidden layers to estimate crop water-related indicators (Traore *et al.* 2021). These hidden layers work collaboratively to learn complex features, enabling the transformation of input data into valuable output information (Chew *et al.* 2020; Bouguettaya *et al.* 2022). Unlike conventional machine learning methods that require prior knowledge of parameters, DNN relies on feature representations acquired directly from the input dataset (Omosalewa *et al.* 2021). This distinct strategy enables the model to comprehend and detect complex non-linear relationships among variables, thereby improving its capacity to reveal intricate patterns and dependencies within the data (Omosalewa *et al.* 2021; Traore *et al.* 2021).

A three-layer neural network model consisting of a comprehensive set of 17 input variables, including five spectral channels, one thermal infrared band, two thermal indices and nine vegetation indices, was assessed individually and used collectively to develop optimal crop water content models (Figure 4.3). The models were stimulated and refined using a Rectified Linear Unit (ReLU) with a maximum of 200 epochs to enhance prediction accuracy. To address the challenge of overfitting, a dropout regularization technique was implemented, with input and hidden layer dropout rates set at 0.4 and 0.2, respectively. Furthermore, the SoftMax activation function was used for the transformation of raw neural network outputs into a vector of probabilities, while the Adaptive Moment Estimation (Adam) optimiser was chosen to achieve optimal results. Finally, the DNN models for crop-water related parameters were fine-tuned with a learning rate of 0.001 and a batch size of 32. Finally, the models were developed and adjusted using Python 3.8 within Anaconda Jupyter Notebooks, with the TensorFlow and Keras libraries used for building and training the model, while Pandas, NumPy, Matplotlib and Scikit-learn libraries were used for data analysis and visualisation.

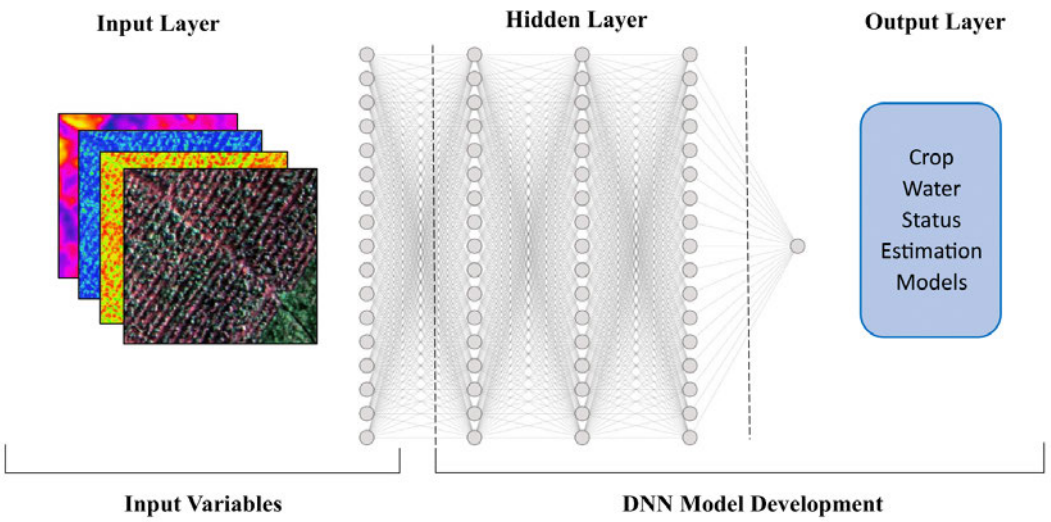

Figure 4.3 Graphical representation of DNN structure, composed of input, hidden, and output layers.

4.2.6 Accuracy assessment

An accuracy assessment was performed using the testing dataset (n = 30) to evaluate the effectiveness of the DNN model in estimating Taro crop water indicators. Three key accuracy metrics were utilised for this evaluation: the Coefficient of Determination (R^2), the Root Mean Square Error (RMSE), and the Relative Root Mean Square Error (rRMSE). These metrics are detailed in Ndlovu *et al.* (2024b). To understand the contribution of predictor variables in model development, the SHapley Additive exPlanations (SHAP) approach was employed. This approach calculates the marginal contribution value of each predictor variable, thereby ranking their importance in the model (Nahiduzzaman *et al.* 2023b). Utilizing SHAP provides a comprehensive understanding of the significance of individual predictor variables in influencing the accuracy of the crop water status physiological indicators estimation models.

4.2.7 A methodological overview on assessing the influence of thermal spectral data in characterising crop water status physiological indicators

Figure 4.4 illustrates the methodology used to evaluate the influence of integrating thermal spectral data on the prediction accuracy of crop water status physiological indicators. The analysis followed a comparative approach across different stages (a-d) to determine the significance of thermal data in enhancing model performance. Firstly, a DNN model was developed for each crop water status physiological indicator using multispectral bands (blue,

green, red, red-edge and NIR) to establish a baseline prediction accuracy (a). Thereafter, the thermal band was integrated into the model in the second stage to assess the impact of raw thermal data on model accuracy (b). In the third stage (c), thermal indices were incorporated to assess the influence of including the raw thermal band and derived thermal indices (NRCT and I3) in the prediction accuracies of crop water indicators. Lastly (d), for comparative purposes against thermal indices, a final analysis was conducted for each crop water status indicator using only spectral indices derived from multispectral wavelengths (i.e., spectral indices (NDVI, SAVI, NDRE, NGRDI, SIPI, TCARI, MCARI, CIrededge)) to compare the efficiency of spectral indices in characterising the water status variations of taro crops. The influence of thermal remote sensing in enhancing the prediction accuracy of crop water status indicators is determined by the model with the highest R^2 and lowest RMSE and rRMSE values.

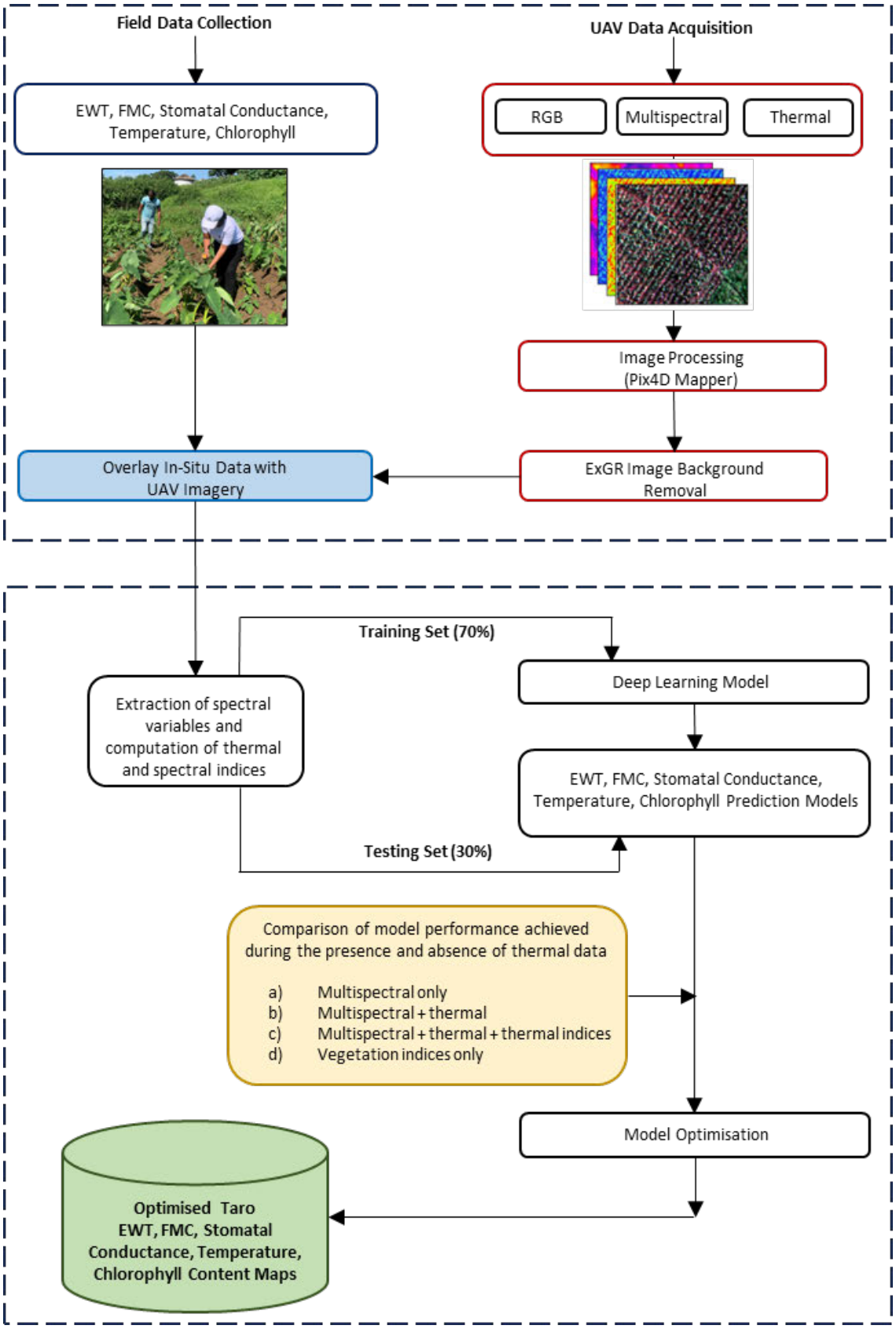

Figure 4.4 Methodological overview of the study.

4.3 **Result**s

4.3.1 Descriptive analysis of taro crop water status indicators

Table 4.2 presents the descriptive analysis results and variability of taro crop water status indicators across the smallholder field. For equivalent water thickness, the range spanned from 8.72 g/m² to 220.77 g/m², with a mean value of 59.77 ± 4.77 g/m². Fuel moisture content ranged from 28.68 % to 84.43 %, with a mean of 68.96 ± 1.15 %. Similarly, stomatal conductance varied from 43.10 mmol m^{-2} s^{-1} to 575.90 mmol m^{-2} s^{-1}, with a mean value of 234.09 ± 16.96 mmol m^{-2} s^{-1}. Leaf temperature varied from 26.10 °C to 33.40 °C, with a mean of 29.90 ± 0.19 °C, while chlorophyll ranged from 587.89 µmol/m^{-2} to 1643.95 µmol/m^{-2}, with a mean value of 1118.07 ± 26 µmol/m^{-2}.

Table 4.2 Descriptive analysis of taro crop water status physiological indicators.

Indicator	**Min**	**Max**	**Mean**	**Median**	**SEM**	**Std**	**CV%**
Equivalent Water Thickness (g/m^2)	8.72	220.77	59.77	48.20	4.77	42.17	70.54
Fuel Moisture Content (%)	28.68	84.43	68.96	70.69	1.15	10.19	14.78
Stomatal Conductance (mmol m^{-2} s^{-1})	43.10	575.90	234.09	174.85	16.96	149.77	63.98
Leaf Temperature (°C)	26.10	33.40	29.90	29.80	0.19	1.65	5.51
Chlorophyll Content (µmol/m^{-2})	587.89	1643.95	1118.07	1135.20	26.00	229.59	20.53

The standard error of mean is denoted by SEM, the standard deviation by Std., and the coefficient of variation by CV.

4.3.2 Estimation of taro crop water status physiological indicators using selected spectral variables

The estimation accuracies of taro crop water status physiological indicators using selected spectral variables are presented in Table 4.3. When considering the prediction accuracies based on multispectral bands alone, poor to moderate model performance was observed across all physiological indicators. Specifically, equivalent water thickness, fuel moisture content and chlorophyll content reported R^2 values between 0.30 and 0.36, while stomatal conductance and leaf temperature recorded R^2 values of 0.46 and 0.47, correspondingly. Furthermore, both RMSE and rRMSE values were relatively high across the indicators, revealing significant

variation between the predicted and observed measurements achieved based on multispectral bands. Meanwhile, incorporating the thermal band into the analysis improved prediction accuracies, particularly for stomatal conductance and leaf temperature, yielding impressive R^2 of 0.80 and 0.65, respectively. The corresponding RMSE values were 66.54 mmol m^{-2} s^{-1} and 0.89 °C with rRMSE values of 29.16 % and 2.96 %, accordingly (Table 4.3).

Similarly, the integration of multispectral and thermal bands with thermal indices further improved prediction accuracies across all crop water status physiological indicators, with higher R^2 and lower RMSE and rRMSE values. Notably, leaf temperature achieved the highest model accuracy based on this integration, yielding R^2 of 0.74, RMSE of 0.76 °C and rRMSE of 2.54 %. Meanwhile, the incorporation of thermal indices did not significantly enhance the predictive performance of fuel moisture content and chlorophyll content, with both indicators achieving moderate accuracies (R^2 = 0.55, RMSE = 6.48 %, rRMSE = 9.22 % and R^2 = 0.53, RMSE = 148.99 µmol/m^{-2}, rRMSE = 13.6 %, accordingly) (Table 4.3).

The analysis revealed that spectral indices yielded the highest prediction accuracies across several physiological indicators. For instance, fuel moisture content and chlorophyll content achieved their peak prediction accuracies when spectral indices were selected as input variables, yielding R^2 values of 0.77 and 0.76, respectively. The corresponding RMSE and rRMSE values were 4.60 % and 6.55 % for fuel moisture content, and 115.77 µmol/m^{-2} and 10.56 %, for chlorophyll content. While equivalent water thickness obtained an R^2 of 0.73, the model produced a relatively high rRMSE of 33.82 %, indicating notable variability between the predicted and actual values. Interestingly, while most physiological indicators performed best with general spectral indices, stomatal conductance and leaf temperature achieved their highest prediction accuracies when integrating multispectral and thermal bands with thermal indices. Stomatal conductance, for example, achieved an impressive R^2 of 0.84, with an RMSE of 59.23 mmol m^{-2} s^{-1} and rRMSE of 25.96%, while leaf temperature exhibited an R^2 of 0.74, with an RMSE of 0.76 °C and rRMSE of 2.54% (Table 4.3).

Table 4.3 Estimation accuracies of taro crop water status physiological indicators using selected spectral variables.

Predictor Variables	Accuracy Metric	Equivalent Water Thickness (g/m^2)	Fuel Moisture Content (%)	Stomatal Conductance (mmol m^{-2} s^{-1})	Leaf Temperature (°C)	Chlorophyll Content (µmol/m^{-2})
Multispectral Bands	R^2	0.36	0.34	0.46	0.47	0.30
	RMSE	36.28	7.88	108.83	1.10	196.09
	rRMSE	52.62	11.21	47.69	3.64	17.88
Multispectral Bands	R^2	0.47	0.43	0.80	0.65	0.43
Thermal Band	RMSE	32.95	7.31	66.54	0.89	177.22
	rRMSE	47.80	10.41	29.16	2.96	16.16
Multispectral Bands	R^2	0.64	0.55	**0.84**	**0.74**	0.53
Thermal Band	RMSE	27.21	6.48	**59.23**	**0.76**	148.99
Thermal Indices	rRMSE	39.47	9.22	**25.96**	**2.54**	13.16
Spectral Indices	R^2	**0.73**	**0.77**	0.77	0.67	**0.76**
	RMSE	**23.32**	**4.60**	71.30	0.86	**115.77**
	rRMSE	**33.82**	**6.55**	31.25	2.84	**10.56**

The highest accuracies achieved for each physiological indicator using optimal spectral variables selected by the DNN algorithm are highlighted in bold text.

4.3.3 Optimised regression models of taro crop water status physiological indicators integrating thermal and multispectral data

Optimised regression models were developed for all crop water status physiological indicators by leveraging the combination of multispectral bands, the thermal band, thermal indices, and spectral indices. For instance, in estimating the equivalent water thickness of taro crops, the optimised regression model achieved an impressive R^2 of 0.95, a corresponding RMSE of 9.76 g/m^2 and rRMSE of 14.15 (Figure 4.5a). The top-most influential predictor variables in the model development were MCARI, Thermal, CIrededge, TCARI, NIR, SIPI and NDRE, in descending order of importance (Figure 4.6a). Similarly, the optimised model for fuel moisture content yielded an exceptional R^2 of 0.94, with an RMSE of 2.33% and an rRMSE of 3.32% (Figure 4.5b). Variables such as MCARI, CIrededge, and SIPI emerged as the most important

predictors, indicating the significance of chlorophyll-based indices in estimating fuel moisture content (Figure 4.6b).

Furthermore, the optimised regression model for stomatal conductance exhibited an optimal R^2 of 0.96, with an RMSE of 29.34 mmol m^{-2} s^{-1} and an rRMSE of 12.86% (Figure 4.5c). Among the top predictors, variables such as CIrededge, thermal band, NRCT, SIPI and MCARI (Figure 4.6c), emerged as significant contributors, highlighting the importance of thermal data and certain spectral indices in predicting stomatal conductance. Similarly, the optimised regression model for leaf temperature produced an impressive R^2 of 0.95, RMSE of 0.33°C and an rRMSE of 1.11% (Figure 4.5d). Again, thermal data including the thermal band and NRCT, along with spectral indices such MCARI, CIrededge, SIPI, NDWI and NDRE, were among the most important predictor variables (Figure 4.6d). Lastly, the chlorophyll content estimation model achieved a strong R^2 of 0.91, with an RMSE of 71.51 μmol/m^{-2} and an rRMSE of 6.52% (Figure 4.5e). Despite being slightly lower than other indicators, these results still demonstrated the model's effectiveness in estimating the chlorophyll content of smallholder taro crops. The top-most influential predictor variables were CIrededge, thermal, MCARI, SIPI, NDRE, TCARI and NDVI, indicating the significance of red-edge-derived spectral indices and the thermal band in predicting chlorophyll content (Figure 4.6e).

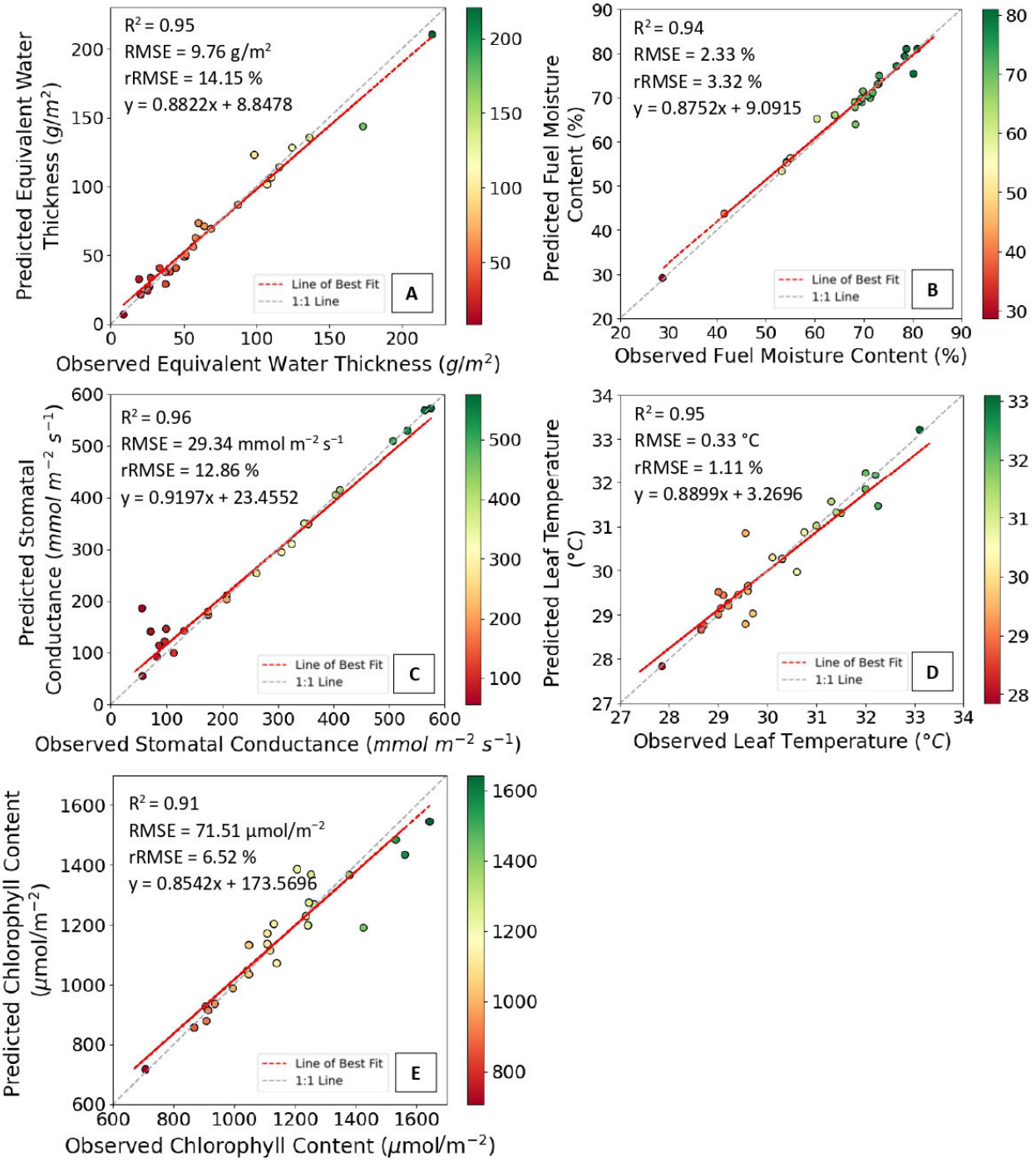

Figure 4.5 Relationship between measured and predicted a) equivalent water thickness, b) fuel moisture content, c) stomatal conductance, d) leaf temperature and e) chlorophyll content.

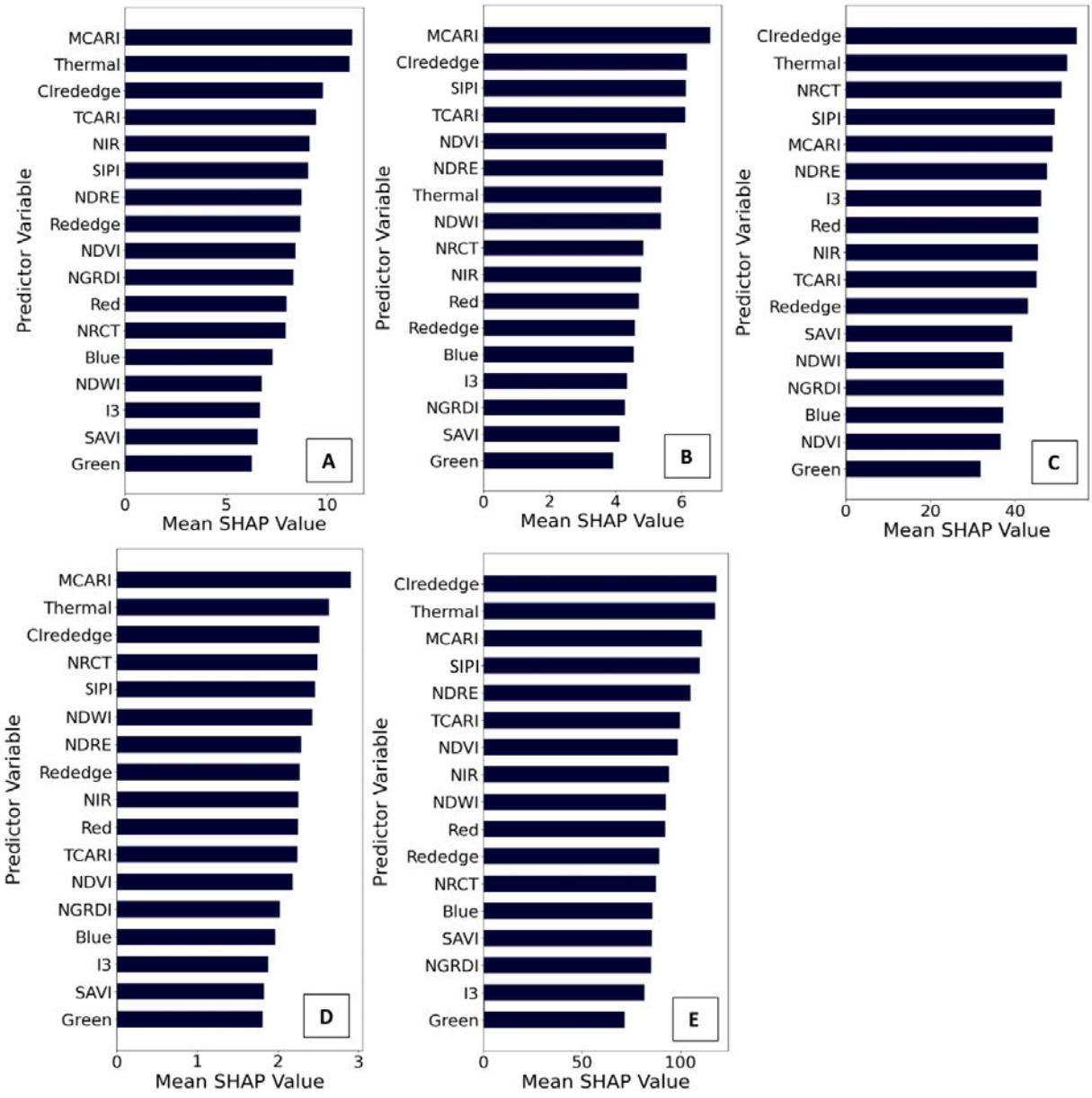

Figure 4.6 SHAP generated variable importance values of predictor variables use in developing the optimal estimation models of a) equivalent water thickness, b) fuel moisture content, c) stomatal conductance, d) leaf temperature and e) chlorophyll content.

4.3.4 Mapping the spatial distribution of taro crop water status physiological indicators

The integration of multispectral and thermal bands with thermal and spectral indices presented the highest prediction accuracies. Figure 4.7 depicts the spatial distribution of the crop water

status physiological indicators of smallholder taro crops. Notably, the southwestern area of the field consistently exhibits higher estimated values for equivalent water thickness, fuel moisture content, stomatal conductance, and chlorophyll content, contrasting with relatively lower values observed in the eastern up-slope regions. Additionally, leaf temperature patterns reveal distinct spatial variations, with lower temperatures prevalent in the southwestern parts and higher temperatures in the northern and southern extremities of the field (Figure 4.7).

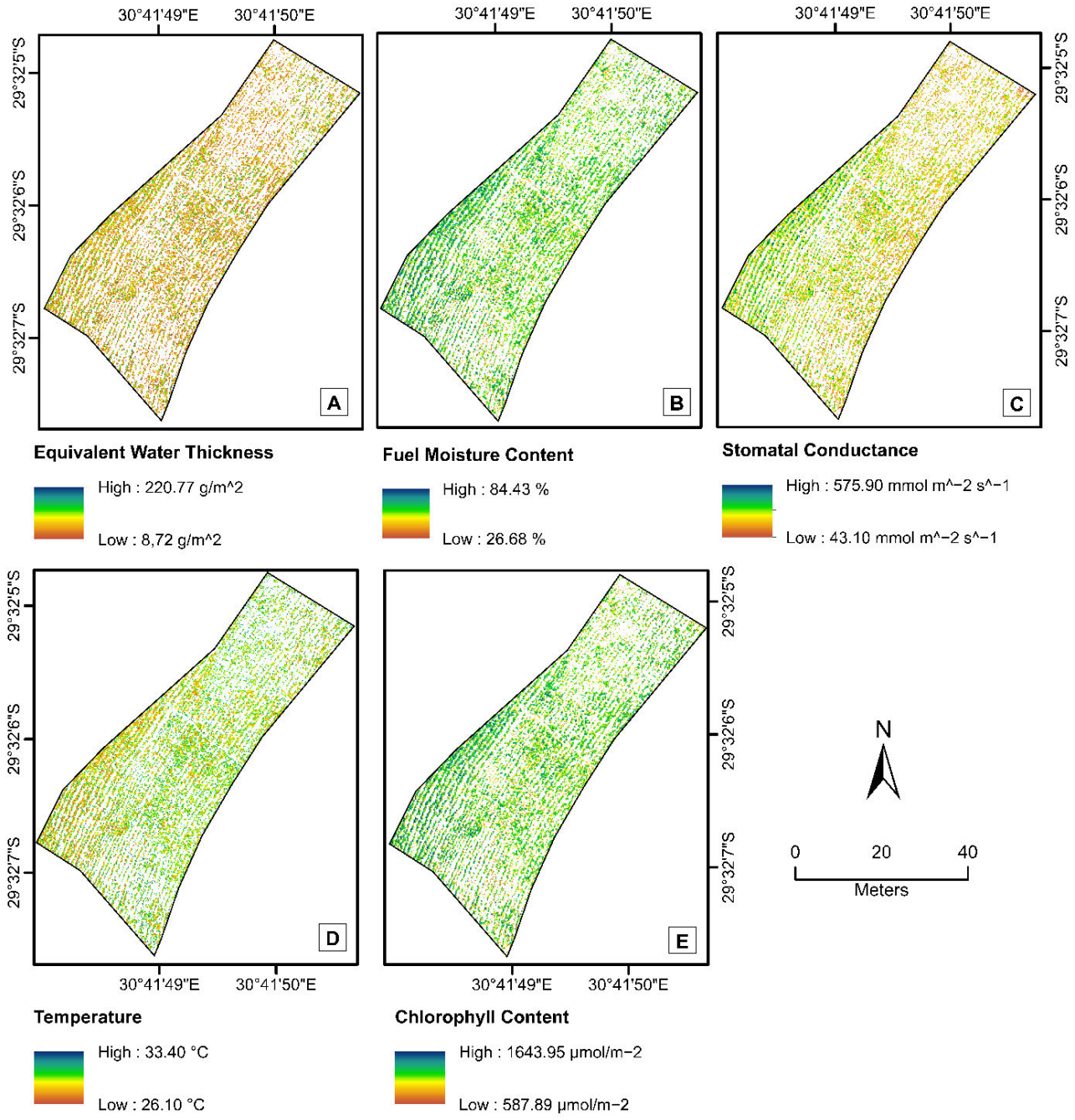

Figure 4.7 Spatial distribution of modelled a) equivalent water thickness, b) fuel moisture content, c) stomatal conductance, d) leaf temperature and e) chlorophyll content.

4.4 Discussion

4.4.1 The performance of integrating multispectral and thermal bands with thermal and spectral indices

The results of this study illustrated that integrating multi-modal features, such as thermal data and multispectral data along with their derived spectral indices, leads to higher estimation accuracies compared to using single-modal variables alone. For instance, the combination of thermal and multispectral data resulted in the most accurate predictions of crop water status physiological indicators, as evidenced by the findings presented in Table 4.3 and Figure 4.6. This improvement can be attributed to the complementary nature of thermal and multispectral data which captured different aspects of crop physiology and water status, thereby enhancing the overall predictive capability of the model (Sobejano-Paz *et al.* 2020). While, thermal imaging provides valuable temperature information associated with leaf moisture, pigmentation, and canopy structure features, it is important to note that a wide range of environmental factors influence crop water status beyond what thermal imaging alone can capture (Zhu *et al.* 2021a). For example, during their evaluation of water status variability using UAV data, Baluja *et al.* (2012a) found that certain vegetation indices derived from multispectral data, as opposed to thermal images, exhibited stronger correlations with stomatal conductance and leaf water potential within a commercial rainfed vineyard. Additionally, physiological indicators such as equivalent water thickness, fuel moisture content, and chlorophyll content were not extensively associated with the variations in the thermal section of the electromagnetic spectrum (Gerhards *et al.* 2019). This could be attributed to the fact that these crop physiological elements are more aligned with biomass accumulation (Quan *et al.* 2015; Liu *et al.* 2019; Sibanda *et al.* 2021b). In contrast, spectral indices that focus on crop greenness and health, derived from multispectral data, complement thermal imaging by providing additional information on plant physiological processes related to water status (Pineda *et al.* 2020; Kang *et al.* 2021).

While integrating thermal and multispectral data improves prediction accuracy overall, it is important to acknowledge that thermal data alone did not consistently correlate with certain physiological indicators such as equivalent water thickness, fuel moisture content, and chlorophyll content. This limitation may be attributed to the complex physiological nature of these traits and their indirect expression in canopy temperature, which is also affected by

external environmental noise such as wind, solar radiation, and humidity (Bellvert *et al.* 2014; Nanda *et al.* 2018). These factors can obscure thermal signals, particularly for traits more tightly linked to biomass and pigment content rather than direct transpiration processes. Therefore, the predictive strength of thermal imaging may be context-dependent and less reliable for certain indicators when used in isolation. Therefore, the integration of various types of variables from multiple modalities could have effectively reduced the influence of noise, thereby enhancing the predictive capabilities of the estimation models (Sobejano-Paz *et al.* 2020; Zhai *et al.* 2023). The findings of this study are supported by those of Zhai *et al.* (2023) who integrated the spectral capabilities of thermal and multispectral data to optimise the estimation of chlorophyll content of maize crops, achieving R^2 of 0.75 and rRMSE of 8.36 %.

This study demonstrated that taro equivalent water thickness was optimally predicted using a combination of spectral variables including MCARI, Thermal, CIrededge, TCARI, NIR, SIPI, and NDRE, resulting in an R^2 of 0.95 and rRMSE of 14.15% (Figure 4.5a and 4.6a). Similarly, for fuel moisture content, the optimised model revealed MCARI, CIrededge, and SIPI as the most influential predictors, achieving a high R^2 of 0.94 and rRMSE of 3.32% (Figure 4b and 5b). Even though the thermal band and derived thermal indices did not emerge as the top most predictor variables, it was not surprising as equivalent water thickness and fuel moisture content are closely linked to leaf matter and accumulated above-ground biomass, which decreases under soil water stress (Zhang and Zhou 2019b; Qi *et al.* 2020). These findings are supported by those of Gunawardena *et al.* (2015) who observed a poor negative correlation between above-ground biomass and land surface temperature, with an R^2 value of 0.35, hence signifying the poor relationship between thermal characteristics and biomass-derived indices. Notably, while spectral indices were important predictors, estimating equivalent water thickness using spectral indices alone yielded an R^2 of 0.73 with a relatively high prediction error (rRMSE of 33.82 %), suggesting limitations in the model's ability to capture trait-specific variability. This limitation was addressed by incorporating thermal data, which significantly improved model performance, highlighting the value of integrating complementary data for enhanced prediction of equivalent water thickness.

Moreover, the result highlights the influential role of the thermal band and derived indices in predicting stomatal conductance and leaf temperature in smallholder taro crops. Specifically, influential predictor variables such as CIrededge, the thermal band, NRCT, SIPI, and MCARI yielded optimal predictions for stomatal conductance, achieving an impressive R^2

of 0.96 and rRMSE of 12.86% (Figure 4.5c and 4.6c). Similarly, for leaf temperature, the thermal band, NRCT, MCARI, CIrededge, SIPI, NDWI, and NDRE emerged as crucial predictor variables, resulting in an optimal R^2 of 0.95 and rRMSE of 1.11% (Figure 4.5d and 4.6d). The significance of the thermal band can be attributed to its ability to capture variations in canopy temperature, which directly affect stomatal conductance and water use (Ahmad *et al.* 2021; Wang *et al.* 2022a). As stomata regulate the release of water vapor from crops, changes in stomatal conductance are reflected in leaf temperature, making the thermal band a valuable predictor for this physiological indicator (Yu *et al.* 2015; Gerhards *et al.* 2019). In a similar study, Brewer *et al.* (2022b) explored the use of integrating optical and thermal infrared UAV imagery to estimate stomatal conductance and leaf temperature, achieving R^2 values of 0.85 and 0.81, respectively, with the thermal band emerging amongst top most influential variables. Furthermore, Katuwal *et al.* (2023) demonstrated that the SIPI exhibits a strong correlation with vegetation water content (R^2 = 0.84), as it captures the balance between chlorophyll and carotenoid pigments, which are sensitive to changes in plant water status. Therefore, the inclusion of thermal data and chlorophyll-based spectral indices such as SIPI in estimation models enhances the ability to accurately estimate stomatal conductance and leaf temperature, offering insightful information about the water status of taro crops.

Finally, the findings revealed that chlorophyll content estimation can be optimally achieved to an R^2 of 0.91 and an rRMSE of 6.52%, with thermal data and red-edge-based indices including CIrededge, MCARI, SIPI, NDRE, and TCARI emerging as the most influential predictor variables (Figure 4.5e and 4.6e). Similarly, Brewer *et al.* (2022a) in smallholder maize farms attained a comparable correlation between chlorophyll content and red-edge-based indices, yielding optimal chlorophyll content prediction models with R^2 values exceeding 0.75 throughout the growing season. Meanwhile, Clevers and Gitelson (2013), in a related study, identified red-edge-based indices such as CIrededge as optimal variables for precisely quantifying the chlorophyll content of maize and soybean, achieving R^2 values of 0.92 and 0.94, respectively.

4.4.2 The performance of selected spectral variables in estimating the crop water status physiological indicators of smallholder taro crops

The findings of this study revealed a suboptimal performance of UAV-derived multispectral bands in predicting crop water status physiological indicators. This limitation can be attributed

to the limited spectral resolution of UAV-acquired multispectral bands which constrain their ability to capture the intricate variations in physiological indicators (Lu and He 2017; Barbedo 2019; Huang *et al.* 2019). These findings are consistent with those of Zhai *et al.* (2023), who investigated the efficacy of gradient boosting machine, random forest regression, and ridge regression in estimating the chlorophyll content of maize crops solely using multispectral bands, achieving R^2 values ranging from 0.54 to 0.61. Consequently, achieving optimal predictions of taro crop water status necessitate the integration of additional data sources, such as thermal bands and spectral indices to enhance the accuracy and reliability of the estimations.

Meanwhile, the findings demonstrated a notable increase in prediction accuracies when the thermal band and thermal indices were integrated with multispectral bands, especially for taro stomatal conductance and leaf temperature. Literature has detailed that thermal data and derived thermal indices offer valuable insights into crop water stress by detecting variations in leaf temperature linked to water availability and transpiration rates (Baluja *et al.* 2012a; García-Tejero *et al.* 2016; Gago *et al.* 2017a). For example, stomatal conductance, which regulates leaf temperature dynamics, influences the closure of stomata under water stress, reducing water vapor loss and increasing leaf temperature (Yu *et al.* 2015; Wang *et al.* 2022a). Therefore, through the correlations between crop temperature and stomatal activity, thermal infrared data can provide rapid and robust data essential for quantifying the stomatal conductance of smallholder taro crops.

Moreover, spectral vegetation indices produced the highest model accuracies for estimating the equivalent water thickness, fuel moisture content, and chlorophyll of smallholder taro crops. These findings are consistent with a substantial and expanding body of literature demonstrating the efficacy of spectral indices developed from water-sensitive portions of the spectrum for estimating physiological indicators of crop water status (Zhang and Zhou 2015; Pasqualotto *et al.* 2018; Zhang *et al.* 2019; Sibanda *et al.* 2021b). For instance, water stress-induced changes in moisture content and chlorophyll levels are intricately linked to leaf pigmentation and biochemical composition, influencing crop canopy spectral reflectance, especially in the near-infrared and red-edge regions of the electromagnetic spectrum (Pasqualotto *et al.* 2018; Parkash and Singh 2020). Therefore, through leveraging the unique spectral properties captured by these bands, vegetation indices provide enhanced sensitivity to changes in chlorophyll content and canopy moisture content (Brewer *et al.* 2022a; Ndlovu *et al.* 2024b).

4.4.3 Implications of the study limitations and recommendations for future research

The study highlights the prospects for high-resolution UAV-acquired thermal remote sensing techniques in assessing crop water status physiological indicators, particularly of NUS smallholder taro crops. Demonstrating the effectiveness of thermal data when used in conjunction with multispectral bands highlights the importance of integrating various spectral variables for comprehensive agricultural monitoring. Understanding the dynamics of crop water status physiological indicators, including equivalent water thickness, fuel moisture content, stomatal conductance, canopy temperature, and chlorophyll content, enables the development of targeted adaptation strategies for smallholder farmers facing climate-related risks. Furthermore, the in-depth analysis of taro crop water status could contribute to agricultural frameworks aimed at redefining existing agricultural landscapes and diversifying cropping systems to include future smart NUS crops such as taro, thus ensuring sustainable food production and food security.

However, this study acknowledges several limitations. Firstly, occlusion effects because of the top-down perspective of the UAV sensor may obscure certain parts of the crop canopy due to overlapping leaves, therefore, potentially influencing the accuracy of crop water status measurements. Therefore, future studies should explore the integration of Light Detection and Ranging technology to account for the effects of occlusion by providing a three-dimensional view of the canopy structure and its influence on crop water monitoring. Furthermore, while interlacing of leaves was not a significant factor in this study due to taro's discontinuous canopy structure, further research is required to understand the effect of intra-plant overlapping of leaves, particularly for leaf-level estimations of crop water status indicators. Additionally, environmental and atmospheric attributes such as solar radiation, can introduce interferences in thermal reflectance properties, therefore affecting the quality of data and reducing the accuracy of estimated crop water physiological indicators. Therefore, further research on the refinement and incorporation of these aspects is required to enhance the reliability and accuracy of estimated crop water status indicators. Furthermore, to gain a comprehensive understanding of crop water status, further research is required to investigate the phenology and water status variations of smallholder taro crops across the growing season. Additionally, there is a need to explore the integration of additional crop water-related indicators, such as soil moisture content, to provide a more holistic understanding of water dynamics in smallholder taro farming systems.

4.5 Conclusion

The study aimed to assess the applicability of UAV multi-modal thermal multispectral data and deep neural network techniques to assess the crop water status of smallholder taro crops. Considering the findings presented in this study, the following conclusions can be drawn:

- Taro crop water content physiological indicators can be optimally estimated using multi-modal UAV-acquired thermal and multispectral data, achieving impressive R^2 values greater than 0.91 and rRSME values less than 14.15% of equivalent water thickness, fuel moisture content, stomatal conductance, canopy temperature, and chlorophyll content.
- Integrating thermal and multispectral bands with thermal and spectral indices results in the most optimal estimation models for equivalent water thickness, fuel moisture content, stomatal conductance, and canopy temperature.

This study serves as a stepping stone toward advancing precision agriculture practices for neglected and underutilised smallholder taro crops. Demonstrating the effectiveness of UAV multi-modal thermal multispectral remote sensing techniques paves the way for more efficient and sustainable management of taro cultivation practices. Furthermore, the integration of advanced remote sensing technologies and deep learning algorithms allows for new avenues for enhancing agricultural monitoring and decision-making processes, ultimately contributing to global efforts towards achieving food security and sustainable agricultural systems.

4.6 Summary

The findings of this chapter demonstrated the advantages of a multi-modal approach integrating thermal and multispectral UAV data for estimating key physiological indicators of taro crop water status. However, the dynamic nature of crop water status necessitates a deeper understanding of the temporal variability of physiological indicators over time. While indicators such as equivalent water thickness and fuel moisture content could be optimally predicted using UAV thermal remotely sensed data, their destructive nature limits their assessment across the growing season. In this regard, Chapter Five extends these findings by introducing a temporal dimension, evaluating the variability of stomatal conductance and leaf temperature across different growth stages of smallholder taro crops. Specifically, this temporal analysis will provide valuable insights into the responsiveness of these indicators to

environmental and phenological changes, identifying the critical growth stages when taro crop water status can be adequately estimated using UAV-based thermal and multispectral data.

CHAPTER FIVE

Multi-Temporal Analysis of Taro Crop Water Stress Using High-Resolution Thermal and Multispectral Proximal Sensing for Improved Resilience of Smallholder Farming Systems

This chapter is based on:

Ndlovu, H. S., Odindi, J., Sibanda, M., & Mutanga, O. (2025). Multi-Temporal Analysis of Taro Crop Water Stress Using High-Resolution Thermal and Multispectral Proximal Sensing for Improved Resilience of Smallholder Farming Systems. *Computers and Electronics in Agriculture*, Under Preparation.

Abstract

Taro, a neglected and underutilised crop species, has been identified as a promising future smart crop with significant potential to enhance food and nutrition security while diversifying cropping systems. Despite its reported resilience to climate change impacts, taro's physiological responses to water stress, such as increased leaf temperature and reduced stomatal conductance, can significantly reduce its productivity and yield. As a result, near-real-time monitoring of taro's water status throughout the growing season is essential for implementing rapid interventions and adaptation strategies aimed at mitigating the adverse effects of water deficits. Over the recent decades, cutting-edge thermal remote sensing technologies and Unmanned Aerial Vehicles (UAVs) have allowed for non-invasive monitoring of crop water status at ultra-high spatial and temporal scales. Therefore, this study explored the utility of UAV-acquired thermal and multispectral proximal sensing and the deep neural network algorithm to estimate the stomatal conductance and leaf temperature of smallholder taro crops during the emergence, vegetative and maturity growth stages. Findings showed that thermal data, together with derived thermal indices, are critical predictor variables for both stomatal conductance and leaf temperature across the taro growth stages. Furthermore, the results illustrated that the vegetative growth stage exhibited the highest prediction accuracies for stomatal conductance (R^2 of 0.96, RMSE of 29.34 mmol m^{-2} s^{-1} and rRMSE of 12.86 %) and leaf temperature (R^2 of 0.95, RMSE of 0.33 °C and rRMSE of 1.11 %). Overall, the study findings underscore the transformative potential of multi-modal high-resolution thermal and multispectral sensing technologies in advancing precision agriculture, particularly in monitoring the water status of smallholder taro crops. The insights of this study contribute to agricultural frameworks aimed at redesigning current cropping landscapes to incorporate climate resilient neglected and underutilised crops, such as taro, for improved food and nutrition security. However, a key limitation is that while the model outputs provide accurate predictions, the actual implementation of these insights on farms may be constrained by how farmers interpret and act on this information. Future research should therefore investigate how to bridge this gap by incorporating farmer decision-making into remote sensing-based advisory systems.

Keywords: Taro, neglected and underutilised, thermal remote sensing, unmanned aerial vehicles, growth stages, physiological indicators.

5.1 Introduction

Despite the substantial increase in agricultural production over the recent decade, food security remains a global challenge (Nhamo *et al.* 2020; Panday *et al.* 2020). To sustain the growing human population, which is expected to reach 9 billion people by 2050, agricultural food production would have to increase by 50% (Chakraborty and Newton 2011; Kumari *et al.* 2022). Meanwhile, studies have shown that efforts to increase crop yield and ensure food security will further be challenged by the impacts of climate variability and change (Kephe *et al.* 2021b). For instance, in southern Africa, climate change has adversely affected agricultural crop sector due to increased frequency and intensity of extreme weather events, hence affecting the region's capacity to meet the increased production demands (Nhamo *et al.* 2019b; Kephe *et al.* 2021b). This is particularly a challenge in smallholder farming systems, where dependence on seasonal rainfall and the use of traditional farm management practices aggravates their vulnerability (Chivenge *et al.* 2015; Nhamo *et al.* 2019a). Therefore, in response to these challenges, there is a pressing need to redesign agricultural landscapes to incorporate crop species that are more resilient to the impacts of climate change to improve crop yields and ensure food security. Furthermore, while the current agricultural systems, based on a limited number of major food crops, have effectively sustained food security in the past, their capacity to maintain this in the twenty-first century remains questionable, prompting calls for increased diversification of cropping systems (Mabhaudhi *et al.* 2017a).

Neglected and Underutilised Crop Species (NUS), have been identified as possible future smart crops with the potential to improve food and nutrition security while transforming agricultural landscapes by enhancing climate resilience (Kapoor *et al.* 2022). Taro (*Colocasia esculenta* (L)), a NUS known in South Africa as *amadumbe*, is a highly nutritious tuber crop widely cultivated for its edible leaves, corms and petioles (Sultana *et al.* 2021). Contrary to traditional major crops, NUS crops, such as taro, are known for their drought and heat tolerance with the ability to adapt to adverse conditions, including those observed under climate variability and change (Mabhaudhi and Modi 2015; Oyeyinka and Amonsou 2020; Mugiyo *et al.* 2021a). Despite its potential, there is a gap in literature describing the water status and stress of taro crops, which hinders their development and promotion in current agricultural systems.

Furthermore, moisture content plays a critical role in determining the quality of taro crops, especially the tubers, as it directly influences their texture and taste (Ferdaus *et al.* 2023). Hence, it is imperative that taro assumes optimal water status conditions throughout the growing season to ensure the desired quality in yield. This underscores the need for robust and evidence-based research to enhance the understanding of taro crop water status and aid its integration as a climate-resilient and future smart crop.

Various physiological indicators, including stomatal conductance and leaf temperature have been widely recognised in the literature as key measures for assessing and monitoring crop water status (Gerhards *et al.* 2019; Ahmad *et al.* 2021; Awais *et al.* 2022a). Research has shown that crops exhibit several physiological mechanisms in response to water stress to conserve water, maintain cellular functions and enhance survival under adverse conditions (Matese *et al.* 2018b). For instance, when crops experience water deficit, stomata cells located in the leaf epidermis initiate stomatal closure to reduce moisture loss through transpiration, consequently increasing leaf and canopy temperature due to the reduced evaporative cooling, which limits the crop's ability to dissipate heat (Sepúlveda-Reyes *et al.* 2016; Matese and Di Gennaro 2018; Sagan *et al.* 2019b). Furthermore, as taro's water status fluctuates during the emergence, vegetative and maturity growth stages, both stomatal conductance and leaf temperature vary in tandem with the crop's photosynthetic activities throughout its phenological development (Brewer *et al.* 2022c). As a result, stomatal conductance and leaf temperature estimates are often used as reliable proxies for the continuous monitoring of crop water status across the growing season.

Traditional methods of estimating stomatal conductance and leaf temperature, including direct measurements and visual observations conducted by trained experts, are time-consuming, laborious, expensive and cannot effectively capture the spatial and temporal variability of crop water status (Maimaitiyiming *et al.* 2020b; Panday *et al.* 2020). Meanwhile, recent advances in earth observation data, particularly thermal remote sensing, have provided a promising tool for monitoring crop water status (Khanal *et al.* 2017; Messina and Modica 2020). Studies have confirmed that thermal infrared imagery shows significant correlations with crop water stress, as the emitted radiance in the thermal region exhibits sensitivity to variations in canopy temperature, which is influenced by physiological changes associated with crop water status (Gerhards *et al.* 2019). Several satellite-based thermal sensors including Ecosystem Spaceborne Thermal Radiometer Experiment on Space Station (ECOSTRESS), Landsat Thermal Infrared

Sensor (Landsat -TIRS), Visible Infrared Imaging Radiometer Suite (VIIRS) and Moderate Resolution Imaging Spectroradiometer (MODIS) have been used to monitor crop water status (Masina *et al.* 2020; Awais *et al.* 2022a). However, these satellite-based sensors are restricted by their relatively coarse spatial resolution, insufficient revisit time, and in the specific case of Landsat, the presence of black stripes which introduce gaps in the data, hence limiting their applicability to the continuous near-real-time monitoring of taro crop water status (Malbéteau *et al.* 2018a; Masina *et al.* 2020).

Over the years, advances in remote sensing technology, specifically the development of unmanned aerial vehicles (UAVs), mounted with ultra-high-resolution thermal and multispectral sensors, have presented an invaluable field phenotyping platform (Nhamo *et al.* 2020; Brewer *et al.* 2022c). Equipped with the ability to provide instantaneous imagery at a sub-centimetre ground resolution, UAVs have enabled high-precision imagery acquisition at high spatial, temporal and spectral resolutions suitable for monitoring crop water status at field scale (Santesteban *et al.* 2017b; Maimaitiyiming *et al.* 2020b). In contrast to satellite platforms, UAVs enable flight planning at low altitudes, allowing for targeted observations of specific areas and the acquisition of imagery on demand, hence facilitating the near-real-time collection of thermal and multispectral imagery suitable for detecting the subtle changes in crop physiology and water status (Malbéteau *et al.* 2018a). For example, a recent study by Shao *et al.* (2023) used UAV remotely sensed data and machine learning techniques to estimate cumulative evapotranspiration of maize crops, achieving an R^2 of 0.89 and RMSE of 0.0089 mm. Meanwhile, Han *et al.* (2020) obtained an R^2 of 0.78 and RMSE of 2.42% by using UAV-based thermal imagery to quantify soil moisture content based on the canopy surface temperature of commercial winter wheat. Despite these successes, the utility of UAVs integrated with high-resolution thermal sensors for continuous monitoring of taro water status in smallholder farming systems remains an underexplored domain (Santesteban *et al.* 2017b; Sagan *et al.* 2019b; Han *et al.* 2020).

While UAV thermal remote sensing has been invaluable in modern agriculture, derived imagery can often have canopy pixels that represent non-target elements such as soil background, hence reducing the quality of the data (Bian *et al.* 2019; Messina and Modica 2020). The mixed pixel problem is particularly an issue in smallholder taro fields where crops are characterised by discontinuous canopies due to low planting density and wide interrow spacing (Tumuhimbise 2015; Sepúlveda-Reyes *et al.* 2016). The Excess Green minus Excess

Red (ExGR) index has been recognised as an effective approach for extracting pure crop pixels, as it utilises green reflectance to isolate the canopy and red reflectance to suppress the soil background, making it suitable for image segmentation in smallholder taro landscapes (Hamuda *et al.* 2016; Riehle *et al.* 2020; Upendar *et al.* 2021). Furthermore, while thermal remote sensing and derived thermal indices have proven to be invaluable for quantifying crop water status, research has shown that the integration of multispectral-based vegetation indices significantly enhance the accuracy of water status assessments (Panday *et al.* 2020; Ndlovu *et al.* 2024a). For instance, Baluja *et al.* (2012a) demonstrated the utility of UAV data in assessing the water status of commercial rainfed vineyards. They observed that some multispectral vegetation indices, including the normalised difference vegetation index, exhibited better correlations with stomatal conductance as they suggest a long-term response of crops to cumulative water deficits. Meanwhile, a recent study by Zhang *et al.* (2023b) demonstrated that multi-sensor data improved the estimation accuracy of maize soil moisture content at the vegetative growth stage from an R^2 of 0.50 when using thermal data only to an R^2 of 0.61 when using thermal and multispectral data. This combined approach leverages the strengths of both thermal and multispectral data, enabling a more comprehensive evaluation of crop water status by capturing additional information related to canopy structure and photosynthetic activity (Panday *et al.* 2020; Sobejano-Paz *et al.* 2020). As a result, the integration of multi-modal thermal and multispectral data provides a comprehensive and reliable method for monitoring and assessing crop water status across various growth stages.

Additionally, incorporating machine learning techniques, particularly Deep Neural Networks (DNN), has shown potential in advancing the analysis of UAV-based proximal remotely sensed agricultural data (Zhou *et al.* 2021; de Melo *et al.* 2022). The efficacy of the DNN algorithm lies in its ability to model complex, non-linear relationships between various environmental factors enabling more precise predictions of crop attributes such as water status (Yuan *et al.* 2020; Omosalewa *et al.* 2022). Despite these advancements, the application of the DNN technique, in conjunction with UAV-based proximal thermal data and image segmentation for crop water estimations within smallholder taro farming systems is yet to be explored. Given the complexity of smallholder farmlands, where factors such as variable planting densities and soil background introduce additional challenges, the DNN approach offers a promising solution for more accurate and continuous crop water monitoring. Nonetheless, additional research is required to fully explore and integrate DNNs into precision

agriculture research, especially for NUS such as taro. This will help unlock their potential to improve crop water management throughout the growing season and enhance overall crop resilience. Considering the potential of UAV-proximal remote sensing multi-modal thermal and multispectral data combined with the ExGR image segmentation and the DNN algorithm, this study aimed to evaluate the utility of high-resolution UAV image data in estimating crop water status attributes across the growth stages of smallholder taro crops. Specifically, the study aimed to 1) predict stomatal conductance and leaf temperature using UAV multi-modal thermal and multispectral data at the emergence, vegetative and maturity growth stages and 2) compare the most optimal growth stage to predict stomatal conductance and leaf temperature of smallholder taro crops.

5.2 Materials and Methods

5.2.1 Study site description

This study was undertaken at Swayimane (-29.534951; 30.697113), a rural community located approximately 58 km north-east of Pietermaritzburg, KwaZulu-Natal, South Africa (Figure 5.1). The area has a sub-humid climate characterised by tropical wet summers and dry cool winters with a mean annual temperature of 17 ℃ and an average rainfall ranging from 600-1100 mm per annum (Brewer *et al.* 2022c; Cele and Mudhara 2024). The area is ranked within the top 2% of high-potential land in South Africa and is characterised by arable soils, which are highly fertile and well-suited for agricultural activities (Ndlovu *et al.* 2021c). As a result, the Swayimane community relies heavily on the land for subsistence agriculture, where crops such as sweet potatoes, beans, maize, sugarcane and taro are widely cultivated. Smallholder farmers in the area follow traditional farming practices, including manual plant, hand-weeding, and the use of organic fertilisers such as animal manure. Despite having arable land, Swayimane is in a high-risk location for climate change impacts, characterised by increasing intensity and frequency of extreme weather events, which significantly threaten crop productivity and local food security.

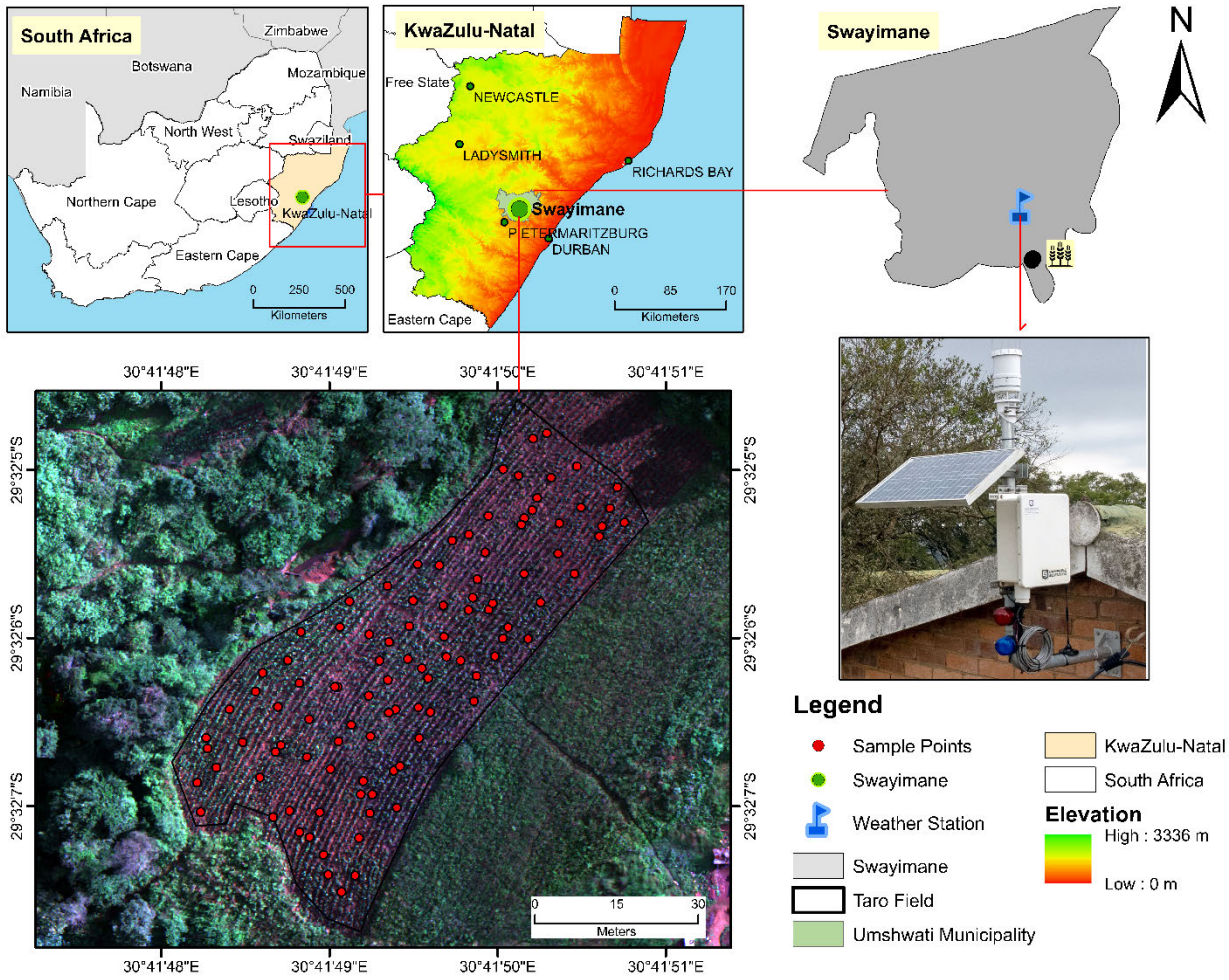

Figure 5.1 Location of the smallholder taro field and automatic weather station in the rural community of Swayimane, Pietermaritzburg, South Africa.

5.2.2 Experimental plot

The rain-fed taro crop was sown on 26 October 2022 in an experimental plot with a spatial coverage of 2864.56 m^2. The study focused on monitoring the three major growth stages of taro; emergence, vegetative, and maturity stages, detailed in Table 5.1. The emergence stage comprises root formation and leaf production, where the initial establishment of the crop occurs, and the plant begins to develop its first leaves (Sibiya 2015). During this stage, propagules play an essential role in supporting crop development as they provide the necessary carbohydrates and nutrients allowing the crop to establish its root system and begin leaf production before it can fully rely on photosynthesis (Sibiya 2015; Lewu *et al.* 2017). During the vegetative growth stage, the plant undergoes significant growth, characterised by the expansion of leaves and the accumulation of above-ground biomass, which is critical for photosynthesis and energy storage

(Sibiya 2015). Lastly, the maturity stage is characterised by a reduction in crop height, active leaves and leaf area, as energy is directed towards the rapid formation of tubers (Lewu *et al.* 2017). The crop enters a leaf senescence period where leaves begin to yellow and tubers are fully developed and prepared for harvest (Miyasaka *et al.* 2003; Chauhan *et al.* 2024).

Table 5.1 Description of taro growth stages

Days After Planting	Growth Stage	Description	Illustration
74	Emergence	The taro crops have emerged from the soil. Small, tender leaves begin to appear as the plant establishes its root system.	
167	Vegetative	The crops are in full vegetative growth, with broad leaves expanding and the canopy thickening. The focus is on leaf production and growth.	
219	Maturity	The taro crops have reached maturity. Leaf growth begins to slow down, and energy is redirected towards tuber development. At this stage, the crop starts to prepare itself for harvest.	

During the study period, the weather conditions in the study area were continuously monitored using an Automatic Weather Station (AWS) located approximately 2 km from the smallholder taro field (Table 5.2). Over the taro growing period, the area had a total rainfall of 870.9 mm and an average maximum air temperature of 24 °C, along with other bioclimatic variables, as shown in Figure 5.2. Furthermore, rainfall typically followed a distinct trend of the lowest rainfall during the autumn and winter months between April and June and the highest precipitation during the spring and summer months between October and March (Figure 5.2).

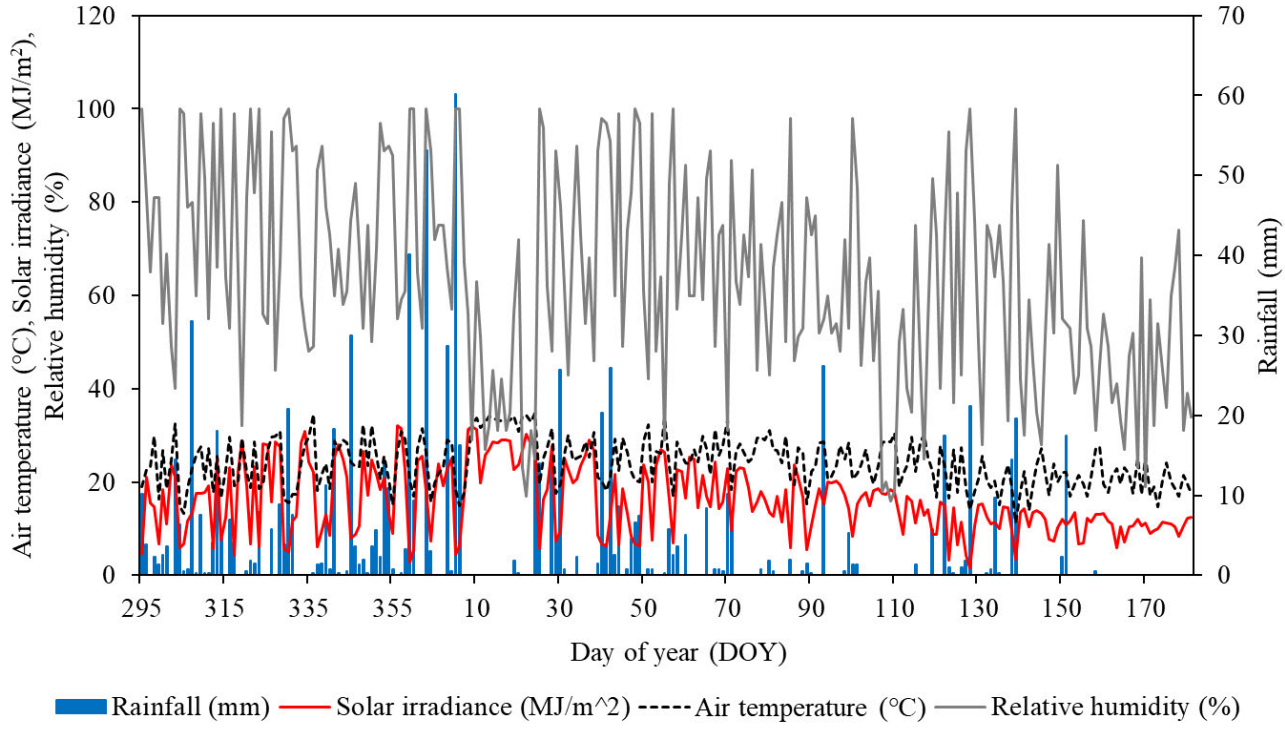

Figure 5.2 Daily weather conditions of the experimental plot in Swayimane over the taro growing period.

Table 5.2 Weather conditions observed during the emergence, vegetative and maturity growth stages of taro.

Taro Growth Stage	Emergence	Vegetative	Maturity
Days after planting	74	167	219
Maximum air temperature (°C)	25.1	21.8	19.6
Minimum air temperature (°C)	10.8	11.0	7.0
Total rainfall (mm)	00.0	01.3	00.0
Wind speed (m/s)	39.7	133.5	9.8
Relative humidity (%)	56	83	39
Mean vapor pressure deficit (kPa)	0.86	0.17	0.87

5.2.3 Field sampling and in-situ measurements

Field data sampling was conducted during the crop's emergence, vegetative and maturity growth stages. Pre-sampling was conducted using Google Earth Pro to delineate the smallholder taro field. Subsequently, the digitised polygon was imported into ArcGIS Pro, where the field was stratified into three elevation-based zones (upper slope, mid-slope, and lower slope) to

account for potential variability in topography and moisture distribution. A total of 100 stratified random sampling points were generated across these elevation strata to ensure comprehensive and representative spatial coverage. The resulting sampling points were transferred to a Trimble handheld Global Positioning System (GPS), which was used to accurately navigate to each sampling location within the field.

An SC-1 Leaf Porometer (Decagon Devices Inc., Pullman, Washington, USA) was used to measure the stomatal conductance of the crop at each sampling point. To confirm the readings accuracy, the leaf porometer was calibrated prior to use to ensure thermal equilibrium between the sensor clip and the environment (Brewer *et al.* 2022b). The calibration process began by placing filter paper saturated with distilled water over the aperture of the calibration (Ganesan *et al.* 2024). The sensor head was then attached to initiate a 30-second measurement period (Brewer *et al.* 2022b). Following each reading, the sensor was allowed to equilibrate before reattachment for subsequent measurements. This procedure was repeated ten times to ensure consistent and standardised readings of stomatal conductance. After calibration, the leaf porometer was carefully positioned on a fully sunlit taro leaf, specifically at the centre of the leaf blade and perpendicular to the midrib. The SC-1 leaf porometer automatically measured leaf stomatal conductance over a 30-second period while recording air temperature and humidity. Stomatal conductance values closer to 0 mmol m^{-2} s^{-1} indicate stomatal closure to reduce water loss, signifying server water stress. In contrast, stomatal conductance measurements closer to 500 mmol m^{-2} s^{-1} signify open stomata, reflecting minimal crop water stress and optimal physiological activity.

Following the measurement of stomatal conductance, taro leaf foliar temperature was measured using a digital laser infrared GM320 handheld thermometer (Shenzhen Jumaoyuan Science and Technology Co., Ltd, Nanshan District, Shenzhen, China). The GM320 thermometer is designed to provide precise temperature readings with a measurement range from -50 °C to 380 °C, an error margin of ± 1.5 °C and a spectral response of 8-14 µm. At each sampling point, five separate temperature measurements were recorded from different areas of the taro leaf to account for potential variability in temperature across the leaf surface. Foliar temperature measurements were obtained at (1) the centre of each leaf blade, near the primary leaf vein, (2) roughly one-third from the tip of the leaf, (3) about two-thirds down from the leaf tip, and (4) at the midpoint between the leaf vein and the leaf margin on both sides. The individual measurements were then averaged to provide a comprehensive representation of taro

leaf foliar temperature. All in-situ measurements were conducted on sunny days during the mid-morning to early afternoon, typically between 10:00 am and 2:00 pm local time, to capture peak photosynthesis activity.

5.2.4 Image acquisition and pre-processing

A DJI Matrice 300 (M300) (DJI-Innovations Inc., Shenzhen, China), equipped with a MicaSense Altum multispectral-thermal camera (MicaSense, Seattle, WA, USA) was used to acquire aerial-view imagery of the study field. The M300 multirotor drone with vertical take-off and landing, is well-suited in rural settlements where space for take-off and landing is limited (Puppala *et al.* 2023). Meanwhile, the MicaSense Altum sensor integrates a radiometrically calibrated thermal channel (11 μm) with five high-resolution spectral bands that measure reflectance in the blue (475 nm), green (560 nm), red (668 nm), red-edge (717 nm), and near-infrared (NIR) (840 nm) sections of the electromagnetic spectrum (Cottrell *et al.* 2024). The selection of the Altum camera is due to its ability to simultaneously capture multispectral and thermal infrared images while equipped with a global shutter that supports a capture rate of up to one second, ensuring high spatial resolution and precisely aligned imagery (Hutton *et al.* 2020b).

To ensure systematic and consistent data collection across the taro growth period, a flight path of the experimental plot was digitised from Google Earth Pro and exported as a Keyhole Markup Language (KML) file. Subsequently, the KML boundary of the study field was imported to the M300 handheld smart controller. Before and after all UAV flights, the Altum sensor was calibrated using a Calibration Reflectance Panel (CRP) equipped with a white balance card. The white balance card uses known reflectance properties across the spectrum to perform radiometric calibration on the sensor. This process involved manually capturing an unshaded image of the CRP, allowing the system to adjust for the prevailing illumination and atmospheric conditions during the flight (Buthelezi *et al.* 2023; Cottrell *et al.* 2024). Autonomous drone flights were conducted under clear sky conditions, simultaneously with field in-situ measurements, between 10:00 am and 2:00 pm local time, coinciding with the period of optimal solar irradiance. Furthermore, the flight mission was carried out using an 80% forward and sideward overlap at an altitude of 100 m above the ground, resulting in the acquisition of high spatial resolution imagery of 10.08 cm per pixel. A total of 1626 raw UAV imagery was captured during each growth stage and imported into Pix4D photogrammetry

software (Pix4D Inc. Denver, USA). The Pix4D software uses the CRP information and the raw images to automatically identify radiometric corrections and generate an ortho-mosaic of the taro field. Thereafter, ground reference points sampled during field data collection were used to refine the geometric accuracy of the UAV imagery, which was then referenced to the Universal Transverse Mercator (UTM zone36S) projection in ArcGIS Pro. Using equation 5.1 below, the thermal infrared data was transformed into absolute temperature values in the Pix4D software (Rutkoski *et al.* 2016; Osroosh *et al.* 2018).

$$Absolute\ Temperature = \frac{Thermal\ infrared}{100} - 273.15 \qquad units: °C \qquad (5.1)$$

Subsequently, the corresponding air temperature (Ta) value at the time of the flight was subtracted from the canopy temperature value (Tc) of each pixel to derive the difference (Tc – Ta °C) at each growth stage of taro (Zhang *et al.* 2019; Marques *et al.* 2020). Finally, the sampled in-situ measurements and associated geolocation data were overlaid with the acquired UAV imagery at each growth stage and crop thermal and multispectral reflectance properties extracted and used to compute spectral indices (Table 5.3). These indices were selected based on their reported direct and indirect correlations with crop water status in literature (Baluja *et al.* 2012a; Gago *et al.* 2017a; Ozelkan 2020). Standard remote sensing techniques were employed to compute spectral indices using the blue, green, red, red-edge and NIR channels of the spectrum. Concurrently, thermal indices, specifically the Normalised Relative Canopy Temperature (NRCT) and the Second Formulation of the Stomatal Conductance Index (I3), were calculated based on the canopy temperature (T_{canopy}) of sampled taro crops. Meanwhile, T_{wet} was established using the lower boundary temperature, under the assumption that these crops were undergoing maximum transpiration with open stomata, and T_{dry} was established using the higher boundary temperature, under the assumption that these crops were experiencing minimal transpiration with closed stomata (Baluja *et al.* 2012a; Crusiol *et al.* 2020b).

Table 5.3 UAV derived spectral indices used in this study.

Vegetation Index	Abbreviation and Equation	Reference
Thermal Indices		
Normalised Relative Canopy Temperature	$NRCT = \frac{T_{canopy} - T_{wet}}{T_{dry} - T_{wet}}$	(Elsayed *et al.* 2015)
Second Formulation of the Stomatal Conductance Index	$I3 = \frac{T_{canopy} - T_{wet}}{T_{dry} - T_{canopy}}$	(Baluja *et al.* 2012b)
Spectral Indices		
Normalised difference vegetation index	$NDVI = \frac{R_{Nir} - R_{red}}{R_{Nir} + R_{red}}$	(Rouse *et al.* 1974)
Soil-Adjusted Vegetation Index	$SAVI = \frac{R_{Nir} - R_{red}}{R_{Nir} + R_{red} + L} \times (1 + L)$	(Huete 1988)
Normalised Difference Red-Edge Index	$NDRE = \frac{R_{Nir} - R_{Redegde}}{R_{Nir} + R_{Rededge}}$	(Gitelson and Merzlyak 1994)
Transformed Chlorophyll Absorption in Reflectance Index	$TCARI = 3 \times (R_{Rededge} - R_{Red}) - 0.2 \times (R_{Rededge} - R_{Green}) \times \frac{R_{Redegde}}{R_{Red}}$	(Haboudane *et al.* 2002)
Modified Chlorophyll Absorption in Reflectance Index	$MCARI = (R_{Rededge} - R_{Red}) - 0.2 \times (R_{Rededge} - R_{Green}) \times \frac{R_{Rededge}}{R_{Red}}$	(Daughtry *et al.* 2000)
Normalised Green-Red Difference Index	$NGRDI = \frac{R_{Green} - R_{Red}}{R_{Green} + R_{Red}}$	(Hunt Jr *et al.* 2013)
Normalised Difference Water Index	$NDWI = \frac{R_{Green} - R_{Nir}}{R_{Green} + R_{Nir}}$	(Gao 1996; McFeeters 1996)
Structural Insensitive Pigment Index	$SIPI = \frac{R_{Nir} - R_{Blue}}{R_{Nir} + R_{Red}}$	(Penuelas *et al.* 1995)

Red-edge Chlorophyll Index	$CIrededge = \frac{R_{Nir}}{R_{rededge}} - 1$	(Gitelson *et al.* 2003; Gitelson *et al.* 2006)

5.2.5 Crop canopy extraction and soil background removal

The Excess Green minus Excess Red (ExGR) index-based segmentation technique was selected for extracting crop canopy and removing soil background following Riehle *et al.* (2020). The advantages of the ExGR index lie in its comprehensive ability to effectively distinguish between crop cover and soil by leveraging the contrast in the green and red bands (Meyer *et al.* 2004; Hamuda *et al.* 2016; Riehle *et al.* 2020; Upendar *et al.* 2021). Following equation 5.2, the ExGR index was used to generate a binary image from the gray-level histogram obtained during the segmentation process in Mathworks MatLab, where a fixed zero threshold was applied to differentiate between crop canopy and background elements (Hamuda *et al.* 2016). Positive pixel values were classified as 1, representing crop canopy, while negative pixels were classified as 0, indicating soil background (Riehle *et al.* 2020). A vegetation mask isolating the crop canopy from the background was converted to a shapefile and overlaid with the UAV imagery of each growth stage to extract the taro crop canopy in ArcGIS Pro.

$$ExGR = (2 \times R_{Green} - R_{Red} - R_{Blue}) - (1.4 \times R_{Red} - R_{Green}) \quad (5.2)$$

where *R* represents the reflectance values obtained from the respective spectral band.

5.2.6 Model development and statistical analysis

In this study, the Deep Neural Network (DNN) was used to develop prediction models of stomatal conductance and leaf temperature at each taro growth stage. The DNN is characterised by multiple interconnected hidden layers that work collectively to learn higher-level features and stimulate the complex relationships between input features and target variables (Chew *et al.* 2020; Traore *et al.* 2021; Bouguettaya *et al.* 2022). This deep learning approach was selected due to its capacity to handle high-dimensional data and non-linear relationships, making the algorithm suitable for predicting crop physiological indicators such as stomatal conductance and leaf temperature under varying growth conditions (Omosalewa *et al.* 2021). The study employed a DNN model with a Rectified Linear Unit (ReLU) transfer function to simulate

stomatal conductance and leaf temperature using a selection of 17 thermal and spectral indices by setting a maximum epoch at 200 interactions. To address the challenge of overfitting and ensure optimal model accuracy, a dropout regularization technique was implemented, with input and hidden layer dropout rates set at 0.4 and 0.2, respectively. Furthermore, the Adaptive Moment Estimation (Adam) was used as an optimisation algorithm in the DNN model and the SoftMax activation function used to transform the raw outputs of the neural network into a vector of probabilities. Lastly, the stomatal conductance and leaf temperature DNN models were fine-tuned to a learning rate of 0.001 and a batch size of 32 using Python 3.8. within Anaconda Jupyter Notebooks.

5.2.7 Accuracy Assessment

An accuracy assessment was conducted to evaluate the performance and overall robustness of the predictive models in estimating stomatal conductance and leaf temperature at each taro growth stage. The sampled data were randomly split into training (70%) and testing data (30%), where the former was used in model development and the latter in assessing the accuracy of predictive models. Three accuracy metrics were evaluated: the Coefficient of Determination (R2), the Root Mean Square Error (RMSE), and the Relative Root Mean Square Error (rRMSE). Specific details on these metrices are outlined in Ndlovu *et al.* (2024b) and Masenyama *et al.* (2023). The SHapley Additive exPlanations (SHAP) technique was employed to understand the contribution of the predictor variables in the model development of each growth stage. The SHAP technique computes the average marginal contribution value of each input variable and ranks their importance from least to most influential in the model development (Nahiduzzaman *et al.* 2023a). Lastly, the accuracy metrices were subjected to a statistical analysis using a Two-Way Analysis of Variance (ANOVA), in IBM SPSS software version 29.0.2, to assess the significant differences between the means of the prediction accuracies. In particular, the Two-Way ANOVA test was performed to statistically compare the estimation accuracies obtained for stomatal conductance and leaf temperature during the crop's emergence, vegetative and maturity growth stages. Based on the analysis, the *f*-value and the *p*-value were obtained to explore the significant relationships between the accuracy metrices achieved at each taro growth stage for both stomatal conductance and leaf temperature estimations. During this study, a significance level of 5% was applied and a p-value < 0.05 considered statically significant

(Sobejano-Paz *et al.* 2020). A detailed methodological workflow of the study is presented in Figure 5.3 below.

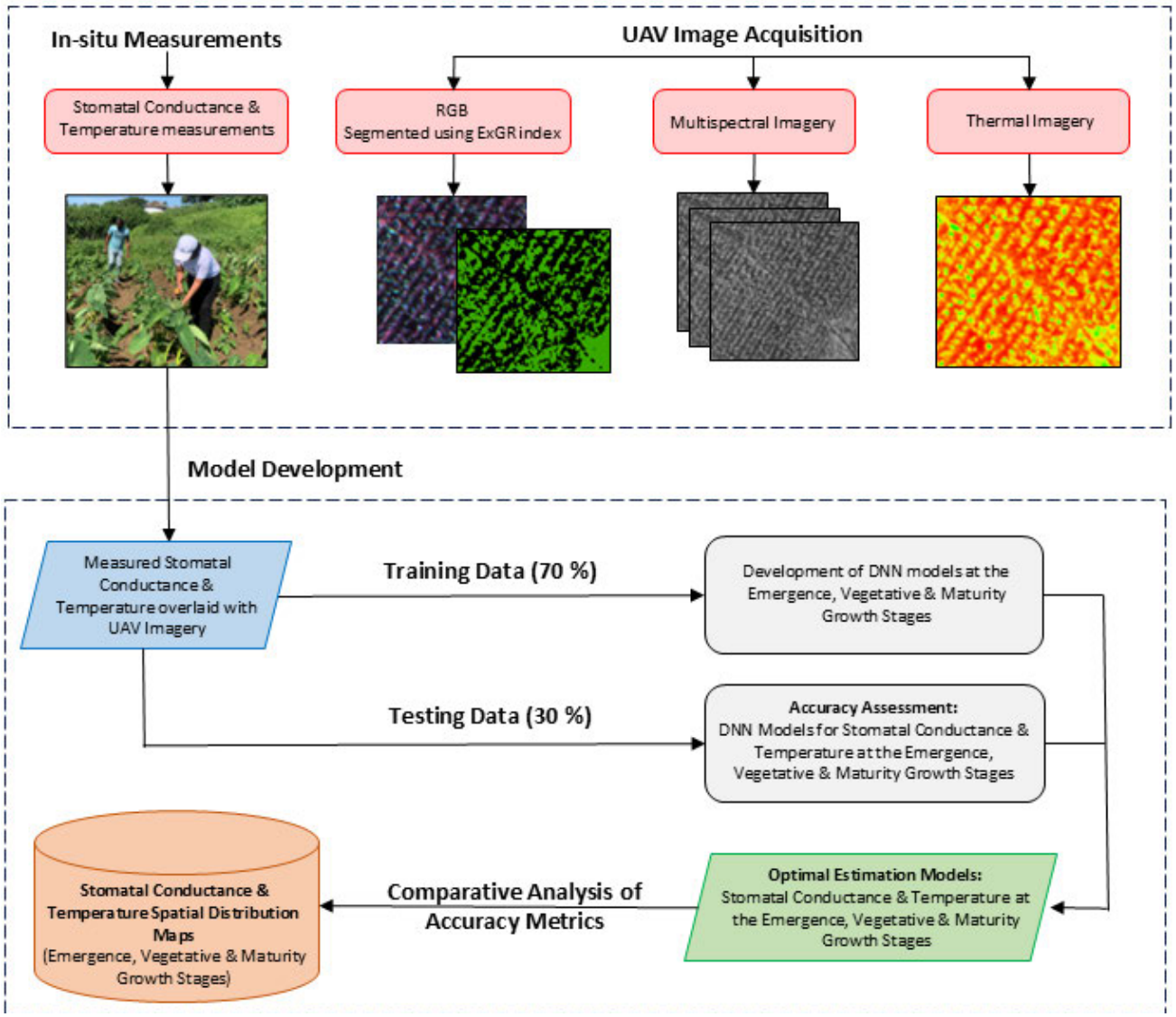

Figure 5.3 Methodological workflow of the study.

5.3 Results

5.3.1 Descriptive statistics

The descriptive statistics and variations in in-situ stomatal conductance and leaf temperature observed at the different growth stages are shown in Table 5.4. Distinct trends in stomatal conductance and leaf temperature were observed across the crop's growth stages. During the vegetative growth stage, mean stomatal conductance increased significantly, rising from 69.66

± 6.50 mmol m^{-2} s^{-1} at the emergence stage to a peak of 234.09 ± 16.96 mmol m^{-2} s^{-1}. This was followed by a decrease to 194.29 ± 11.03 mmol m^{-2} s^{-1} at the maturity stage. Meanwhile, mean leaf temperature decreased during the emergence stage from 36.93 ± 0.08 °C to 29. 90 ± 0.19 °C in the vegetative growth stage, thereafter, a slight increase to 31.84 ± 0.25 °C in the maturity growth stage.

Table 5.4 Descriptive statistics of in-situ taro stomatal conductance and leaf temperature.

Growth Stage	Min	Max	Median	Mean	Std.	SEM.	CV (%)
			Stomatal Conductance (mmol m^{-2} s^{-1})				
Emergence	22,70	333,20	49,00	69,66	58,13	6,50	83,45
Vegetative	43,10	575,90	174,85	234,09	149,77	16,96	63,98
Maturity	34,20	452,70	192,10	194,29	92,91	11,03	47,82
			Leaf Temperature (°C)				
Emergence	34,50	38,90	37,00	36,93	0,71	0,08	1,92
Vegetative	26,10	33,40	29,80	29,90	1,65	0,19	5,51
Maturity	28,00	36,30	31,60	31,84	2,07	0,25	6,50

The standard error of mean is denoted by SEM, the standard deviation by Std., and the coefficient of variation by CV.

It is worth noting that an inverse relationship between stomatal conductance and leaf temperature was observed, yielding an R^2 of 0.9986 (Figure 5.4a). The strong negative correlation between these variables illustrates that as stomatal conductance decreases, leaf temperature increases, resulting in a "hot canopy" effect, a potential indication of crop water stress. Conversely, an increase in stomatal conductance was associated with a decrease in leaf temperature, indicating a "cool canopy" with higher transpiration rates and optimal water productivity within the smallholder taro field. For instance, during the vegetative growth stage, average leaf temperatures were lowest at 29.9 °C and stomatal conductance highest at 234.09 mmol m^{-2} s^{-1}, potentially indicating optimal taro crop conditions.

Furthermore, the difference between canopy and air temperature (Tc – Ta) fluctuated throughout the crop's growth stages (Figure 5.4b). The emergence growth stage demonstrated the highest Tc – Ta difference of 11.83 °C. In contrast, the vegetative growth stage showed a significant reduction in the Tc -Ta difference, with a value of 8.1 °C. Meanwhile, during the maturity growth, a slight increase in the Tc -Ta differences was observed, yielding a mean difference value of 9.64 °C (Figure 5.4b).

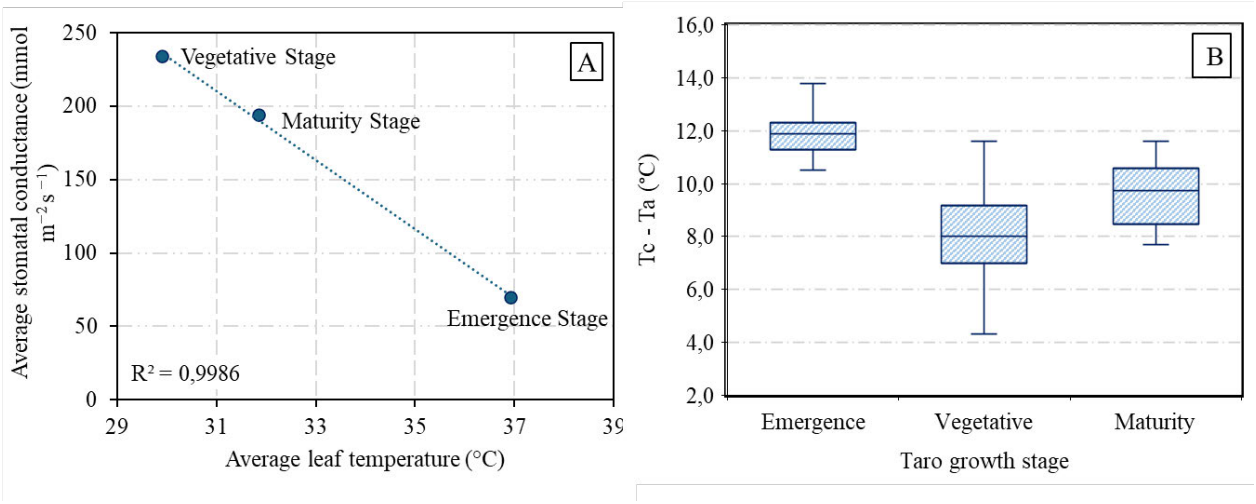

Figure 5.4 a) Correlation between average stomatal conductance and leaf temperature across the taro growth stages, and b) distribution of temperature gradients (Tc-Ta) between canopy temperature and air temperature.

5.3.2 Estimation of taro stomatal conductance and leaf temperature across the growth stages

Figure 5.5 represents the predictive accuracies obtained in the estimation of stomatal conductance and leaf temperature of smallholder taro crops across the growth stages based on the multisource feature fusion of thermal and multispectral canopy features. For the prediction of taro stomatal conductance, the vegetative growth stage yielded the most optimal model with an R^2 of 0.96, RMSE of 29.34 mmol m^{-2} s^{-1} and rRMSE of 12.86 % (Figure 5.5b1), based on the CIrededge, thermal, NCRT, SIPI, MCARI, NDRE and I3, in order of importance (Figure 5.6b1). Meanwhile, the emergence growth stage yielded the poorest prediction of stomatal conductance, producing an R^2 of 0.87, RMSE of 32.66 mmol m^{-2} s^{-1} and rRMSE of 26.87 % (Figure 5.5a1). The most suitable predictor variables which generated this model were the NCRT, NDWI, Thermal, Green, Red and NGRDI, in descending importance (Figure 5.6a1). Lastly, the maturity growth stage produced moderately high prediction accuracies, exhibiting an R^2 of 0.92, RMSE of 30.11 mmol m^{-2} s^{-1} and rRMSE of 13.89 % (Figure 5.5c1), with the thermal, NGRDI, NCRT, CIrededge, I3 and SAVI emerging as the top-most influential predictor variables, in order of importance (Figure 5.6c1).

When estimating leaf temperature, the emergence growth stage yielded the model with the lowest estimation accuracy, with an R^2 of 0.84, RMSE of 0.38 °C and rRMSE of 1.76 % (Figure 5.5a2). Based on the derived model, Thermal, NCRT, red-edge, NGRDI, NDWI, and NDRE were among the most important predictor variables, in order of importance (Figure 5.6a2). Meanwhile, a notable improvement in prediction accuracy was observed during the vegetative growth stage, where the model achieved the highest accuracy for estimating leaf temperature, with an R^2 of 0.95, RMSE of 0.33 °C and rRMSE of 1.11 % (Figure 5.5b2). The most significant predictor variables, in order of importance, were MCARI, Thermal, CIrededge, NRCT, SIPI, NDWI and NDRE (Figure 5.6b2). Then the matured growth stage model exhibited the most optimal estimation accuracies characterised by an R^2 of 0.90, RMSE of 0.57 °C and rRMSE of 1.81 % (Figure 5.5c2), based on the CIrededge, MCARI, NCRT, Thermal, I3 and NGRDI, in descending order of importance (Figure 5.6c2).

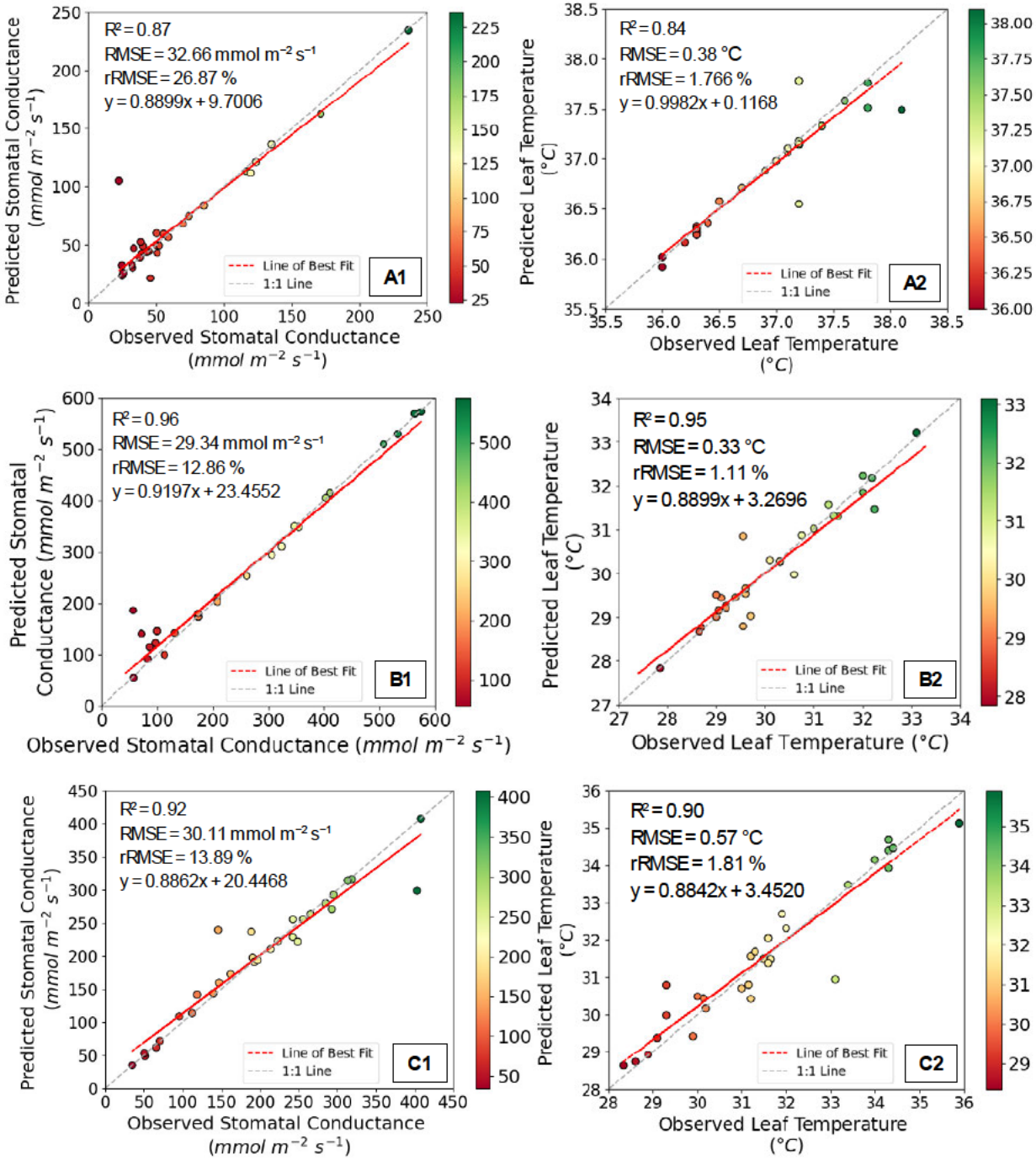

Figure 5.5 Relationship between observed and predicted a) stomatal conductance and b) leaf temperature during the 1) emergence, 2) vegetative and 3) maturity growth stages.

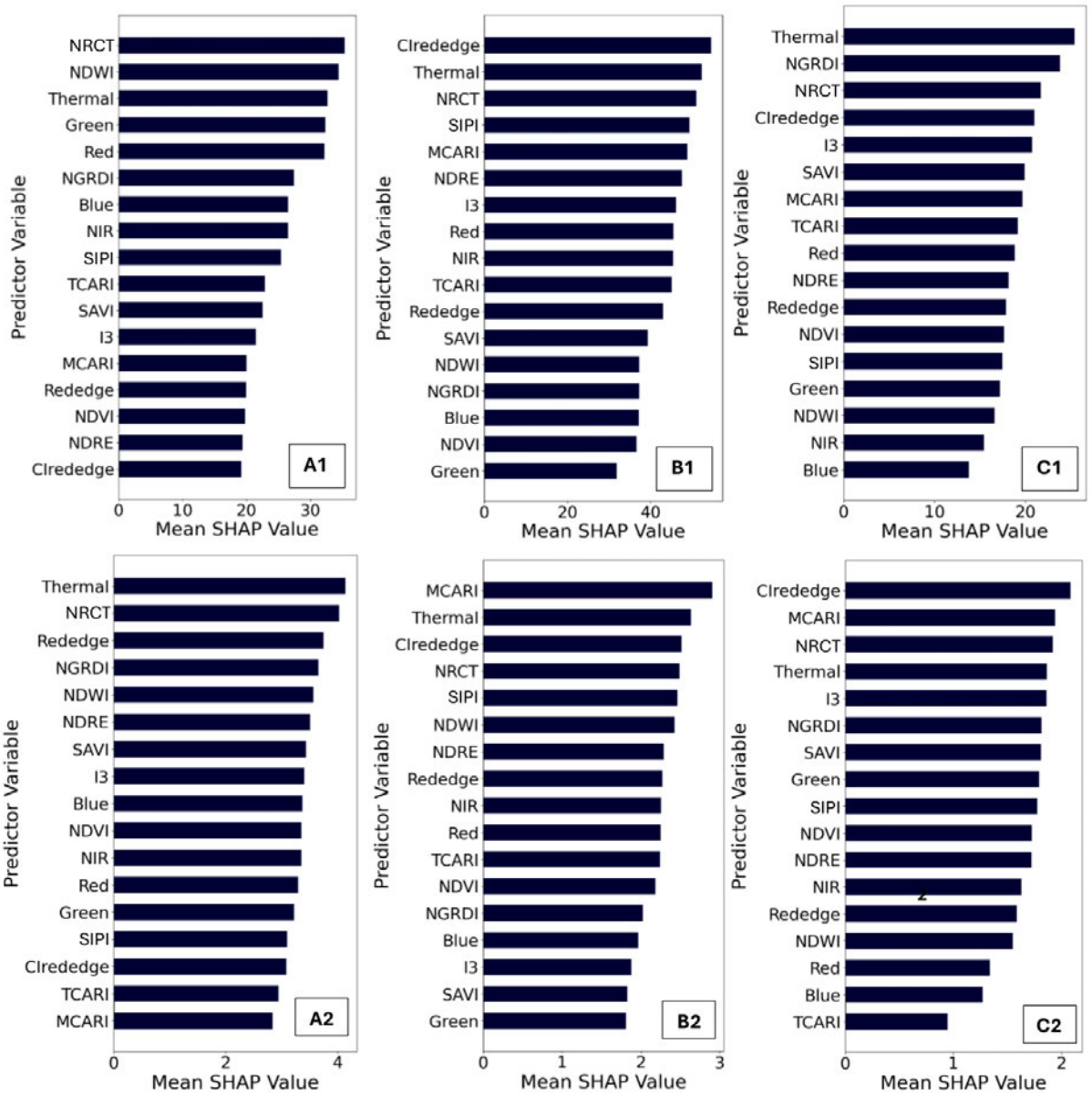

Figure 5.6 SHAP generated variable importance values of predictor variables used in developing the estimation models of a) stomatal conductance and b) leaf temperature during the 1) emergence, 2) vegetative and 3) maturity growth stages.

5.3.3 Comparative analysis between the prediction accuracies of taro stomatal conductance and leaf temperature across the growth stages

The crop's vegetative growth stage produced the most optimal prediction models for both stomatal conduce and leaf temperature, in comparison to the emergence and maturity growth stages. This pattern is consistent across the R^2, RMSE and rRMSE metrics for both stomatal conductance and leaf temperature, with generally higher estimation accuracies achieved during the vegetative growth stage of taro crops (Figure 5.7a & b). The Kolmogorov-Smirnov test indicated a normal distribution of residuals ($p > 0.05$), confirming that the residuals followed an approximately normal distribution. For stomatal conductance, the ANOVA test indicated a statistically significant difference in prediction performance, with the vegetative growth stage yielding the highest accuracy ($R^2 = 0.96$, RMSE = 29.34 mmol m^{-2} s^{-1} and rRMSE = 12.86 % (Figure 5.5b1), compared to the emergence and maturity stages. The ANOVA results produced a p-value of 0.0023, indicating a significant difference in the accuracy metrics achieved in predicting stomatal conductance amongst the emergence, vegetative and maturity growth stages. Similarly, for leaf temperature estimation, the ANOVA results confirmed significant variation in model performance across the growth stages, with the vegetative growth stage exhibiting the highest prediction accuracy (R^2 of 0.95, RMSE of 0.33 °C and rRMSE of 1.11 % (Figure 5.5b2)). Specifically, the ANOVA showed a significant difference in the accuracy metrics for predicting leaf temperature across the different growth stages, yielding a p-value of 0.0093. These findings highlight the variability in model accuracy across the different growth stages, suggesting that the vegetative stage provides the most reliable estimates for both stomatal conductance and leaf temperature, potentially due to optimal canopy conditions and enhanced physiological activity during this period. While the vegetative growth stage yielded the most accurate predictions, model performance was significantly lower during the emergence and maturity stages, indicating limited reliability of the models outside the vegetative phase.

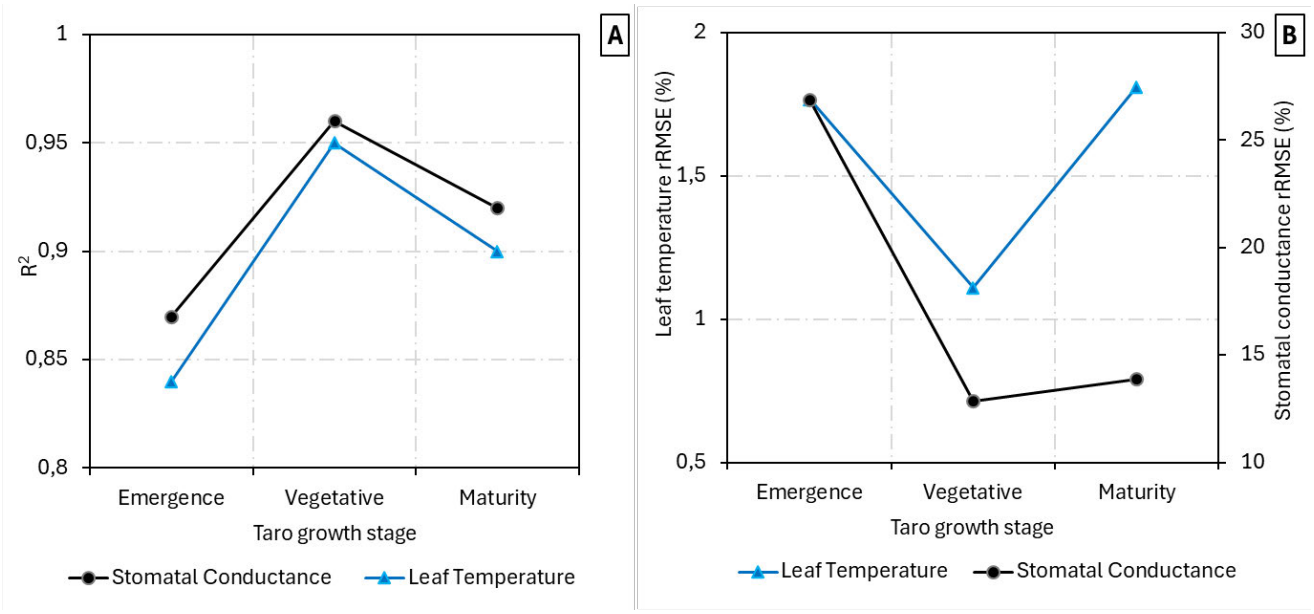

Figure 5.7 Comparative analysis of performance metrics, including a) R^2 and b) rRMSE across emergence, vegetative and maturity growth stages of taro.

5.3.4 Spatial and temporal variability of taro stomatal conductance and leaf temperature across the growth stages

The modelled spatial and temporal variability of stomatal conductance and leaf temperature of smallholder taro crops across the emergence, vegetative and maturity growth stages are presented in Figure 5.8. Overall, distinct temporal and spatial patterns were observed of stomatal conductance and leaf temperature across the growth stages. Taro stomatal conductance was relatively high during the vegetative growth stage, with the northwestern regions of the field displaying higher levels of stomatal conductance (Figure 5.8 a2). In contrast, the lowest stomatal conductance of 27.70 mmol m^{-2} s^{-1} was observed during the emergence growth stage, particularly in the western and central portions of the field (Figure 5.8 a1). As crops transitioned to the maturity stage, lower stomatal conductance was observed, coinciding with the reduced above-ground biomass and onset of the senescence phase (Figure 5.8 a3).

Conversely, leaf temperature was highest during the emergence stage, with elevated temperatures spread across the field (Figure 5.8 b1). During the vegetative stage, leaf temperature was lowest, with only a few areas reaching a maximum of 33.40 °C (Figure 5.8 b2). Lastly, moderate leaf temperatures were recorded during the maturity stage, with the highest values concentrated in the northwestern parts of the field (Figure 5.8 b3).

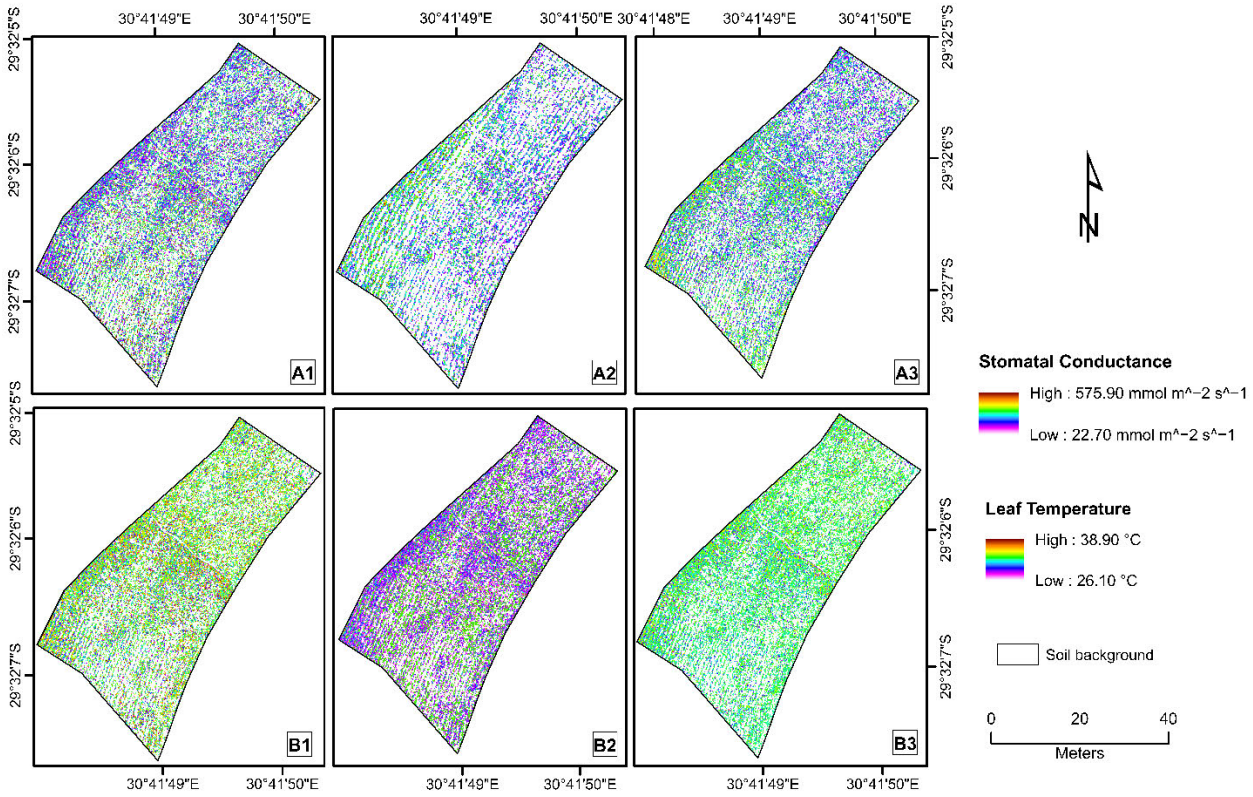

Figure 5.8 Spatial and temporal distribution of a) stomatal conductance and b) leaf temperature during the 1) emergence, 2) vegetative and 3) maturity growth stages.

5.4 Discussion

This study sought to assess the utility of UAV-based multimodal thermal and multispectral data in estimating the stomatal conductance and leaf temperature as indicators of crop water status within smallholder taro fields. The primary objectives were twofold: 1) to estimate stomatal conductance and leaf temperature using UAV multimodal thermal and multispectral at the emergence, vegetative and maturity growth stages of taro and 2) to compare the most optimal growth stage for estimating these physiological indicators of water status.

5.4.1 Predicting taro canopy water status using UAV multimodal thermal and multispectral remotely sensed features

Literature has confirmed that improved assessments of crop water status can be achieved by integrating thermal and multispectral datasets (Gerhards *et al.* 2019; Panday *et al.* 2020; Sobejano-Paz *et al.* 2020). This integrated approach allows for a comprehensive evaluation by capturing not only the thermal emissions related to crop transpiration but also additional crop

water status and overall health indicators, such as canopy structure, photosynthetic activity and chlorophyll content, which are optimally detected through multispectral wavelengths (Santesteban *et al.* 2017b; Zhang *et al.* 2023b). Findings of this study demonstrated that the fusion of multimodal thermal and multispectral data produced optimal prediction accuracies, with R^2 values greater than 0.80 and rRMSE's less than 30% error (Figure 5.5). These results are in agreement with Cheng *et al.* (2022), who also reported that combining thermal and multispectral spectra yielded the highest accuracies in predicting maize soil moisture to an R^2 of 0.78 and RMSE of 11.2 %. At the vegetative growth stage, the findings of this study illustrated that red-edge-based indices such as CIrededge, SIPI, MCARI and NDRE were top predictor variables in estimating both stomatal conductance and leaf temperature (Figure 5.6).

This is attributed to the fact that the red-edge channel is sensitive to variations in water content, which, when reduced, leads to decreased photosynthetic activity and stomatal closure (Colovic *et al.* 2022). As a result, chlorophyll content diminishes, causing a shift in the red-edge reflectance towards longer wavelengths (Xie *et al.* 2018; Ali and Imran 2020). When chlorophyll levels are higher, the red-edge position shifts to shorter wavelengths, reflecting optimal water status, whereas lower chlorophyll levels indicate reduced moisture and crop stress (Ballester *et al.* 2019; Li *et al.* 2022c). For example, a study by Zarco-Tejada *et al.* (2003) demonstrated that the red-edge region aligns with fluorescence emissions, which are closely associated with photosynthetic efficiency, reinforcing the link between stomatal conductance and photosynthesis, as changes in fluorescence reflect variations in the physiological processes governing water use and gas exchange in plants. However, it is important to acknowledge that the strong performance of red-edge indices in this study was observed specifically in taro during its vegetative growth stage. The ability of these indices to reliably predict physiological traits such as stomatal conductance and leaf temperature may not extend to other crops or growth stages, as spectral responses can vary significantly across species and phenological phases. For example, crop architecture, leaf structure, and pigment composition differ between species and over time, potentially altering reflectance behaviours and reducing the efficacy of red-edge-based indices (Xie *et al.* 2018; Omia *et al.* 2023). Therefore, caution must be exercised when generalising these findings, and further validation is needed across different crop types and phenological stages to confirm the broader applicability of red-edge indices in crop water status monitoring. Overall, the combination of thermal and multispectral data, including red-edge-

derived indices, provides a powerful complementary dataset conducive to characterising smallholder taro crop water status.

5.4.2 Comparison of stomatal conductance and leaf temperature predictions across the growth stages of taro crops

The findings revealed that the vegetative growth stage produced the most optimal estimations of taro stomatal conductance (R^2 of 0.96, RMSE of 29.34 mmol m^{-2} s^{-1} and rRMSE of 12.86 %) and leaf temperature (R^2 of 0.95, RMSE of 0.33 °C and rRMSE of 1.11 %). This can be explained by the higher above-ground biomass accumulation during the vegetative stage, leading to increased foliage and canopy density (Chauhan *et al.* 2024). At this stage, the plants allocate more resources to foliage growth, which supports more efficient regulation of water loss and optimal photosynthetic activity (Badr *et al.* 2012). In contrast, during the maturity stage, resource allocation shifts towards underground tuber development, reducing the foliage and affecting the model's predictions (Kunz *et al.* 2024b). Furthermore, although soil background removal was performed, the dense canopy at this growth stage reduces soil exposure, allowing for accurate estimations of stomatal conductance and leaf temperature in the absence of external influences such as soil temperature (Maimaitiyiming *et al.* 2020b; Messina and Modica 2020). This contrasts with taro's emergence growth stage where canopy coverage is poor, resulting in the observation of higher leaf temperatures due to heat absorption from the soil, as evident in this study.

Furthermore, the emergence growth stage demonstrated the highest Tc -Ta difference, indicating greater levels of thermal stress during this stage (Figure 5.4b). When crops are in a state of water deficit and are experiencing water shortages, the Tc -Ta difference tends to increase as plants struggle to regulate their leaf temperatures and maintain their physiological functions (Yi *et al.* 2020; Guo *et al.* 2023). In contrast, the vegetative growth stage exhibited the lowest Tc – Ta difference, indicating that taro crops effectively managed heat stress due to increased stomatal conductance and adequate water intake (Luan and Vico 2021; Brewer *et al.* 2022b). Therefore, the relatively high stomatal conductance, coupled with low leaf temperature and Tc - Ta difference values during the vegetative growth stage, suggest optimal crop water status, aligning with the optimal prediction accuracies achieved for both stomatal conductance and leaf temperature during this stage. Meanwhile, during the maturity growth stage, reduced prediction accuracies are observed as taro crop leaves become yellow and canopy coverage

decreases due to optimised tuber development and crop senescence. These findings are supported by Zhang *et al.* (2023b), who found that maize vegetative growth stage facilitated the most accurate soil moisture predictions, yielding an optimal R^2 of 0.78 and rRMSE of 19.63%. Additionally, Wang *et al.* (2024a) reported that the vegetative growth stage produced optimal accuracies for stomatal conductance predictions, achieving an RMSE of 15%.

While the vegetative stage allows for highly accurate predictions of stomatal conductance and leaf temperature due to optimal canopy and physiological conditions, the model's reduced accuracy during emergence and maturity stages limits its effectiveness for full-season monitoring. For instance, it will be difficult to monitor the water stress during the emergence stage, where low canopy coverage and high soil background interference hinder the accurate assessment of plant physiological traits. Under these conditions, the elevated Tc - Ta values suggest that monitoring water stress becomes more challenging, and physiological signals may be masked by soil heat influence. These stage-specific variations underscore the need for tailored modelling approaches or additional correction methods to improve reliability during early and late growth phases.

5.4.3 Implications of the study and recommendations for future research

Through providing spatially detailed and near-real-time data on taro crop water status, the findings of this research contribute toward enhancing water stress detection and improving water management strategies within smallholder farming systems. The ability to accurately estimate stomatal conductance and leaf temperature at optimal growth stages introduce a data-driven approach to assessing crop water status, allowing for the development of timely interventions to mitigate moisture deficits. Furthermore, this research supports the diversification of crop systems by advocating for the inclusion of NUS, such as taro, into mainstream farming frameworks, which could bolster food security and sustainability, particularly in water-scarce regions of the global south.

Nonetheless, this study does not come without its limitations. Although high-resolution UAV imagery was utilised, the spectral resolution of the multispectral sensor is limited, restricting the ability to compute certain vegetation indices, particularly those that require shortwave infrared wavelengths, which are crucial for accurately quantifying water status. Therefore, it is recommended that future studies explore the integration of sensors with higher

spectral resolution to capture more detailed information on crop water status. Additional research is also required to enhance the calibration of thermal sensors, addressing issues such as non-uniformity correction and temperature drift to improve data quality. By refining these calibration processes, future studies can achieve greater accuracy and reliability in UAV-based temperature measurements, particularly in diverse environmental conditions. A further limitation of the study is that while the DNN models were trained and tested using in-situ stomatal conductance and leaf temperature data, the dataset was field-specific and may not fully capture the broader variability across different smallholder taro fields. As such, the spatial and temporal patterns observed may have been influenced by environmental or management factors not explicitly accounted for in this analysis. Caution is therefore advised when generalising these findings beyond the study site or season. Future studies should explore the application of DNN models at a larger scale to enhance the generalizability and robustness of taro crop water status estimations. Additionally, while the study estimated crop water status across various growth stages, it mainly focused on the major growth stages of smallholder taro crops. Therefore, it is essential that future research assess the intermediary growth stages as well to gain a comprehensive understanding of crop development and water status, thereby enhancing the precision of water management strategies in taro farmlands.

5.5 Conclusion

This study investigated the utility of multi-modal UAV thermal and multispectral data in estimating the spatial and temporal variability of stomatal conductance and leaf temperature as proxies of crop water status in neglected and underutilised taro crops within smallholder farming systems. The primary conclusions are as follows:

- Thermal remotely sensed proximal data has proven critical in estimating taro stomatal conductance and leaf temperature, with the thermal band and derived indices emerging as important predictor variables across the taro growth stages.
- The vegetative growth stage exhibited the highest prediction accuracies for stomatal conductance (R^2 of 0.96, RMSE of 29.34 mmol m^{-2} s^{-1} and rRMSE of 12.86 %) and leaf temperature (R^2 of 0.95, RMSE of 0.33 °C and rRMSE of 1.11 %).

These findings underscore the effectiveness of integrating thermal imagery with multispectral data, allowing for the near-real-time and continuous monitoring of taro crops. By

harnessing the capabilities of UAV technology, this study provides a powerful tool for assessing smallholder taro crop water status at unprecedented accuracy and frequency, allowing for timely interventions and informed decision-making on crop and water management. Moreover, the insights gained from this research contribute to the broader body of scientific knowledge on precision agriculture and pave the way for transforming current cropping systems to more climate-resilient NUS, such as taro, especially in smallholder farming where the impacts of climate variability are exacerbated because of limited resources. Ultimately, this research support Sustainable Development Goal 2: Zero Hunger and 13: Climate Action, as it addresses the challenges posed by climate variability while contributing to continental efforts to enhance food security and nutrition in the global south.

5.6 Summary

Chapter Five evaluated the multi-temporal variability of taro water status, particularly stomatal conductance and leaf temperature across the emergence, vegetative and maturity growth stages, using UAV-acquired thermal and multispectral data. The findings of the study observed distinct variations in stomatal conductance and leaf temperature, with the vegetative growth stage exhibiting the highest prediction accuracies. While UAV remotely sensed thermal and multispectral data are critical for monitoring crop water status, the comprehensive integration of multiple data sources and environmental factors can enhance model accuracies. Therefore, Chapter Six presents a data-driven approach to optimising the estimation of taro crop water status, using UAV-derived thermal and multispectral remotely sensed data, topographic variables, and advanced machine learning techniques. Furthermore, this chapter will explore the application of critical water stress thresholds of taro crops to identify areas of water stress, enabling targeted interventions for mitigating smallholder taro crop water deficit.

CHAPTER SIX

Optimising Neglected and Underutilised Taro Crop Water Status Estimations using UAV-Acquired Thermal and Multispectral Remotely Sensed Data

This chapter is based on:

Ndlovu, H. S., Odindi, J., Sibanda, M., & Mutanga, O. (2025). Optimising Neglected and Underutilised Taro Crop Water Status Estimations using UAV-Acquired Thermal and Multispectral Remotely Sensed Data. *Smart Agricultural Technology*, Under Preparation.

Abstract

Accurate estimation of crop water status is crucial for enhancing agricultural productivity and sustainability, particularly in rainfed smallholder farming systems. Taro (*Colocasia esculenta* (L)), a neglected and underutilised crop, has been identified as a climate-smart crop due to its drought and heat tolerance abilities. Nonetheless, the overall productivity and yield of taro, as well as the palatability of its tubers, is largely affected by inadequate moisture availability and crop water stress that induce physiological responses such as increased leaf temperatures and reduced stomatal conductance. While Unmanned Aerial Vehicle (UAV)-acquired thermal and multispectral data are critical for assessing crop water dynamics, literature have argued that integrating topographic features, such as slope, topographic wetness and aspect can enhance model accuracy and predictive performance. Hence, this study sought to evaluate the utility of a data-driven approach using UAV-based thermal and multispectral remotely sensed data, along with topographic variables, to estimate the stomatal conductance and leaf temperature of smallholder taro crops across different growth stages (emergence, vegetative, and maturity) as proxies for crop water status. The findings revealed that multispectral bands and thermal data, together with derived thermal indices, are critical for estimating both stomatal conductance and leaf temperature across the taro growth stages (R^2 values ranging between 0.61 and 0.84). To ensure reliability and accuracy of crop water status models, advanced feature selection and optimisation techniques were applied to deep neural network models developed on a combination of all feature subsets. The optimised analysis revealed that the vegetative stage exhibited the highest predictive accuracy, with R^2 values exceeding 0.95 and rRMSE values below 11 %, for both stomatal conductance and leaf temperature. In contrast, although generally accurate, the emergence and maturity stages showed slightly lower accuracies, with R^2 values above 0.91 and rRMSEs less than 17%. The findings of this study underscore the utility of integrating high-resolution UAV-derived proximal data with advanced modelling techniques to develop efficient and scalable methods for monitoring crop water status of neglected and underutilised taro crops and supporting sustainable agricultural practices in resource-constrained smallholder farming systems.

Keywords: unmanned aerial vehicle, thermal imagery, multispectral data, stomatal conductance, leaf temperature, model optimisation, crop water stress, precision agriculture

6.1 Introduction

The global demand for food production, driven by a growing human population and changing dietary patterns, is expected to rise by over 50% by 2050 (Turk 2016; Van Dijk *et al.* 2021; Falcon *et al.* 2022). However, the ability of traditional agricultural systems to meet this rising demand is being compromised by a range of challenges, with climate change being one of the most significant stressors (Vos and Bellù 2019; Das 2024). Rising temperatures, erratic rainfall patterns and more frequent extreme weather events have led to adverse effects on crop production globally (Gomez-Zavaglia *et al.* 2020). These impacts are particularly acute in developing regions, such as southern Africa, where pre-existing issues of hunger and food insecurity intersect with a semi-arid climate (Ebhuoma *et al.* 2020; Chakona and Mushangai 2021). Furthermore, smallholder farming systems, responsible for approximately 80% of local food production, are particularly vulnerable due to their reliance on seasonal rainfall for irrigation, limited resources and dependence on traditional farming techniques (Gomez y Paloma *et al.* 2020; Hlophe-Ginindza and Mpandeli 2020). Consequently, food and nutrition security remain persistent concerns, as conventional crops struggle to thrive under increasingly variable climate conditions (Chivenge *et al.* 2015; Aryal *et al.* 2020). This reality has prompted the urgent need for innovative and climate-smart approaches aimed at redesigning current agricultural landscapes to include crop species that are more resilient to the effects of climate change.

The above challenges necessitate a rethink of traditional farming practices to embrace a more holistic approach to agriculture that prioritises climate resilience, human nutrition and food security (Mabhaudhi *et al.* 2018). Notably, Neglected and Underutilised Crop Species (NUS) offer a promising solution to climate-resilient and nutrition-sensitive agriculture. For instance, Taro (*Colocasia esculenta* (L)), also known as Amadumbe in South Africa, holds exceptional adaptability, drought and heat tolerance and the ability to thrive in challenging environmental conditions, making it well suited to smallholder farming systems in vulnerable regions (Mabhaudhi and Modi 2015; Oyeyinka and Amonsou 2020). Furthermore, taro's nutritional profile, rich in carbohydrates, protein, vitamins and natural sterols, is valuable in addressing micronutrient deficiencies, while promoting food security (Chivenge *et al.* 2015; Haerussana *et al.* 2022). Although taro presents an opportunity to diversify agricultural systems, a critical gap remains in the literature regarding the spatial and temporal monitoring of its water status and stress responses across its growing season. Moreover, the accurate monitoring of taro

moisture content is crucial for determining the quality of its tubers, as it directly impacts their texture and palatability (Ferdaus *et al.* 2023). Therefore, development of spatially and temporally explicit evidence-based information on taro's water status is essential for maintaining optimal moisture levels, informing climate-adaptive management practices and optimising overall crop yields and quality.

The dynamics of crop water status can be effectively captured through physiological indicators, with stomatal conductance and leaf temperature as key metrics for quantifying crop moisture levels (Pirasteh-Anosheh *et al.* 2016; Gerhards *et al.* 2019; Wang *et al.* 2022a). Literature shows that water stress activates a series of physiological responses in crops, including stomatal closure, which serves as a critical adaptation mechanism to conserve water and ensure survival under unfavourable conditions (Matese *et al.* 2015; Gracia-Romero *et al.* 2019a; Sobejano-Paz *et al.* 2020). The closure of stomata in response to water deficits limits transpiration and results in increased leaf and canopy temperatures due to reduced evaporative cooling (Gerhards *et al.* 2019). Furthermore, as taro progresses through its emergence, vegetative, and maturity stages, changes in stomatal conductance and leaf temperature reflect variations in photosynthetic activity, making these indicators essential for tracking water status over the growing season (Brewer *et al.* 2022b). Studies have identified critical physiological thresholds for tuber crops (including taro), where crop growth and development become adversely affected (Hassanpanah and Khorshidi Benam 2004; Soureshjani *et al.* 2019). Ramírez *et al.* (2016) and Ninanya *et al.* (2021) for instance established that values below 50 mmol m^{-2} s^{-1} stomatal conductance lead to significant stress in tuber crops, while Luo QunYing (2011), Mabhaudhi *et al.* (2014), and Kunz *et al.* (2024b) noted that a minimum of 10 °C and a maximum of 35 °C are required for taro's growth and optimal productivity, respectively, with temperatures exceeding these thresholds inducing stress. To identify critical thresholds for stomatal conductance and leaf temperature, previous research has employed linear regression models to analyse the relationship between these indicators and physiological processes affected by water deficits, such as net photosynthesis, carbon isotope discrimination, and the crop water stress index (Ramírez *et al.* 2016; Gerhards *et al.* 2019; Kim and Lee 2019). For instance, plotting the net photosynthesis of tuber crops against stomatal conductance has been used to determine the point at which the relationship between these variables changes slope, referred to as the "breakpoint" by Ahumada-Orellana *et al.* (2019). This breakpoint represents the stomatal conductance threshold, below which net photosynthesis declines significantly,

indicating the onset of water stress (Ahumada-Orellana *et al.* 2019). While predefined thresholds are invaluable for identifying water-stressed crops, there is a pressing need for innovative, efficient, and scalable strategies to accurately assess and quantify stomatal conductance and leaf temperature throughout the growing season, capturing the spatiotemporal dynamics of taro crop water status.

Even though conventional techniques for assessing and quantifying stomatal conductance and leaf temperature have proven reliable, these methods are resource-intensive, prone to human error, expensive and not well suited for the continuous spatial and temporal monitoring of water status across the growing season (Maimaitiyiming *et al.* 2020a; Panday *et al.* 2020). Recent developments in the field of earth observation technologies, particularly thermal remote sensing, have offered a transformative tool for monitoring crop water status (Messina and Modica 2020; Awais *et al.* 2022a). Literature has demonstrated that thermal infrared imaging has significant correlation with crop water stress, as the thermal radiation emitted from crop canopy is highly sensitive to changes in canopy temperature, reflecting its physiological responses to water availability (Maes and Steppe 2012; Gerhards *et al.* 2019; Krishna *et al.* 2021). The launch of advanced satellite-based thermal sensors, including Ecosystem Spaceborne Thermal Radiometer Experiment on Space Station (ECOSTRESS), Advanced Spaceborne Thermal Emission and Reflection Radiometer (ASTER) and Landsat Thermal Infrared Sensor (Landsat -TIRS) marked a significant milestone in crop water status monitoring (Piekarczyk *et al.* 2012; Xue *et al.* 2020a). While thermal remote sensing provides a robust framework for monitoring crop water status, the integration of thermal data with multispectral imagery has been noted to provide a more comprehensive understanding of crop water dynamics and overall health, enabling the capture of subtle variations in crop water status that may not be detectable through thermal remotely sensed data alone (Gerhards *et al.* 2019; Messina and Modica 2020; Gao *et al.* 2024). Multispectral sensors, such as Multispectral Instrument (MSI), Landsat Thematic Mapper (TM)/Enhanced TM Plus (ETM+), WorldView-2/3, and PlanetScope, which capture spectral variability from the visible to shortwave infrared regions, provide complementary information to thermal data, capturing key indicators of crop moisture, health, and overall productivity (Misra *et al.* 2020; Tsvetkov 2023). Although satellite-based thermal and multispectral sensors offer valuable insights, their relatively coarse spatial resolution and limited revisit time restrict their ability to provide continuous, field-scale monitoring of crop water status (Mohamed *et al.* 2017; Reddy 2018). Moreover, while high-

resolution sensors such as WorldView-3 and PlanetScope offer finer spatial detail, their high cost and restricted data availability limit their practicality for sustained crop monitoring (Kpienbaareh *et al.* 2021; Sagan *et al.* 2021). Consequently, novel and spatially explicit alternatives are essential for detecting intricate variations in crop water status, thereby facilitating data-driven precision agriculture.

The launch of advanced proximal remote sensing technologies, particularly Unmanned Aerial Vehicles (UAVs), has opened up new opportunities for crop water status monitoring by enabling the acquisition of high-resolution thermal and multispectral data at ultra-high spatial and temporal resolutions (Hussain *et al.* 2020; Nhamo *et al.* 2020). By harnessing the versatility of UAVs, near-real-time imagery can be obtained at sub-centimeter pixel scales, enabling targeted observations and on-demand imagery acquisition (Malbéteau *et al.* 2018b; Chivasa *et al.* 2020). This capability is instrumental for addressing the limitations of traditional satellite-based methods and facilitating the continuous, precise, and temporally frequent monitoring of crop moisture at field scale (Santesteban *et al.* 2017a; Malbéteau *et al.* 2018b). Recently, Kapari *et al.* (2024) demonstrated the efficacy of UAV-based remote sensing for estimating maize crop water stress, with R^2 values of 0.85 and RMSE of 0.05, while Guimarães *et al.* (2024) employed UAV-acquired multispectral and thermal imagery to predict stomatal conductance in almond orchards, yielding an optimal R^2 value of 0.87 and an MSE of 0.0016 mmol m^{-2} s^{-1}. Despite this progress, to the best of our knowledge, the use of high-resolution UAV-based thermal and multispectral sensors for monitoring water status in neglected and underutilised taro crops within rainfed smallholder farming systems remains largely underexplored (Santesteban *et al.* 2017a; Sagan *et al.* 2019a).

Meanwhile, deep learning approaches, particularly the Deep Neural Networks (DNNs) algorithm, has emerged as a powerful tool in crop monitoring and assessments (Nguyen *et al.* 2020; Zhou *et al.* 2021). Compared to other machine learning algorithms, DNNs excel in processing high-dimensional dataset and capturing non-linear and hierarchical patterns, making them ideal for modelling complex crop water dynamics (de Melo *et al.* 2022; Rajwade *et al.* 2023). Additionally, its ability to automatically learn and extract intricate features from raw inputs provides an advantage in scenarios where complex interactions between variables require advanced modelling (Yuan *et al.* 2020; Omosalewa *et al.* 2021). A study by Elsherbiny *et al.* (2021) integrated visible and thermal imagery, including thermal indices and vegetation indices, to predict the canopy water content of rice paddies to an R^2 of 0.98 and RMSE of 0.59 %, using

deep learning techniques. Whereas thermal and multispectral data are essential for capturing crop water dynamics, recent studies have argued that integrating topographic features, such as slope, topographic wetness index and aspect can further enhance model accuracy (Allen *et al.* 2011; Singh and Das 2022; Shi *et al.* 2024). These variables provide additional critical information that accounts for spatial variability in crop growth and water stress across the landscape, thereby improving the robustness of predictive models (Maestrini and Basso 2018a). For instance, slope controls surface water runoff and infiltration while aspect determines the exposure of the crop to sunlight, which influences crop thermal signatures (McTavish *et al.* 2020; Zhu *et al.* 2023). Nonetheless, Saravi *et al.* (2021) argue that while deep learning offers immense potential for agricultural applications through hierarchical data processing, the inclusion of too many variables can result in information redundancy, multicollinearity and computation complexity, thereby reducing computational efficiency and model accuracy (Garg and Tai 2013; Chan *et al.* 2022). Furthermore, Wei *et al.* (2023) demonstrated that different crop growth stages exhibit distinct temporal growth characteristics, highlighting the necessity of selecting stage-specific input features that are sensitive to the unique crop attributes of each stage. As a result, optimisation of predictive models by selecting only the most relevant features is essential for maintaining performance and accuracy, particularly when assessing moisture variability across crop growth stages and conditions (Abdolrasol *et al.* 2021; Saravi *et al.* 2021; Liao *et al.* 2022).

In this regard, this study sought to assess the utility of UAV-derived thermal and multispectral imagery in estimating the stomatal conductance and leaf temperature as proxies of crop water status and stress across the growth stages of smallholder taro farming systems. Specifically, the study sought to evaluate the predictive performance of feature subsets (thermal data, multispectral bands, vegetation indices and topographic variables) in estimating stomatal conductance and leaf temperature of smallholder taro crops.

6.2 Materials and Methods

6.2.1 Study site description

This study was conducted in the rural village of Swayimane (29°31′24″ S; 30°41′37″ E) (Figure 6.1), located northeast of Pietermaritzburg city in uMshwathi Municipality, KwaZulu-Natal, South Africa. Situated within the moist midland mistbelt bioresource group (Camp 1999; Cele

and Mudhara 2024), Swayimane is characterised by a sub-humid climate with average temperatures ranging from 11.8 °C to 24 °C, and a mean annual temperature of 17 °C (Gokool *et al.* 2024; Kapari *et al.* 2025). The region experiences hot and wet summers, and cool dry winters, with annual rainfall ranging between 600 mm and 1100 mm (Brewer *et al.* 2022c; Cele and Mudhara 2024). The soils in the study area are primarily arable clay loam, and rank among the top 2% of high-potential land in South Africa (Ndlovu *et al.* 2021c), making them highly suitable for crop cultivation, that include maize, sugarcane, sweet potato, and taro. Farming systems in Swayimane are rooted in traditional practices, where manual labour is employed for field management, and livestock manure is commonly utilised as natural fertiliser. Smallholder subsistence farming is prevalent, with crops grown for both local consumption and sale. This farming system plays a crucial role in supporting food security and sustaining local livelihoods, highlighting the importance of the region for agricultural research focused on enhancing productivity and resilience. Although characterised by arable land, Swayimane has been identified as a region of high climate change risk, with projections suggesting an increase in temperature and unpredictable changes in precipitation (Mthethwa *et al.* 2022).

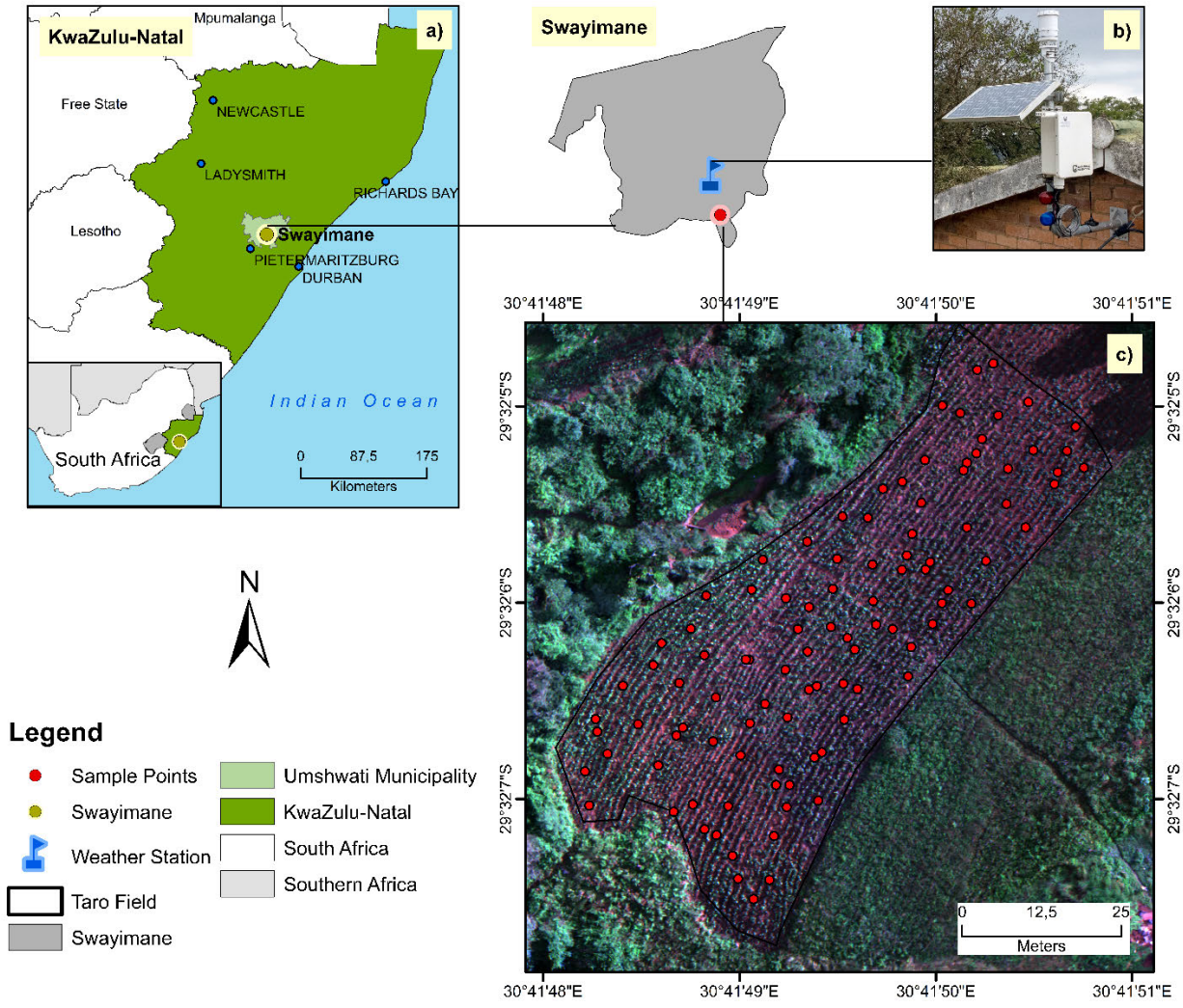

Figure 6.1 Location of the study site in Swayimane, KwaZulu-Natal, South Africa, illustrating the location of a) Swayimane within the province, b) the automatic weather station, and c) the specific experimental taro field.

6.2.2 Experimental field and growth stage characteristics

This study was conducted in a smallholder rainfed experimental field spanning 2864.56 m², where taro was planted on the 26th of October 2022. An Automatic Weather Station (AWS), following the World Meteorological Organisation's standards, proximal to the experimental field was used to continuously monitor the local microclimatic conditions across the sampling period. Additional details on the AWS setup and instrumentation can be sourced from project documentation and related work by Mahomed *et al.* (2021). Along with other microclimatic factors, the experimental field received a total precipitation of 870.9 mm and an average maximum air temperature of 24 °C for the taro growing season (Figure 6.2). Additionally,

precipitation trends in the study area followed a distinct pattern of the highest level of precipitation occurring in the spring and summer months between October and March and the lowest during the autumn and winter months between April and June.

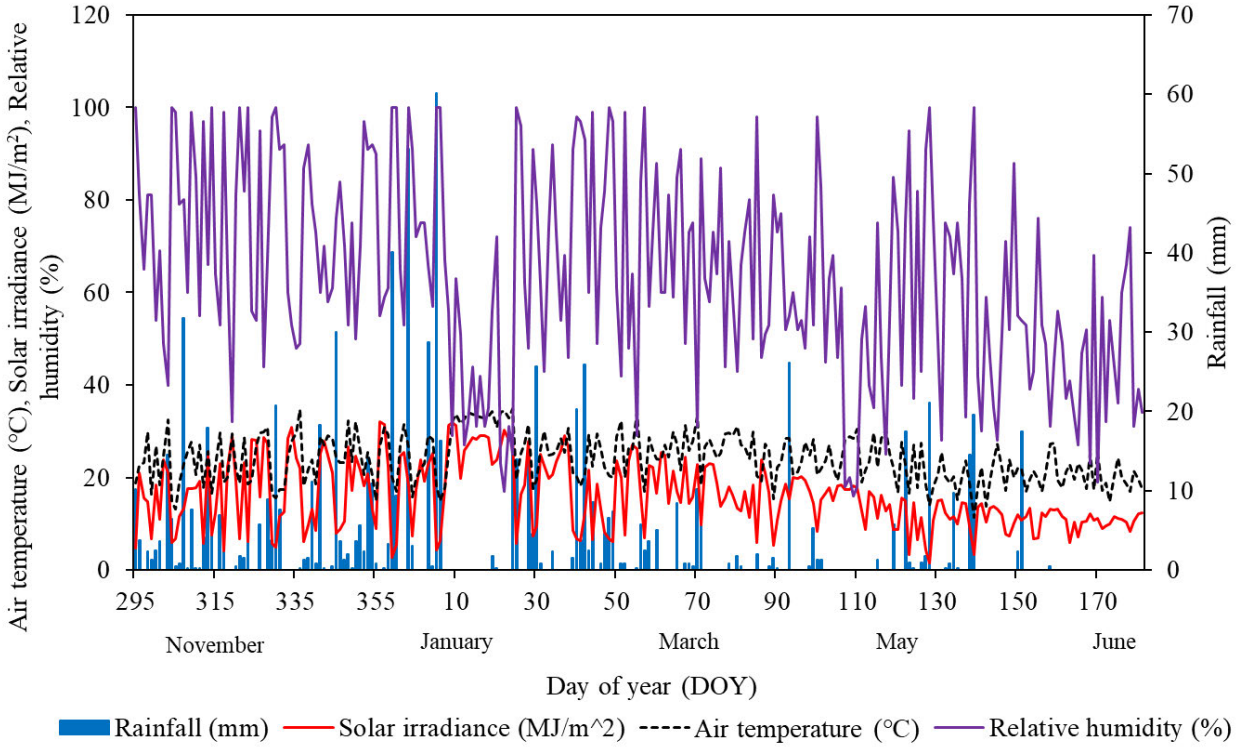

Figure 6.2 Microclimatic conditions of the experimental field in Swayimane over the taro growing period.

Three main stages of taro growth, i.e. the emergence, vegetative and maturity stages were assessed. The microclimatic conditions of the experimental field during each growth stage are detailed in Table 6.1. Crop establishment, root formation and the production of leaves occur at the emergence growth stage (Sibiya 2015) (Table 6.2). During this stage of taro growth, propagules are crucial for crop development as they offer nutrients and carbohydrates required to initiate the rooting system and leaf emergence before the crop completely depends on photosynthesis (Sibiya 2015; Lewu *et al.* 2017). At the subsequent vegetative stage, the crop experiences substantial growth, with leaves fully expanding and above-ground biomass increasing significantly, both essential for photosynthesis and energy storage (Sibiya 2015). Finally, as energy is focused on the rapid development of tubers, the maturity growth stage is marked by a decrease in crop height, leaf area and active leaves (Lewu *et al.* 2017). Once the crop reaches full maturity, it enters a phase of leaf senescence, marked by the yellowing of

leaves, while the tubers become fully developed and are ready for harvest (Miyasaka *et al.* 2003; Chauhan *et al.* 2024) (Table 6.2).

Table 6.1 Microclimatic conditions observed during the emergence, vegetative and maturity growth stages of taro.

Taro Growth Stage	Emergence	Vegetative	Maturity
Days after planting	74	167	219
Maximum air temperature (°C)	25.1	21.8	19.6
Minimum air temperature (°C)	10.8	11.0	7.0
Total rainfall (mm)	00.0	01.3	00.0
Wind speed (m/s)	39.7	133.5	9.8
Relative humidity (%)	56	83	39
Mean vapor pressure deficit (kPa)	0.86	0.17	0.87

Table 6.2 Description of taro growth stages

Growth Stage	Taro	Days After Planting	Description
Emergence		74	The taro crops are now visible through the soil. As the crop grows its root system, small delicate leaves start to emerge.
Vegetative		167	The crops are fully developing vegetatively, characterised by the thickening canopy and the expansion of broad leaves. The focus of this growth stage is above-ground growth and leaf production.

Maturity		219	The taro crops are fully grown. Energy is shifted to the formation of tubers as leaf growth slows down. The crop is now beginning to get ready for harvest.

6.2.3 Field sampling and in-situ measurements

Field data collection and in-situ measurements were carried out during the emergence, vegetative and maturity stages of taro growth. The boundary of the smallholder experimental field was digitised using Google Earth Pro and subsequently exported into ArcGIS Pro. To ensure spatial variability linked to topography was captured, the field was visually assessed and divided into three elevation-based strata: stratum A (upper slope), stratum B (mid-slope), and stratum C (lower slope). A total of 100 stratified random sampling points were then generated within each of the defined elevation strata. This sampling design aimed to ensure a representative distribution of points across the slope-driven gradients influencing water availability and plant physiology. The predefined point locations were uploaded to a Trimble handheld Global Positioning System (GPS), which was then used to navigate the field. At each sampling point, in-situ measurements of stomatal conductance and leaf temperature were recorded, as described below.

6.2.3.1 Stomatal conductance

The stomatal conductance was measured using an SC-1 Leaf Porometer (Decagon Devices Inc., Pullman, Washington, USA). Prior to use, the leaf porometer was calibrated using the Decagon calibration kit to establish thermal equilibrium with the surrounding environment, ensuring accurate readings (Brewer *et al.* 2022b). A plastic bead included in the calibration kit was inserted into the aperture of the sensor head to facilitate air mixing within the chamber, ensuring that the sensor readings are stabilised and remain within 2% relative humidity before proceeding with the equilibration process. Thereafter, filter paper soaked in distilled water was placed over the calibration plate, and the sensor head securely positioned on the plate to begin a 30-second measurement period (Ganesan *et al.* 2024). To ensure precision and consistency, this calibration process was repeated ten times. Following calibration, the leaf porometer was placed at the middle of the taro leaf blade exposed to full sun and perpendicular to the midrib.

The SC-1 leaf porometer recorded air temperature and humidity, while automatically measuring leaf stomatal conductance over a 30-second period. Server water stress was indicated by stomatal conductance values closer to 0 mmol m^{-2} s^{-1}, which suggests stomatal closing to minimise water loss. Meanwhile, minimal crop water stress and optimal physiological activity were indicated by stomatal conductance measurements closer to 500 mmol m^{-2} s^{-1}, suggesting open stomata.

6.2.3.2 Foliar temperature

A digital laser infrared GM320 handheld thermometer (Shenzhen Jumaoyuan Science and Technology Co., Ltd, Nanshan District, Shenzhen, China) was used to measure taro leaves foliar temperature. The GM320 thermometer can provide temperature readings at ± 1.5 °C error margin, with a measurement range from -50 °C to 380 °C and a spectral response of 8-14 μm. To account for possible variations in temperature across the leaf surface, five distinct temperature readings were taken from various parts of the taro leaf at each sampling location. These measurements were obtained at (1) the centre of each leaf blade, close to the principal leaf vein, (2) approximately one-third of the leaf tip, (3) approximately two-thirds of the leaf tip, and (4) the midpoint on both sides between the leaf vein and the leaf border. The resultant measurements were then averaged to obtain an overall representation of taro foliar temperature.

Lastly, all field measurement was taken at the optimal interval for crop photosynthesis, 10:00 am to 2:00 pm local time, on a sunny day. This timing was chosen to guarantee that the collected data accurately reflects the taros' peak reflectance and photosynthetic activity.

6.2.4 Image acquisition and pre-processing

The multirotor platform DJI Matrice 300 (M300) (DJI-Innovations Inc., Shenzhen, China), integrated with the MicaSense Altum multispectral-thermal camera (MicaSense, Seattle, WA, USA) was employed to capture high-resolution aerial imagery of the experimental field across the taro growth stages. Equipped with Vertical Take-Off and Landing (VTOL) capabilities, the M300 quadcopter drone is well suited to rural environments with constrained take-off and landing areas. The MicaSense Altum sensor features a radiometrically calibrated thermal channel (11 μm) alongside five precise spectral bands for reflectance measurements in the blue (475 nm), green (560 nm), red (668 nm), red-edge (717 nm), and near-infrared (NIR) (840 nm) regions of the electromagnetic spectrum (Cottrell *et al.* 2024). The novelty of the Altum camera

lie in its capacity to concurrently collect multispectral and thermal infrared images while equipped with a global shutter that supports a capture rate of up to one second, ensuring high spatial resolution and accurately aligned imagery (Hutton *et al.* 2020a).

The flight path for the experimental field was mapped in Google Earth Pro and exported as a Keyhole Markup Language (KML) file to ensure consistent image acquisition throughout the taro growth period. The flight path was then uploaded to the M300's portable smart controller for precise navigation and systematic data collection. Prior to and post all aerial flights, a Calibration Reflectance Panel (CRP) with a white balance card was used to radiometrically calibrate the Altum sensor by using known reflectance properties throughout the electromagnetic spectrum, ensuring accurate reflectance measurements. This process included manually capturing an unshaded image of the CRP, enabling the sensor to adapt to the current lighting and air conditions throughout the flight (Buthelezi *et al.* 2023; Cottrell *et al.* 2024). Thereafter, autonomous aerial flights of the experimental field were conducted concurrently with in-situ measurements, between 10:00 am and 2:00 pm local time, corresponding to the period of optimal solar irradiance. The UAV flight missions were carried out at an altitude of 100 m above the ground to provide a ground sampling distance of 10.08 cm per pixel at a forward and sideward image overlap of 80%. During each growth stage, a total of 1626 raw UAV images were acquired and exported to the Pix4D photogrammetry software (Pix4D Inc. Denver, USA). The Pix4D software instantaneously identifies the CRP images to radiometrically correct the acquired raw images and generate an ortho-mosaic of the experimental field at each taro growth stage. Subsequently, the acquired thermal infrared data was converted into absolute temperature values in the Pix4D software using equation 6.2 below (Rutkoski *et al.* 2016; Osroosh *et al.* 2018).

$$Absolute\ Temperature = \frac{Thermal\ infrared}{100} - 273.15 \qquad units: °C \qquad (6.2)$$

Following data acquisition, multispectral reflectance properties were extracted and leveraged to compute vegetation indices (Table 6.3) selectively chosen for their established correlations with crop water status reported in literature (Baluja *et al.* 2012a; Gago *et al.* 2015; Zhang and Zhou 2019a; Ozelkan 2020). Additionally, the canopy temperature (T_{canopy}) of each sampled taro crop was used to compute thermal indices, including the Normalised Relative Canopy Temperature (NRCT) and the Second Formulation of the Stomatal Conductance Index

(I3). Specifically, the wet temperatures (T_{wet}) was calculated using the lower boundary temperature, assuming maximum transpiration with open stomata, while the dry temperature (Tdry) was set using the higher boundary temperature, assuming minimal transpiration with closed stomata (Baluja *et al.* 2012a; Crusiol *et al.* 2020b). A digital elevation model acquired from the Altum MicaSense sensor was used to compute seven topographic indices: elevation, slope, aspect, flow direction, Topographic Wetness Index (TWI), Terrain Ruggedness Index (TRI) and Stream Power Index (SPI). These indices were computed in ArcGIS Pro using the Spatial Analyst and 3D Analyst extensions, accessible through the ArcToolbox (Alexander *et al.* 2016; Chowdhury 2023). Thereafter, the UAV thermal-multispectral imagery together with the derived thermal, vegetation and topographic indices were superimposed with the in-situ measurements and corresponding geolocational data recorded at each growth stage. Finally, the data samples were divided into training (70%) and testing (30%) sets, with the training data employed for model calibrations and the testing data used for validating model performance.

Table 6.3 Thermal and spectral indices used in this study.

Vegetation Index	Abbreviation and Equation	Reference
	Thermal Indices	
Normalised Relative Canopy Temperature	$NRCT = \frac{T_{canopy} - T_{wet}}{T_{dry} - T_{wet}}$	(Elsayed *et al.* 2015)
Second Formulation of the Stomatal Conductance Index	$I3 = \frac{T_{canopy} - T_{wet}}{T_{dry} - T_{canopy}}$	(Baluja *et al.* 2012b)
	Spectral Indices	
Normalised difference vegetation index	$NDVI = \frac{R_{Nir} - R_{red}}{R_{Nir} + R_{red}}$	(Rouse *et al.* 1974)
Soil-Adjusted Vegetation Index	$SAVI = \frac{R_{Nir} - R_{red}}{R_{Nir} + R_{red} + L} \times (1 + L)$	(Huete 1988)
Normalised Difference Red-Edge Index	$NDRE = \frac{R_{Nir} - R_{Redegde}}{R_{Nir} + R_{Rededge}}$	(Gitelson and Merzlyak 1994)
Transformed Chlorophyll Absorption in Reflectance Index	$TCARI = 3 \times (R_{Rededge} - R_{Red}) - 0.2 \times (R_{Rededge} - R_{Green}) \times \frac{R_{Redegde}}{R_{Red}}$	(Haboudane *et al.* 2002)
Modified Chlorophyll Absorption in Reflectance Index	$MCARI = (R_{Rededge} - R_{Red}) - 0.2 \times (R_{Rededge} - R_{Green}) \times \frac{R_{Rededge}}{R_{Red}}$	(Daughtry *et al.* 2000)
Structural Insensitive Pigment Index	$SIPI = \frac{R_{Nir} - R_{Blue}}{R_{Nir} + R_{Red}}$	(Penuelas *et al.* 1995)
Normalised Green-Red Difference Index	$NGRDI = \frac{R_{Green} - R_{red}}{R_{Green} + R_{red}}$	(Hunt Jr *et al.* 2013)
Normalised difference water index	$NDWI = \frac{R_{Green} - R_{Nir}}{R_{Green} + R_{Nir}}$	(Gao 1996; McFeeters 1996)
Red-edge Chlorophyll Index	$CIrededge = \frac{R_{Nir}}{R_{rededge}} - 1$	(Gitelson *et al.* 2003; Gitelson *et al.* 2006)

6.2.5 Crop canopy extraction and soil background removal

To ensure that the acquired imagery contained only taro pixels, the Excess Green minus Excess Red (ExGR) index, as described by Riehle *et al.* (2020), was selected to optimally isolate the crop canopy from the soil background. By using the contrast between the green and red regions of the electromagnetic spectrum, the ExGR index has the capability to effectively differentiate between soil and crop cover (Meyer *et al.* 2004; Hamuda *et al.* 2016; Riehle *et al.* 2020; Upendar *et al.* 2021). Using equation 6.3, the ExGR index generated a binary image from the gray-level histogram within Mathworks MATLAB, where a fixed zero threshold was applied to distinguish between crop canopy and background features (Hamuda *et al.* 2016). The crop canopy was represented by a positive pixel value of 1, while soil cover was indicated by a negative pixel value of 0 (Riehle *et al.* 2020). To extract the taro crop canopy in ArcGIS Pro, a vegetation mask that separated the crop canopy from the background was converted into a shapefile and superimposed with the UAV imagery at each growth stage.

$$ExGR = (2 \times R_{Green} - R_{Red} - R_{Blue}) - (1.4 \times R_{Red} - R_{Green}) \quad (6.3)$$

where the reflectance values from the corresponding spectral band are denoted by *R*.

6.2.6 Model development, hyperparameters optimisation and statistical analysis

6.2.6.1 Development of DNN models for each feature subset

The study applied the Deep Neural Network (DNN) model to estimate the stomatal conductance and leaf temperature of smallholder taro crops at each growth stage. The DNN algorithm, a type of artificial neural network, was employed due to its exceptional ability to learn complex and high-dimensional relationships between input features (Chew *et al.* 2020; Traore *et al.* 2021). Furthermore, the algorithm has the ability to handle high-dimensional data and non-linear relationships, making the algorithm suitable for predicting crop physiological indicators such as stomatal conductance and leaf temperature under varying growth conditions (Omosalewa *et al.* 2021).

The derived thermal and multispectral data, together with topographic variables were grouped into feature subsets. The analysis adopted a comparative approach to assess the predictive power of each feature subset (a – g) in estimating the stomatal conductance and leaf temperature of smallholder taro crops at each growth stage. The DNN models were developed

using a) multispectral bands (blue, green, red, red-edge and NIR), b) multispectral and thermal bands, c) multispectral and thermal bands combined with thermal indices, d) the thermal band and derived thermal indices (NRCT and I3), e) vegetation indices (NDVI, NDRE, NGRDI, NDWI, SAVI, SIPI, TCARI, MCARI, CIrededge) and f) topographic indices (elevation, slope, aspect, flow direction, TWI, TRI, SPI). Subsequently, g) a comprehensive DNN model was developed using the combination of all feature subsets, including multispectral bands, the thermal band and indices, vegetation indices and topographic variables.

The DNN model consisted of 24 input features, including five multispectral bands, one thermal band, two thermal indices, nine vegetation indices and seven topographic indices that were assessed individually per feature subset and collectively as a combined subset. The models were stimulated and refined using a rectified linear unit (ReLU) with a maximum of 200 epochs to enhance prediction accuracy. To prevent overfitting, L2 dropout regularisation was applied with dropout rates of 0.4 (input layer) and 0.2 (hidden layers). Additionally, the SoftMax activation function was employed to transform the raw outputs of the neural network into a vector of probabilities, while the Adaptive Moment Estimation (Adam) optimiser was chosen to achieve optimal results. Lastly, the DNN models developed at a learning rate of 0.001 and a batch size of 32 with this configuration being consistently applied across all iterations (a-g). All models were developed within Anaconda Jupyter Notebooks using Python 3.8.

6.2.6.2 Optimisation of best-performing DNN model

Thereafter, a multi-faceted approach was used to employ advanced model optimisation on the most optimal feature subset to ensure robust predictions of stomatal conductance and leaf temperature at each taro growth stage.

Following the evaluation of predictive performance across all feature subsets, the best-performing subset was further optimised to enhance accuracy and robustness. Specifically, the Grid Search Cross Validation was used in conjunction with the Keras Regressor to perform a grid search to identify the optimal combination of hyperparameters, including the learning rate, dropout rate, and epochs. Thereafter, to reduce the dimensionality of data and ensure optimal model accuracies, the Least Absolute Shrinkage and Selection Operator (LASSO) feature selection technique was applied to identify the most optimal features for inclusion in the optimised model. This technique was used to select the most informative features, minimising the absolute value of regression coefficients, effectively setting coefficients of less important

features to zero. Using the optimal hyperparameters (Table 6.4) and selected optimal features, optimal DNN models of taro stomatal conductance and leaf temperature was developed for each growth stage. Thereafter, to ensure consistent feature scales and prevent features with large ranges from dominating the model, the Standard Scaler from Scikit-Learn was employed to standardise the features. Subsequently, the L2 regularisation (Ridge Regression) was applied to prevent overfitting by adding a penalty term to the loss function, therefore discouraging large weights and encouraging sparse solutions. Lastly, the Adaptive Moment Estimation (Adam) optimiser was used to optimise the model parameters and ensure accurate results.

Table 6.4 Optimised hyperparameters for taro stomatal conductance and leaf temperature models at derived at each growth stage.

Growth Stage	Physiological Indicator	Learning Rate	Dropout Rate	L2 Regularisation	Epochs	Batch Size
Emergence	Stomatal conductance	0.001	0.4	0.005	400	32
	Leaf temperature	0.001	0.4	0.005	500	32
Vegetative	Stomatal conductance	0.01	0.3	0.001	400	32
	Leaf temperature	0.01	0.2	0.001	400	32
Maturity	Stomatal conductance	0.01	0.3	0.001	400	32
	Leaf temperature	0.01	0.2	0.001	300	32

6.2.7 Accuracy Assessment

To evaluate the predictive accuracy and reliability of models estimating taro stomatal conductance and leaf temperature at each growth stage, an accuracy assessment was performed. Model accuracy was measured using three key metrics: the Coefficient of Determination (R^2), the Root Mean Square Error (RMSE), and the Relative Root Mean Square Error (rRMSE), as detailed in Masenyama *et al.* (2023) and Ndlovu *et al.* (2024b). The dataset, consisting of 100

samples, was split into training (70 %) and testing (30 %) sets, with the latter used for evaluating the performance of the models. Furthermore, to ensure a robust assessment of model generalisability, a 5-fold cross-validation analysis was conducted to further validate the performance of the optimised taro stomatal conductance and leaf temperature models at each growth stage. K-fold cross-validation is a widely adopted resampling technique in machine learning and statistical modelling due to its capacity to provide a more reliable and unbiased estimate of model performance (Wong and Yeh 2019; Nti *et al.* 2021). By systematically partitioning the data into multiple subsets and ensuring that each observation is used for both training and validation, the method reduces the variance associated with a single train-test split and enhances the robustness of performance metrics (Lumumba *et al.* 2024). In this study, a 5-fold approach was selected to strike a balance between bias and variance in the performance metrics while maintaining approximately 80 % of the data for training and 20 % for testing in each iteration (Costa *et al.* 2022; Kumar *et al.* 2023). In particular, the dataset was randomly partitioned into five subsets (folds) containing approximately 20 samples, where for each iteration, four of these folds were used to train the model, while the remaining fold was used for testing (Yang *et al.* 2021; Skobalski *et al.* 2024; Zhao *et al.* 2025) (Wong and Yeh 2019). This process was repeated five times, each time with a different fold serving as the test set. During this validation process, the k-fold R^2 and rRMSE values were calculated for each fold, providing an additional measure of model performance at each growth stage.

Thereafter, the SHapley Additive exPlanations (SHAP) were used to quantify each predictor's contribution within the model at each growth stage. The SHAP analysis calculates the average impact of each input variable, ranking their influence from least to most significant for model accuracy (Nahiduzzaman *et al.* 2023b). Finally, temporal maps illustrating the spatial distribution of estimated taro stomatal conductance and leaf temperature were developed at each growth stage using the best-performing model and optimal features. Subsequently, to identify areas of potential stress, specific literature-informed thresholds of stomatal conductance and leaf temperature were applied. Specifically, Ramírez *et al.* (2016) and Ninanya *et al.* (2021) confirmed that values below 50 mmol m^{-2} s^{-1} stomatal conductance lead to significant stress in tuber crops. Meanwhile, studies by Luo QunYing (2011), Mabhaudhi *et al.* (2014), and Kunz *et al.* (2024b) established that taro requires a minimum of 10 °C and a maximum of 35 °C for optimal growth and productivity, with temperatures beyond this range inducing stress. Therefore, the derived distribution maps were reclassified to highlight crops

with estimated stomatal conductance values below 50 mmol m^{-2} s^{-1}, indicating potential stress conditions. Similarly, taro crops with leaf temperatures below 10 °C and exceeding 35 °C were identified as potentially stressed crops. A detailed outline of the study workflow is presented in Figure 6.3.

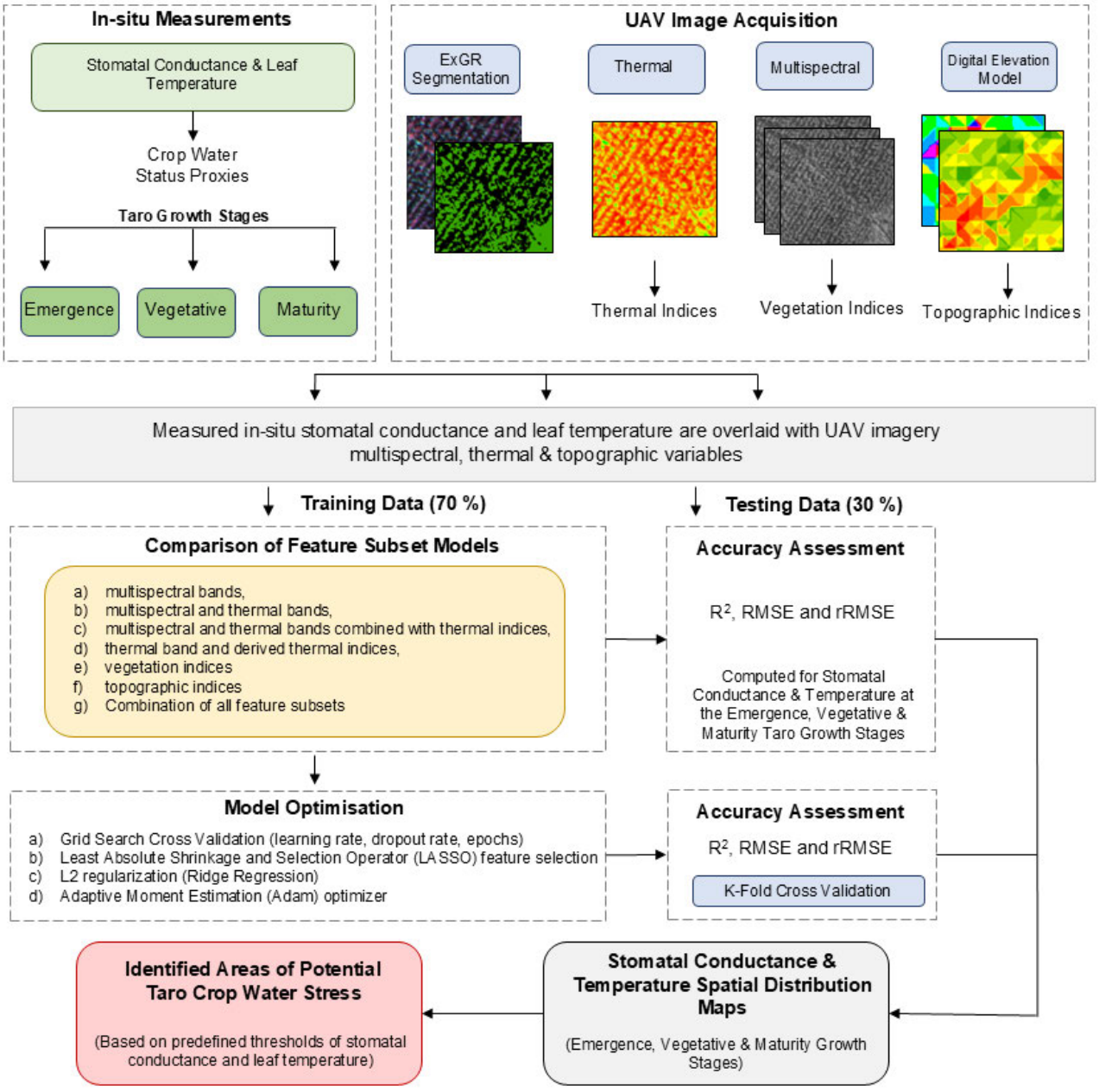

Figure 6.3 Detailed outline of the study workflow.

6.3 Results

6.3.1 Descriptive statistics

Table 6.5 illustrates the descriptive statistics of in-situ stomatal conductance and leaf temperature reported at the various growth stages of smallholder taro. The emergence growth stage had the lowest mean stomatal conductance of 69.66 ± 6.50 mmol m^{-2} s^{-1} and the highest mean leaf temperature of 36.93 ± 0.08 °C. Meanwhile, an increase in mean stomatal conductance was observed in the vegetative growth stage, 234.09 ± 16.96 mmol m^{-2} s^{-1}. Contrastingly, the vegetative stage had the lowest mean leaf temperature of 29. 90 ± 0.19 °C, while the maturity growth stage had a slight increase in mean leaf temperature to 31.84 ± 0.25 °C and a decrease in mean stomatal conductance to 194.29 ± 11.03 mmol m^{-2} s^{-1}. Additionally, the coefficient of variation (CV) was also calculated to describe the relative variability of the parameters across growth stages. Notably, the CV of stomatal conductance is highest during the emergence stage (83.45 %), indicating substantial physiological variability at early growth. The CV gradually decreases across subsequent stages, reflecting more consistent crop water regulation. In contrast, the relatively low CVs for leaf temperature across all stages (ranging from 1.92 % to 6.5 %) suggest that this parameter remains relatively stable and less influenced by growth stage variability. To further assess the distributional characteristics of the in-situ measurements, the Kolmogorov-Smirnov test indicated that leaf temperature conformed to normality at all growth stages (p-values ranging from 0.188 to 0.947). In contrast, stomatal conductance deviated significantly from normality during the emergence ($p = 0.001$) and vegetative stages ($p = 0.023$), while conforming to normality at the maturity stage ($p= 0.286$), suggesting skewness in the data at the earlier stages.

Table 6.5 Descriptive statistics of in-situ taro stomatal conductance and leaf temperature (n = 100).

Indicator	Stomatal Conductance (mmol m^{-2} s^{-1})			Leaf Temperature (°C)		
Growth Stage	Emergence	Vegetative	Maturity	Emergence	Vegetative	Maturity
Min	22,7	43,1	34,2	34,5	26,1	28
Max	333,2	575,9	452,7	38,9	33,4	36,3
Median	49	174,85	192,1	37	29,8	31,6
Mean	69,66	234,09	194,29	36,93	29,9	31,84
Std.	58,13	149,77	92,91	0,71	1,65	2,07
SEM.	6,5	16,96	11,03	0,08	0,19	0,25
CV (%)	83,45	63,98	47,82	1,92	5,51	6,5

The standard error of the mean is denoted by SEM, the standard deviation by Std., and the coefficient of variation by CV.

6.3.2 Estimation of taro crop stomatal conductance and leaf temperature using selected spectral feature subsets

The accuracies achieved for predicting taro crop stomatal conductance (mmol m^{-2} s^{-1}) and leaf temperature (°C) across the different growth stages using selected spectral features subsets are presented in Table 6.6.

When using selected spectral features to estimate stomatal conductance, the combination of multispectral bands, thermal band and thermal indices achieved the highest estimation accuracies across all growth stages, except for the emergence growth stage. During the vegetative stage, this subset recorded the highest R^2 value of 0.84, indicating a moderately high predictive power, with RMSE and rRMSE values of 59.23 mmol m^{-2} s^{-1} and 25.96 %, respectively. At maturity, this combination achieved a moderate R^2 of 0.70, RMSE of 60.41 mmol m^{-2} s^{-1} and rRMSE of 26.23 %. In contrast, vegetation indices performed moderately well in estimating stomatal conductance during the emergence stage, achieving an R^2 of 0.62, with an RMSE of 28.93 mmol m^{-2} s^{-1} and an rRMSE of 46.26 %. While the combination of multispectral bands, thermal band and thermal indices produced the same R^2 of 0.62, this model exhibited a greater RMSE error of 39.98 mmol m^{-2} s^{-1}. Furthermore, the combination of

multispectral bands with the thermal band showed moderate accuracy, with the vegetative growth stage producing the highest accuracy (R^2 = 0.80, RMSE = 66.54 mmol m^{-2} s^{-1} and rRMSE = 29.16 %) in this subset. The use of the thermal band and thermal indices, and the topographic indices subsets exhibited relatively low predictive accuracy for stomatal conductance across all stages, with R^2 values ranging from 0.21 to 0.57 (Table 6.6).

For leaf temperature, the combination of multispectral bands, thermal band, and thermal indices had the best performance across all growth stages. The vegetative stage exhibited the highest prediction accuracy, with an R^2 of 0.74, an RMSE of 0.76 °C, and an rRMSE of 2.54 %. Meanwhile, during the emergence and maturity stages, this feature subset achieved moderate R^2 values of 0.61 and 0.64, RMSE values of 0.85 °C and 0.81 °C, and rRMSE values of 2.79 % and 2.59%, respectively. The subset of multispectral and thermal bands, along with the subset of vegetation indices, performed moderately across the growth stages, achieving their highest accuracies during the vegetative growth stage, with R^2 = 0.65, rRMSE = 2.96 % and R^2 = 0.67, rRMSE = 2.84 %, respectively. Meanwhile, the use of the thermal band and thermal indices subset exhibited the lowest prediction accuracies at all stages of growth, with poor R^2 values ranging between 0.23 and 0.3. Similarly, the use of topographic variables in predicting leaf temperature exhibited a low predictive power across all growth stages, with R^2 values below 0.57 (Table 6.6).

Overall, the combination of all spectral feature subsets outperformed other subsets, producing the highest estimation accuracies for both stomatal conductance and leaf temperature across all growth stages, with R^2 values exceeding 0.86 and rRMSE values less than 25.45%. In particular, the vegetative growth stages yielded the highest predictive power with R^2 = 0.94, RMSE = 26.25 mmol m^{-2} s^{-1} and rRMSE = 14.63% for stomatal conductance and R^2 = 0.90, RMSE = 0.27 °C and rRMSE = 1.08 % for leaf temperature. This was followed by the maturity growth stage, with stomatal conductance reporting R^2 of 0.92, RMSE of 27.07 mmol m^{-2} s^{-1} and rRMSE of 15.16 % and leaf temperature of R^2 of 0.92, an RMSE of 0.30°C, and an rRMSE of 1.53% (Table 6.6). The reported results highlight the varying contributions of feature subsets at different growth stages.

Table 6.6 Growth stage estimation accuracies of taro crop stomatal conductance and leaf temperature using selected feature subsets.

	Feature Subsets	Accuracy Metric	Taro Physiological Indicator and Growth Stage					
			Stomatal Conductance (mmol m^{-2} s^{-1})			Leaf Temperature (°C)		
			Emergence	Vegetative	Maturity	Emergence	Vegetative	Maturity
A	Multispectral Bands	R^2	0,31	0,46	0,42	0,23	0,47	0,44
		RMSE	43,05	108,83	39,53	1,77	1,1	1,58
		rRMSE (%)	62,49	11,21	52,45	3,83	3,64	3,67
B	Multispectral Bands Thermal Band	R^2	0,42	0,8	0,65	0,39	0,65	0,56
		RMSE	72,91	66,54	43,5	1,68	0,89	1,53
		rRMSE	62,49	29,16	19,48	3,51	2,96	3,43
C	Multispectral Bands Thermal Band Thermal Indices	R^2	0,62	**0,84**	**0,70**	**0,61**	**0,74**	**0,64**
		RMSE	68,91	**59,23**	**60,41**	**0,85**	**0,76**	**0,81**
		rRMSE	46,33	**25,96**	**26,23**	**2,79**	**2,54**	**2,59**
D	Thermal Band Thermal Indices	R^2	0,21	0,33	0,23	0,23	0,3	0,28
		RMSE	50,36	210,68	110,18	1,98	1,39	1,63
		rRMSE	73,41	32,1	29,64	3,61	4,66	4,72
E	Vegetation Indices	R^2	**0,62**	0,77	0,61	0,44	0,67	0,61
		RMSE	**28,93**	71,3	77,63	0,49	0,86	0,69
		rRMSE	**46,26**	31,25	38,75	1,34	2,84	2,57
F	Topographic Indices	R^2	0,29	0,56	0,51	0,46	0,57	0,51
		RMSE	54,7	131,99	89,47	0,5	1,01	0,72
		rRMSE	73,78	18,81	23,47	1,35	3,39	2,66
G	Combination Model	R^2	**0.89**	**0.94**	**0.92**	**0.86**	**0.90**	**0.92**
		RMSE	**27.96**	**26.25**	**27.07**	**0.35**	**0.27**	**0.30**
		rRMSE	**25.45**	**14.63**	**15.16**	**1.61**	**1.08**	**1.53**

The highest estimation accuracies achieved for using selected spectral features across the different growth stages are highlighted in bold text.

6.3.3 Optimised estimation of taro stomatal conductance and leaf temperature across the growth stages

Optimised estimation models of taro stomatal conductance and leaf temperature were developed across the growth stages (Figure 6.4). The predictive models for stomatal conductance showed strong agreement with observed values across all growth stages. During the emergence growth stage, the model yielded an R^2 of 0.92, RMSE of 20.65 mmol m^{-2} s^{-1} and rRMSE of 16.86 % (Figure 6.4a). The model showed a strong relationship between the observed and predicted values based on NRCT, thermal, NDWI, slope, I3, NDVI, TWI, red, SIPI, CIrededge, red-edge, aspect, MCARI, TCARI, TRI, NDRE and NIR selected variables, in descending order of importance (Figure 6.5a). Cross-validation using K-Fold analysis further confirmed the model's robustness, yielding an R^2 of 0.87 and an rRMSE of 22.75 %. Meanwhile, during the vegetative stage, a stronger predictive performance was observed, achieving the highest R^2 value of 0.95, a lower RMSE of 10.26 mmol m^{-2} s^{-1}, and an rRMSE of 10.23 % (Figure 6.4b). This optimal accuracy was supported by the K-Fold cross-validation, exhibiting an R^2 of 0.90 and an rRMSE of 17.71 %, indicating reliability in model performance. The top-most predictor variables selected in the model development were thermal, SIPI, NRCT, CIrededge, I3, red-edge, NDVI, NIR, MCARI, slope, NDWI, TWI, red and NDRE, in decreasing order of importance (Figure 6.5b). While the maturity growth stage maintained a strong performance, with an R^2 of 0.94, an RMSE of 15.78 mmol m^{-2} s^{-1}, and an rRMSE of 11.91 % (Figure 6.4c). Cross-validation yielded an R^2 of 0.89 and an rRMSE of 19.22 %, demonstrating the model's robustness in estimating stomatal conductance during the final growth stage. Specifically, CIrededge, thermal, NDWI, NRCT, NDVI, SIPI, NDRE, MCARI, I3, NIR, TWI, slope, red and red-edge emerged as the selected variables for optimised model performance (Figure 3.5c).

For leaf temperature, the emergence stage achieved high predictive accuracy, with an R^2 of 0.91, RMSE of 0.30 °C, and rRMSE of 1.52 % (Figure 6.4d). The regression model demonstrated a strong relationship between observed and predicted leaf temperature values with the K-Fold yielding an R^2 of 0.88 and an rRMSE of 1.60 %. The top-most predictor variables selected in the model development were thermal, NDWI, NGRDI, NDRE, aspect, NRCT, NDVI, red-edge, TWI, blue and slope, in decreasing order of importance (Figure 6.5d). The vegetative growth stage exhibited the highest estimation accuracy for leaf temperature,

with an R^2 of 0.95, RMSE of 0.20 °C, and rRMSE of 0.74 % (Figure 6.4e). The model showed a strong relationship between the observed and predicted values based on NRCT, thermal, NDWI, NIR, NDRE, NDVI, CIrededge, MCARI, aspect, TWI, TCARI, red and slope selected features, in descending order of importance (Figure 6.5e). The K-Fold cross-validation further confirmed the model's robustness, with an R^2 of 0.91 and an rRMSE of 1.04 %. Additionally, the maturity growth stage model maintained similar accuracy, achieving an R^2 of 0.94, RMSE of 0.24 °C, and rRMSE of 0.96 % (Figure 6.4f). Specifically, CIrededge, thermal, MCARI, NDVI, NDWI, I3, NDRE, NRCT, aspect, TWI, SIPI, slope, NGRDI, NIR and red-edge emerged as the selected variables for optimised model performance (Figure 6.5f). The K-Fold cross-validation results, with an R^2 of 0.89 and an rRMSE of 1.41 %, further validated the model's robustness in estimating leaf temperature during the maturity growth stage.

Overall, the optimised prediction models demonstrated exceptional performance across all taro growth stages for both stomatal conductance and leaf temperature, with R^2 values ranging from 0.91 to 0.95 (Figure 6.4). Furthermore, the rRMSE values achieved for all predictive models were well below the generally accepted threshold of 30% error, indicating that the models maintained an acceptable level of precision across the growth stages. Additionally, the RMSE values were generally low across the growth stages, highlighting the model's ability to minimise deviations from observed stomatal conductance and leaf temperature measurements. While rRMSE values were generally low throughout growth stages, a slight increase in K-Fold rRMSE and a decrease in K-Fold R2 was observed for all models.

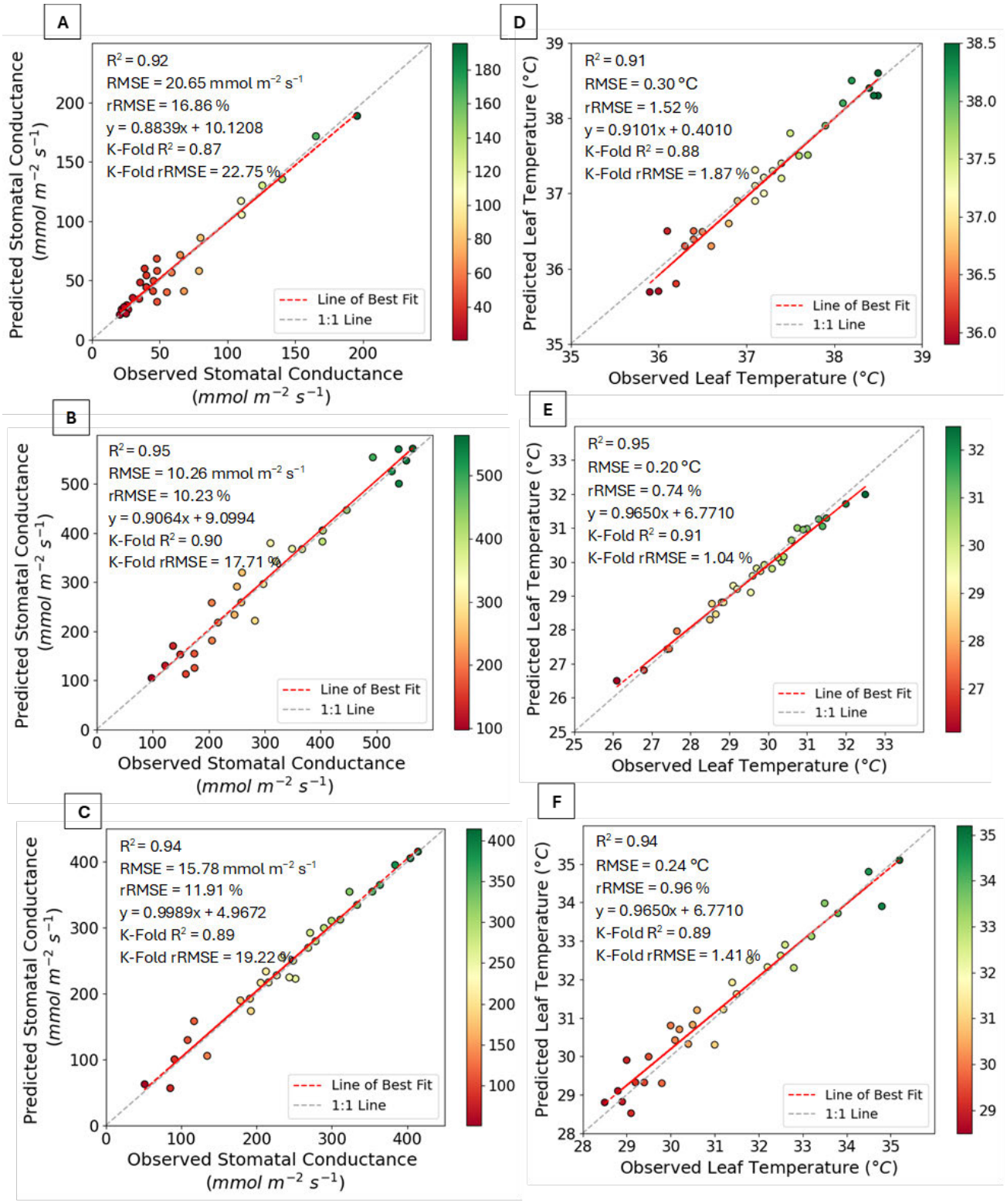

Figure 6.4 Relationship between observed and predicted stomatal conductance (a-c) and leaf temperature (d-f) across taro growth stages: emergence (a, d), vegetative (b, e), and maturity (c, f).

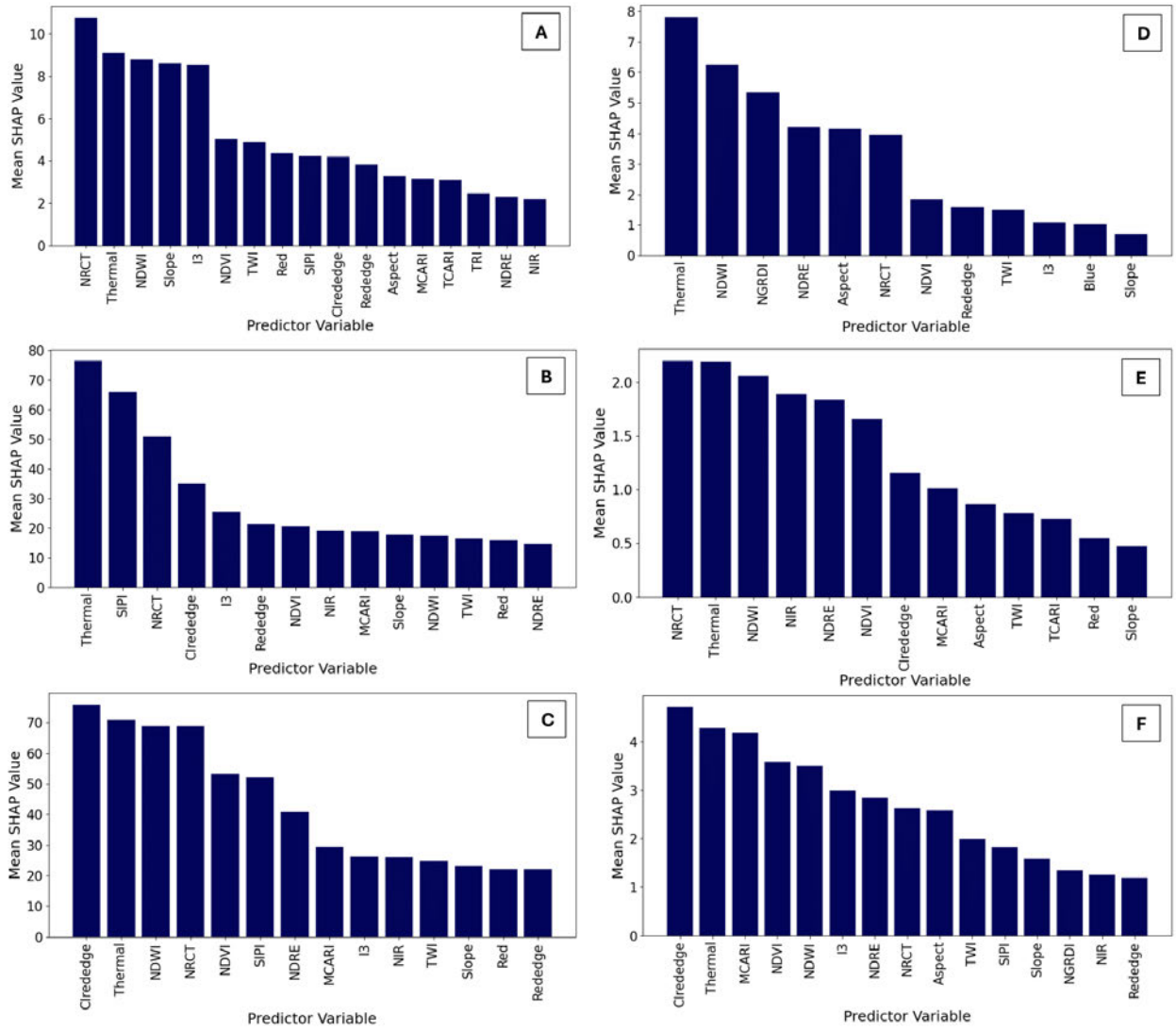

Figure 6.5 SHAP generated variable importance values of predictor variables used in developing the optimised estimation models of stomatal conductance (a-c) and leaf temperature (d-f) across taro growth stages: emergence (a, d), vegetative (b, e), and maturity (c, f).

6.3.4 Mapping the spatial and temporal distribution of taro stomatal conductance and leaf temperature

Figure 6.6 illustrates the modelled spatial and temporal distribution of stomatal conductance and leaf temperature across taro's emergence, vegetative and maturity growth stages. Notably, the emergence stage exhibited low stomatal conductance values, especially in the central and western regions of the experimental field recording the lowest values of 27.70 mmol m^{-2} s^{-1} (Figure 6.6a). Meanwhile, taro stomatal conductance peaked during the vegetative stage, with elevated values concentrated in the northwestern regions of the study field (Figure 6.6b). As taro entered maturity, stomatal conductance values decreased again, aligning with reduced above-ground biomass and the onset of crop senescence (Figure 6c). Meanwhile, taro leaf temperature was highest during the emergence growth stage, with elevated temperatures observed across the experimental field (Figure 6.6d). Lower leaf temperatures were exhibited during the vegetative growth stage coupled with small pockets of high leaf temperatures across the field (Figure 6.6e). Finally, moderate taro leaf temperatures characterised the maturity stage, concentrated throughout the experimental field (Figure 6.6f).

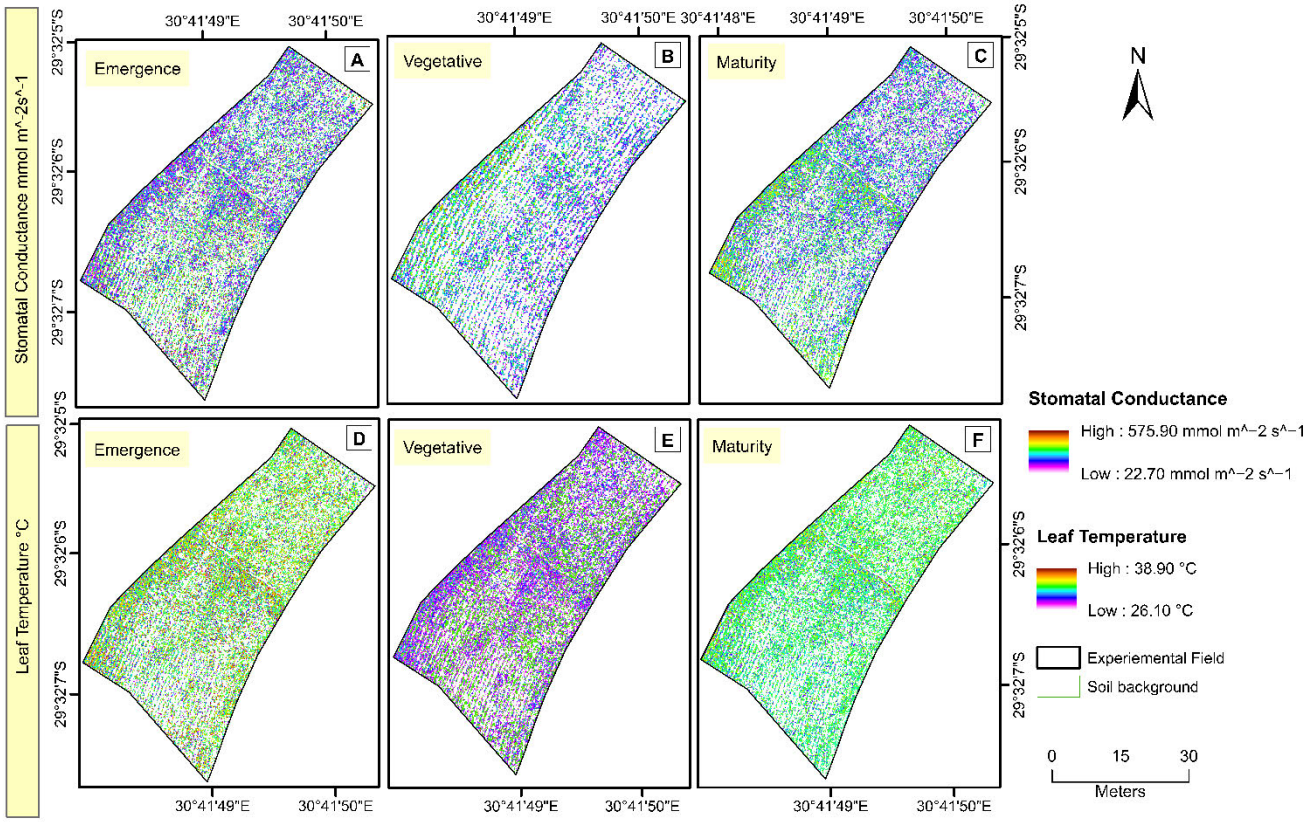

Figure 6.6 The spatial and temporal distribution of stomatal conductance (a-c) and leaf temperature (d-f) across taro growth stages: emergence (a, d), vegetative (b, e), and maturity (c, f).

Figure 6.7 illustrates the spatial distribution of estimated water-stressed areas across the emergence, vegetative, and maturity growth stages, generated using the stomatal conductance threshold of 50 mmol m^{-2} s^{-1} and the leaf temperature threshold of 35 °C. During the emergence growth stage, a significant proportion of taro crops exhibited stress. Specifically, 14.18 % (406.22 m²) of the crops fell below the stomatal conductance threshold (Figure 6.7a), while 37.14 % (1 063.85 m²) exceeded the leaf temperature threshold (Figure 6.7d). This indicates a notable level of estimated potential water stress during the early growth stage of the smallholder taro field. In the vegetative growth stage, water stress was minimal, with most of the field categorised as non-stressed. Only 1.85 % (52.88 m²) of the field was identified as stressed based on stomatal conductance (Figure 6.7b), and an insignificant 0.004 % (0.11 m²) exceeded the leaf temperature threshold (Figure 6.7e), highlighting optimal growing conditions during this stage. The maturity stage exhibited a slight increase in stressed areas compared to the vegetative stage. Stomatal conductance stress remained relatively low, with 7.23 % (207.07 m²) of the crop below the threshold (Figure 6.7c). In contrast, leaf temperature stress was more

pronounced, with 9.36 % (268.22 m²) of the field exceeding the threshold (Figure 6.7f). Despite this increase, much of the smallholder taro field remained non-stressed. The combined trends in stress percentages and areas across all growth stages are visualised in Figure 6.8.

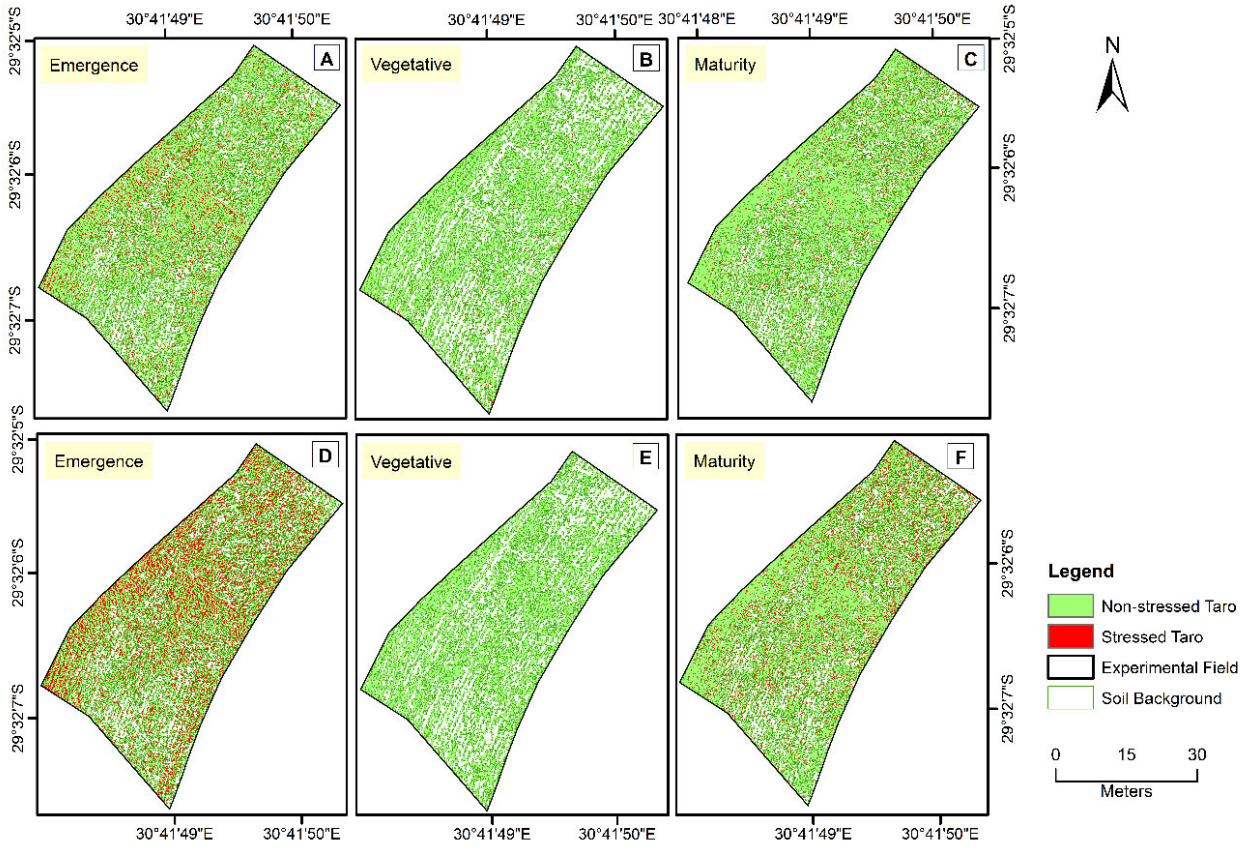

Figure 6.7 Spatial distribution of potential water-stressed taro crops based on the stomatal conductance (a-c) and leaf temperature (d-f) thresholds across taro growth stages: emergence (a, d), vegetative (b, e), and maturity (c, f).

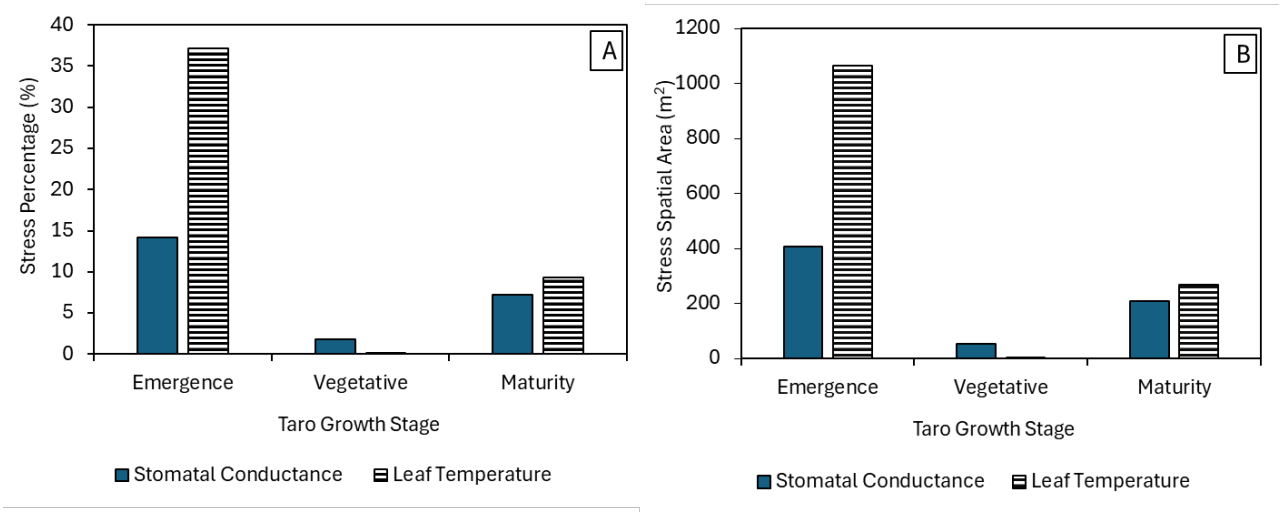

Figure 6.8 (a) Stress percentages and (b) Stressed areas (m²) for stomatal conductance and leaf temperature across the emergence, vegetative, and maturity growth stages of taro.

6.4 Discussion

6.4.1 Performance of selected spectral feature subsets in estimating taro stomatal conductance and leaf temperature

In assessing individual spectral feature subsets, the combination of multispectral bands, the thermal band, and thermal indices generally outperformed other subsets across all growth stages for both stomatal conductance and leaf temperature estimations (R^2 values ranging between 0.61 and 0.84) (Table 6.6), while the use of the multispectral band's feature subset and the thermal data feature subset individually demonstrated moderately low performance (R^2 values ranging from 0.23 to 0.46 and 0.21 to 0.33, respectively). The strong performance of multispectral bands, the thermal band, and the thermal indices feature subset can be attributed to the complementary nature of integrating thermal datasets with multispectral bands (Sobejano-Paz *et al.* 2020). For instance, thermal data directly reflects the thermal properties of crops intricately linked to transpiration rates and stomatal activity, while multispectral bands provide critical information on crop physiology and structural attributes, which vary as a function of water availability (Khanal *et al.* 2017; Gerhards *et al.* 2019; Ahmad *et al.* 2021). When combined, these datasets capture both the energy balance and physiological responses of taro to provide comprehensive information on crop water status, allowing for more accurate estimations of stomatal conductance and leaf temperature.

The findings further revealed that vegetation indices generated moderate accuracies, with the highest predictive power recorded during the vegetative growth stage (R^2 = 0.77 and 0.67 for stomatal conductance and leaf temperature, respectively). These results are consistent with Mwinuka *et al.* (2021a), who found that UAV-derived vegetation indices, such as NDVI, as particularly sensitive to crop moisture content, especially during the vegetative growth stage of the African eggplant crop. Vegetation indices, particularly those derived from the red-edge and NIR regions of the electromagnetic spectrum, are well-established for their ability to capture subtle changes in vegetation vigour, dry matter accumulation, chlorophyll content and photosynthetic activity, which are physiological responses closely linked to the availability of water for crop development (Zhang and Zhou 2019a; Mukiibi *et al.* 2024). For example, a recent study by Suyala *et al.* (2024) integrated the NDWI and NDVI with other indices highly correlated with crop moisture to model the leaf water content of local potato tuber varieties to an R^2 of 0.90, highlighting the effectiveness of vegetation indices in estimating crop water status at critical growth stages. Nonetheless, the performance of vegetation indices became less apparent during the emergence growth stage, where insufficient canopy development and interference of soil temperatures affect predictive accuracy (R^2 = 0.44) (Table 6.6). Similarly, while vegetation indices achieved a moderate R^2 of 0.62 for stomatal conductance during this stage, the rRMSE of 46.26% reflects significant variability between the observed and modelled data (Table 6.6). This limitation aligns with findings by Wang *et al.* (2024c), who highlighted that measurements of canopy reflectance and derived indices along the visible and NIR spectra are typically most effective in advanced stages of crop growth, where structural and physiological changes in canopy are highly responsive to variations in water content. This result highlights a key limitation of using vegetation indices for early-stage crop monitoring, where spectral signals are weak and physiological traits are not yet sufficiently developed to allow for robust prediction. The large variability observed in the emergence stage suggests that additional data types, such as thermal or environmental variables, may be necessary to improve prediction accuracy during this critical establishment phase.

Additionally, the findings of the study reported moderate prediction accuracies (R^2 up to 0.57) in estimating stomatal conductance and leaf temperature using the topographic indices (Table 6.6). Studies have shown topographic indices, including slope, aspect and TWI as terrain attributes that are closely associated with hydrological processes that directly and indirectly influence crop water availability (Oliveira *et al.* 2022; Rabia *et al.* 2022). These indices,

capturing water movement and accumulation within a landscape, significantly influence the moisture available to crops and therefore play an essential role in understanding the relationship between topography and crop physiological processes, such as leaf transpiration and thermoregulation (Rabia *et al.* 2022).

Overall, the highest predictive accuracy for stomatal conductance and leaf temperature was achieved using the combination of feature subsets, with R^2 values exceeding 0.86 across the growth stages (Table 6.6). These findings are in agreement with those of Guimarães *et al.* (2024), who successfully combined UAV multispectral and thermal data to predict the stomatal conductance of almond crops to an R^2 of 0.87 and MSE of 0.0016 mmol m^{-2} s^{-1}. Similar trends were observed by Liu *et al.* (2025), who found that regardless of the modelling technique, the fusion of thermal and multispectral data outperforms individual feature subsets in estimating citrus stomatal conductance with R^2 ranging from 0.91 to 0.98, and RMSE from 1.62 mmol to 3.99 mmol H_2O $m^{-2} \cdot s^{-2}$. In a similar study, Yu *et al.* (2021) integrated UAV multispectral imagery with topographic metrics to estimate the nitrogen content of wheat fields, achieving an optimal R^2 of 0.92 and RMSE of 1.75 g/m^2. Meanwhile, a related study by Usta (2022) obtained optimal R^2 values ranging between 0.75 to 0.90 when combining multispectral data, thermal data and topographic indices (including slope and TWI) to estimate the soil water content of agricultural fields. Nonetheless, combining feature subsets is not without limitations as the inclusion of diverse variables can introduce redundancy, multicollinearity, and increased computational complexity (Omia *et al.* 2023; Wang *et al.* 2024b). Moreover, despite the overall high predictive performance, some models still reported relatively high error margins, with rRMSE values reaching up to 25.45% (Table 6.6). These findings highlight the need for further optimisation, such as feature selection to minimise redundancy and advanced calibration techniques to optimise model robustness and refine predictions.

6.4.2 Performance of optimised models in estimating stomatal conductance and leaf temperature across the taro growth stages

The optimised models demonstrated exceptional predictive performance in estimating taro stomatal conductance and leaf temperature across all growth stages, with R^2 values exceeding 0.91 and rRMSE values less than 17 % (Figure 6.4). Among the growth stages, the vegetative stage consistently exhibited the highest predictive accuracy (Figure 6.4b and e). The strong performance during the vegetative stage can be attributed to the optimal growth conditions and

increased physiological activity, which likely resulted in higher variability in predictor variables, allowing the model to identify stronger correlations among input features (Maestrini and Basso 2018b). Additionally, the increase of crop canopy and accumulation of above-ground biomass during the vegetative stage strengthens the robustness of taro spectral signatures, minimising residual soil background interference (Maimaitiyiming *et al.* 2020a; Messina and Modica 2020; Chauhan *et al.* 2024). Meanwhile, the emergence and maturity stages exhibited slightly lower prediction accuracies in estimating stomatal conductance and leaf temperature compared to the vegetative stage, though the results remained generally high, with R^2 values above 0.91 (Figure 6.4). During the emergence stage, the sparse canopy coverage and early developmental phase of the crop limit the effectiveness of spectral data in capturing the relevant physiological responses associated with water stress, resulting in reduced model performance (Khanal *et al.* 2017). During the maturity stage, physiological processes begin to slow as the crop enters senescence and resources are allocated towards tuber development, therefore reducing the above-ground biomass visible for the sensor to accurately capture crop attributes (Kunz *et al.* 2024b). These findings are consistent with those of Brewer *et al.* (2022b) who achieved the highest prediction accuracies during the vegetative growth stage in estimating the foliar temperature of smallholder maize fields. A similar trend was observed by Wang *et al.* (2018) who demonstrated the optimal prediction of maize stomatal conductance at the vegetative growth stage (R^2 of 0.82 and NRMSE of 23.1%).

The findings illustrated that the optimal features for estimating taro stomatal conductance include thermal, NRCT, I3, SIPI, CIrededge, red-edge, NDVI, NDWI, NDRE, MCARI, slope, TWI, NIR, and red, while thermal, NRCT, NDWI, NIR, NDRE, NDVI, CIrededge, MCARI, aspect, TWI and slope were consistently selected for estimating leaf temperature across the growth stages (Figure 6.5). The consistency of thermal data as optimal features across both stomatal conductance and leaf temperature estimations highlights the documented utility of thermal remote sensing in crop water assessments and monitoring (Khanal *et al.* 2017; Zhou *et al.* 2021; Awais *et al.* 2022a). These findings are supported by those of Brewer *et al.* (2022b) who found the thermal band to be the most important predictor variable of both stomatal conductance and foliar temperature estimations across multiple maize growth stages. Similarly, Elsayed *et al.* (2017) demonstrated a strong correlation, with an R^2 of 0.87, between the thermal index NRCT and canopy water status. Furthermore, vegetation indices (NDWI, NDVI, NDRE) and chlorophyll-based indices (SIPI, CIrededge, MCARI) were consistently selected as

important input features for estimating both taro stomatal conductance and leaf temperature (Figure 6.5). Studies have shown that vegetation indices, particularly those in the red-edge and NIR regions of the electromagnetic spectrum, are highly sensitive to variations in crop water content due to their ability to capture key physiological and structural changes in vegetation induced by water stress (Colovic *et al.* 2022; Li *et al.* 2022c). These findings are supported by Guimarães *et al.* (2024), who reported NDVI, NDRE, and CIrededge as significant predictor variables for estimating stomatal conductance in rainfed almond crops, with correlation values exceeding R^2 of 0.70. Similarly, Zhang and Zhou (2019a) reported the CIrededge as the most sensitive indirect indicator of water variation in maize, recording a correlation R^2 of 0.75. Studies have also shown chlorophyll-based indices, such as the CIrededge and SIPI, as invaluable in assessing crop water status, as they capture essential information on crop photosynthetic efficiency and are sensitive to changes in water content and stress, making them excellent predictors of stomatal conductance and leaf temperature under varying water availability (Suárez *et al.* 2008; Ryu *et al.* 2022). Lastly, the reported utility of topographic indices, such as slope, aspect and TWI lies in their ability to modulate the local microclimate, influence spatiotemporal water distribution and regulate soil moisture retention, consequently affecting crop thermoregulation and water uptake (Rabia *et al.* 2022).

6.4.3 The spatial and temporal variability of taro stomatal conductance and leaf temperature across the taro growth stages

The variation in stomatal conductance and leaf temperature across the taro growth stages revealed critical insights into the crop's water status dynamics and potential water-stress areas. During the emergence growth stage, leaf temperature peaked while stomatal conductance was at its lowest, resulting in significant water stress levels, with an estimated 37 % of crops surpassing the temperature threshold and 14.18 % exceeding the stomatal conductance threshold (Figure 6.8). This early-stage stress can be attributed to limited canopy development, which left the soil exposed to higher evaporation rates, combined with the underdeveloped rhizomatous root systems that restricted the plant's ability to uptake water effectively, making taro more susceptible to stress (Dathe *et al.* 2014; Delogu *et al.* 2018; Costa *et al.* 2019). Additionally, the emergence stage represents a critical period of physiological establishment for taro, during which the crop is more vulnerable to environmental extremes such as elevated temperatures and water scarcity (Kashyap and Panda 2003; Dahal *et al.* 2019; Lal *et al.* 2022).

In contrast, the vegetative growth stage observed peak stomatal conductance while leaf temperature reached its lowest levels, resulting minimal crop moisture stress observed (Figure 8). This is explained by the fact that crops at this stage are characterised by fully established physiological processes, including the crop's ability to adequately produce osmolytes, heat shock protein and other growth regulators, to mitigate water deficits and maintain their growth functions under mild moisture stress (Daryanto *et al.* 2017). However, under severe water stress, taro crops exhibit dehydration avoidance by reducing stomatal conductance as a mechanism to minimise transpirational water losses (Mabhaudhi *et al.* 2013), therefore explaining the low stomatal conductance observed during the emergence growth stage. Consistent with our results, Mthembu *et al.* (2022) observed that tuber crops characterised by water stress conditions exhibited significantly lower stomatal conductance rates compared to those cultivated under optimal moisture conditions.

Lastly, it is important to note that the vegetative stage also showed the highest variability in stomatal conductance measurements (234.09 ± 149.77 mmol m^{-2} s^{-1}), as revealed in the descriptive statistics (Table 6.5). This substantial within-stage variability may reflect environmental heterogeneity, such as uneven water availability or microclimatic fluctuations. Although the optimised models performed well overall, such variability may have contributed to higher residuals in model predictions or reduced generalisability across microenvironments. This underscores the complexity of modelling stomatal behaviour during periods of heightened physiological activity. Moreover, the limited number of discrete growth stages assessed may not fully capture the continuous and dynamic shifts in stomatal conductance and leaf temperature, potentially masking transitional physiological processes between stages. As such, more frequent temporal sampling strategy is recommended to further enhance model accuracy and interpretation of crop water stress patterns.

6.4.4 Implications of the study, limitations and recommendations for future research

The findings of this study highlight the value of integrating UAV-acquired multispectral and thermal data, vegetation indices and topographic metrics, with advanced model optimisation techniques, to facilitate comprehensive and near-real-time analysis of crop water status. By using stomatal conductance and leaf temperature as proxies, this study demonstrates a robust, scalable, and innovative approach to monitoring the water status of taro crops, offering the potential for targeted interventions that mitigate the adverse impacts of water stress on rainfed

smallholder farming systems. Furthermore, the application of UAV technologies in this study represents a transformative and cost-effective solution for the continuous monitoring of crop water status, enabling the early detection of water deficits in the absence of extensive ground-based measurements. On a broader scale, the findings of this study contribute to the ongoing efforts to enhance food security, advance sustainable agricultural practices and build the resilience of smallholder farming systems in light of climate change and variability. As water scarcity becomes an increasing challenge in many regions, particularly in the global south, adopting innovative technologies such as UAV proximal sensing can support sustainable farming practices, ensuring that smallholder farmers can adapt to changing environmental conditions, while enhancing food production. Moreover, this study advocates for the diversification of agricultural systems by promoting the integration of NUS, such as taro, into mainstream farming practices, therefore enhancing resilience and supporting agricultural sustainability and food security.

Despite the strengths of this study, some limitations warrant attention. Although the study followed a data-driven approach to modelling crop water status, the restricted spectral resolution of the multispectral sensor used in this study limited the computation of additional vegetation indices that are known to be valuable in assessing crop water status. Therefore, further research is needed to explore the integration of higher-resolution multispectral or hyperspectral sensors that would enable the computation of a broader range of vegetation indices, particularly those derived from the shortwave infrared region. Moreover, the DNN models developed in this study were trained and tested using in-situ stomatal conductance and leaf temperature data that were specific to the field site, hence may not fully represent the variability across different smallholder taro fields. Therefore, future research should focus on applying DNN models on a larger scale to improve the generalisability and reliability of taro crop water status predictions. Furthermore, it is recommended that future studies compare the performance of additional feature selection methods and model optimisation techniques to improve the accuracy and efficiency of crop water status predictions. Finally, while this study provided valuable insights into the temporal dynamics of crop water status, it was conducted over a single growing season, limiting the ability to assess long-term variability in taro stomatal conductance and leaf temperature. To address this gap, future studies should evaluate seasonal fluctuations in water status across multiple growth stages and growing seasons to capture the

full variability and inform more effective water management strategies within smallholder taro farmlands.

6.5 Conclusion

This study aimed to address the critical need for monitoring and quantifying the taro crop water status, particularly within resource-constrained, rainfed smallholder farming systems. By leveraging UAV-derived thermal and multispectral imagery, combined with topographic indices variables, the study sought to estimate stomatal conductance and leaf temperature as proxies for crop water status and stress, while identifying areas of potential water stress across different growth stages. Based on the primary findings of this research, it can be concluded that:

- The optimised models for taro stomatal conductance across the growth stages achieved exceptional predictive performance in this study, with R^2 values exceeding 0.92 and rRMSE below 17 %. Key predictor variables included thermal, NRCT, I3, SIPI, CIrededge, red-edge, NDVI, NDWI, NDRE, MCARI, slope, TWI, NIR, and the red band.

- The optimised models of taro leaf temperature yielded high estimation accuracies across the growth stages, with R^2 values ranging from 0.91 to 0.95 and rRMSE below 1.52 %. Consistently selected key predictor variables in this study were thermal, NRCT, NDWI, NIR, NDRE, NDVI, CIrededge, MCARI, aspect, TWI and slope.

In conclusion, this study contributes to the discourse on sustainable agriculture, highlighting the role of innovative technologies in addressing the challenges posed by climate variability. By providing a robust framework for assessing crop water stress, this study contributes to enhancing the anecdotal knowledge on neglected and underutilised crops, such as taro, thereby highlighting their potential for promoting climate-smart and nutrition-sensitive agricultural practices. The ability to identify and manage water stress in taro not only enhances crop resilience and productivity but also supports food security and sustainable livelihoods in smallholder farming communities. Furthermore, the integration of UAV technology and advanced modelling approaches offers a scalable solution for monitoring other neglected and underutilised crops, reinforcing the imperative for transformative adaptation strategies in agriculture. By bridging the knowledge gap in spatiotemporal taro water dynamics, the study

sets the foundation for future research and policy interventions aimed at achieving climate-resilient agricultural landscapes that prioritise human well-being, food security, and environmental sustainability.

6.6 Summary

Chapter Six presented a comprehensive data-driven approach for optimising taro crop water status estimations within smallholder taro farming systems. By leveraging UAV-acquired thermal and multispectral data, alongside topographic variables, the chapter highlights the importance of integrating diverse datasets for accurately predicting stomatal conductance and leaf temperature across the emergence, vegetative and reproductive growth stages. The analysis also explored the application of literature-informed critical water stress thresholds to precisely identify areas of potential water stress within taro crops, facilitating targeted interventions that mitigate the impacts of water deficits. The following Chapter Seven synthesises the key findings from this study, contextualises their implications and provides recommendations for future research, offering a comprehensive conclusion to this dissertation.

CHAPTER SEVEN: SYNTHESIS AND CONCLUSION

7.1 Introduction

Due to the exponentially increasing human population, ensuring food and nutrition security has become an urgent priority (Mugiyo *et al.* 2021c; Din *et al.* 2022a). Climate change and variability have presented a significant challenge in agriculture, particularly in sub-Saharan Africa, where smallholder farming systems account for up to 80% of food production but remain disproportionately vulnerable to climate change impacts (Hlophe-Ginindza and Mpandeli 2020; Lee *et al.* 2023). As smallholder agricultural crop production becomes increasingly affected by erratic rainfall patterns, rising temperatures and escalating water scarcity, there is an urgent need for innovative approaches aimed at sustaining agricultural productivity, while promoting climate resilience (Nhamo *et al.* 2019b; Kumar *et al.* 2020). Meanwhile, taro (*Colocasia esculenta* (L)), a Neglected and Underutilised Crop Species (NUS) characterised by drought and heat tolerance, adaptability to diverse environmental conductions, and a high nutritional profile, has been identified as a future-smart-crop capable of diversifying current agricultural cropping systems and advancing climate-resilient and nutrition-sensitive agriculture (Chivenge *et al.* 2015; Mabhaudhi and Modi 2015; Oyeyinka and Amonsou 2020). Nonetheless, while taro has demonstrated significant potential in enhancing smallholder climate resilience and ensuring food and nutrition security, there is limited research available on the spatial and temporal dynamics of its water status and stress responses throughout the growing season. Therefore, there is an urgent need for spatially and temporally explicit evidence-based information on taro's water status to guide adaptive water management practices, optimise crop productivity and promote its broader adoption and integration into mainstream agriculture.

Proximal remote sensing technologies, particularly Unmanned Aerial Vehicles (UAVs) mounted with ultra-high-resolution thermal cameras and multispectral sensors, have emerged as an innovative and effective tool for crop water status monitoring at field scale (Gerhards *et al.* 2019; Hussain *et al.* 2020; Nhamo *et al.* 2020). While the integration of near-real time UAV remotely sensed data with advanced deep learning modelling techniques and robust datasets facilitates rapid and accurate crop monitoring, its applicability in quantifying the crop water status of neglected and underutilised smallholder taro crops remains insufficiently explored. In this regard, this study sought to evaluate the utility of UAV thermal remote sensing in assessing

and monitoring the crop water status of taro crops within smallholder farming systems. To address the overarching aim, the following specific objectives were drawn:

- To review and offer an in-depth systematic assessment of the progress, challenges, and opportunities presented in the literature on the adoption of UAV thermal remote sensing in assessing and monitoring crop water status.

- To assess the utility of UAV thermal remotely sensed data and index-based segmentation techniques in enhancing the estimation of smallholder taro equivalent water thickness as a proxy of crop water status.

- To evaluate the utility of UAV remotely sensed data for high-throughput crop phenotyping of taro equivalent water thickness, fuel moisture content, stomatal conductance, foliar temperature and chlorophyll content as proxies for water status within smallholder farms.

- To conduct a multi-temporal analysis of neglected and underutilised taro crop water status using multimodal UAV remotely sensed data to estimate stomatal conductance and foliar temperature as key physiological indicators across different growth stages of smallholder taro crops.

- To optimise the estimation of taro stomatal conductance and leaf temperature through a data-driven approach that integrates UAV-derived thermal and multispectral data with topographic variables, enabling the quantification of crop water stress based on predefined stress thresholds.

7.2 Synthesis of findings aligned to objectives

7.2.1 A Systematic Review of the Application of UAV-Based Thermal Remote Sensing for Assessing and Monitoring Crop Water Status in Crop Farming Systems

Noticeable gaps exist in the literature, particularly on the application of UAV thermal remote sensing in assessing crop biophysical and biochemical properties related to crop water status. In this regard, a systematic review was conducted to understand the progress, challenges, and opportunities in utilising UAV thermal remotely sensed data to assess and map the crop water status within agricultural systems (Chapter Two). While notable progress has been achieved in

this field, research efforts remain disproportionately concentrated in the global north, with a strong focus on mainstream crops and commercial irrigated farming systems. In contrast, there is a notable paucity of studies on water status within neglected and underutilised crops and smallholder rainfed cropping systems in the global south. Furthermore, there is a lack of consensus on the most effective biophysical indicators for assessing crop water status. While some studies have explored the use of stomatal conductance, equivalent water thickness, canopy water content, and leaf temperature as proxies of crop water status, their applicability remains inadequately researched, highlighting the need for comprehensive investigations in this area. Furthermore, the findings revealed that while UAV-derived thermal datasets have garnered increased popularity over the decades, numerous studies have investigated the combination of thermal imagery and multispectral channels for estimating crop water status, leveraging the complementary nature of these data types to enhance accuracy and provide a more comprehensive assessment of crop water conditions. Moreover, there is a notable scarcity of studies that probe the efficacy of robust machine algorithms, including deep learning techniques, in conjunction with thermal and spectral indices in mapping and monitoring crop water status. Therefore, this study highlights the need for additional research to explore the utility of UAV remotely sensed thermal data, alongside multi-source datasets and deep learning techniques, in estimating the crop water status of neglected and underutilised taro crops, especially in smallholder farming systems in the global south. The systematic literature review informed the other forth coming chapters regarding the optimal machine learning techniques, spectral variables and image processing techniques suitable for mapping crop water status elements of taro in smallholder cropland systems.

7.2.2 Enhancing the Estimation of Equivalent Water Thickness in Neglected and Underutilised Taro Crops using UAV acquired Multispectral Thermal Image Data and Index-Based Image Segmentation

Image segmentation to remove soil background is crucial to accurately assess crop water status, especially in set-ups such as smallholder taro fields, where the soil background effect is pronounced due to low planting density and high interrow spacing. In this regard, this specific objective sought to assess the performance of UAV thermal remote sensing and index-based segmentation techniques in improving the estimation of canopy Equivalent Water Thickness (EWT_{canopy}) as a proxy of water status within smallholder taro crops (Chapter Three). To

achieve this objective, a comparative analysis was conducted to evaluate the predictive performance of models with and without the thermal band, while assessing the effectiveness of Excess Green (ExG), Excess Red (ExR), and Excess Green minus Excess Red (ExGR) image segmentation techniques in enhancing taro EWT_{canopy} estimations. The results demonstrated that incorporating the thermal band and applying image segmentation, particularly using the ExGR technique, significantly enhanced the prediction accuracy of taro EWT_{canopy}, increasing the R^2 value from 0.32 to 0.92 and reducing the rRMSE from 60.51% to 15.31%. These findings are consistent with a recent study by Guan and Grote (2023), which reported an improvement in the estimation of vineyard water status by incorporating the thermal channel, achieving an R^2 of 0.74 compared to an R^2 of 0.63 when the model relied solely on multispectral data. The results of this study highlight the critical importance of combining thermal data with effective image segmentation techniques, such as the ExGR method, to enhance the accuracy of EWT estimations, serving as a benchmark for optimising the assessment of other crop water status indicators within smallholder taro cropping systems.

7.2.3 Assessing Neglected and Underutilised Taro Crop Water Status using Physiological Indicators and UAV Multi-Modal Thermal-Multispectral Data

Although taro exhibits tolerance to drought conditions, variations in physiological attributes such as leaf temperature that rises during water stress and the associated stomatal closure initiated to conserve water, compromise crop productivity and overall yield (Gerhards *et al.* 2019; Wang *et al.* 2022a). Therefore, monitoring the variations in these physiological indicators allows for the effective quantification of crop water status and the timely implementation of targeted interventions aimed at mitigating the impacts of water deficit on taro crop productivity. Therefore, this specific objective aimed to evaluate the utility of UAV remotely sensed data for high-throughput crop phenotyping of taro equivalent water thickness, fuel moisture content, stomatal conductance, foliar temperature and chlorophyll content as proxies for water status within smallholder farms (Chapter Four). The findings showed that the multi-modal approach, integrating both thermal and multispectral data, yields the highest estimation accuracy in comparison to single-modal predictions, achieving R^2 values greater than 0.91 and rRSME values less than 14.15% for all crop water status physiological indicators. The findings of this study are supported by those of Zhai *et al.* (2023) who integrated the spectral capabilities of thermal and multispectral data to optimise the estimation of chlorophyll content of maize crops,

achieving R^2 of 0.75 and RMSE of 8.36 %. The results also highlighted that the thermal waveband and derived thermal indices were the most influential variables in estimating crop water status physiological indicators, particularly stomatal conductance and leaf temperature, yielding R^2 of 0.96 and 0.95, respectively. The significance of the thermal band can be explained by the fact that as stomata regulate the release of water vapor from crop leaves, changes in stomatal conductance are reflected in leaf temperature, making thermal data valuable predictors of these physiological indicators (Yu *et al.* 2015; Gerhards *et al.* 2019). These findings are corroborated by Brewer *et al.* (2022b) who explored the use of integrating optical and thermal infrared UAV imagery to estimate maize stomatal conductance and leaf temperature, achieving R^2 values of 0.85 and 0.81, respectively, with the thermal band emerging amongst top most influential variables. Additionally, the results highlighted the importance of spectral indices, particularly those derived from the near-infrared and red-edge regions of the electromagnetic spectrum, as key predictors of crop water status physiological indicators such as equivalent water thickness, fuel moisture content, and chlorophyll content. The sensitivity of these regions is attributed to their ability to detect subtle changes in vegetation structure and leaf pigmentation due to water stress, thereby, making the region invaluable for crop water assessments (Ballester *et al.* 2019; Colovic *et al.* 2022). Overall, the results of this study demonstrated the effectiveness of UAV thermal remote sensing, in concert with multispectral data, for providing rapid and accurate spatially explicit data on smallholder taro crop water status physiological indicators, crucial for improving crop productivity and developing early warning systems for water stress.

7.2.4 Multi-Temporal Analysis of Taro Crop Water Stress Using High-Resolution Thermal and Multispectral Proximal Sensing for Improved Resilience of Smallholder Farming Systems

Effective monitoring of taro's water status throughout the growing season is essential for timely interventions and adaptation strategies aimed at mitigating the negative effects of water deficits. With the increasing challenges of climate change, it is critical to implement robust methods for tracking crop water stress, particularly for smallholder farming systems, throughout the growing season of taro. In this regard, this specific objective aimed to explore the potential of UAV-acquired thermal and multispectral proximal sensing, integrated with the deep neural

network algorithm, to assess the multitemporal variability of stomatal conductance and leaf temperature of smallholder taro crops during the emergence, vegetative, and maturity growth stages (Chapter Five). The observed patterns in stomatal conductance and leaf temperature indicate critical trends in the physiological responses of taro under varying growth stages. During the emergence stage, taro exhibited notably high leaf temperatures paired with low stomatal conductance, reflecting limited transpiration and reduced cooling efficiency. In contrast, the vegetative stage displayed the lowest leaf temperature and a peak in stomatal conductance, highlighting effective stomatal cooling through enhanced transpiration. Furthermore, the emergence stage showed the highest canopy-to-air temperature difference (Tc-Ta), signifying elevated thermal stress. This trend aligns with the principle that crops experiencing water deficits struggle to regulate their leaf temperature, resulting in an increased Tc-Ta as their cooling capacity diminishes, while stomatal conductance declines as a protective response to conserve water and maintain physiological functions (Luan and Vico 2021; Brewer *et al.* 2022b). Additionally, the results demonstrated that thermal data, alongside derived thermal indices, were critical predictors for both stomatal conductance and leaf temperature across all taro growth stages. Notably, the vegetative stage yielded the highest prediction accuracies for both physiological indicators: stomatal conductance (R^2 = 0.96, RMSE = 29.34 mmol m^{-2} s^{-1}, rRMSE = 12.86 %) and leaf temperature (R^2 = 0.95, RMSE = 0.33 °C, rRMSE = 1.11 %). These findings are consistent with those by Wang *et al.* (2024a) who reported that the vegetative growth stage produced optimal accuracies for stomatal conductance predictions, achieving an RMSE of 15%. The optimal accuracies during this stage can be attributed to the dense canopy, which minimises soil temperature influence and enhances physiological regulation (Badr *et al.* 2012; Sobejano-Paz *et al.* 2020; Chauhan *et al.* 2024). In contrast, the reduced canopy cover during the emergence stage, due to early crop development, and during the maturity stage, due to senescence and the crop shifting its resource allocation to underground tuber development, impacted model predictions by increasing soil heat absorption (Maimaitiyiming *et al.* 2020a; Messina and Modica 2020; Kunz *et al.* 2024b). Overall, these findings highlight the transformative potential of combining high-resolution thermal and multispectral sensing technologies for precision agriculture, particularly in the context of monitoring smallholder taro stomatal conductance and leaf temperature variability across different growth stages, as proxies of crop water status.

7.2.5 Optimising Neglected and Underutilised Taro Crop Water Status Estimations using UAV-Acquired Thermal and Multispectral Remotely Sensed Data

This study presents a data-driven approach to optimising the estimation of water status in neglected and underutilised taro crops, at the emergence, vegetative, and maturity growth stages. The aim of the study was to enhance the accuracy of crop water status estimations by integrating UAV-derived thermal and multispectral remotely sensed data and topographic variables within an advanced modelling framework using stomatal conductance and leaf temperature as water stress proxies (Chapter Six). While integrating multi-source datasets provides a comprehensive insight to crop water conditions, combining feature subsets introduces challenges such as redundancy, multicollinearity, and increased computational complexity (Omia *et al.* 2023; Wang *et al.* 2024b). To overcome these challenges, optimised predictive models that employed advanced feature selection techniques were utilised to enhance model performance and accuracy in estimating water stress proxies in this chapter. The results demonstrated the significant potential of advanced feature selection and deep learning techniques in optimising predictive models for estimating taro crop water status. The optimised models exhibited strong performance, with R^2 values consistently exceeding 0.91 and rRMSE values remaining below 16.86%. Furthermore, thermal, NRCT, I3, SIPI, CIrededge, red-edge, NDVI, NDWI, NDRE, MCARI, slope, TWI, NIR and red were observed as the optimal feature combination for estimating stomatal conductance, while thermal NRCT, NDWI, NIR, NDRE, NDVI, CIrededge, MCARI, aspect, TWI and slope were optimal features for leaf temperature models. These findings highlighted the utility of integrating diverse yet relevant datasets, including thermal, multispectral, and topographic data into a unified, data-driven framework for estimating crop water status. Moreover, this study applied critical water stress thresholds (50 mmol m^{-2} s^{-1} for stomatal conductance and 35 °C for leaf temperature) on optimised estimation models, allowing for a spatially explicit quantification of water-stressed areas across the taro field. The study findings revealed that during the emergence stage, a significant portion of the taro field exhibited stress, with 14.18 % of crops showing below-threshold stomatal conductance and 37.14 % exceeding the leaf temperature threshold, indicating potential water stress during early growth. In contrast, the vegetative stage exhibited minimal stress, with only 1.85 % of the field identified as stressed based on stomatal conductance, while the maturity stage saw a slight increase in stress, particularly in leaf temperature, with 9.36% of the area exceeding the stress threshold. These findings align with the variability of stomatal conductance

and leaf temperature observed in Chapter Five, where the emergence stage exhibited high leaf temperatures coupled with low stomatal conductance, reflecting potential water stress. These findings are particularly significant when considering the implications for crop management, highlighting the critical need for early-stage monitoring and targeted interventions, especially during the emergence stage, to manage potential negative impacts caused by water stress on taro. Overall, the results demonstrated the significant potential of UAV-derived thermal and multispectral remotely sensed data, integrated with advanced modelling techniques, in optimising the estimation of crop water status for smallholder neglected and underutilised crops such as taro. These findings contribute to the development of a practical, efficient, and scalable framework for monitoring taro croplands within smallholder farming systems. By accurately predicting taro water status and quantifying areas of water stress, this framework can inform evidence-based crop management, ultimately improving NUS productivity and sustainability in the face of increasing climate variability.

7.3 Conclusions

This study aimed to evaluate the utility of UAV thermal remote sensing in assessing and monitoring the crop water status of neglected and underutilised taro crops within smallholder farming systems. The study focused on leveraging UAV remotely sensed data, in concert with deep learning modelling, to estimate key crop water physiological indicators, including equivalent water thickness, fuel moisture content, stomatal conductance, foliar temperature and chlorophyll content as proxies for water status within smallholder taro farming systems. The findings demonstrated that UAV thermal and multispectral imagery, combined with image segmentation techniques and machine learning algorithms, such as deep neural networks, can accurately estimate and quantify crop water status at a field scale.

The conclusions drawn from the findings of each objective are:

i. Based on the literature, UAV-based thermal remote sensing is an invaluable tool and holds significant promise in advancing crop water status assessments and monitoring. The use of proximal thermal remote sensing for crop water monitoring has gained traction over the years, with the recent decade noting a proliferation of cutting-edge sensors and related studies in this field, particularly in the global north. Nonetheless, the value and performance of thermal remote sensing is largely dependent on its integration

with multispectral sensor technologies. Additionally, challenges, such as the mixed-pixel effect and soil background noise, have been identified as contributing factors to inconsistencies in thermal imagery, thereby compromising the accuracy of crop water status assessments. Opportunities to enhance crop water status monitoring exist in refining data processing methods, evaluating the effectiveness of robust machine learning algorithms such as deep learning techniques, and exploring their potential to monitor seasonal and diurnal moisture variability in tuber crops, particularly within smallholder rainfed systems in the global south.

ii. The use of UAV thermal remotely sensed data combined with image segmentation, particularly through the ExGR technique, substantially enhances the predictive accuracy of EWT_{canopy} estimations in smallholder taro crops. Overall, the study deduced that integrating thermal with multispectral data is essential for accurately capturing the variability of EWT_{canopy} across taro fields, with the absence of this combined data leading to a noticeable reduction in the predictive performance of crop water status models. Moreover, the ExGR segmentation technique was the most effective in isolating pure crop canopy spectra and eliminating soil background interference, notably improving the accuracy of EWT_{canopy} predictions. The conclusions of this study provide a foundational framework for optimal image segmentation technique for isolating taro crop pixels and highlight the critical importance of combining thermal and multispectral data to enhance the estimation of crop water status physiological indicators.

iii. UAV remotely sensed data is valuable for high-throughput crop phenotyping of multiple water status proxies, including taro equivalent water thickness, fuel moisture content, stomatal conductance, foliar temperature, and chlorophyll content. Overall, the integration of thermal and multispectral data yielded the highest predictive accuracies of taro crop water status, with thermal data, thermal indices and vegetation indices derived from the near-infrared and red-edge regions of the electromagnetic spectrum emerging as important predictor variables of smallholder taro crop water status. This demonstrates the power of multi-modal approaches in high-throughput crop phenotyping.

iv. UAV multi-modal remotely sensed data is valuable in assessing the spatial and temporal variability of crop water status physiological indicators, particularly stomatal conductance and leaf temperature across the emergence, vegetative and maturity growth stages of taro. The variability of stomatal conductance and leaf temperature can be accurately captured through the combination of thermal and multispectral data, with the thermal band and derived indices emerging as essential predictor variables across the taro growth stages. Moreover, the vegetative growth stage is the optimal period for crop water status assessments, with the highest prediction accuracies for stomatal conductance and leaf temperature observed during this stage.

v. The integration of advanced feature selection techniques and model optimisation methods improves the estimation of smallholder taro stomatal conductance and leaf temperature across the various growth stages. The optimisation of crop water status models, together with the inclusion of crucial UAV and non-UAV data configurations, including thermal data, multispectral bands, vegetation indices and topographic variables, results in optimal prediction accuracies of taro stomatal conductance and leaf temperature. Additionally, the application of critical water stress thresholds allows for the spatially explicit identification of water-stressed areas across taro fields, essential for pinpointing areas requiring immediate intervention and targeted water management strategies. This data-driven approach enhances the quantification of crop water stress based on predefined stress thresholds, offering a robust tool for managing water resources within neglected and underutilised smallholder taro farming systems.

7.4 Study limitations, challenges, and recommendations for future research

The application of UAV thermal remote sensing for assessing and monitoring crop water status has demonstrated immense potential in advancing precision agriculture. By leveraging high-resolution thermal and multispectral data, this technology offers solutions to addressing water management challenges in smallholder farming systems, particularly in the light of climate change impacts. However, the adoption of UAV thermal remote sensing for agricultural crop water monitoring, particularly for neglected and underutilised crops such as taro, is not without challenges. This study, therefore, notes the following limitations and proposes corresponding recommendations and future research opportunities:

- Existing literature highlights a significant gap in research exploring the efficacy of advanced machine learning algorithms, particularly deep learning techniques integrated with thermal and spectral indices for mapping and monitoring crop water status within smallholder farmlands. To the best of our knowledge, this study represents the first attempt at deep learning-based modelling of crop water status using UAV-derived remote sensing data for smallholder neglected and underutilised taro crops in the global south. However, a critical limitation of this study is the specificity of the dataset used for training and testing the Deep Neural Network (DNN) models. While the models provided high accuracy estimates of taro crop water status, the data was collected from a single field, hence limiting the generalisability of the findings across other smallholder farming contexts. Furthermore, DNN models are challenged by their high computational requirements, the potential for overfitting, and the need for extensive datasets to ensure reliable performance. As a result, future research should focus on scaling the application of DNN models to include multiple fields with varying conditions. Such expansion would not only enhance the robustness and reliability of model predictions but also provide a more comprehensive understanding of taro water status across diverse smallholder environments.

- The spectral resolution of the multispectral sensor used in this study posed a limitation. While UAVs offer exceptional spatial resolution imagery, the limited spectral bands available constrain the ability to compute additional vegetation indices, particularly those derived from the shortwave infrared region, which are critical for assessing crop water status. The restricted spectral range limited the ability to fully exploit the potential of additional water-sensitive indices in monitoring taro water stress. To address this, future studies should explore the integration of advanced multispectral or hyperspectral sensors, that can enable the computation of a broader array of vegetation indices.

- The precise calibration of thermal imagery is essential to ensure the accuracy of derived datasets, as errors can directly affect the reliability of water stress assessments. Factors such as atmospheric interference, variable solar radiation, and soil background effects have been demonstrated to introduce variability in the thermal data. Addressing these challenges requires rigorous calibration protocols, alongside the adoption of advanced image segmentation techniques to isolate vegetation from background elements. Therefore, it is recommended that future studies explore the utility of other calibration and image

segmentation techniques to refine the accuracy and applicability of thermal imagery for precision crop monitoring.

- While EWT_{canopy} has proved a valuable indicator of taro water status, its destructive nature poses a limitation for continuous monitoring across the growing season as repeated destructive sampling can result in crop mortality, hence unsustainable for multi-temporal assessment. Additionally, future research should extend the scope of this study by investigating the influence of soil moisture content at various depths corresponding to the growth stages of taro tubers. Such an approach can provide a comprehensive understanding of water dynamics within smallholder taro farming systems, offering valuable insights into the interplay between soil moisture variability and crop water status.

- This study focused on quantifying the water status of rainfed taro crops planted in low densities and over high inter-row spacing, a characteristic of smallholder farming systems. Meanwhile, previous studies within this domain have extensively applied UAV thermal remote sensing for the crop water monitoring of high-density commercial irrigated crops such as maize, wheat and vineyards. While this research provides valuable contributions to advancing water status assessments of taro, its applicability to other tuber crops and varying farm settings remains largely unexplored. Further studies are needed to assess the utility of UAV thermal remote sensing for monitoring other tuber crops, including sweet potatoes, cassava and yams, under diverse soil types, climates, and management practices. Expanding the scope of research would enhance the generalisability of the findings and provide a foundation for scaling UAV applications to other NUS crop types and smallholder farming contexts.

- This study was conducted over a single growing season and primarily focused on major growth stages of taro, limiting its ability to capture the temporal variability of crop water status across seasons and intermediary growth stages. Seasonal fluctuations in water status, influenced by environmental conditions and crop development, play a critical role in understanding taro water dynamics. Therefore, future research should prioritise multi-seasonal studies that encompass the full spectrum of growth stages, facilitating the development of long-term water management strategies suitable for smallholder taro farming systems.

- Economic and regulatory barriers pose significant challenges to the broader adoption of UAV thermal remote sensing technologies within smallholder taro farms. High costs associated with UAVs equipped with thermal and multispectral cameras render them inaccessible to many smallholder farmers and researchers with limited budgets. Additionally, UAV operation requires specialised knowledge and adherence to stringent regulatory frameworks, such as those imposed by the South African Civil Aviation Authority (SACAA). These regulations necessitate costly and time-intensive training and certification processes, further restricting the use of UAVs in agricultural research and practice. Addressing these barriers requires capacity-building initiatives aimed at training farmers and researchers in UAV operation and data interpretation. Furthermore, the development of cost-effective platforms, such as real-time dashboards, could enable smallholder farmers to access actionable information on crop water status, fostering data-driven decision-making and improving farm-level water management.

Overall, this study contributes to advancing crop water status assessments, particularly within smallholder farming systems, by integrating cutting-edge UAV thermal remote sensing with advanced machine learning techniques. Focusing on neglected and underutilised taro crops, this study provides actionable solutions for enhancing the spatial and temporal monitoring of taro water variability, thereby informing water management strategies and ultimately improving crop productivity and yields in resource-constrained taro farming systems. The findings of this study further promote climate-smart agriculture and climate resilience, highlighting the importance of innovative technologies in addressing the multifaceted challenges posed by climate variability in agriculture. This study contributes to building adaptive capacities within smallholder farming communities, fostering sustainable agricultural practices that mitigate the impacts of water scarcity and ensuring the long-term viability of taro cultivation under changing climatic conditions. Moreover, these findings can assist policymakers and practitioners seeking to implement evidence-based strategies for sustainable water resource management and climate adaptation in smallholder agriculture. The study aligns with global and regional developmental goals, contributing to Sustainable Development Goal (SDG) 2: Zero Hunger by addressing food security challenges and promoting nutritional diversity through improved taro crop productivity, and SDG 13: Climate Action by enhancing the resilience of agricultural systems to climate-related shocks and stresses. Lastly, this research contributes to the African Union's Agenda 2063, particularly

Aspiration 1, Goal 5: Modern Agriculture for Increased Productivity and Production by leveraging modern cutting-edge technologies for transforming smallholder farming into robust, productive, and climate-resilient systems.

REFERENCES

Abd El-Aal, M., El-Anany, A. & Rizk, S. 2019. Rationalization of water consumption for taro plant through the rationing of irrigation and expand the plant ability to resist stress conditions. *International Journal of Plant & Soil Science,* 29(4)**,** 1-23.

Abdolrasol, M. G., Hussain, S. S., Ustun, T. S., Sarker, M. R., Hannan, M. A., Mohamed, R., Ali, J. A., Mekhilef, S. & Milad, A. 2021. Artificial neural networks based optimization techniques: A review. *Electronics,* 10(21)**,** 2689.

Aboutalebi, M., Torres-Rua, A. F., McKee, M., Kustas, W. P., Nieto, H., Alsina, M. M., White, A., Prueger, J. H., McKee, L., Alfieri, J., Hipps, L., Coopmans, C., Sanchez, L. & Dokoozlian, N. 2022. Downscaling UAV land surface temperature using a coupled wavelet-machine learning-optimization algorithm and its impact on evapotranspiration.

Abrahams, M., Sibanda, M., Dube, T., Chimonyo, V. G. & Mabhaudhi, T. 2023. A systematic review of UAV applications for mapping neglected and underutilised crop species' spatial distribution and health. *Remote Sensing,* 15(19)**,** 4672.

Acorsi, M. G. & Gimenez, L. M. 2021. Predicting Soil Water Content on Rainfed Maize through Aerial Thermal Imaging.

Ahmad, U., Alvino, A. & Marino, S. 2021. A review of crop water stress assessment using remote sensing. *Remote Sensing,* 13(20)**,** 4155.

Ahumada-Orellana, L., Ortega-Farías, S., Poblete-Echeverría, C. & Searles, P. S. 2019. Estimation of stomatal conductance and stem water potential threshold values for water stress in olive trees (cv. Arbequina). *Irrigation Science,* 37**,** 461-467.

Alexander, C., Deák, B. & Heilmeier, H. 2016. Micro-topography driven vegetation patterns in open mosaic landscapes. *Ecological indicators,* 60**,** 906-920.

Alexandris, S., Psomiadis, E., Proutsos, N., Philippopoulos, P., Charalampopoulos, I., Kakaletris, G., Papoutsi, E. M., Vassilakis, S. & Paraskevopoulos, A. 2021. Integrating drone technology into an innovative agrometeorological methodology for the precise and real-time estimation of crop water requirements.

Ali, A. & Imran, M. 2020. Evaluating the potential of red edge position (REP) of hyperspectral remote sensing data for real time estimation of LAI & chlorophyll content of kinnow mandarin (Citrus reticulata) fruit orchards. *Scientia Horticulturae,* 267**,** 109326.

Alimonti, C., Baiocchi, V., Spadaro, C. & Spadaro, R. 2020. Integration of UAV data with soil water balance models for evaluation/monitoring of maize water stress.

Allen, R., Irmak, A., Trezza, R., Hendrickx, J. M., Bastiaanssen, W. & Kjaersgaard, J. 2011. Satellite-based ET estimation in agriculture using SEBAL and METRIC. *Hydrological processes,* 25(26)**,** 4011-4027.

Antonaci, L., Demeke, M. & Vezzani, A. 2014. The challenges of managing agricultural price and production risks in sub-Saharan Africa.

Araújo-Paredes, C., Portela, F., Mendes, S. & Valín, M. I. 2022. Using Aerial Thermal Imagery to Evaluate Water Status in Vitis vinifera cv. Loureiro.

Aryal, J. P., Sapkota, T. B., Khurana, R., Khatri-Chhetri, A., Rahut, D. B. & Jat, M. L. 2020. Climate change and agriculture in South Asia: Adaptation options in smallholder production systems. *Environment, Development and Sustainability,* 22(6)**,** 5045-5075.

Awais, M., Li, W., Cheema, M., Zaman, Q., Shaheen, A., Aslam, B., Zhu, W., Ajmal, M., Faheem, M. & Hussain, S. 2022a. UAV-based remote sensing in plant stress imagine using high-resolution thermal sensor for digital agriculture practices: A meta-review. *International Journal of Environmental Science and Technology***,** 1-18.

Awais, M., Li, W., Cheema, M. J. M., Hussain, S., AlGarni, T. S., Liu, C. & Ali, A. 2021. Remotely sensed identification of canopy characteristics using UAV-based imagery under unstable environmental conditions.

Awais, M., Li, W., Hussain, S., Cheema, M. J. M., Li, W., Song, R. & Liu, C. 2022b. Comparative Evaluation of Land Surface Temperature Images from Unmanned Aerial Vehicle and Satellite Observation for Agricultural Areas Using In Situ Data.

Ayamga, M., Tekinerdogan, B. & Kassahun, A. 2021. Exploring the challenges posed by regulations for the use of drones in agriculture in the African context. *Land,* 10(2)**,** 164.

Badr, M., El-Tohamy, W. & Zaghloul, A. 2012. Yield and water use efficiency of potato grown under different irrigation and nitrogen levels in an arid region. *Agricultural Water Management,* 110**,** 9-15.

Ballester, C., Brinkhoff, J., Quayle, W. C. & Hornbuckle, J. 2019. Monitoring the effects of water stress in cotton using the green red vegetation index and red edge ratio. *Remote Sensing,* 11(7)**,** 873.

Baluja, J., Diago, M. P., Balda, P., Zorer, R., Meggio, F., Morales, F. & Tardaguila, J. 2012a. Assessment of vineyard water status variability by thermal and multispectral imagery using an unmanned aerial vehicle (UAV). *Irrigation Science,* 30**,** 511-522.

Baluja, J., Diago, M. P., Balda, P., Zorer, R., Meggio, F., Morales, F. & Tardaguila, J. 2012b. Assessment of vineyard water status variability by thermal and multispectral imagery using an unmanned aerial vehicle (UAV).

Barbedo, J. G. A. 2019. A review on the use of unmanned aerial vehicles and imaging sensors for monitoring and assessing plant stresses. *Drones,* 3(2)**,** 40.

Basile, A., Albrizio, R., Autovino, D., Bonfante, A., De Mascellis, R., Terribile, F. & Giorio, P. 2020. A modelling approach to discriminate contributions of soil hydrological properties and slope gradient to water stress in Mediterranean vineyards. *Agricultural Water Management,* 241**,** 106338.

Basukala, A. K., Oldenburg, C., Schellberg, J., Sultanov, M. & Dubovyk, O. 2017. Towards improved land use mapping of irrigated croplands: Performance assessment of different image classification algorithms and approaches. *European Journal of Remote Sensing,* 50(1)**,** 187-201.

Bayat, B., Van der Tol, C. & Verhoef, W. 2016. Remote sensing of grass response to drought stress using spectroscopic techniques and canopy reflectance model inversion. *Remote Sensing,* 8(7)**,** 557.

Bellvert, J., Zarco-Tejada, P. J., Girona, J. & Fereres, E. 2014. Mapping crop water stress index in a 'Pinot-noir'vineyard: comparing ground measurements with thermal remote sensing imagery from an unmanned aerial vehicle. *Precision agriculture,* 15**,** 361-376.

Berni, J. A. J., Zarco-Tejada, P. J., Sepulcre-Cantó, G., Fereres, E. & Villalobos, F. 2009a. Mapping canopy conductance and CWSI in olive orchards using high resolution thermal remote sensing imagery.

Berni, J. A. J., Zarco-Tejada, P. J., Suárez, L. & Fereres, E. 2009b. Thermal and narrowband multispectral remote sensing for vegetation monitoring from an unmanned aerial vehicle.

Bhatti, S., Heeren, D. M., Barker, J. B., Neale, C. M. U., Woldt, W. E., Maguire, M. S. & Rudnick, D. R. 2020. Site-specific irrigation management in a sub-humid climate using a spatial evapotranspiration model with satellite and airborne imagery.

Bian, J., Zhang, Z., Chen, J., Chen, H., Cui, C., Li, X., Chen, S. & Fu, Q. 2019. Simplified evaluation of cotton water stress using high resolution unmanned aerial vehicle thermal imagery.

Bouguettaya, A., Zarzour, H., Kechida, A. & Taberkit, A. M. 2022. Deep learning techniques to classify agricultural crops through UAV imagery: A review. *Neural Computing and Applications,* 34(12)**,** 9511-9536.

Brewer, K., Clulow, A., Sibanda, M., Gokool, S., Naiken, V. & Mabhaudhi, T. 2022a. Predicting the Chlorophyll Content of Maize over Phenotyping as a Proxy for Crop Health in Smallholder Farming Systems. *Remote Sensing,* 14(3)**,** 518.

Brewer, K., Clulow, A., Sibanda, M., Gokool, S., Odindi, J., Mutanga, O., Naiken, V., Chimonyo, V. G. & Mabhaudhi, T. 2022b. Estimation of maize foliar temperature and stomatal conductance as indicators of water stress based on optical and thermal imagery acquired using an unmanned aerial vehicle (UAV) platform. *Drones,* 6(7)**,** 169.

Brewer, K., Clulow, A., Sibanda, M., Gokool, S., Odindi, J., Mutanga, O., Naiken, V., Chimonyo, V. G. P. & Mabhaudhi, T. 2022c. Estimation of Maize Foliar Temperature and Stomatal Conductance as Indicators of Water Stress Based on Optical and Thermal Imagery Acquired Using an Unmanned Aerial Vehicle (UAV) Platform. *DRONES,* 6(7).

Buthelezi, S., Mutanga, O., Sibanda, M., Odindi, J., Clulow, A. D., Chimonyo, V. G. & Mabhaudhi, T. 2023. Assessing the prospects of remote sensing maize leaf area index using UAV-derived multi-spectral data in smallholder farms across the growing season. *Remote Sensing,* 15(6)**,** 1597.

Byambadorj, S.-O., Hernandez, J. O., Lkhagvasuren, S., Erma, G., Sharavdorj, K., Park, B. B. & Nyam-Osor, B. 2023. Leaf morpho-physiological traits of Populus sibirica and Ulmus pumila in different irrigation regimes and fertilizer types. *PeerJ,* 11**,** e16107.

Calderón, R., Navas-Cortés, J. A., Lucena, C. & Zarco-Tejada, P. J. 2013. High-resolution airborne hyperspectral and thermal imagery for early detection of Verticillium wilt of olive using fluorescence, temperature and narrow-band spectral indices.

Calicioglu, O., Flammini, A., Bracco, S., Bellù, L. & Sims, R. 2019. The future challenges of food and agriculture: An integrated analysis of trends and solutions. *Sustainability,* 11(1)**,** 222.

Camp, K. 1999. *The Bioresource Groups of KwaZulu-Natal: Mistbelt Including BRG 5: Moist Midlands Mistbelt, BRG 6: Dry Midlands Mistbelt, BRG 7: Northern Mistbelt, BRG 11: Moist Transitional Tall Grassveld*, KwaZulu-Natal Department of Agriculture.

Caruso, G., Palai, G., Tozzini, L. & Gucci, R. 2022. Using Visible and Thermal Images by an Unmanned Aerial Vehicle to Monitor the Plant Water Status, Canopy Growth and Yield of Olive Trees (cvs. Frantoio and Leccino) under Different Irrigation Regimes.

Cele, T. & Mudhara, M. 2024. Impacts of Crop Production and Value Chains on Household Food Insecurity in Kwazulu-Natal: An Ordered Probit Analysis. *Sustainability,* 16(2)**,** 700.

Chakona, G. & Mushangai, D. 2021. Understanding the food crises in southern Africa and the ways of transitioning the food systems to combat hunger. *Working paper. Centre for researching education and labour–university of the witwatersrand/environmental research learning centre–rhodes university.*

Chakraborty, M., Khot, L. R. & Peters, R. T. 2020. Assessing suitability of modified center pivot irrigation systems in corn production using low altitude aerial imaging techniques.

Chakraborty, S. & Newton, A. C. 2011. Climate change, plant diseases and food security: an overview. *Plant pathology,* 60(1)**,** 2-14.

Chan, J. Y.-L., Leow, S. M. H., Bea, K. T., Cheng, W. K., Phoong, S. W., Hong, Z.-W. & Chen, Y.-L. 2022. Mitigating the multicollinearity problem and its machine learning approach: a review. *Mathematics,* 10(8)**,** 1283.

Chauhan, V. B. S., Mallick, S. N., Mohapatra, P., Pati, K., Gowda, H., Arutselvan, R., Verma, A. K. & Nedunchezhiyan, M. 2024. Codification and description of phenological growth stages of taro (Colocasia esculenta var. antiquorum) according to the extended BBCH Scale. *Annals of Applied Biology,* 184(3)**,** 352-364.

Chávez, J. L., Zhang, H., Capurro, M. C., Masih, A. & Altenhofen, J. Year: Published. Evaluation of multispectral unmanned aerial systems for irrigation management.

Chen, A., Orlov-Levin, V., Elharar, O. & Meron, M. Year: Published. Comparing satellite and high-resolution visible and thermal aerial imaging of field crops for precision irrigation management and plant biomass forecast.

Chen, B., Han, M., Peng, K., Zhou, S., Shao, L., Wu, X., Wei, W., Liu, S., Li, Z. & Li, J. 2018. Global land-water nexus: Agricultural land and freshwater use embodied in worldwide supply chains. *Science of the Total Environment,* 613**,** 931-943.

Chen, J. M. 1996. Evaluation of vegetation indices and a modified simple ratio for boreal applications. *Canadian Journal of Remote Sensing,* 22(3)**,** 229-242.

Cheng, M., Jiao, X., Liu, Y., Shao, M., Yu, X., Bai, Y., Wang, Z., Wang, S., Tuohuti, N., Liu, S., Shi, L., Yin, D., Huang, X., Nie, C. & Jin, X. 2022. Estimation of soil moisture

content under high maize canopy coverage from UAV multimodal data and machine learning.

Cheng, M., Sun, C., Nie, C., Liu, S., Yu, X., Bai, Y., Liu, Y., Meng, L., Jia, X., Liu, Y., Zhou, L., Nan, F., Cui, T. & Jin, X. 2023. Evaluation of UAV-based drought indices for crop water conditions monitoring: A case study of summer maize. *Agricultural Water Management,* 287.

Chew, R., Rineer, J., Beach, R., O'Neil, M., Ujeneza, N., Lapidus, D., Miano, T., Hegarty-Craver, M., Polly, J. & Temple, D. S. 2020. Deep neural networks and transfer learning for food crop identification in UAV images. *Drones,* 4(1)**,** 7.

Chivasa, W., Mutanga, O. & Biradar, C. 2020. UAV-based multispectral phenotyping for disease resistance to accelerate crop improvement under changing climate conditions. *Remote Sensing,* 12(15)**,** 2445.

Chivenge, P., Mabhaudhi, T., Modi, A. T. & Mafongoya, P. 2015. The potential role of neglected and underutilised crop species as future crops under water scarce conditions in Sub-Saharan Africa. *International journal of environmental research and public health,* 12(6)**,** 5685-5711.

Chowdhury, M. S. 2023. Modelling hydrological factors from DEM using GIS. *MethodsX,* 10**,** 102062.

Clarke, R. 2014. Understanding the drone epidemic. *Computer Law & Security Review,* 30(3)**,** 230-246.

Clevers, J. G. & Gitelson, A. A. 2013. Remote estimation of crop and grass chlorophyll and nitrogen content using red-edge bands on Sentinel-2 and-3. *International Journal of Applied Earth Observation and Geoinformation,* 23**,** 344-351.

Colovic, M., Yu, K., Todorovic, M., Cantore, V., Hamze, M., Albrizio, R. & Stellacci, A. M. 2022. Hyperspectral vegetation indices to assess water and nitrogen status of sweet maize crop. *Agronomy,* 12(9)**,** 2181.

Costa, J., Egipto, R., Sánchez-Virosta, A., Lopes, C. & Chaves, M. 2019. Canopy and soil thermal patterns to support water and heat stress management in vineyards. *Agricultural Water Management,* 216**,** 484-496.

Costa, J. M., Grant, O. M. & Chaves, M. M. 2013. Thermography to explore plant–environment interactions. *Journal of experimental botany,* 64(13)**,** 3937-3949.

Costa, L., Kunwar, S., Ampatzidis, Y. & Albrecht, U. 2022. Determining leaf nutrient concentrations in citrus trees using UAV imagery and machine learning. *Precision agriculture***,** 1-22.

Cottrell, B., Kalacska, M., Arroyo-Mora, J.-P., Lucanus, O., Inamdar, D., Løke, T. & Soffer, R. J. 2024. Limitations of a Multispectral UAV Sensor for Satellite Validation and Mapping Complex Vegetation. *Remote Sensing,* 16(13)**,** 2463.

Cracknell, A. P. 2017. UAVs: regulations and law enforcement. *International Journal of Remote Sensing,* 38(8-10)**,** 3054-3067.

Crusiol, L. G. T., Nanni, M. R., Furlanetto, R. H., Sibaldelli, R. N. R., Cezar, E., Mertz-Henning, L. M., Nepomuceno, A. L., Neumaier, N. & Farias, J. R. B. 2020a. UAV-based thermal imaging in the assessment of water status of soybean plants.

Crusiol, L. G. T., Nanni, M. R., Furlanetto, R. H., Sibaldelli, R. N. R., Cezar, E., Mertz-Henning, L. M., Nepomuceno, A. L., Neumaier, N. & Farias, J. R. B. 2020b. UAV-based thermal imaging in the assessment of water status of soybean plants. *International Journal of Remote Sensing,* 41(9)**,** 3243-3265.

Dahal, K., Li, X.-Q., Tai, H., Creelman, A. & Bizimungu, B. 2019. Improving potato stress tolerance and tuber yield under a climate change scenario–a current overview. *Frontiers in plant science,* 10**,** 563.

Danson, F. M. & Bowyer, P. 2004. Estimating live fuel moisture content from remotely sensed reflectance. *Remote Sensing of Environment,* 92(3)**,** 309-321.

Daryanto, S., Wang, L. & Jacinthe, P.-A. 2017. Global synthesis of drought effects on cereal, legume, tuber and root crops production: A review. *Agricultural Water Management,* 179**,** 18-33.

Das, K. 2024. Traditional Agronomic Practices: Understanding and Mitigating the Risks of Climate Change. *Recent Advancements in Sustainable Agricultural Practices: Harnessing Technology for Water Resources, Irrigation and Environmental Management.* Springer.

Das, S., Christopher, J., Apan, A., Choudhury, M. R., Chapman, S., Menzies, N. W. & Dang, Y. P. 2021a. Evaluation of water status of wheat genotypes to aid prediction of yield on sodic soils using UAV-thermal imaging and machine learning.

Das, S., Christopher, J., Apan, A., Roy Choudhury, M., Chapman, S., Menzies, N. W. & Dang, Y. P. 2021b. UAV-Thermal imaging and agglomerative hierarchical clustering

techniques to evaluate and rank physiological performance of wheat genotypes on sodic soil.

Das, S., Christopher, J., Roy Choudhury, M., Apan, A., Chapman, S., Menzies, N. W. & Dang, Y. P. 2022. Evaluation of drought tolerance of wheat genotypes in rain-fed sodic soil environments using high-resolution UAV remote sensing techniques.

Dathe, A., Fleisher, D., Timlin, D., Fisher, J. & Reddy, V. 2014. Modeling potato root growth and water uptake under water stress conditions. *Agricultural and Forest Meteorology,* 194**,** 37-49.

Daughtry, C. S., Walthall, C., Kim, M., De Colstoun, E. B. & McMurtrey Iii, J. 2000. Estimating corn leaf chlorophyll concentration from leaf and canopy reflectance. *Remote sensing of Environment,* 74(2)**,** 229-239.

de Melo, L. L., de Melo, V. G. M. L., Marques, P. A. A., Frizzone, J. A., Coelho, R. D., Romero, R. A. F. & da Silva Barros, T. H. 2022. Deep learning for identification of water deficits in sugarcane based on thermal images. *Agricultural Water Management,* 272**,** 107820.

Deepan, P. & Sudha, L. 2020. Object classification of remote sensing image using deep convolutional neural network. *The cognitive approach in cloud computing and internet of things technologies for surveillance tracking systems.* Elsevier.

DeJonge, K. C., Taghvaeian, S., Trout, T. J. & Comas, L. H. 2015. Comparison of canopy temperature-based water stress indices for maize. *Agricultural water management,* 156**,** 51-62.

Delavarpour, N., Koparan, C., Nowatzki, J., Bajwa, S. & Sun, X. 2021. A technical study on UAV characteristics for precision agriculture applications and associated practical challenges. *Remote Sensing,* 13(6)**,** 1204.

Delegido, J., Vergara, C., Verrelst, J., Gandía, S. & Moreno, J. 2011. Remote Estimation of Crop Chlorophyll Content by Means of High-Spectral-Resolution Reflectance Techniques. *Agronomy journal,* 103(6)**,** 1834-1842.

Delogu, E., Boulet, G., Olioso, A., Garrigues, S., Brut, A., Tallec, T., Demarty, J., Soudani, K. & Lagouarde, J.-P. 2018. Evaluation of the SPARSE dual-source model for predicting water stress and evapotranspiration from thermal infrared data over multiple crops and climates. *Remote Sensing,* 10(11)**,** 1806.

Din, M. S. U., Mubeen, M., Hussain, S., Ahmad, A., Hussain, N., Ali, M. A., El Sabagh, A., Elsabagh, M., Shah, G. M. & Qaisrani, S. A. 2022a. World nations priorities on climate

change and food security. *Building climate resilience in agriculture: theory, practice and future perspective***,** 365-384.

Din, M. S. U., Mubeen, M., Hussain, S., Ahmad, A., Hussain, N., Ali, M. A., Sabagh, A. E., Elsabagh, M., Shah, G. M. & Qaisrani, S. A. 2022b. World nations priorities on climate change and food security. *Building Climate Resilience in Agriculture.* Springer.

Dinar, A., Tieu, A. & Huynh, H. 2019. Water scarcity impacts on global food production. *Global Food Security,* 23**,** 212-226.

Ebhuoma, E. E., Donkor, F. K., Ebhuoma, O. O., Leonard, L. & Tantoh, H. B. 2020. Subsistence farmers' differential vulnerability to drought in Mpumalanga province, South Africa: Under the political ecology spotlight. *Cogent Social Sciences,* 6(1)**,** 1792155.

Ekinzog, E. K., Schlerf, M., Kraft, M., Werner, F., Riedel, A., Rock, G. & Mallick, K. 2022. Revisiting crop water stress index based on potato field experiments in Northern Germany. *Agricultural Water Management,* 269.

El-Hendawy, S. E., Al-Suhaibani, N. A., Elsayed, S., Hassan, W. M., Dewir, Y. H., Refay, Y. & Abdella, K. A. 2019. Potential of the existing and novel spectral reflectance indices for estimating the leaf water status and grain yield of spring wheat exposed to different irrigation rates. *Agricultural Water Management,* 217**,** 356-373.

Elsayed, S., Elhoweity, M., Ibrahim, H. H., Dewir, Y. H., Migdadi, H. M. & Schmidhalter, U. 2017. Thermal imaging and passive reflectance sensing to estimate the water status and grain yield of wheat under different irrigation regimes. *Agricultural Water Management,* 189**,** 98-110.

Elsayed, S., Rischbeck, P. & Schmidhalter, U. 2015. Comparing the performance of active and passive reflectance sensors to assess the normalized relative canopy temperature and grain yield of drought-stressed barley cultivars. *Field Crops Research,* 177**,** 148-160.

Elsherbiny, O., Zhou, L., Feng, L. & Qiu, Z. 2021. Integration of visible and thermal imagery with an artificial neural network approach for robust forecasting of canopy water content in rice. *Remote Sensing,* 13(9)**,** 1785.

Espinoza, C. Z., Khot, L. R., Sankaran, S. & Jacoby, P. W. 2017. High resolution multispectral and thermal remote sensing-based water stress assessment in subsurface irrigated grapevines.

Falcon, W. P., Naylor, R. L. & Shankar, N. D. 2022. Rethinking global food demand for 2050. *Population and Development Review,* 48(4)**,** 921-957.

Ferdaus, M. J., Chukwu-Munsen, E., Foguel, A. & da Silva, R. C. 2023. Taro roots: An underexploited root crop. *Nutrients,* 15(15)**,** 3337.

Fukai, S. & Mitchell, J. 2022. Role of canopy temperature depression in rice. *Crop and Environment*.

Gago, J., Douthe, C., Coopman, R., Gallego, P., Ribas-Carbo, M., Flexas, J., Escalona, J. & Medrano, H. 2015. UAVs challenge to assess water stress for sustainable agriculture. *Agricultural water management,* 153**,** 9-19.

Gago, J., Fernie, A. R., Nikoloski, Z., Tohge, T., Martorell, S., Escalona, J. M., Ribas-Carbo, M., Flexas, J. & Medrano, H. 2017a. Integrative field scale phenotyping for investigating metabolic components of water stress within a vineyard. *Plant Methods,* 13**,** 1-14.

Gago, J., Fernie, A. R., Nikoloski, Z., Tohge, T., Martorell, S., Escalona, J. M., Ribas-Carbó, M., Flexas, J. & Medrano, H. 2017b. Integrative field scale phenotyping for investigating metabolic components of water stress within a vineyard.

Gamon, J., Penuelas, J. & Field, C. 1992. A narrow-waveband spectral index that tracks diurnal changes in photosynthetic efficiency. *Remote Sensing of environment,* 41(1)**,** 35-44.

Ganesan, S. P., Bordoloi, S., Cai, W., Garg, A., Sekharan, S. & Sahoo, L. 2024. Effect of soil type on tipping point hydrological requirements for Axonopus compressus grass under extreme drought stress. *Science of The Total Environment***,** 175928.

Gao, B.-C. 1996. NDWI—A normalized difference water index for remote sensing of vegetation liquid water from space. *Remote sensing of environment,* 58(3)**,** 257-266.

Gao, C., Liu, S., Wu, P., Wang, Y., Wu, K., Li, L., Wang, J., Liu, S., Gao, P. & Zhao, Z. 2024. Estimation of Canopy Water Content by Integrating Hyperspectral and Thermal Imagery in Winter Wheat Fields. *Agronomy,* 14(11)**,** 2569.

García-Tejero, I., Costa, J., Egipto, R., Durán-Zuazo, V., Lima, R., Lopes, C. & Chaves, M. 2016. Thermal data to monitor crop-water status in irrigated Mediterranean viticulture. *Agricultural Water Management,* 176**,** 80-90.

García-Tejero, I., Rubio, A., Viñuela, I., Hernández, A., Gutiérrez-Gordillo, S., Rodríguez-Pleguezuelo, C. & Durán-Zuazo, V. 2018. Thermal imaging at plant level to assess the crop-water status in almond trees (cv. Guara) under deficit irrigation strategies. *Agricultural water management,* 208**,** 176-186.

Garg, A. & Tai, K. 2013. Comparison of statistical and machine learning methods in modelling of data with multicollinearity. *International Journal of Modelling, Identification and Control,* 18(4)**,** 295-312.

Gerhards, M., Schlerf, M., Mallick, K. & Udelhoven, T. 2019. Challenges and future perspectives of multi-/Hyperspectral thermal infrared remote sensing for crop water-stress detection: A review. *Remote Sensing,* 11(10)**,** 1240.

Ghosh, A., Kumar, A. & Biswas, G. 2024. Exponential population growth and global food security: challenges and alternatives. *Bioremediation of Emerging Contaminants from Soils.* Elsevier.

Gitelson, A. & Merzlyak, M. N. 1994. Spectral reflectance changes associated with autumn senescence of Aesculus hippocastanum L. and Acer platanoides L. leaves. Spectral features and relation to chlorophyll estimation. *Journal of plant physiology,* 143(3)**,** 286-292.

Gitelson, A. A., Gritz, Y. & Merzlyak, M. N. 2003. Relationships between leaf chlorophyll content and spectral reflectance and algorithms for non-destructive chlorophyll assessment in higher plant leaves. *Journal of plant physiology,* 160(3)**,** 271-282.

Gitelson, A. A., Keydan, G. P. & Merzlyak, M. N. 2006. Three-band model for noninvasive estimation of chlorophyll, carotenoids, and anthocyanin contents in higher plant leaves. *Geophysical research letters,* 33(11).

Gokool, S., Mahomed, M., Brewer, K., Naiken, V., Clulow, A., Sibanda, M. & Mabhaudhi, T. 2024. Crop mapping in smallholder farms using unmanned aerial vehicle imagery and geospatial cloud computing infrastructure. *Heliyon,* 10(5).

Gomez-Zavaglia, A., Mejuto, J. C. & Simal-Gandara, J. 2020. Mitigation of emerging implications of climate change on food production systems. *Food Research International,* 134**,** 109256.

Gomez y Paloma, S., Riesgo, L. & Louhichi, K. 2020. *The Role of Smallholder Farms in Food and Nutrition Security*, Springer Nature.

Gonzalez-Dugo, V., Zarco-Tejada, P., Nicolás, E., Nortes, P. A., Alarcón, J. J., Intrigliolo, D. S. & Fereres, E. 2013. Using high resolution UAV thermal imagery to assess the variability in the water status of five fruit tree species within a commercial orchard.

Gonzalez-Dugo, V., Zarco-Tejada, P. J. & Fereres, E. 2014. Applicability and limitations of using the crop water stress index as an indicator of water deficits in citrus orchards. *Agricultural and Forest Meteorology,* 198-199**,** 94-104.

Gouveia, C. S., Ganança, J. F., de Nóbrega, H. G., de Freitas, J. G., Lebot, V. & Pinheiro de Carvalho, M. A. 2020. Phenotypic flexibility and drought avoidance in taro (Colocasia esculenta (L.) Schott).

Gracia-Romero, A., Kefauver, S. C., Fernandez-Gallego, J. A., Vergara-Díaz, O., Nieto-Taladriz, M. T. & Araus, J. L. 2019a. UAV and ground image-based phenotyping: A proof of concept with durum wheat. *Remote sensing,* 11(10)**,** 1244.

Gracia-Romero, A., Kefauver, S. C., Fernandez-Gallego, J. A., Vergara-Díaz, O., Nieto-Taladriz, M. T. & Araus, J. L. 2019b. UAV and ground image-based phenotyping: A proof of concept with durum wheat.

Guan, Y. & Grote, K. 2023. Assessing the Potential of UAV-Based Multispectral and Thermal Data to Estimate Soil Water Content Using Geophysical Methods. *Remote Sensing,* 16(1)**,** 61.

Guimarães, N., Sousa, J. J., Couto, P., Bento, A. & Pádua, L. 2024. Combining UAV-Based Multispectral and Thermal Infrared Data with Regression Modeling and SHAP Analysis for Predicting Stomatal Conductance in Almond Orchards. *Remote Sensing,* 16(13)**,** 1-19.

Gunawardena, A., Nissanka, S., Dayawansa, N. & Fernando, T. 2015. Estimation of above ground biomass in Horton Plains National Park, Sri Lanka using Optical, thermal and RADAR remote sensing data.

Guo, Z., Zhang, K., Lin, H., Majcher, B. M., Lee, C. K., Still, C. J. & Wu, J. 2023. Plant canopies exhibit stronger thermoregulation capability at the seasonal than diurnal timescales. *Agricultural and Forest Meteorology,* 339**,** 109582.

Haboudane, D., Miller, J. R., Tremblay, N., Zarco-Tejada, P. J. & Dextraze, L. 2002. Integrated narrow-band vegetation indices for prediction of crop chlorophyll content for application to precision agriculture. *Remote sensing of environment,* 81(2-3)**,** 416-426.

Haerussana, A. N. E. M., Ayuhastuti, A., Yuniar, S. F., Bustami, H. A. & Widyastiwi, W. 2022. Taro (Colosia esculenta) Leaves Extract Inhibits Streptococcus mutans ATCC 31987. *Borneo Journal of Pharmacy,* 5(3)**,** 268-278.

Hamuda, E., Glavin, M. & Jones, E. 2016. A survey of image processing techniques for plant extraction and segmentation in the field. *Computers and electronics in agriculture,* 125**,** 184-199.

Han, M., Zhang, H., DeJonge, K. C., Comas, L. H. & Trout, T. J. 2016. Estimating maize water stress by standard deviation of canopy temperature in thermal imagery. *Agricultural Water Management,* 177**,** 400-409.

Han, X., Thomasson, J. A., Swaminathan, V., Wang, T., Siegfried, J., Raman, R., Rajan, N. & Neely, H. 2020. Field-based calibration of unmanned aerial vehicle thermal infrared imagery with temperature-controlled references.

Han, Y., Tarakey, B. A., Hong, S. J., Kim, S. Y., Kim, E., Lee, C. H. & Kim, G. 2021. Calibration and Image Processing of Aerial Thermal Image for UAV Application in Crop Water Stress Estimation.

Hassanpanah, D. & Khorshidi Benam, M. Year: Published. Study of Thermal Different Thresholds on Different Potatoe Cultivers' Tuber Growth in Ardebil Region *III Balkan Symposium on Vegetables and Potatoes 729*. 221-225.

Hefferon, K. L. 2015. Nutritionally enhanced food crops; progress and perspectives. *International journal of molecular sciences,* 16(2)**,** 3895-3914.

Hernández-Hernández, J. L., García-Mateos, G., González-Esquiva, J., Escarabajal-Henarejos, D., Ruiz-Canales, A. & Molina-Martínez, J. M. 2016. Optimal color space selection method for plant/soil segmentation in agriculture. *Computers and Electronics in Agriculture,* 122**,** 124-132.

Hilary van Wyk, R. & Oscar Amonsou, E. 2021. Physiochemical and functional properties of albumin and globulin from amadumbe (Colocasia esculenta) corms. *Food Science and Technology*.

Hlophe-Ginindza, S. N. & Mpandeli, N. 2020. The role of small-scale farmers in ensuring food security in Africa. *Food Security in Africa***,** 1-12.

Hodgkinson, D. & Johnston, R. 2018. *Aviation law and drones: Unmanned aircraft and the future of aviation*, Routledge.

Hoffmann, H., Jensen, R., Thomsen, A., Nieto, H., Rasmussen, J. & Friborg, T. 2016a. Crop water stress maps for an entire growing season from visible and thermal UAV imagery.

Hoffmann, H., Jensen, R., Thomsen, A., Nieto, H., Rasmussen, J. & Friborg, T. 2016b. Crop water stress maps for an entire growing season from visible and thermal UAV imagery. *Biogeosciences,* 13(24)**,** 6545-6563.

Hoffmann, H., Nieto, H., Jensen, R., Guzinski, R., Zarco-Tejada, P. & Friborg, T. 2016c. Estimating evaporation with thermal UAV data and two-source energy balance models.

Hou, M., Tian, F., Ortega-Farias, S., Riveros-Burgos, C., Zhang, T. & Lin, A. 2021. Estimation of crop transpiration and its scale effect based on ground and UAV thermal infrared remote sensing images.

Hou, M., Tian, F., Zhang, L., Li, S., Du, T., Huang, M. & Yuan, Y. 2018. Estimating crop transpiration of soybean under different irrigation treatments using thermal infrared remote sensing imagery. *Agronomy,* 9(1)**,** 8.

Huang, C.-y., Wei, H.-L., Rau, J.-Y. & Jhan, J.-P. 2019. Use of principal components of UAV-acquired narrow-band multispectral imagery to map the diverse low stature vegetation fAPAR. *GIScience & remote sensing,* 56(4)**,** 605-623.

Huang, Z., Liu, Y., Tian, F.-P. & Wu, G.-L. 2020. Soil water availability threshold indicator was determined by using plant physiological responses under drought conditions. *Ecological Indicators,* 118**,** 106740.

Huete, A., Didan, K., Miura, T., Rodriguez, E. P., Gao, X. & Ferreira, L. G. 2002. Overview of the radiometric and biophysical performance of the MODIS vegetation indices. *Remote sensing of environment,* 83(1-2)**,** 195-213.

Huete, A. R. 1988. A soil-adjusted vegetation index (SAVI). *Remote sensing of environment,* 25(3)**,** 295-309.

Hunt Jr, E. R., Doraiswamy, P. C., McMurtrey, J. E., Daughtry, C. S., Perry, E. M. & Akhmedov, B. 2013. A visible band index for remote sensing leaf chlorophyll content at the canopy scale. *International journal of applied earth observation and Geoinformation,* 21**,** 103-112.

Hussain, S., Gao, K., Din, M., Gao, Y., Shi, Z. & Wang, S. 2020. Assessment of UAV-Onboard Multispectral Sensor for non-destructive site-specific rapeseed crop phenotype variable at different phenological stages and resolutions. *Remote Sensing,* 12(3)**,** 397.

Hutton, J., Lipa, G., Baustian, D., Sulik, J. & Bruce, R. 2020a. High accuracy direct georeferencing of the Altum multi-spectral UAV camera and its application to high throughput plant phenotyping. *The International Archives of Photogrammetry, Remote Sensing and Spatial Information Sciences,* 43**,** 451-456.

Hutton, J., Lipa, G., Baustian, D., Sulik, J. & Bruce, R. 2020b. High accuracy direct georeferencing of the Altum multi-spectral UAV camera and its application to high throughput plant phenotyping. *The International Archives of the Photogrammetry, Remote Sensing and Spatial Information Sciences,* 43**,** 451-456.

Idso, S., Jackson, R., Pinter Jr, P., Reginato, R. & Hatfield, J. 1981. Normalizing the stress-degree-day parameter for environmental variability. *Agricultural meteorology,* 24**,** 45-55.

Ihuoma, S. O. & Madramootoo, C. A. 2017. Recent advances in crop water stress detection. *Computers and Electronics in Agriculture,* 141**,** 267-275.

Ihuoma, S. O. & Madramootoo, C. A. 2019. Sensitivity of spectral vegetation indices for monitoring water stress in tomato plants. *Computers and Electronics in Agriculture,* 163**,** 104860.

Ishimwe, R., Abutaleb, K. & Ahmed, F. 2014. Applications of thermal imaging in agriculture—A review. *Advances in remote Sensing,* 3(03)**,** 128.

Jones, H. G. 1999. Use of infrared thermometry for estimation of stomatal conductance as a possible aid to irrigation scheduling. *Agricultural and forest meteorology,* 95(3)**,** 139-149.

Joshi, B. K., Shrestha, R., Gauchan, D. & Shrestha, A. 2020. Neglected, underutilized, and future smart crop species in Nepal. *Journal of Crop Improvement,* 34(3)**,** 291-313.

Kang, J., Hao, X., Zhou, H. & Ding, R. 2021. An integrated strategy for improving water use efficiency by understanding physiological mechanisms of crops responding to water deficit: Present and prospect. *Agricultural Water Management,* 255**,** 107008.

Kapari, M., Hlophe-Ginindza, S., Nhamo, L. & Mpandeli, S. 2023. Contribution of smallholder farmers to food security and opportunities for resilient farming systems. *Frontiers in Sustainable Food Systems,* 7**,** 1149854.

Kapari, M., Sibanda, M., Magidi, J., Mabhaudhi, T., Mpandeli, S. & Nhamo, L. 2025. Assessment of the Maize Crop Water Stress Index (CWSI) Using Drone-Acquired Data Across Different Phenological Stages. *Drones,* 9(3)**,** 192.

Kapari, M., Sibanda, M., Magidi, J., Mabhaudhi, T., Nhamo, L. & Mpandeli, S. 2024. Comparing Machine Learning Algorithms for Estimating the Maize Crop Water Stress Index (CWSI) Using UAV-Acquired Remotely Sensed Data in Smallholder Croplands. *Drones,* 8(2)**,** 61.

Kapoor, B., Singh, S. & Kumar, P. 2022. Taro (Colocasia esculenta): Zero wastage orphan food crop for food and nutritional security. *South African Journal of Botany,* 145**,** 157-169.

Kashyap, P. & Panda, R. 2003. Effect of irrigation scheduling on potato crop parameters under water stressed conditions. *Agricultural water management,* 59(1)**,** 49-66.

Katsigiannis, P., Misopolinos, L., Liakopoulos, V., Alexandridis, T. K. & Zalidis, G. Year: Published. An autonomous multi-sensor UAV system for reduced-input precision agriculture applications.

Katuwal, K. B., Yang, H. & Huang, B. 2023. Evaluation of phenotypic and photosynthetic indices to detect water stress in perennial grass species using hyperspectral, multispectral and chlorophyll fluorescence imaging. *Grass Research,* 3(1).

Kephe, P. N., Ayisi, K. K. & Petja, B. M. 2021a. Challenges and opportunities in crop simulation modelling under seasonal and projected climate change scenarios for crop production in South Africa. *Agriculture & Food Security,* 10**,** 1-24.

Kephe, P. N., Ayisi, K. K. & Petja, B. M. 2021b. Challenges and opportunities in crop simulation modelling under seasonal and projected climate change scenarios for crop production in South Africa. *Agriculture & Food Security,* 10(1)**,** 1-24.

Khanal, S., Fulton, J. & Shearer, S. 2017. An overview of current and potential applications of thermal remote sensing in precision agriculture. *Computers and Electronics in Agriculture,* 139**,** 22-32.

Kim, Y.-U. & Lee, B.-W. 2019. Differential mechanisms of potato yield loss induced by high day and night temperatures during tuber initiation and bulking: photosynthesis and tuber growth. *Frontiers in Plant Science,* 10**,** 300.

Kogan, F. N. 1995. Application of vegetation index and brightness temperature for drought detection. *Advances in space research,* 15(11)**,** 91-100.

Kpienbaareh, D., Sun, X., Wang, J., Luginaah, I., Bezner Kerr, R., Lupafya, E. & Dakishoni, L. 2021. Crop type and land cover mapping in northern Malawi using the integration of sentinel-1, sentinel-2, and planetscope satellite data. *Remote Sensing,* 13(4)**,** 700.

Krishna, G., Sahoo, R. N., Singh, P., Bajpai, V., Patra, H., Kumar, S., Dandapani, R., Gupta, V. K., Viswanathan, C. & Ahmad, T. 2019. Comparison of various modelling approaches for water deficit stress monitoring in rice crop through hyperspectral remote sensing. *Agricultural Water Management,* 213**,** 231-244.

Krishna, G., Sahoo, R. N., Singh, P., Patra, H., Bajpai, V., Das, B., Kumar, S., Dhandapani, R., Vishwakarma, C. & Pal, M. 2021. Application of thermal imaging and hyperspectral remote sensing for crop water deficit stress monitoring. *Geocarto International,* 36(5)**,** 481-498.

Kullberg, E. G., DeJonge, K. C. & Chávez, J. L. 2017. Evaluation of thermal remote sensing indices to estimate crop evapotranspiration coefficients. *Agricultural water management,* 179**,** 64-73.

Kumar, C., Mubvumba, P., Huang, Y., Dhillon, J. & Reddy, K. 2023. Multi-stage corn yield prediction using high-resolution UAV multispectral data and machine learning models. *Agronomy,* 13(5)**,** 1277.

Kumar, S., Roshni, T., Kahya, E. & Ghorbani, M. A. 2020. Climate change projections of rainfall and its impact on the cropland suitability for rice and wheat crops in the Sone river command, Bihar. *Theoretical and Applied Climatology,* 142(1)**,** 433-451.

Kumari, V. V., Banerjee, P., Verma, V. C., Sukumaran, S., Chandran, M. A. S., Gopinath, K. A., Venkatesh, G., Yadav, S. K., Singh, V. K. & Awasthi, N. K. 2022. Plant nutrition: An effective way to alleviate abiotic stress in agricultural crops. *International Journal of Molecular Sciences,* 23(15)**,** 8519.

Kunz, R., Reddy, K., Mthembu, T., Lake, S., Mabhaudhi, T., Chimonyo, V. & Naiken, V. 2024a. CROP AND NUTRITIONAL WATER PRODUCTIVITY OF SWEET POTATO AND TARO.

Kunz, R., Reddy, K., Mthembu, T., Lake, S., Mabhaudhi, T., Chimonyo, V. & Naiken, V. 2024b. Crop and Nutritional Water Productivity of Sweet Potato and Taro

Lacerda, L. N., Snider, J. L., Cohen, Y., Liakos, V., Gobbo, S. & Vellidis, G. 2022. Using UAV-based thermal imagery to detect crop water status variability in cotton.

Lal, M. K., Tiwari, R. K., Kumar, A., Dey, A., Kumar, R., Kumar, D., Jaiswal, A., Changan, S. S., Raigond, P. & Dutt, S. 2022. Mechanistic concept of physiological, biochemical, and molecular responses of the potato crop to heat and drought stress. *Plants,* 11(21)**,** 2857.

Lee, D. H. & Park, J. H. Year: Published. Comparison between NDVI and CWSI for waxy corn growth monitoring in field soil conditions.

Lee, H., Calvin, K., Dasgupta, D., Krinner, G., Mukherji, A., Thorne, P., Trisos, C., Romero, J., Aldunce, P. & Barret, K. 2023. IPCC, 2023: Climate Change 2023: Synthesis Report, Summary for Policymakers. Contribution of Working Groups I, II and III to the Sixth Assessment Report of the Intergovernmental Panel on Climate Change [Core Writing Team, H. Lee and J. Romero (eds.)]. IPCC, Geneva, Switzerland.

Lewu, M. N., Mulidzi, A. R., Gerrano, A. S. & Adebola, P. O. 2017. Comparative growth and yield of taro (Colocasia esculenta) accessions cultivated in the Western Cape, South Africa. *International Journal of Agriculture and Biology,* 19(3).

Li, H., Wang, Y., Fan, K., Mao, Y., Shen, Y. & Ding, Z. 2022a. Evaluation of important phenotypic parameters of tea plantations using multi-source remote sensing data.

Li, J., Schachtman, D. P., Creech, C. F., Wang, L., Ge, Y. & Shi, Y. 2022b. Evaluation of UAV-derived multimodal remote sensing data for biomass prediction and drought tolerance assessment in bioenergy sorghum.

Li, Q., Gao, M. & Li, Z.-L. 2022c. Ground hyper-spectral remote-sensing monitoring of wheat water stress during different growing stages. *Agronomy,* 12(10)**,** 2267.

Li, W., Liu, C., Yang, Y., Awais, M., Li, W., Ying, P., Ru, W. & Cheema, M. 2022d. A UAV-aided prediction system of soil moisture content relying on thermal infrared remote sensing. *International Journal of Environmental Science and Technology,* 19(10)**,** 9587-9600.

Li, W., Liu, C., Yang, Y., Awais, M., Li, W., Ying, P., Ru, W. & Cheema, M. J. M. 2022e. A UAV-aided prediction system of soil moisture content relying on thermal infrared remote sensing.

Li, X. & Siddique, K. H. 2018. Future smart food. *Rediscovering hidden treasures of neglected and underutilized species for Zero Hunger in Asia, Bangkok*.

Liakos, K. G., Busato, P., Moshou, D., Pearson, S. & Bochtis, D. 2018. Machine learning in agriculture: A review. *Sensors,* 18(8)**,** 2674.

Liao, L., Li, H., Shang, W. & Ma, L. 2022. An empirical study of the impact of hyperparameter tuning and model optimization on the performance properties of deep neural networks. *ACM Transactions on Software Engineering and Methodology (TOSEM),* 31(3)**,** 1-40.

Ling, Q., Huang, W. & Jarvis, P. 2011. Use of a SPAD-502 meter to measure leaf chlorophyll concentration in Arabidopsis thaliana. *Photosynthesis research,* 107(2)**,** 209-214.

Liu, C., Liu, Y., Lu, Y., Liao, Y., Nie, J., Yuan, X. & Chen, F. 2019. Use of a leaf chlorophyll content index to improve the prediction of above-ground biomass and productivity. *PeerJ,* 6**,** e6240.

Liu, N., Deng, Z., Wang, H., Luo, Z., Gutiérrez-Jurado, H. A., He, X. & Guan, H. 2020. Thermal remote sensing of plant water stress in natural ecosystems. *Forest Ecology and Management,* 476**,** 118433.

Liu, Q., Wu, Z., Cui, N., Zheng, S., Jiang, S., Wang, Z., Gong, D., Wang, Y., Zhao, L. & Wei, R. 2025. Estimating stomatal conductance of citrus orchard based on UAV multi-modal information in Southwest China. *Agricultural Water Management,* 307**,** 109253.

Lu, B. & He, Y. 2017. Species classification using Unmanned Aerial Vehicle (UAV)-acquired high spatial resolution imagery in a heterogeneous grassland. *ISPRS Journal of Photogrammetry and Remote Sensing,* 128**,** 73-85.

Lu, S., Xuan, J., Zhang, T., Bai, X., Tian, F. & Ortega-Farias, S. 2022a. Effect of the Shadow Pixels on Evapotranspiration Inversion of Vineyard: A High-Resolution UAV-Based and Ground-Based Remote Sensing Measurements.

Lu, Y., Young, S., Wang, H. & Wijewardane, N. 2022b. Robust plant segmentation of color images based on image contrast optimization. *Computers and Electronics in Agriculture,* 193**,** 106711.

Luan, X. & Vico, G. 2021. Canopy temperature and heat stress are increased by compound high air temperature and water stress and reduced by irrigation–a modeling analysis. *Hydrology and Earth System Sciences,* 25(3)**,** 1411-1423.

Lumumba, V. W., Kiprotich, D., Makena, N., Kavita, M. & Mpaine, M. 2024. Comparative Analysis of Cross-Validation Techniques: LOOCV, K-Folds Cross-Validation, and Repeated K-Folds Cross-Validation in Machine Learning Models. *Am. J. Theor. Appl. Stat,* 13**,** 127-137.

Luo QunYing, L. Q. 2011. Temperature thresholds and crop production: a review. *Climate Change,* 109(3/4)**,** 583-598.

Mabhaudhi, T., Chibarabada, T. P., Chimonyo, V. G. P., Murugani, V. G., Pereira, L. M., Sobratee, N., Govender, L., Slotow, R. & Modi, A. T. 2018. Mainstreaming underutilized indigenous and traditional crops into food systems: A South African perspective. *Sustainability,* 11(1)**,** 172.

Mabhaudhi, T., Chimonyo, V. G., Chibarabada, T. P. & Modi, A. T. 2017a. Developing a roadmap for improving neglected and underutilized crops: A case study of South Africa. *Frontiers in plant science,* 8**,** 2143.

Mabhaudhi, T., Chimonyo, V. G. & Modi, A. T. 2017b. Status of underutilised crops in South Africa: Opportunities for developing research capacity. *Sustainability,* 9(9)**,** 1569.

Mabhaudhi, T. & Modi, A. 2015. Drought tolerance of selected South African taro (Colocasia esculenta L. Schott) landraces. *Experimental Agriculture,* 51(3)**,** 451-466.

Mabhaudhi, T. & Modi, A. Year: Published. Yield response of selected taro (Colocasia esculenta) landraces from South Africa to irrigated and rain-fed field conditions. *3rd International conference on neglected*. 8.

Mabhaudhi, T., Modi, A. & Beletse, Y. Year: Published. Growth response of selected taro [Colocasia esculenta (L.) schott] landraces to water stress. *II International Symposium on Underutilized Plant Species: Crops for the Future-Beyond Food Security 979*. 327-334.

Mabhaudhi, T., Modi, A. & Beletse, Y. 2013. Response of taro (Colocasia esculenta L. Schott) landraces to varying water regimes under a rainshelter. *Agricultural water management,* 121**,** 102-112.

Mabhaudhi, T., Modi, A. T. & Beletse, Y. G. 2014. Parameterisation and evaluation of the FAO-AquaCrop model for a South African taro (Colocasia esculenta L. Schott) landrace. *Agricultural and Forest Meteorology,* 192**,** 132-139.

Maes, W. & Steppe, K. 2012. Estimating evapotranspiration and drought stress with ground-based thermal remote sensing in agriculture: a review. *Journal of experimental botany,* 63(13)**,** 4671-4712.

Maestrini, B. & Basso, B. 2018a. Drivers of within-field spatial and temporal variability of crop yield across the US Midwest. *Scientific reports,* 8(1)**,** 14833.

Maestrini, B. & Basso, B. 2018b. Predicting spatial patterns of within-field crop yield variability. *Field Crops Research,* 219**,** 106-112.

Maguire, M. S., Neale, C. M. U. & Woldt, W. E. 2021. Improving accuracy of unmanned aerial system thermal infrared remote sensing for use in energy balance models in agriculture applications.

Mahomed, M., Clulow, A. D., Strydom, S., Mabhaudhi, T. & Savage, M. J. 2021. Assessment of a ground-based lightning detection and near-real-time warning system in the rural community of Swayimane, Kwazulu-Natal, South Africa. *Weather, Climate, and Society,* 13(3)**,** 605-621.

Maimaitiyiming, M., Sagan, V., Sidike, P., Maimaitijiang, M., Miller, A. J. & Kwasniewski, M. 2020a. Leveraging very-high spatial resolution hyperspectral and thermal UAV imageries for characterizing diurnal indicators of grapevine physiology. *Remote Sensing,* 12(19)**,** 3216.

Maimaitiyiming, M., Sagan, V., Sidike, P., Maimaitijiang, M., Miller, A. J. & Kwasniewski, M. 2020b. Leveraging very-high spatial resolution hyperspectral and thermal UAV imageries for characterizing diurnal indicators of grapevine physiology.

Malbéteau, Y., Parkes, S., Aragon, B., Rosas, J. & McCabe, M. F. 2018a. Capturing the diurnal cycle of land surface temperature using an unmanned aerial vehicle.

Malbéteau, Y., Parkes, S., Aragon, B., Rosas, J. & McCabe, M. F. 2018b. Capturing the diurnal cycle of land surface temperature using an unmanned aerial vehicle. *Remote Sensing,* 10(9)**,** 1407.

Mall, R. K., Gupta, A. & Sonkar, G. 2017. Effect of climate change on agricultural crops. *Current developments in biotechnology and bioengineering.* Elsevier.

Markwell, J., Osterman, J. C. & Mitchell, J. L. 1995. Calibration of the Minolta SPAD-502 leaf chlorophyll meter. *Photosynthesis research,* 46(3)**,** 467-472.

Marques, P., Padua, L., Brito, T., Sousa, J. J. & Fernandes-Silva, A. Year: Published. Monitoring of Olive Trees Temperatures under Different Irrigation Strategies by UAV Thermal Infrared Imagery.

Martínez, J., Egea, G., Agüera, J. & Pérez-Ruiz, M. 2017. A cost-effective canopy temperature measurement system for precision agriculture: a case study on sugar beet.

Masenyama, A., Mutanga, O., Dube, T., Sibanda, M., Odebiri, O. & Mabhaudhi, T. 2023. Inter-seasonal estimation of grass water content indicators using multisource remotely sensed data metrics and the cloud-computing google earth engine platform. *Applied Sciences,* 13(5)**,** 3117.

Masina, M., Lambertini, A., Daprà, I., Mandanici, E. & Lamberti, A. 2020. Remote sensing analysis of surface temperature from heterogeneous data in a maize field and related water stress.

Matese, A., Baraldi, R., Berton, A., Cesaraccio, C., Di Gennaro, S. F., Duce, P., Facini, O., Mameli, M. G., Piga, A. & Zaldei, A. 2018a. Estimation of water stress in grapevines using proximal and remote sensing methods. *Remote Sensing,* 10(1)**,** 114.

Matese, A., Baraldi, R., Berton, A., Cesaraccio, C., Di Gennaro, S. F., Duce, P., Facini, O., Mameli, M. G., Piga, A. & Zaldei, A. 2018b. Estimation of Water Stress in grapevines using proximal and remote sensing methods.

Matese, A. & Di Gennaro, S. F. 2018. Practical applications of a multisensor UAV platform based on multispectral, thermal and RGB high resolution images in precision viticulture.

Matese, A., Toscano, P., Di Gennaro, S. F., Genesio, L., Vaccari, F. P., Primicerio, J., Belli, C., Zaldei, A., Bianconi, R. & Gioli, B. 2015. Intercomparison of UAV, aircraft and satellite remote sensing platforms for precision viticulture. *Remote Sensing,* 7(3)**,** 2971-2990.

Mawoyo, B., Adebola, P., Gerrano, A. S. & Amonsou, E. 2017. Effect of genotypes and growth locations on composition and functional properties of amadumbe flours. *Journal of food science and technology,* 54(11)**,** 3577-3586.

McFeeters, S. K. 1996. The use of the Normalized Difference Water Index (NDWI) in the delineation of open water features. *International journal of remote sensing,* 17(7)**,** 1425-1432.

McTavish, C. K., Poirier, B. C., Torres, C. A., Mattheis, J. P. & Rudell, D. R. 2020. A convergence of sunlight and cold chain: The influence of sun exposure on postharvest apple peel metabolism. *Postharvest Biology and Technology,* 164**,** 111164.

Messina, G. & Modica, G. 2020. Applications of UAV thermal imagery in precision agriculture: State of the art and future research outlook. *Remote Sensing,* 12(9)**,** 1491.

Meyer, G. E., Hindman, T. W. & Laksmi, K. Year: Published. Machine vision detection parameters for plant species identification. *Precision agriculture and biological quality*. SPIE, 327-335.

Meyer, G. E. & Neto, J. C. 2008. Verification of color vegetation indices for automated crop imaging applications. *Computers and electronics in agriculture,* 63(2)**,** 282-293.

Meyer, G. E., Neto, J. C., Jones, D. D. & Hindman, T. W. 2004. Intensified fuzzy clusters for classifying plant, soil, and residue regions of interest from color images. *Computers and electronics in agriculture,* 42(3)**,** 161-180.

Misra, G., Cawkwell, F. & Wingler, A. 2020. Status of phenological research using Sentinel-2 data: A review. *Remote Sensing,* 12(17)**,** 2760.

Miyasaka, S. C., Ogoshi, R. M., Tsuji, G. Y. & Kodani, L. S. 2003. Site and planting date effects on taro growth: comparison with aroid model predictions. *Agronomy journal,* 95(3)**,** 545-557.

Mo, F., Li, H., Jing, Q., Zhang, X., Cao, B. & Liu, Q. Year: Published. Research on high resolution thermal infrared satellite technology and applications. *IGARSS 2018-2018 IEEE International Geoscience and Remote Sensing Symposium*. IEEE, 5674-5677.

Mobasheri, M. R. & Fatemi, S. B. 2013a. Leaf Equivalent Water Thickness assessment using reflectance at optimum wavelengths. *Theoretical and Experimental Plant Physiology,* 25(3)**,** 196-202.

Mobasheri, M. R. & Fatemi, S. B. 2013b. Leaf Equivalent Water Thickness assessment using reflectance at optimum wavelengths. *Theoretical and Experimental Plant Physiology,* 25**,** 196-202.

Mohamed, A. A., Odindi, J. & Mutanga, O. 2017. Land surface temperature and emissivity estimation for Urban Heat Island assessment using medium-and low-resolution space-borne sensors: A review. *Geocarto international,* 32(4)**,** 455-470.

Mokari, E., Samani, Z., Heerema, R., Dehghan-Niri, E., DuBois, D., Ward, F. & Pierce, C. 2022. Development of a new UAV-thermal imaging based model for estimating pecan evapotranspiration.

Mokoena, Q., Daniyan, I., Mpofu, K. & Abisuga, O. 2022. Towards strategic management of drone application process and regulation in South Africa. *South African Journal of Industrial Engineering,* 33(4)**,** 177-196.

Moral-Muñoz, J. A., Herrera-Viedma, E., Santisteban-Espejo, A. & Cobo, M. J. 2020. Software tools for conducting bibliometric analysis in science: An up-to-date review. *Profesional de la Información,* 29(1).

Moran, M., Clarke, T., Inoue, Y. & Vidal, A. 1994. Estimating crop water deficit using the relation between surface-air temperature and spectral vegetation index. *Remote sensing of environment,* 49(3)**,** 246-263.

Mthembu, S. G., Magwaza, L. S., Mashilo, J., Mditshwa, A. & Odindo, A. 2022. Drought tolerance assessment of potato (Solanum tuberosum L.) genotypes at different growth stages, based on morphological and physiological traits. *Agricultural Water Management,* 261**,** 107361.

Mthethwa, K. N., Ngidi, M. S. C., Ojo, T. O. & Hlatshwayo, S. I. 2022. The determinants of adoption and intensity of climate-smart agricultural practices among smallholder maize farmers. *Sustainability,* 14(24)**,** 16926.

Mugiyo, H., Chimonyo, V., Sibanda, M., Kunz, R., Masemola, C., Modi, A. & Mabhaudhi, T. 2021a. Evaluation of land suitability methods with reference to neglected and underutilised crop species: A scoping review. *Land,* 10(2)**,** 125.

Mugiyo, H., Chimonyo, V. G., Sibanda, M., Kunz, R., Masemola, C. R., Modi, A. T. & Mabhaudhi, T. 2021b. Evaluation of land suitability methods with reference to neglected and underutilised crop species: A scoping review. *Land,* 10(2)**,** 125.

Mugiyo, H., Chimonyo, V. G., Sibanda, M., Kunz, R., Nhamo, L., Masemola, C. R., Dalin, C., Modi, A. T. & Mabhaudhi, T. 2021c. Multi-criteria suitability analysis for neglected and underutilised crop species in South Africa. *Plos one,* 16(1)**,** e0244734.

Mukiibi, A., Machakaire, A., Franke, A. & Steyn, J. 2024. A Systematic Review of Vegetation Indices for Potato Growth Monitoring and Tuber Yield Prediction from Remote Sensing. *Potato Research***,** 1-40.

Munialo, S., Siddique, K. H., Barker, N. P., Onyango, C. M., Amissah, J. N., Wamalwa, L. N., Qwabe, Q., Dougill, A. J. & Sibanda, L. M. 2024. Reorienting research investments toward under-researched crops for sustainable food systems. *Food and Energy Security,* 13(2)**,** e538.

Mwinuka, P. R., Mbilinyi, B. P., Mbungu, W. B., Mourice, S. K., Mahoo, H. & Schmitter, P. 2021a. The feasibility of hand-held thermal and UAV-based multispectral imaging for canopy water status assessment and yield prediction of irrigated African eggplant (Solanum aethopicum L). *Agricultural Water Management,* 245**,** 106584.

Mwinuka, P. R., Mbilinyi, B. P., Mbungu, W. B., Mourice, S. K., Mahoo, H. F. & Schmitter, P. 2021b. The feasibility of hand-held thermal and UAV-based multispectral imaging for canopy water status assessment and yield prediction of irrigated African eggplant (Solanum aethopicum L).

Nahiduzzaman, M., Chowdhury, M. E., Salam, A., Nahid, E., Ahmed, F., Al-Emadi, N., Ayari, M. A., Khandakar, A. & Haider, J. 2023a. Explainable deep learning model for automatic mulberry leaf disease classification. *Frontiers in Plant Science,* 14**,** 1175515.

Nahiduzzaman, M., Chowdhury, M. E., Salam, A., Nahid, E., Ahmed, F., Al-Emadi, N., Ayari, M. A., Khandakar, A. & Haider, J. 2023b. Explainable deep learning model for automatic mulberry leaf disease classification. *Frontiers in Plant Science,* 14.

Nanda, M. K., Giri, U. & Bera, N. 2018. Canopy temperature-based water stress indices: potential and limitations. *Advances in crop environment interaction***,** 365-385.

Ndlovu, H. S., Odindi, J., Sibanda, M. & Mutanga, O. 2024a. A systematic review on the application of UAV-based thermal remote sensing for assessing and monitoring crop water status in crop farming systems. *International Journal of Remote Sensing,* 45(15)**,** 4923-4960.

Ndlovu, H. S., Odindi, J., Sibanda, M., Mutanga, O., Clulow, A., Chimonyo, V. G. & Mabhaudhi, T. 2021a. A Comparative Estimation of Maize Leaf Water Content Using

Machine Learning Techniques and Unmanned Aerial Vehicle (UAV)-Based Proximal and Remotely Sensed Data. *Remote Sensing,* 13(20)**,** 4091.

Ndlovu, H. S., Odindi, J., Sibanda, M., Mutanga, O., Clulow, A., Chimonyo, V. G. & Mabhaudhi, T. 2024b. Use of unmanned aerial vehicle-derived multi-spectral data for the early detection of multi-temporal maize leaf equivalent water thickness and fuel moisture content for the improved resilience of smallholder maize farming. *Journal of Applied Remote Sensing,* 18(1)**,** 014520-014520.

Ndlovu, H. S., Odindi, J., Sibanda, M., Mutanga, O., Clulow, A., Chimonyo, V. G. P. & Mabhaudhi, T. 2021b. A Comparative Estimation of Maize Leaf Water Content Using Machine Learning Techniques and Unmanned Aerial Vehicle (UAV)-Based Proximal and Remotely Sensed Data. *REMOTE SENSING,* 13(20).

Ndlovu, M., Scheelbeek, P., Ngidi, M. & Mabhaudhi, T. 2024c. Underutilized crops for diverse, resilient and healthy agri-food systems: A systematic review of sub-Saharan Africa. *Frontiers in Sustainable Food Systems,* 8**,** 1498402.

Ndlovu, P., Thamaga-Chitja, J. & Ojo, T. 2021c. Factors influencing the level of vegetable value chain participation and implications on smallholder farmers in Swayimane KwaZulu-Natal. *Land Use Policy,* 109**,** 105611.

Neinavaz, E., Skidmore, A. K., Darvishzadeh, R. & Groen, T. A. 2017. Retrieving vegetation canopy water content from hyperspectral thermal measurements. *Agricultural and forest meteorology,* 247**,** 365-375.

Nguyen, T. T., Hoang, T. D., Pham, M. T., Vu, T. T., Nguyen, T. H., Huynh, Q.-T. & Jo, J. 2020. Monitoring agriculture areas with satellite images and deep learning. *Applied Soft Computing,* 95**,** 106565.

Nhamo, L., Mabhaudhi, T. & Modi, A. 2019a. Preparedness or repeated short-term relief aid? Building drought resilience through early warning in southern Africa. *Water Sa,* 45(1)**,** 75-85.

Nhamo, L., Magidi, J., Nyamugama, A., Clulow, A. D., Sibanda, M., Chimonyo, V. G. & Mabhaudhi, T. 2020. Prospects of improving agricultural and water productivity through unmanned aerial vehicles. *Agriculture,* 10(7)**,** 256.

Nhamo, L., Matchaya, G., Mabhaudhi, T., Nhlengethwa, S., Nhemachena, C. & Mpandeli, S. 2019b. Cereal production trends under climate change: Impacts and adaptation strategies in southern Africa. *Agriculture,* 9(2)**,** 30.

Nhemachena, C., Nhamo, L., Matchaya, G., Nhemachena, C. R., Muchara, B., Karuaihe, S. T. & Mpandeli, S. 2020. Climate change impacts on water and agriculture sectors in Southern Africa: Threats and opportunities for sustainable development. *Water,* 12(10)**,** 2673.

Nieto, H., Kustas, W. P., Torres-Rúa, A., Alfieri, J. G., Gao, F., Anderson, M. C., White, W. A., Song, L., Alsina, M. M., Prueger, J. H., McKee, M., Elarab, M. & McKee, L. G. 2019. Evaluation of TSEB turbulent fluxes using different methods for the retrieval of soil and canopy component temperatures from UAV thermal and multispectral imagery.

Ninanya, J., Ramírez, D. A., Rinza, J., Silva-Díaz, C., Cervantes, M., García, J. & Quiroz, R. 2021. Canopy temperature as a key physiological trait to improve yield prediction under water restrictions in potato. *Agronomy,* 11(7)**,** 1436.

Nti, I. K., Nyarko-Boateng, O. & Aning, J. 2021. Performance of machine learning algorithms with different K values in K-fold cross-validation. *International Journal of Information Technology and Computer Science,* 13(6)**,** 61-71.

Oliveira, M. F. d., Ortiz, B. V., Morata, G. T., Jiménez, A.-F., Rolim, G. d. S. & Silva, R. P. d. 2022. Training machine learning algorithms using remote sensing and topographic indices for corn yield prediction. *Remote Sensing,* 14(23)**,** 6171.

Omia, E., Bae, H., Park, E., Kim, M. S., Baek, I., Kabenge, I. & Cho, B.-K. 2023. Remote sensing in field crop monitoring: A comprehensive review of sensor systems, data analyses and recent advances. *Remote Sensing,* 15(2)**,** 354.

Omosalewa, O., Mutanga, O., Odindi, J. & Naicker, R. 2022. Modelling soil organic carbon stock distribution across different land-uses in South Africa: A remote sensing and deep learning approach. *ISPRS Journal of Photogrammetry and Remote Sensing,* 188**,** 351-362.

Omosalewa, O., Odindi, J. & Mutanga, O. 2021. Basic and deep learning models in remote sensing of soil organic carbon estimation: A brief review. *International Journal of Applied Earth Observation and Geoinformation,* 102**,** 102389.

Orduña-Malea, E. & Costas, R. 2021. Link-based approach to study scientific software usage: The case of VOSviewer. *Scientometrics,* 126(9)**,** 8153-8186.

Osroosh, Y., Khot, L. R. & Peters, R. T. 2018. Economical thermal-RGB imaging system for monitoring agricultural crops. *Computers and Electronics in Agriculture,* 147**,** 34-43.

Otsu, N. 1979. A threshold selection method from gray-level histograms. *IEEE transactions on systems, man, and cybernetics,* 9(1)**,** 62-66.

Oyeyinka, S. A. & Amonsou, E. O. 2020. Composition, pasting and thermal properties of flour and starch derived from amadumbe with different corm sizes. *Journal of Food Science and Technology,* 57(10)**,** 3688-3695.

Ozelkan, E. 2020. Water body detection analysis using NDWI indices derived from landsat-8 OLI. *Polish Journal of Environmental Studies,* 29(2)**,** 1759-1769.

Pádua, L., Bernardo, S., Dinis, L. T., Correia, C., Moutinho-Pereira, J. & Sousa, J. J. 2022. The Efficiency of Foliar Kaolin Spray Assessed through UAV-Based Thermal Infrared Imagery.

Page, M. J., McKenzie, J. E., Bossuyt, P. M., Boutron, I., Hoffmann, T. C., Mulrow, C. D., Shamseer, L., Tetzlaff, J. M., Akl, E. A. & Brennan, S. E. 2021. The PRISMA 2020 statement: an updated guideline for reporting systematic reviews. *International journal of surgery,* 88**,** 105906.

Panday, U. S., Pratihast, A. K., Aryal, J. & Kayastha, R. B. 2020. A review on drone-based data solutions for cereal crops. *Drones,* 4(3)**,** 41.

Park, S., Ryu, D., Fuentes, S., Chung, H., Hernández-Montes, E. & O'Connell, M. 2017. Adaptive estimation of crop water stress in nectarine and peach orchards using high-resolution imagery from an unmanned aerial vehicle (UAV).

Park, S., Ryu, D., Fuentes, S., Chung, H., O'connell, M. & Kim, J. 2021a. Dependence of cwsi-based plant water stress estimation with diurnal acquisition times in a nectarine orchard.

Park, S., Ryu, D., Fuentes, S., Chung, H., O'Connell, M. & Kim, J. 2021b. Mapping very-high-resolution evapotranspiration from unmanned aerial vehicle (UAV) imagery.

Parkash, V. & Singh, S. 2020. A review on potential plant-based water stress indicators for vegetable crops. *Sustainability,* 12(10)**,** 3945.

Pasqualotto, N., Delegido, J., Van Wittenberghe, S., Verrelst, J., Rivera, J. P. & Moreno, J. 2018. Retrieval of canopy water content of different crop types with two new hyperspectral indices: Water Absorption Area Index and Depth Water Index. *International journal of applied earth observation and geoinformation,* 67**,** 69-78.

Pawlak, K. & Kołodziejczak, M. 2020. The role of agriculture in ensuring food security in developing countries: Considerations in the context of the problem of sustainable food production. *Sustainability,* 12(13)**,** 5488.

Peng, J., Nieto, H., Neumann Andersen, M., Kørup, K., Larsen, R., Morel, J., Parsons, D., Zhou, Z. & Manevski, K. 2023. Accurate estimates of land surface energy fluxes and irrigation requirements from UAV-based thermal and multispectral sensors.

Peng, Z., Lin, S., Zhang, B., Wei, Z., Liu, L., Han, N., Cai, J. & Chen, H. 2020. Winter wheat canopy water content monitoring based on spectral transforms and “three-edge” parameters. *Agricultural Water Management,* 240**,** 106306.

Penuelas, J., Baret, F. & Filella, I. 1995. Semi-empirical indices to assess carotenoids/chlorophyll a ratio from leaf spectral reflectance. *Photosynthetica,* 31(2)**,** 221-230.

Perich, G., Hund, A., Anderegg, J., Roth, L., Boer, M. P., Walter, A., Liebisch, F. & Aasen, H. 2020. Assessment of Multi-Image Unmanned Aerial Vehicle Based High-Throughput Field Phenotyping of Canopy Temperature.

Piekarczyk, J., Kaźmierowski, C. & Krolewicz, S. 2012. Relationships between soil properties of the abandoned fields and spectral data derived from the advanced spaceborne thermal emission and reflection radiometer (ASTER). *Advances in space research,* 49(2)**,** 280-291.

Pineda, M., Barón, M. & Pérez-Bueno, M.-L. 2020. Thermal imaging for plant stress detection and phenotyping. *Remote Sensing,* 13(1)**,** 68.

Pirasteh-Anosheh, H., Saed-Moucheshi, A., Pakniyat, H. & Pessarakli, M. 2016. Stomatal responses to drought stress. *Water stress and crop plants: A sustainable approach,* 1**,** 24-40.

Poblete, T., Ortega-Farías, S. & Ryu, D. 2018. Automatic coregistration algorithm to remove canopy shaded pixels in UAV-borne thermal images to improve the estimation of crop water stress index of a drip-irrigated cabernet sauvignon vineyard.

Popoola, J., Ojuederie, O., Omonhinmin, C. & Adegbite, A. 2019. Neglected and underutilized legume crops: Improvement and future prospects. *Recent advances in grain crops research.* IntechOpen.

Puppala, H., Peddinti, P. R., Tamvada, J. P., Ahuja, J. & Kim, B. 2023. Barriers to the adoption of new technologies in rural areas: The case of unmanned aerial vehicles for precision agriculture in India. *Technology in Society,* 74**,** 102335.

Qi, D., Hu, T. & Liu, T. 2020. Biomass accumulation and distribution, yield formation and water use efficiency responses of maize (Zea mays L.) to nitrogen supply methods under partial root-zone irrigation. *Agricultural Water Management,* 230**,** 105981.

Quan, X., He, B., Li, X. & Tang, Z. 2015. Estimation of grassland live fuel moisture content from ratio of canopy water content and foliage dry biomass. *IEEE Geoscience and Remote Sensing Letters,* 12(9)**,** 1903-1907.

Quiroga-Garza, A., Garza-Cisneros, A. N., Elizondo-Omaña, R. E., Vilchez-Cavazos, J. F., de-Oca-Luna, R. M., Villarreal-Silva, E., Guzman-Lopez, S. & Gonzalez-Gonzalez, J. G. 2022. Research barriers in the global south: Mexico. *Journal of Global Health,* 12.

Rabia, A. H., Neupane, J., Lin, Z., Lewis, K., Cao, G. & Guo, W. 2022. Principles and applications of topography in precision agriculture. *Advances in agronomy,* 171**,** 143-189.

Rajwade, Y. A., Chandel, N. S., Dubey, K., Anakkallan, S., Upender, K. & Jat, D. 2023. Assessment of water stress in rainfed maize using RGB and thermal imagery. *Arabian Journal of Geosciences,* 16(2)**,** 119.

Ramírez, D. A., Yactayo, W., Rens, L. R., Rolando, J. L., Palacios, S., De Mendiburu, F., Mares, V., Barreda, C., Loayza, H. & Monneveux, P. 2016. Defining biological thresholds associated to plant water status for monitoring water restriction effects: Stomatal conductance and photosynthesis recovery as key indicators in potato. *Agricultural Water Management,* 177**,** 369-378.

Rapholo, M. T. & Diko Makia, L. 2020. Are smallholder farmers' perceptions of climate variability supported by climatological evidence? Case study of a semi-arid region in South Africa. *International Journal of Climate Change Strategies and Management,* 12(5)**,** 571-585.

Reddy, G. P. O. 2018. Satellite Remote Sensing Sensors: Principles and Applications. *In:* Reddy, G. P. O. & Singh, S. K. (eds.) *Geospatial Technologies in Land Resources Mapping, Monitoring and Management.* Cham: Springer International Publishing.

Riehle, D., Reiser, D. & Griepentrog, H. W. 2020. Robust index-based semantic plant/background segmentation for RGB-images. *Computers and Electronics in Agriculture,* 169**,** 105201.

Roujean, J.-L. & Breon, F.-M. 1995. Estimating PAR absorbed by vegetation from bidirectional reflectance measurements. *Remote sensing of Environment,* 51(3)**,** 375-384.

Rouse, J., Haas, J., Schell, J. & Deering, D. Year: Published. Monitoring vegetation systemsin the Great Plains witherts. *Proceedings of the 3rd ERTS Symposium, Washington, DC, USA*.

Rutkoski, J., Poland, J., Mondal, S., Autrique, E., Pérez, L. G., Crossa, J., Reynolds, M. & Singh, R. 2016. Canopy temperature and vegetation indices from high-throughput phenotyping improve accuracy of pedigree and genomic selection for grain yield in wheat. *G3: Genes, Genomes, Genetics,* 6(9)**,** 2799-2808.

Ryu, J.-H., Oh, D., Ko, J., Kim, H.-Y., Yeom, J.-M. & Cho, J. 2022. Remote sensing-Based evaluation of heat stress damage on paddy rice using NDVI and PRI measured at leaf and canopy scales. *Agronomy,* 12(8)**,** 1972.

Sabzi, S., Abbaspour-Gilandeh, Y., García-Mateos, G., Ruiz-Canales, A. & Molina-Martínez, J. M. 2018. Segmentation of apples in aerial images under sixteen different lighting conditions using color and texture for optimal irrigation. *Water,* 10(11)**,** 1634.

Sagan, V., Maimaitijiang, M., Bhadra, S., Maimaitiyiming, M., Brown, D. R., Sidike, P. & Fritschi, F. B. 2021. Field-scale crop yield prediction using multi-temporal WorldView-3 and PlanetScope satellite data and deep learning. *ISPRS journal of photogrammetry and remote sensing,* 174**,** 265-281.

Sagan, V., Maimaitijiang, M., Sidike, P., Eblimit, K., Peterson, K. T., Hartling, S., Esposito, F., Khanal, K., Newcomb, M. & Pauli, D. 2019a. UAV-based high resolution thermal imaging for vegetation monitoring, and plant phenotyping using ICI 8640 P, FLIR Vue Pro R 640, and thermomap cameras. *Remote Sensing,* 11(3)**,** 330.

Sagan, V., Maimaitijiang, M., Sidike, P., Eblimit, K., Peterson, K. T., Hartling, S., Esposito, F., Khanal, K., Newcomb, M., Pauli, D., Ward, R., Fritschi, F., Shakoor, N. & Mockler, T. 2019b. UAV-based high resolution thermal imaging for vegetation monitoring, and plant phenotyping using ICI 8640 P, FLIR Vue Pro R 640, and thermomap cameras.

SANBI 2018. *South African National Biodiversity Institute: Project Proposal to the Adaptation Fund*.

Sandholt, I., Rasmussen, K. & Andersen, J. 2002. A simple interpretation of the surface temperature/vegetation index space for assessment of surface moisture status. *Remote Sensing of environment,* 79(2-3)**,** 213-224.

Sankaran, S., Quirós, J. J. & Miklas, P. N. 2019. Unmanned aerial system and satellite-based high resolution imagery for high-throughput phenotyping in dry bean.

Santesteban, L., Di Gennaro, S., Herrero-Langreo, A., Miranda, C., Royo, J. & Matese, A. 2017a. High-resolution UAV-based thermal imaging to estimate the instantaneous and seasonal variability of plant water status within a vineyard. *Agricultural Water Management,* 183**,** 49-59.

Santesteban, L. G., Di Gennaro, S. F., Herrero-Langreo, A., Miranda, C., Royo, J. B. & Matese, A. 2017b. High-resolution UAV-based thermal imaging to estimate the instantaneous and seasonal variability of plant water status within a vineyard.

Saravi, B., Nejadhashemi, A. P., Jha, P. & Tang, B. 2021. Reducing deep learning network structure through variable reduction methods in crop modeling. *Artificial Intelligence in Agriculture,* 5**,** 196-207.

Sepúlveda-Reyes, D., Ingram, B., Bardeen, M., Zúñiga, M., Ortega-Farías, S. & Poblete-Echeverría, C. 2016. Selecting canopy zones and thresholding approaches to assess grapevine water status by using aerial and ground-based thermal imaging.

Shafiq, S., Akram, N. A. & Ashraf, M. 2019. Assessment of physio-biochemical indicators for drought tolerance in different cultivars of maize (Zea mays L.). *Pakistan Journal of Botany,* 51(4)**,** 1241-1247.

Shahzad, A., Ullah, S., Dar, A. A., Sardar, M. F., Mehmood, T., Tufail, M. A., Shakoor, A. & Haris, M. 2021. Nexus on climate change: Agriculture and possible solution to cope future climate change stresses. *Environmental Science and Pollution Research,* 28**,** 14211-14232.

Shao, G., Han, W., Zhang, H., Zhang, L., Wang, Y. & Zhang, Y. 2023. Prediction of maize crop coefficient from UAV multisensor remote sensing using machine learning methods. *Agricultural Water Management,* 276.

Shi, J., Sang, Y.-F., Sun, S., Aghakouchak, A., Hu, S. & Dash, S. S. 2024. Development of a leaf area index-based relative threshold method for identifying agricultural drought areas. *Journal of Hydrology,* 641**,** 131846.

Shu, M., Zuo, J., Shen, M., Yin, P., Wang, M., Yang, X., Tang, J., Li, B. & Ma, Y. 2021. Improving the estimation accuracy of SPAD values for maize leaves by removing UAV hyperspectral image backgrounds. *International Journal of Remote Sensing,* 42(15)**,** 5862-5881.

Sibanda, M., Mutanga, O., Chimonyo, V. G., Clulow, A. D., Shoko, C., Mazvimavi, D., Dube, T. & Mabhaudhi, T. 2021a. Application of drone technologies in surface water resources monitoring and assessment: a systematic review of progress, challenges, and opportunities in the global south. *Drones,* 5(3)**,** 84.

Sibanda, M., Mutanga, O., Chimonyo, V. G., Clulow, A. D., Shoko, C., Mazvimavi, D., Dube, T. & Mabhaudhi, T. 2022. Correction: Sibanda et al. Application of drone technologies in surface water resources monitoring and assessment: A systematic review of progress, challenges, and opportunities in the Global South. Drones 2021, 5, 84. *Drones,* 6(5)**,** 131.

Sibanda, M., Ndlovu, H. S., Brewer, K., Buthelezi, S., Matongera, T. N., Mutanga, O., Odidndi, J., Clulow, A. D., Chimonyo, V. G. & Mabhaudhi, T. 2023. Remote sensing hail damage on maize crops in smallholder farms using data acquired by remotely piloted aircraft system. *Smart Agricultural Technology,* 6**,** 100325.

Sibanda, M., Onisimo, M., Dube, T. & Mabhaudhi, T. 2021b. Quantitative assessment of grassland foliar moisture parameters as an inference on rangeland condition in the mesic rangelands of southern Africa. *International Journal of Remote Sensing,* 42(4)**,** 1474-1491.

Sibiya, S. G. 2015. *Planting density effect on growth and yield of taro (Colocasia esculenta) landraces.*

Silici, L., Knox, J., Rowe, A. & Nanthikesan, S. 2022. Evaluating Transformational Adaptation in Smallholder Farming: Insights from an Evidence Review. *Transformational Change for People and the Planet: Evaluating Environment and Development***,** 187-202.

Sims, D. A. & Gamon, J. A. 2002. Relationships between leaf pigment content and spectral reflectance across a wide range of species, leaf structures and developmental stages. *Remote sensing of environment,* 81(2-3)**,** 337-354.

Singh, G. & Das, N. N. 2022. A data-driven approach using the remotely sensed soil moisture product to identify water-demand in agricultural regions. *Science of The Total Environment,* 837**,** 155893.

Sishodia, R. P., Ray, R. L. & Singh, S. K. 2020. Applications of remote sensing in precision agriculture: A review. *Remote Sensing,* 12(19)**,** 3136.

Skobalski, J., Sagan, V., Alifu, H., Al Akkad, O., Lopes, F. A. & Grignola, F. 2024. Bridging the gap between crop breeding and GeoAI: Soybean yield prediction from multispectral UAV images with transfer learning. *ISPRS Journal of Photogrammetry and Remote Sensing,* 210**,** 260-281.

Sobejano-Paz, V., Mikkelsen, T. N., Baum, A., Mo, X., Liu, S., Köppl, C. J., Johnson, M. S., Gulyas, L. & García, M. 2020. Hyperspectral and thermal sensing of stomatal conductance, transpiration, and photosynthesis for soybean and maize under drought. *Remote Sensing,* 12(19)**,** 3182.

Soureshjani, H. K., Dehkordi, A. G. & Bahador, M. 2019. Temperature effect on yield of winter and spring irrigated crops. *Agricultural and Forest Meteorology,* 279**,** 107664.

Suárez, L., Zarco-Tejada, P. J., Sepulcre-Cantó, G., Pérez-Priego, O., Miller, J., Jiménez-Muñoz, J. & Sobrino, J. 2008. Assessing canopy PRI for water stress detection with diurnal airborne imagery. *Remote Sensing of Environment,* 112(2)**,** 560-575.

Sullivan, D. G., Fulton, J. P., Shaw, J. N. & Bland, G. L. 2007. Evaluating the sensitivity of an unmanned thermal infrared aerial system to detect water stress in a cotton canopy.

Sultana, N., Jahan, F. & Rahim, M. 2021. Status and Scope of Promoting Underutilized Taro for Sustainable biodiversity and nutrition security in SAARC Countries. *Promotion of Underutilized Taro for Sustainable Biodiversity and Nutrition Security in SAARC Countries,* 281**,** 1.

Suyala, Q., Li, Z., Zhang, Z., Jia, L., Fan, M., Sun, Y. & Xing, H. 2024. Developing a hyperspectral remote sensing-based algorithm to diagnose potato moisture for water-saving irrigation. *Horticulturae,* 10(8)**,** 811.

Taghvaeian, S., Comas, L., DeJonge, K. C. & Trout, T. J. 2014. Conventional and simplified canopy temperature indices predict water stress in sunflower. *Agricultural water management,* 144**,** 69-80.

Talucder, M. S. A., Ruba, U. B. & Robi, M. A. S. 2024. Potentiality of Neglected and Underutilized Species (NUS) as a future resilient food: A systematic review. *Journal of Agriculture and Food Research***,** 101116.

Tang, T., Radomski, M., Stefan, M., Perrelli, M. & Fan, H. 2020a. UAV-based high spatial and temporal resolution monitoring and mapping of surface moisture status in a vineyard. *Papers in Applied Geography,* 6(4)**,** 402-415.

Tang, T., Radomski, M., Stefan, M., Perrelli, M. & Fan, H. 2020b. UAV-based high spatial and temporal resolution monitoring and mapping of surface moisture status in a vineyard.

Tang, Z., Jin, Y., Brown, P. H. & Park, M. 2023. Estimation of tomato water status with photochemical reflectance index and machine learning: Assessment from proximal sensors and UAV imagery. *Frontiers in Plant Science,* 14**,** 1057733.

Tanner, C. 1963. Plant temperatures. *Agron. J.,* 55**,** 210-211.

Tattaris, M., Reynolds, M. P. & Chapman, S. C. 2016. A direct comparison of remote sensing approaches for high-throughput phenotyping in plant breeding.

Thomas, H. 2018. Some like it hot: The impact of next generation FLIR Systems thermal cameras on archaeological thermography. *Archaeological Prospection,* 25(1)**,** 81-87.

Tilling, A. K., O'Leary, G. J., Ferwerda, J. G., Jones, S. D., Fitzgerald, G. J., Rodriguez, D. & Belford, R. 2007. Remote sensing of nitrogen and water stress in wheat. *Field Crops Research,* 104(1-3)**,** 77-85.

Traore, A., Ata-Ul-Karim, S. T., Duan, A., Soothar, M. K., Traore, S. & Zhao, B. 2021. Predicting Equivalent Water Thickness in Wheat Using UAV Mounted Multispectral Sensor through Deep Learning Techniques. *Remote Sensing,* 13(21)**,** 4476.

Tsvetkov, M. Y. Year: Published. Satellite and drone multi-spectral and thermal images data fusion for intelligent agriculture monitoring and decision making support. *Remote Sensing for Agriculture, Ecosystems, and Hydrology XXV*. SPIE, 378-384.

Tumuhimbise, R. 2015. Plant spacing and planting depth effects on corm yield of taro (Colocasia esculenta (L.) Schott). *Journal of Crop Improvement,* 29(6)**,** 747-757.

Turk, J. 2016. Meeting projected food demands by 2050: Understanding and enhancing the role of grazing ruminants. *Journal of Animal Science,* 94(suppl_6)**,** 53-62.

Uddling, J., Gelang-Alfredsson, J., Piikki, K. & Pleijel, H. 2007. Evaluating the relationship between leaf chlorophyll concentration and SPAD-502 chlorophyll meter readings. *Photosynthesis research,* 91(1)**,** 37-46.

United Nations. 2024. *UN projects world population to peak within this century* [Online]. Available: https://www.un.org/en/UN-projects-world-population-to-peak-within-this-century [Accessed 21/12/2024.

Upendar, K., Agrawal, K., Chandel, N. & Singh, K. 2021. Greenness identification using visible spectral colour indices for site specific weed management. *Plant Physiology Reports,* 26**,** 179-187.

Usta, A. 2022. Prediction of soil water contents and erodibility indices based on artificial neural networks: using topography and remote sensing. *Environmental Monitoring and Assessment,* 194(11)**,** 794.

Van Dijk, M., Morley, T., Rau, M. L. & Saghai, Y. 2021. A meta-analysis of projected global food demand and population at risk of hunger for the period 2010–2050. *Nature Food,* 2(7)**,** 494-501.

Van Eck, N. & Waltman, L. 2010. Software survey: VOSviewer, a computer program for bibliometric mapping. *scientometrics,* 84(2)**,** 523-538.

Van Wyk, H. R. A., O E 2021. Physiochemical and functional properties of albumin and globulin from amadumbe (Colocasia esculenta) corms. *Food Science and Technology*.

Veysi, S., Naseri, A. A., Hamzeh, S. & Bartholomeus, H. 2017. A satellite based crop water stress index for irrigation scheduling in sugarcane fields. *Agricultural water management,* 189**,** 70-86.

Virnodkar, S. S., Pachghare, V. K., Patil, V. & Jha, S. K. 2020. Remote sensing and machine learning for crop water stress determination in various crops: a critical review. *Precision Agriculture,* 21(5)**,** 1121-1155.

Vos, R. & Bellù, L. G. 2019. Global trends and challenges to food and agriculture into the 21st century. *Sustainable food and agriculture***,** 11-30.

Wang, C., Zhu, K., Bai, Y., Li, C., Li, M. & Sun, Y. 2024a. Response of Stomatal Conductance to Crop Water Stress In Buffalograss: Observation with Uav Thermal Infrared Imagery. *Available at SSRN 4580414*.

Wang, E., Huang, T., Liu, Z., Bao, L., Guo, B., Yu, Z., Feng, Z., Luo, H. & Ou, G. 2024b. Improving Forest Above-Ground Biomass Estimation Accuracy Using Multi-Source Remote Sensing and Optimized Least Absolute Shrinkage and Selection Operator Variable Selection Method. *Remote Sensing,* 16(23)**,** 4497.

Wang, J., Lou, Y., Wang, W., Liu, S., Zhang, H., Hui, X., Wang, Y., Yan, H. & Maes, W. H. 2024c. A robust model for diagnosing water stress of winter wheat by combining UAV multispectral and thermal remote sensing. *Agricultural Water Management,* 291**,** 108616.

Wang, J., Zhang, X., Han, Z., Feng, H., Wang, Y., Kang, J., Han, X., Wang, L., Wang, C. & Li, H. 2022a. Analysis of physiological indicators associated with drought tolerance in wheat under drought and re-watering conditions. *Antioxidants,* 11(11)**,** 2266.

Wang, N., Clevers, J. G. P. W., Wieneke, S., Bartholomeus, H. & Kooistra, L. 2022b. Potential of UAV-based sun-induced chlorophyll fluorescence to detect water stress in sugar beet. *Agricultural and Forest Meteorology,* 323.

Wang, N., Yang, P., Clevers, J. G. P. W., Wieneke, S. & Kooistra, L. 2023. Decoupling physiological and non-physiological responses of sugar beet to water stress from sun-induced chlorophyll fluorescence. *Remote Sensing of Environment,* 286.

Wang, Q., He, Q. & Zhou, G. 2018. Applicability of common stomatal conductance models in maize under varying soil moisture conditions. *Science of the Total Environment,* 628**,** 141-149.

Wei, M., Wang, H., Zhang, Y., Li, Q., Du, X., Shi, G. & Ren, Y. 2023. Investigating the potential of crop discrimination in early growing stage of change analysis in remote sensing crop profiles. *Remote Sensing,* 15(3)**,** 853.

Wijewardana, C., Alsajri, F. A., Irby, J. T., Krutz, L. J., Golden, B., Henry, W. B., Gao, W. & Reddy, K. R. 2019. Physiological assessment of water deficit in soybean using midday leaf water potential and spectral features. *Journal of Plant Interactions,* 14(1)**,** 533-543.

Williamson, E., Ross, I. L., Wall, B. T. & Hankamer, B. 2024. Microalgae: Potential novel protein for sustainable human nutrition. *Trends in Plant Science,* 29(3)**,** 370-382.

Woebbecke, D. M., Meyer, G. E., Von Bargen, K. & Mortensen, D. A. 1995. Color indices for weed identification under various soil, residue, and lighting conditions. *Transactions of the ASAE,* 38(1)**,** 259-269.

Wong, T.-T. & Yeh, P.-Y. 2019. Reliable accuracy estimates from k-fold cross validation. *IEEE Transactions on Knowledge and Data Engineering,* 32(8)**,** 1586-1594.

Xie, Q., Dash, J., Huang, W., Peng, D., Qin, Q., Mortimer, H., Casa, R., Pignatti, S., Laneve, G. & Pascucci, S. 2018. Vegetation indices combining the red and red-edge spectral information for leaf area index retrieval. *IEEE Journal of selected topics in applied earth observations and remote sensing,* 11(5)**,** 1482-1493.

Xu, X., Fan, L., Li, Z., Meng, Y., Feng, H., Yang, H. & Xu, B. 2021. Estimating leaf nitrogen content in corn based on information fusion of multiple-sensor imagery from UAV. *Remote Sensing,* 13(3)**,** 340.

Xue, J., Anderson, M. C., Gao, F., Hain, C., Sun, L., Yang, Y., Knipper, K. R., Kustas, W. P., Torres-Rua, A. & Schull, M. 2020a. Sharpening ECOSTRESS and VIIRS land surface temperature using harmonized Landsat-Sentinel surface reflectances. *Remote sensing of environment,* 251**,** 112055.

Xue, J., Anderson, M. C., Gao, F., Hain, C., Sun, L., Yang, Y., Knipper, K. R., Kustas, W. P., Torres-Rua, A. & Schull, M. 2020b. Sharpening ECOSTRESS and VIIRS land surface temperature using harmonized Landsat-Sentinel surface reflectances.

Yang, M.-D., Tseng, H.-H., Hsu, Y.-C., Yang, C.-Y., Lai, M.-H. & Wu, D.-H. 2021. A UAV open dataset of rice paddies for deep learning practice. *Remote Sensing,* 13(7)**,** 1358.

Yi, K., Smith, J. W., Jablonski, A. D., Tatham, E. A., Scanlon, T. M., Lerdau, M. T., Novick, K. A. & Yang, X. 2020. High heterogeneity in canopy temperature among co-occurring tree species in a temperate forest. *Journal of Geophysical Research: Biogeosciences,* 125(12)**,** e2020JG005892.

Yi, Q., Wang, F., Bao, A. & Jiapaer, G. 2014. Leaf and canopy water content estimation in cotton using hyperspectral indices and radiative transfer models. *International Journal of Applied Earth Observation and Geoinformation,* 33**,** 67-75.

Yilmaz, M. T., Hunt Jr, E. R. & Jackson, T. J. 2008. Remote sensing of vegetation water content from equivalent water thickness using satellite imagery. *Remote Sensing of Environment,* 112(5)**,** 2514-2522.

Yin, Q., Zhang, Y., Li, W., Wang, J., Wang, W., Ahmad, I., Zhou, G. & Huo, Z. 2023. Estimation of winter wheat SPAD values based on UAV multispectral remote sensing. *Remote Sensing,* 15(14)**,** 3595.

Yinka-Banjo, C. & Ajayi, O. 2019. Sky-farmers: Applications of unmanned aerial vehicles (UAV) in agriculture. *Autonomous vehicles***,** 107-128.

Yousaf, W., Awan, W. K., Kamran, M., Ahmad, S. R., Bodla, H. U., Riaz, M., Umar, M. & Chohan, K. 2021. A paradigm of GIS and remote sensing for crop water deficit assessment in near real time to improve irrigation distribution plan. *Agricultural Water Management,* 243**,** 106443.

Yu, J., Wang, J., Leblon, B. & Song, Y. 2021. Nitrogen estimation for wheat using UAV-based and satellite multispectral imagery, topographic metrics, leaf area index, plant height, soil moisture, and machine learning methods. *Nitrogen,* 3(1)**,** 1-25.

Yu, M.-H., Ding, G.-D., Gao, G.-L., Zhao, Y.-Y., Yan, L. & Sai, K. 2015. Using plant temperature to evaluate the response of stomatal conductance to soil moisture deficit. *Forests,* 6(10)**,** 3748-3762.

Yuan, Q., Shen, H., Li, T., Li, Z., Li, S., Jiang, Y., Xu, H., Tan, W., Yang, Q. & Wang, J. 2020. Deep learning in environmental remote sensing: Achievements and challenges. *Remote Sensing of Environment,* 241**,** 111716.

Zaca, F. N., Ngidi, M. S. C., Chipfupa, U., Ojo, T. O. & Managa, L. R. 2023. Factors influencing the uptake of agroforestry practices among rural households: Empirical evidence from the KwaZulu-Natal province, South Africa. *Forests,* 14(10)**,** 2056.

Zarco-Tejada, P. J., González-Dugo, V., Williams, L. E., Suárez, L., Berni, J. A. J., Goldhamer, D. & Fereres, E. 2013. A PRI-based water stress index combining structural and chlorophyll effects: Assessment using diurnal narrow-band airborne imagery and the CWSI thermal index. *Remote Sensing of Environment,* 138**,** 38-50.

Zarco-Tejada, P. J., Pushnik, J., Dobrowski, S. & Ustin, S. 2003. Steady-state chlorophyll a fluorescence detection from canopy derivative reflectance and double-peak red-edge effects. *Remote Sensing of Environment,* 84(2)**,** 283-294.

Zhai, W., Li, C., Cheng, Q., Ding, F. & Chen, Z. 2023. Exploring Multisource Feature Fusion and Stacking Ensemble Learning for Accurate Estimation of Maize Chlorophyll Content Using Unmanned Aerial Vehicle Remote Sensing. *Remote Sensing,* 15(13)**,** 3454.

Zhang, F. & Zhou, G. 2015. Estimation of canopy water content by means of hyperspectral indices based on drought stress gradient experiments of maize in the north plain China. *Remote Sensing,* 7(11)**,** 15203-15223.

Zhang, F. & Zhou, G. 2019a. Estimation of vegetation water content using hyperspectral vegetation indices: A comparison of crop water indicators in response to water stress treatments for summer maize. *BMC ecology,* 19(1)**,** 1-12.

Zhang, F. & Zhou, G. 2019b. Estimation of vegetation water content using hyperspectral vegetation indices: A comparison of crop water indicators in response to water stress treatments for summer maize. *BMC ecology,* 19**,** 1-12.

Zhang, L., Zhang, H., Han, W., Niu, Y., Chávez, J. L. & Ma, W. 2022. Effects of image spatial resolution and statistical scale on water stress estimation performance of MGDEXG: A new crop water stress indicator derived from RGB images. *Agricultural Water Management,* 264.

Zhang, L., Zhang, H., Niu, Y. & Han, W. 2019. Mapping maize water stress based on UAV multispectral remote sensing. *Remote Sensing,* 11(6)**,** 605.

Zhang, Y., Han, W., Zhang, H., Niu, X. & Shao, G. 2023a. Evaluating maize evapotranspiration using high-resolution UAV-based imagery and FAO-56 dual crop coefficient approach. *Agricultural Water Management,* 275.

Zhang, Y., Han, W., Zhang, H., Niu, X. & Shao, G. 2023b. Evaluating soil moisture content under maize coverage using UAV multimodal data by machine learning algorithms.

Zhao, J., Liu, D. & Huang, R. 2023. A Review of Climate-Smart Agriculture: Recent Advancements, Challenges, and Future Directions. *Sustainability,* 15(4)**,** 3404.

Zhao, P., Yan, Y., Jia, S., Zhao, J. & Zhang, W. 2025. Construction and Evaluation of a Cross-Regional and Cross-Year Monitoring Model for Millet Canopy Phenotype Based on UAV Multispectral Remote Sensing. *Agronomy,* 15(4)**,** 789.

Zhou, J., Zhou, J., Ye, H., Ali, M. L., Nguyen, H. T. & Chen, P. 2020. Classification of soybean leaf wilting due to drought stress using UAV-based imagery.

Zhou, Z., Majeed, Y., Naranjo, G. D. & Gambacorta, E. M. 2021. Assessment for crop water stress with infrared thermal imagery in precision agriculture: A review and future prospects for deep learning applications. *Computers and Electronics in Agriculture,* 182**,** 106019.

Zhu, P., Zhang, G., Yang, Y., Wang, C., Chen, S. & Wan, Y. 2023. Infiltration properties affected by slope position on cropped hillslopes. *Geoderma,* 432**,** 116379.

Zhu, W., Sun, Z., Huang, Y., Yang, T., Li, J., Zhu, K., Zhang, J., Yang, B., Shao, C. & Peng, J. 2021a. Optimization of multi-source UAV RS agro-monitoring schemes designed for field-scale crop phenotyping. *Precision Agriculture,* 22(6)**,** 1768-1802.

Zhu, W., Sun, Z., Huang, Y., Yang, T., Li, J., Zhu, K., Zhang, J., Yang, B., Shao, C., Peng, J., Li, S., Hu, H. & Liao, X. 2021b. Optimization of multi-source UAV RS agro-monitoring schemes designed for field-scale crop phenotyping.

Zulu, N. N. 2022. Water Scarcity and Household Food Security: A Case of Ulundi Local Municipality in KwaZulu-Natal, South Africa. *Handbook of Research on Resource Management and the Struggle for Water Sustainability in Africa.* IGI Global.